

August 2018

# Ghrelin Processing and Maturation: Developing a Molecular-Level Framework for Hormone Activation and Biological Function

Elizabeth Rose Cleverdon  
*Syracuse University*

Follow this and additional works at: <https://surface.syr.edu/etd>

 Part of the [Physical Sciences and Mathematics Commons](#)

---

## Recommended Citation

Cleverdon, Elizabeth Rose, "Ghrelin Processing and Maturation: Developing a Molecular-Level Framework for Hormone Activation and Biological Function" (2018). *Dissertations - ALL*. 913.  
<https://surface.syr.edu/etd/913>

This Dissertation is brought to you for free and open access by the SURFACE at SURFACE. It has been accepted for inclusion in Dissertations - ALL by an authorized administrator of SURFACE. For more information, please contact [surface@syr.edu](mailto:surface@syr.edu).

## Abstract

Ghrelin is a 28 amino acid hormone involved in appetite stimulation, maintenance of energy balance, and a range of other neuroendocrine functions. Over the course of its expression and maturation, proghrelin (the prohormone of ghrelin) undergoes a unique posttranslational modification whereby a serine side chain is esterified with octanoic acid. Proghrelin then undergoes subsequent proteolysis to yield ghrelin. This octanoylation modification has been demonstrated to be required for ghrelin to activate its cognate receptor. Since acylated ghrelin has been linked with a variety of disease states, ghrelin signaling is a prime target for inhibition and inhibitor development. Biochemical and structural studies of the enzyme responsible for ghrelin octanoylation, ghrelin *O*-acyltransferase (GOAT), have identified features required for recognition of ghrelin by GOAT. A majority of these studies have utilized peptide mimetics of the N-terminal sequence of ghrelin. However, the impact of downstream elements in ghrelin and its 94 amino acid precursor proghrelin remains to be fully defined. To investigate this, we have developed bacterial expression systems to explore the role of both ghrelin and C-terminal ghrelin in proghrelin's biological activity and maturation. The work presented in this dissertation is the first instance of expression and structural characterization of human proghrelin and C-ghrelin, as well as an unidentified self-cleavage behavior which has implications in hormone maturation. In complementary studies to characterize ghrelin binding to GOAT, ghrelin peptide mimetics incorporating an amine-substituted Dap residue at the site of acylation provided a superior system for exploring the molecular requirements for ghrelin recognition by GOAT. These studies have identified previously unidentified binding contacts and provides a comprehensive model of peptide binding in the hGOAT active site. The work utilizing Dap-substituted peptides provides a comprehensive peptide scaffold for future inhibitor design for targeting ghrelin signaling.

# Ghrelin Processing and Maturation: Developing a Molecular-Level Framework for Hormone Activation and Biological Function

Elizabeth R. Cleverdon

B.S., University of Wyoming, 2013  
M.Phil., Syracuse University, 2015

Dissertation  
Submitted in partial fulfillment of the requirements for the degree of  
Doctor of Philosophy in *Chemistry*

Syracuse University  
August 2018

Copyright © Elizabeth R. Cleverdon 2018  
All Rights Reserved

## **Acknowledgements**

Firstly, I would like to thank my advisor Dr. James L. Hougland. I have valued his mentorship and scientific acumen throughout my time in his laboratory. His thirst for knowledge and inquisitive mind encouraged the same in me as well as his other students. He was always available for advice or to answer any questions that I had, which were many. He helped me to develop into the scientist that I am today, to be more skeptical and thorough when planning and evaluating experimental data. I thank him for always being very willing for discussion of theories, data, and of course the question of biological relevance. I would also like to thank my committee; Dr. Jason Fridley, Dr. Michael Cosgrove, Dr. Carlos Castañeda, Dr. Mathew Maye and Dr. Robert Doyle for their time and assistance for serving on my defense committee. I want to express my appreciation to Dr. Maye and Dr. Doyle as well as Dr. Dabrowiak for their assistance for serving on my graduate committee throughout my time at Syracuse University. Their help and input into my project was invaluable.

I want to thank the Hougland lab, my family for the past five years. They were a pleasure to work with and I continue to appreciate their mentorship, fellowship and friendship. I want to thank Dr. Susan Flynn, Dr. Joe Darling, Dr. Soumya Gangopadhyay, Dr. Kayleigh McGovern-Gooch and Melanie Blanden for welcoming into the laboratory and for their support throughout my PhD. I also want to thank Maria Campana, Tasha Davis, Sudhat Ashok, Jacob Moose and Mariah Pierce for their support and friendship. Michelle Sieberg, our lab technician and lab mom, has been there throughout my PhD and has always been supportive, both emotionally and scientifically, as well as, a great teacher and resource. My undergraduates, Naomi Rivera-Robles and Casey Cabrinha gave me the opportunity to teach, to test my scientific knowledge and have taught me patience. I am very grateful to have been a member of this laboratory; everyone was

always willing to teach, mentor and support each other. The environment was always friendly and encouraging; you guys were there on both good and bad days, when there was good data and when experiments weren't going so well, and I am very thankful to everyone.

Finally, I would like to thank my family. My parents have always fostered my inquisitive nature. They were always there to answer any questions I had, and if they couldn't answer them they would help me to figure it out. They were always supportive and I know that it would have been much harder to achieve my goals had they not been there. I want to thank my brother for his love and support throughout my studies; as well as, my grandparents for their love and encouragement not only during my training but throughout my life. As a first generation PhD there were many unknowns and a number of struggles were very present but they seemed much less apparent with my family's love and support. Even though they had no idea what I was studying or researching throughout my education and training, it did not matter, they still championed me.

## Table of Contents

|  |      |
|--|------|
| <b>List of figures</b> .....   | x    |
| <b>List of tables</b> .....  | xiii |
| <b>List of abbreviations</b> .....   | xiv  |
| <b>Chapter 1: Introduction</b>   |      |
| 1.1 Post-translational modifications.....  | 2    |
| 1.2 Ghrelin .....  | 5    |
| 1.2.1 Discovery .....  | 5    |
| 1.2.2 Tissue distribution.....   | 6    |
| 1.2.3 Ghrelin processing .....   | 6    |
| 1.2.4 Binding partners for ghrelin within the body.....                                      | 9    |
| 1.2.5 Physiological effects .....  | 15   |
| 1.3 GOAT .....   | 16   |
| 1.3.1 Discovery .....  | 16   |
| 1.3.2 GOAT conservation across species .....   | 17   |
| 1.4 GOAT inhibitors .....  | 20   |
| 1.4.1 Ghrelin product mimetics as GOAT inhibitors.....                                       | 20   |
| 1.4.2 Small molecule GOAT inhibitors .....   | 24   |
| 1.5 GOAT recognition of ghrelin- the role of the N-terminal “GSSF” sequence and beyond ..... | 28   |
| 1.6 Obestatin .....  | 29   |
| 1.7 Aims of this work.....   | 31   |
| 1.8 References.....  | 33   |

## Chapter 2: Proghrelin and C-ghrelin: Expression, purification and structural analysis

|  |     |
|--|-----|
| 2.1 Introduction.....  | 59  |
| 2.2 Results.....   | 64  |
| 2.2.1 Human proghrelin expression system.....  | 64  |
| 2.2.2 Induction method optimization for proghrelin-His <sub>6</sub> .....  | 65  |
| 2.2.3 C-ghrelin insolubility utilizing autoinduction.....  | 68  |
| 2.2.4 C-ghrelin expression optimization.....   | 70  |
| 2.2.5 Purification method for proghrelin-His <sub>6</sub> .....  | 72  |
| 2.2.5.1 Ni <sup>2+</sup> -Sephrose Purifications .....   | 72  |
| 2.2.5.2 Proghrelin purity improved after GST-Sephrose added to purification.....                                 | 78  |
| 2.2.5.3 Size exclusion chromatography affords purified proghrelin-His <sub>6</sub> .....                         | 81  |
| 2.2.6 Purification approaches for C-ghrelin.....   | 83  |
| 2.2.6.1 Ni <sup>2+</sup> -Sephrose based purifications .....   | 83  |
| 2.2.6.2 C-ghrelin purification using established GThPH protocol .....  | 84  |
| 2.2.7 Analysis of purified proghrelin-His <sub>6</sub> .....   | 87  |
| 2.2.8 Circular dichroism analysis of proghrelin-His <sub>6</sub> .....   | 92  |
| 2.2.8.1 pH and buffer effects on proghrelin CD spectrum.....   | 92  |
| 2.2.8.2 Proghrelin secondary structure enhancement with detergents.....  | 95  |
| 2.2.8.3 Comparison of ghrelin and proghrelin isolates the secondary structure<br>contribution of C-ghrelin ..... | 98  |
| 2.2.9 Nuclear magnetic resonance studies of proghrelin-His <sub>6</sub> .....                                    | 100 |
| 2.3 Conclusions.....   | 104 |
| 2.4 Materials and Methods.....   | 107 |
| 2.5 References.....  | 123 |

### **Chapter 3: Processing behavior of proghrelin and C-ghrelin**

|   |     |
|---|-----|
| 3.1 Introduction.....   | 128 |
| 3.2 Results.....  | 131 |
| 3.2.1 Proghrelin cleavage behavior in bacterial lysate .....                              | 131 |
| 3.2.2 Proghrelin cleavage in purified samples .....                                       | 136 |
| 3.2.3 Mass spectrometry analysis of proghrelin cleavage .....                             | 140 |
| 3.2.4 Alanine mutagenesis studies towards inhibition of proghrelin cleavage.....          | 144 |
| 3.2.5 Development of a fluorescence-based system to investigate proghrelin cleavage ..... | 148 |
| 3.2.6 Cleavage behavior of GST-C-ghrelin fusion protein.....                              | 167 |
| 3.3 Conclusions.....  | 169 |
| 3.4 Materials and Methods.....  | 172 |
| 3.5 References.....   | 189 |

### **Chapter 4: Structure-activity relationship determination of ghrelin *O*-acyltransferase substrate binding utilizing unnatural amino acid incorporated peptides**

|   |     |
|---|-----|
| 4.1 Introduction.....   | 193 |
| 4.2. Results.....   | 197 |
| 4.2.1 A 2, 3-diaminopropanoic acid (Dap) substituted ghrelin peptide acts as an inefficient hGOAT substrate. .... | 197 |
| 4.2.2 A Dap-substituted peptide acts as a potent hGOAT inhibitor. ....  | 201 |
| 4.2.3 Length dependence of GOAT inhibition by Dap-containing peptides. ....                                       | 203 |
| 4.2.4 Sequence dependence of GOAT inhibition by Dap-containing peptides .....                                     | 205 |
| 4.2.5 D-amino acid substitution at S3 and F4 impedes ghrelin octanoylation by hGOAT. ....                         | 207 |
| 4.2.6 hGOAT tolerates backbone methylation within ghrelin peptides.....   | 211 |
| 4.2.7 Cell studies into Dap-peptide permeability.....   | 213 |
| 4.3 Conclusions.....  | 219 |

4.4 Materials and Methods..... 226

4.5 References..... 234

## **Chapter 5: Conclusions and Future Directions**

5.1 Introduction..... 243

5.2 Development of a method for purification and structural analysis of proghrelin..... 244

5.3 The cleavage of proghrelin ..... 245

5.4 Unnatural amino acid-containing peptides to study GOAT binding ..... 246

5.5 Summary and future directions..... 248

5.6 References..... 253

## **Appendices**

Appendix I: Reprint permission for reference 20, Chapter 1.....260

Appendix II: Reprint permission for reference 46, Chapter I, reference 6, Chapter 3.....261

Appendix III: Reprint permission for reference 123, Chapter 1 .....262

Appendix IV: Reprint permission for reference 21, Chapter 3.....264

Appendix V: Reprint permission for reference 57, Chapter 4.....266

Appendix VI: Reprint permission for reference 52, Chapter 4.....267

Appendix VII: Curriculum vitae.....268

## **List of figures**

|   |    |
|---|----|
| Figure 1.1. Different forms of protein acylation. ....  | 4  |
| Figure 1.2. The processing of proghrelin to ghrelin. ....   | 8  |
| Figure 1.3. Ghrelin interacts with multiple partners in circulation. ....   | 14 |
| Figure 1.4. The proposed membrane topology of GOAT. ....  | 19 |
| Figure 1.5. Peptide mimetic inhibitors of GOAT ....   | 23 |
| Figure 1.6. Small molecule GOAT inhibitors. ....  | 27 |
| Figure 2.1. Human and mouse proghrelin (1-94) protein sequence alignment. ....  | 63 |
| Figure 2.2. Expression analysis of recombinantly expressed GThPH. ....  | 66 |
| Figure 2.3. Western blot analysis of recombinantly expressed GThPH. ....  | 67 |
| Figure 2.4. GThCgH autoinduction expression analysis. ....  | 69 |
| Figure 2.5. IPTG induction of GThCgH expression. ....   | 71 |
| Figure 2.6. FPLC purification of GThPH from bacterial lysate. ....  | 74 |
| Figure 2.8. Ni <sup>2+</sup> -IMAC purification following TEV digestion of GThPH. ....  | 77 |
| Figure 2.9. GThPH purification using tandem GST and His <sub>6</sub> affinity purifications. ....   | 80 |
| Figure 2.10. Size exclusion chromatography purification of proghrelin-His <sub>6</sub> using a HiLoad16/60<br>Superdex 75pg size exclusion column. .... | 82 |
| Figure 2.11. GST-Sepharose FPLC purification of GThCgH. ....  | 85 |
| Figure 2.13. Anti-His Western Blot of purified proghrelin-His <sub>6</sub> . ....   | 88 |
| Figure 2.14. Verification of proghrelin-His <sub>6</sub> using silver staining of purified proghrelin. ....   | 89 |
| Figure 2.15. Verification of proghrelin-His <sub>6</sub> mass by ESI-MS (monoisotopic). ....  | 90 |
| Figure 2.17. pH dependence of proghrelin-His <sub>6</sub> CD spectrum in 25 mM phosphate buffer. ....   | 93 |
| Figure 2.18. Concentration dependence of proghrelin-His <sub>6</sub> CD spectrum in 25 mM phosphate<br>buffer. ....                                     | 94 |

|  |     |
|--|-----|
| Figure 2.19. Impact of SDS on the CD spectrum of proghrelin-His <sub>6</sub> .....   | 96  |
| Figure 2.20. Impact of detergents on the CD spectra of proghrelin-His <sub>6</sub> .....   | 97  |
| Figure 2.21. Comparison of CD spectra between ghrelin and proghrelin in aqueous environment.<br>.....                            | 99  |
| Figure 2.22. Natural abundance NMR of proghrelin-His <sub>6</sub> .....  | 101 |
| Figure 2.23. pH dependence of proghrelin-His <sub>6</sub> NMR spectrum. ....   | 102 |
| Figure 3.1. The proghrelin processing pathway.....   | 130 |
| Figure 3.2. Addition of a protease cocktail during bacterial lysis and purification does not inhibit<br>cleavage.....            | 132 |
| Figure 3.3. Bacterial pellet lysis in the presence of 6 M GuHCl. ....  | 135 |
| Figure 3.4. Increased proghrelin-His <sub>6</sub> cleavage observed following protein concentration.....                         | 137 |
| Figure 3.5. Addition of EDTA stabilized proghrelin-His <sub>6</sub> against cleavage. ....                                       | 139 |
| Figure 3.6. MALDI-TOF mass spectrometry analysis of time-dependent proghrelin-His <sub>6</sub><br>cleavage.....                  | 141 |
| Figure 3.7. Proghrelin-derived peptides observed by mass spectrometry analysis of a 144 hour<br>time course. ....                | 143 |
| Figure 3.8. Alanine mutations of GThPH lead to no change in protein cleavage. ....   | 145 |
| Figure 3.9. Hormone products from proghrelin processing.....   | 147 |
| Figure 3.10. Schematic of hedgehog cholesterolysis and the FRET construct used to study it,<br>developed by Brian Callahan. .... | 149 |
| Figure 3.11. Cloning schematic of obtaining CpgY from the GST-based GThPH. ....  | 150 |
| Figure 3.12. Expression of bacterially expressed pET23a CpgY .....   | 152 |
| Figure 3.13. Initial FRET readings of CpgY in bacterial lysate. ....   | 153 |
| Figure 3.14. Proghrelin cleavage using FRET signal. ....   | 155 |

|  |     |
|--|-----|
| Figure 3.15. Cleavage of purified CpgY.....  | 156 |
| Figure 3.16. Proghrelin N- and C-terminal truncation constructs. ....  | 158 |
| Figure 3.17. Fluorescent imaging of CpgY proghrelin truncation constructs. ....  | 160 |
| Figure 3.20. Fluorescent imaging of CpgY transfected in HEK 293FT cells.....   | 166 |
| Figure 3.21. Fragments from MALDI-TOF analysis of GThCgH fusion protein.....   | 168 |
| Figure 4.1. Structure of GSSLFC <sub>AcDan</sub> and GSDapFLC <sub>AcDan</sub> peptides. ....  | 196 |
| Figure 4.2. Analysis of acylation of a ghrelin mimetic peptide substrate incorporating a Dap<br>residue. ....  | 198 |
| Figure 4.3. Inhibition of hGOAT-catalyzed octanoylation of GSSFLC <sub>AcDan</sub> by GSSFL and<br>GSDapFL. ....   | 202 |
| Figure 4.4. Defining the N- and C-terminal length dependence of Dap-containing ghrelin<br>mimetic peptide GOAT inhibitors. ....  | 204 |
| Figure 4.5. Protection from chymotryptic digestion confirmed presence of D-phenylalanine<br>residue in GSSFLC <sub>AcDan</sub> substrate. ....   | 209 |
| Figure 4.6. The impact of D-amino acid substitution on peptide acylation by hGOAT.....   | 210 |
| Figure 4.7 Cell viability of Dap-incorporated peptides in PC3 or HEK 293FT cells.....  | 215 |
| Figure 4.8. Schematic of fluorescamine labeling.....   | 217 |
| Figure 4.9. Fluorescamine labeling of SarSDapN-MeF-treated HEK 293FT cells.....  | 218 |
| Figure 4.10. Functional groups composing the pharmacophore for GOAT substrate-mimetic<br>inhibitors, as defined by Dap-containing<br>peptide inhibitor structure-activity analysis. .... | 222 |
| Figure 4.11. Conservation analysis indicates the F4 position is conserved.....   | 223 |

## **List of Tables**

|  |     |
|--|-----|
| Table 3.1. Fragmentation analysis of proghrelin-His <sub>6</sub> cleavage. ....                                      | 142 |
| Table 4.1. Impact on mutations within GSDapFL and GSDapF peptides on inhibitor potency<br>against hGOAT. ....        | 206 |
| Table 4.2. Impact of peptide backbone methylation on Dap peptide inhibitor potency against<br>hGOAT. ....            | 212 |
| Table 4.3 Analytical data of Dap-containing peptides.....  | 227 |
| Table 4.4. MALDI-TOF mass spectrometry (m/z) characterization of acrylodan labeled hGOAT<br>peptide substrates. .... | 229 |

## **List of abbreviations**

|                  |  |
|------------------|--|
| 3XSB             | 3X sample buffer   |
| ACAT1            | Acyl-CoA:cholesterol acyltransferase                           |
| AcDan            | Acrylodan  |
| Amp              | Ampicillin   |
| APT1             | Acyl-protein thioesterase 1                                    |
| BChE             | Butyrylcholinesterase  |
| BPER             | Bacterial protein extraction reagent                           |
| CD               | Circular dichroism   |
| CDDO             | 2-cyano-3,12-dioxooleana-1,9(11)-dien-28-oic acid              |
| CFP              | Cyan fluorescent protein                                       |
| CHAPS            | (3-((3-cholamidopropyl) dimethylammonio)-1-propanesulfonate)   |
| Chl              | Chloramphenicol  |
| CoA              | Coenzyme A   |
| CMV promoter     | Cytomegalovirus promoter                                       |
| CpgY             | Cyan fluorescent protein-proghrelin-Yellow fluorescent protein |
| Dap              | 2,3-diaminopropanoic acid                                      |
| DGAT1            | Diglyceride acyltransferase                                    |
| DM               | n-decyl- $\beta$ -D-maltoside                                  |
| DMEM             | Dulbecco's Modified Eagle's Medium                             |
| DMSO             | Dimethyl sulfoxide   |
| DNA              | Deoxyribonucleic acid  |
| dNTP             | Deoxynucleotide triphosphate                                   |
| <i>E. coli</i>   | Escherichia coli   |
| EDTA             | Ethylenediaminetetraacetic acid                                |
| ELISA            | Enzyme-linked immunosorbent assay                              |
| ER               | Endoplasmic reticulum  |
| FPLC             | Fast protein liquid chromatography                             |
| FRET             | Forester resonance energy transfer                             |
| GH               | Growth hormone   |
| GHS-R1a          | Growth hormone secretagogue receptor type 1a                   |
| GOAT             | Ghrelin <i>O</i> -acyltransferase                              |
| GPI              | Glycosylphosphatidylinositol                                   |
| GPCR             | G-protein coupled receptor                                     |
| GuHCl            | Guanidine hydrochloride  |
| GST              | Glutathione <i>S</i> -transferase                              |
| GThCgH           | GST-TEV-human-C-ghrelin-His <sub>6</sub>                       |
| GThPH            | GST-TEV-human-Proghrelin-His <sub>6</sub>                      |
| HEPES            | 4-(2-hydroxyethyl)-1-piperazineethanesulfonic acid             |
| HEK              | Human embryonic kidney   |
| HDL              | High density lipoprotein                                       |
| hGOAT            | Human ghrelin <i>O</i> -acyltransferase                        |
| mGOAT            | Mouse ghrelin <i>O</i> -acyltransferase                        |
| Hhat             | Hedgehog acyltransferase                                       |
| His <sub>6</sub> | Histidine 6 tag  |
| HIV              | Human immunodeficiency virus                                   |
| HPLC             | High performance liquid chromatography                         |
| HRP              | Horseradish peroxidase   |
| IC <sub>50</sub> | Inhibitor concentration at which activity is reduced by half   |

|           |  |
|-----------|--|
| IgG       | Immunoglobulin G   |
| IMAC      | Immobilized metal affinity chromatography                  |
| IPTG      | Isopropyl $\beta$ -D-1-thiogalactopyranoside               |
| LB        | Lysogeny broth   |
| LDL       | Low density lipoprotein                                    |
| MAFP      | Methyl arachidonyl fluorophosphate                         |
| MALDI-TOF | Matrix-assisted laser desorption/ionization-time of flight |
| MBOAT     | Membrane-bound <i>O</i> -acyltransferase                   |
| MBP       | Maltose binding protein                                    |
| MD        | Molecular dynamics   |
| mRNA      | Messenger ribonucleic acid                                 |
| NaCl      | Sodium chloride  |
| NOESY     | Nuclear Overhauser Spectroscopy                            |
| NEM       | N-Ethylmaleimide   |
| NMR       | Nuclear magnetic resonance                                 |
| NPY       | Neuropeptide Y   |
| OBD       | Octa- $\beta$ -D -glucopyranoside                          |
| PAF       | Platelet activating factor                                 |
| PAM       | Peptidyl glycine $\alpha$ -amidating monooxygenase         |
| PBS       | Phosphate buffered saline                                  |
| PC        | Pancreatic cancer  |
| PCR       | Polymerase chain reaction                                  |
| PMSF      | Phenylmethylsulfonyl fluoride                              |
| PON1      | Serum paraoxonase/arylesterase 1                           |
| PORCN     | Porcupine  |
| TEV       | Tobacco etch virus   |
| Tris      | 2-Amino-2-hydroxymethyl-propane-1,3-diol                   |
| RIPA      | Radioimmunoprecipitation assay buffer                      |
| RNA       | Ribonucleic acid   |
| RP-HPLC   | Reverse phase high performance liquid chromatography       |
| RT-PCR    | Reverse transcriptase polymerase chain reaction            |
| SDS       | Sodium dodecyl sulfate                                     |
| SDS-PAGE  | SDS-polyacrylamide gel electrophoresis                     |
| SUMO      | Small ubiquitin-like modifier                              |
| Tat       | Transactivator of transcription                            |
| TFA       | Trifluoroacetic acid                                       |
| TOCSY     | Total Correlated Spectroscopy                              |
| VLDL      | Very low density lipoprotein                               |
| YFP       | Yellow fluorescent protein                                 |
| WT        | Wild type  |

## Chapter 1: Introduction

Portions of this chapter have been previously published and reprinted with permission from the publisher, reference 46, Cleverdon, E. R.; McGovern-Gooch, K. R.; Hougland, J. L., The octanoylated energy regulating hormone ghrelin: An expanded view of ghrelin's biological interactions and avenues for controlling ghrelin signaling. *Mol Membr Biol* **2016**, *33* (6-8), 111-124. Copyright © 2016 Taylor & Francis.

## 1.1 Post-translational modifications

After a gene is transcribed into RNA and translated into a protein by the ribosome, this polypeptide can be further modified using either co- or post-translational modification(s) through one of two mechanisms: the first is enzyme-catalyzed covalent attachment of chemical groups; and the second being through proteolytic or autocatalytic covalent cleavage of peptide backbones.<sup>1</sup> Chemical modifications of proteins are wide-spread with more than 200 distinct types of chemical group attachment having been characterized.<sup>1</sup> Common forms of post-translational modifications that occur on a variety of protein substrates that include phosphorylation,<sup>2</sup> acylation (acetylation,<sup>3</sup> N-myristoylation,<sup>4</sup> N/S-palmitoylation,<sup>5-8</sup> ubiquitylation,<sup>9</sup> O-acylation<sup>10</sup>) (Figure 1.1), alkylation (S-Prenylation<sup>11-13</sup>), glycosylation,<sup>14-16</sup> and oxidation,<sup>17-18</sup> all of which are catalyzed by enzymes.<sup>1, 12</sup> These small chemical modifications diversify the proteome and can cause changes in structure, localization, protein-protein interactions, and recognition motifs in comparison to their unmodified forms.<sup>1, 12</sup>

Lipidation is a specific class of modification which includes prenylation, palmitoylation and O-acylation among others (Figure 1.1).<sup>19-20</sup> Prenylation is the attachment of 15 or 20 carbon long isoprenoid group to a C-terminal cysteine residue by protein farnesyltransferase and protein geranylgeranyltransferase types I and II, respectively, which serve as the first step in a modification pathway often leading to protein membrane localization.<sup>11, 13</sup> This attachment establishes a thioether bond which is very stable and is not likely to hydrolyze in the cell.<sup>11, 13</sup> Palmitoylation most commonly involves the attachment of a 16-carbon chain to a cysteine, threonine or serine residue.<sup>7-8, 21</sup> This attachment commonly occurs through formation of either an amide bond through N-terminal attachment of the carbon chain or through formation of a thioester linkage, although an ester linkage is possible with serine or threonine palmitoylation.<sup>7-8,</sup>

<sup>21</sup> This modification has been demonstrated in a number of proteins and increases trafficking to intracellular membranes.<sup>7, 12</sup> O-acylation occurs when a serine or threonine residue is modified with the attachment of a lipid moiety.<sup>10, 22</sup> This type of acylation has been associated with intracellular trafficking, receptor binding and activation in both Wnt proteins and also ghrelin.<sup>10, 22-26</sup> This acylation forms an ester linkage and is more susceptible to hydrolysis than the other forms of lipidation.<sup>7</sup>

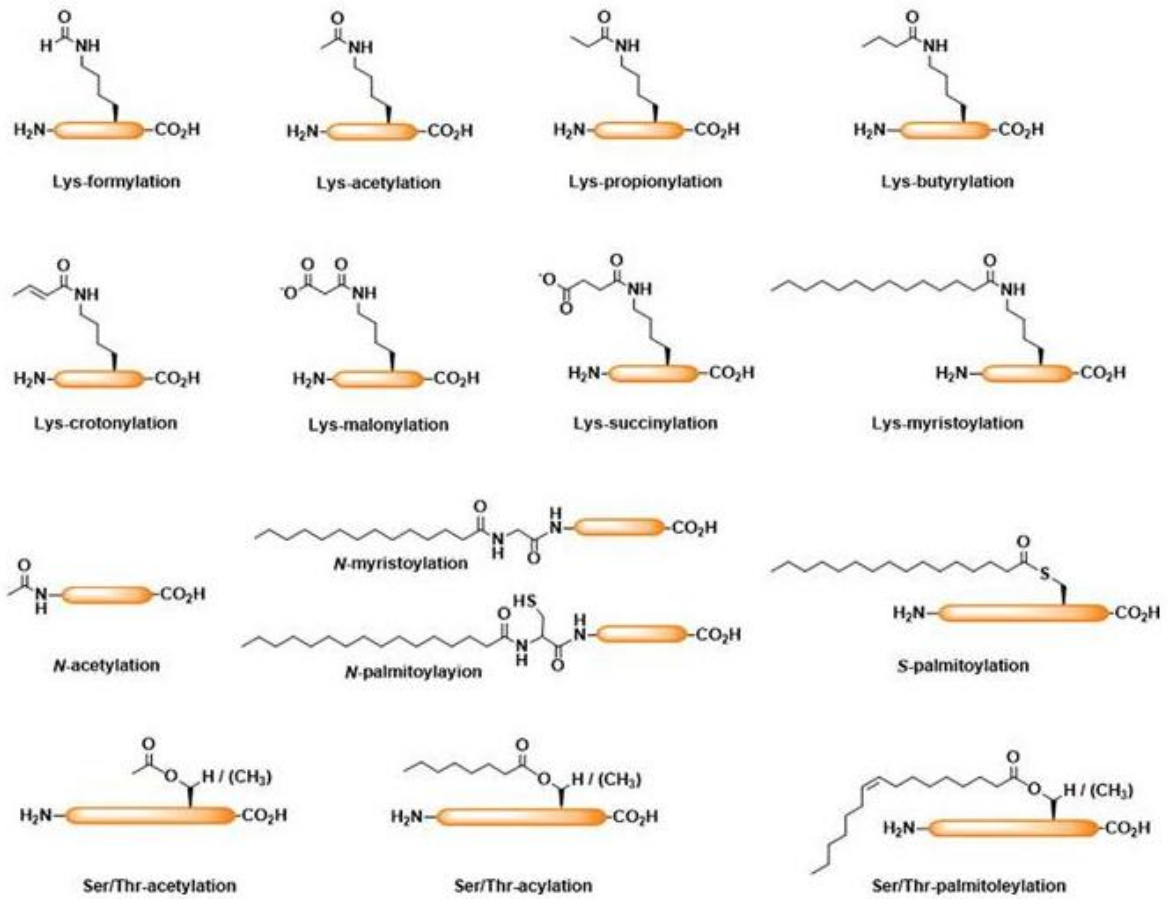


**Figure 1.1. Different forms of protein acylation.** Figure is reproduced with permission from Reference 20 (Appendix I). © 2015 Portland Printed Press.

## 1.2 Ghrelin

### 1.2.1 Discovery

The peptide hormone ghrelin is one of several biological signaling molecules that require a lipidation modification for receptor recognition and biological function. Ghrelin was initially discovered in 1999 as a result of the search for the endogenous ligand for an orphan receptor, the growth hormone secretagogue receptor 1a (GHS-R1a).<sup>10, 27-28</sup> Through the use of a synthetic ghrelin compared to ghrelin extracted from the stomachs of rats, there was a difference in retention time using reverse phase HPLC (high performance liquid chromatography) which is indicative of the presence of a large hydrophobic group.<sup>10</sup> Further analysis using mass spectrometry indicated that this was an 8 carbon long (n-octanoyl) chain which was attached at the N-terminal S3 residue.<sup>10</sup> This discovery presented the first instance of post-translational modification with an n-octanoyl group, and O-acylation of a serine residue is also exceedingly rare among characterized examples of protein modifications.<sup>12</sup>

Ghrelin's post-translational modification, octanoylation, has been demonstrated to be absolutely essential for GHS-R1a receptor recognition and activation.<sup>26</sup> Desacyl ghrelin is unable to bind to and activate the GHS-R1a receptor even though both forms are freely circulating throughout the bloodstream and present in the same tissues.<sup>26</sup> While there is evidence suggesting that the deacylated form of ghrelin is playing a physiological role, the exact nature of this signaling by desacyl ghrelin remains unclear.<sup>29</sup> There is recent evidence suggesting that ghrelin can be reacylated extracellularly, which could provide another avenue of investigation into the biological role of desacyl ghrelin and the regulation between the two forms.<sup>30-31</sup>

### 1.2.2 Tissue distribution

Ghrelin was originally found to be expressed by endocrine X/A cells in mice and rats (P/D cells in humans) in the gastric mucosa of the stomach and small intestine,<sup>10, 32-35</sup> with subsequent investigations demonstrating that ghrelin and its receptor (GHS-R1a) are expressed in various tissues such as pancreatic alpha cells, the pituitary gland and the hypothalamus.<sup>10, 32, 36-37</sup> There is indication based on RT-PCR (reverse transcription polymerase chain reaction) studies of mRNA for ghrelin and its receptor in almost all tissue types in the body; however, this does not necessarily mean there is protein expression found in all of the identified tissue types.<sup>38-</sup><sup>39</sup> This RT-PCR mRNA evidence is supported by a plethora of biochemical techniques including: *in situ* hybridization, immunohistochemistry monitored by optical microscopy, and immunostaining coupled with electron microscopy, which found that ghrelin and its receptor are present in a range of tissues through the body, including the kidney, lung, gall bladder, prostate and liver.<sup>10, 27, 32, 36, 40-41</sup> This expression pattern indicates that ghrelin expression is wide-spread throughout the body and could explain the multiple physiological effects attributed to ghrelin.

### 1.2.3 Ghrelin processing

Ghrelin must undergo a series of processing steps following translation to generate the mature peptide hormone found in circulation (Figure 1.2).<sup>42-46</sup> Proghrelin is translated by the ribosome as a 117 amino acid protein, preproghrelin, which contains a signal sequence which directs the protein to the endoplasmic reticulum where the signal sequence is cleaved by signal peptidase.<sup>44, 47</sup> The resulting prohormone, proghrelin, is post-translationally modified by the attachment of an n-octanoyl moiety in a reaction catalyzed by the integral membrane enzyme ghrelin *O*-acyltransferase (GOAT).<sup>44, 48-49</sup> After modification by GOAT, the acylated proghrelin

is trafficked to the Golgi apparatus and packaged into secretory vesicles where prohormone convertase 1/3 or furin cleaves amino acids 29-94 (C-ghrelin) from amino acids 1-28 (ghrelin).<sup>44</sup>

<sup>47</sup> Subsequent cleavage of the C-terminal portion of proghrelin is proposed to generate the hormone obestatin (amino acids 53-76). The exact mechanism in which obestatin is processed from C-ghrelin is unknown but is hypothesized to involve processing by carboxypeptidase E and peptidyl glycine  $\alpha$ -amidating monooxygenase (PAM) leading to C-terminal amidation.<sup>50</sup>

Following this array of modifications, ghrelin and obestatin are released into the bloodstream in order to fulfill their biological signaling roles.

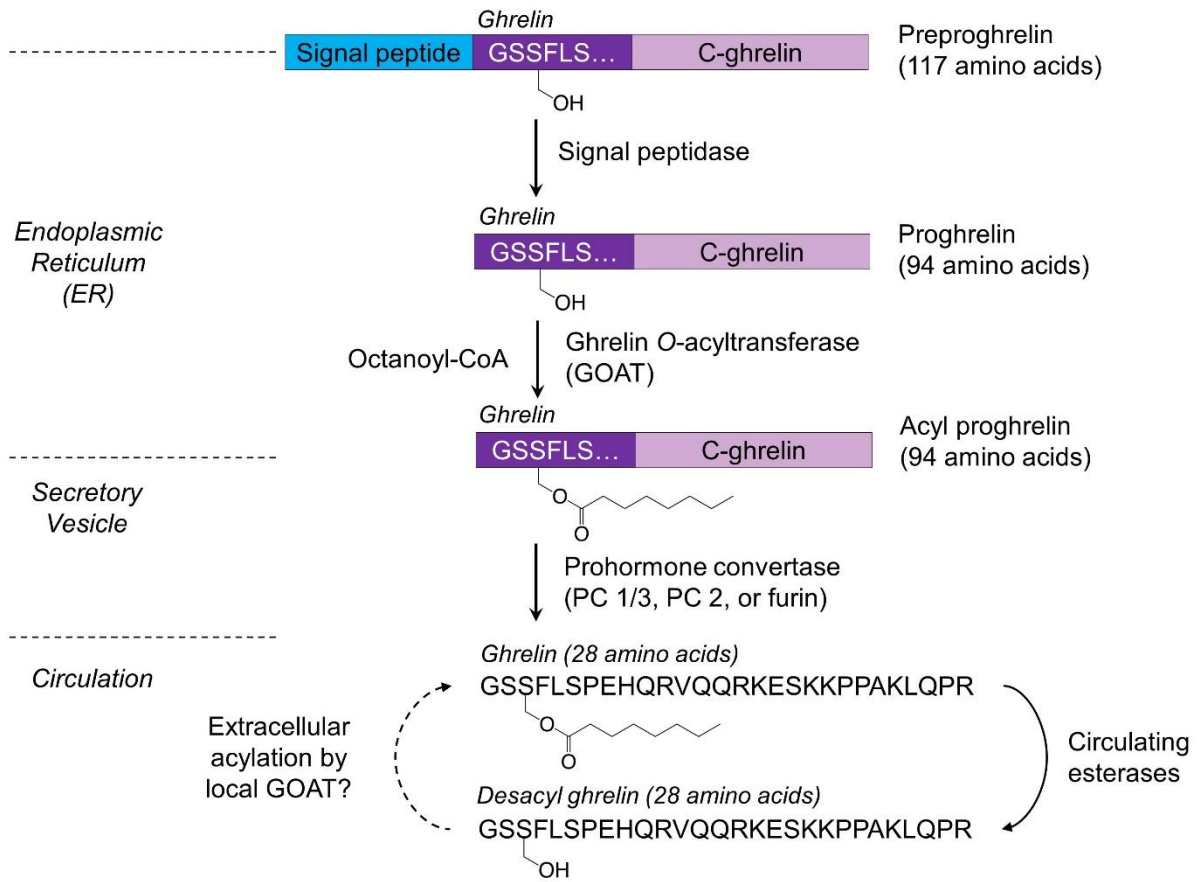


**Figure 1.2. The processing of preproghrelin to ghrelin.** Figure is reproduced with permission from Reference 46 (Appendix II). © 2016 Taylor and Francis.

#### 1.2.4 Binding partners for ghrelin within the body

After their release into the bloodstream, there are a variety of binding partners that desacyl and acylated ghrelin can interact with including lipoproteins, esterases, antibodies and the GHS-R1a receptor (Figure 1.3). There are three major classes of lipoproteins in blood serum, VLDL (very low density lipoproteins, responsible for endogenous fat transport), HDL (high density lipoproteins, responsible for reverse cholesterol transport), and LDL (low density lipoproteins, major carrier of cholesterol in the blood) which are used to traffic proteins throughout the bloodstream.<sup>51</sup> Cholesterol and triacylglycerols are transported in lipoprotein particles which consist of hydrophobic lipids surrounded by outer shells of more polar lipids and proteins (apoproteins), with these apoproteins synthesized in the liver and the intestines.<sup>51</sup> Recent studies support that lipoproteins in the bloodstream act as ghrelin (acyl and desacyl) transporters.<sup>52</sup> The level of cholesterol lipoproteins increase with the increased production of ghrelin, demonstrating a potential relationship between availability of lipoproteins and ghrelin in the body.<sup>52</sup> Ghrelin and desacyl ghrelin show distinct binding preferences for different lipoproteins in circulation, with ghrelin binding VLDL, LDL and HDL equally, while desacyl ghrelin primarily associates with HDL lipoproteins.<sup>53-54</sup> Since HDL particles contain esterases involved in reverse cholesterol transport,<sup>53</sup> the preference for desacyl ghrelin to bind HDL is interesting since the HDL-associated esterase PON1 increases the deacylation and degradation of acylated ghrelin.<sup>55</sup> This data suggests that HDLs can store ghrelin and effectively immobilize it within the bloodstream.<sup>52</sup> The same can be said of VLDL and LDL with acylated ghrelin, which protect the octanoyl group on acylated ghrelin from hydrolysis and serve to shield ghrelin from degradation in circulation.<sup>52-54</sup> Further investigation into the interactions between ghrelin and

lipoproteins is needed to better understand its trafficking in the bloodstream leading to GHS-R1a activation and the ability of lipoproteins to affect acylated ghrelin's half-life in the blood serum.

Due to its hydrolytic susceptibility, the ester-linked acyl chain attached to ghrelin has a limited lifetime in circulation. This has been demonstrated in the collection of blood serum from both rodents and humans, with complete hydrolysis of the acylated ghrelin in 240 minutes in one study and another yielding an estimated half-life of 10 minutes, although these times have been shown to be variable between serum samples.<sup>56</sup> Ester hydrolysis (cleavage of the octanoyl moiety) initially was demonstrated by adding blood serum to a synthetic acylated ghrelin (1-28) that resulted in complete conversion to its desacyl form.<sup>56</sup> This esterase activity has complicated studies of ghrelin concentration in blood serum, with ester hydrolysis rendering accurate sample analysis problematic. Sample treatment with phenylmethylsulfonyl fluoride (PMSF) or other common protease inhibitors was shown to slow ghrelin hydrolysis in blood samples;<sup>56-57</sup> and addition of alkyl fluorophosphonate esterase inhibitors provide complete protection of ghrelin from esterase hydrolysis.<sup>58</sup>

There has been discussion in the literature about which esterase is the “ghrelin” esterase, with a range of esterases that have been demonstrated to have ghrelin hydrolytic activity including: platelet activating factor (PAF), paraoxanase (PON), carboxypeptidase, butyrylcholinesterase, carboxylesterases, APT1, and alpha 2-macroglobulin.<sup>53, 56, 59-61</sup> Among these enzymes, the strongest body of evidence supports butyrylcholinesterase (abbreviated BChE or BuChE) as the most likely esterase responsible for a majority of the ghrelin hydrolysis in circulation.<sup>62-65</sup> Recombinantly expressed BChE has been shown to hydrolyze ghrelin when it was added externally to acylated ghrelin.<sup>65-66</sup> There are also implications in BChE in ghrelin's

biological role, with BChE deficient mice that were fed a high fat diet showing weight gain and were overall heavier than wild-type mice.<sup>63-65, 67</sup> The BChE deficient mice also demonstrated reduced insulin sensitivity compared to their wild-type counterparts (BChE present), both of these observed results could indicate that this esterase has implications in weight control and glucose metabolism via ghrelin hydrolysis.<sup>63-65, 67</sup> There are also indications that BChE has other implications in ghrelin's biological role, including its effects on aggressive behavior in mice.<sup>67</sup> In resident/intruder testing (a provocation test) there was an increase in behavior consistent with stress and increased aggression in mice which had knockout BChE resulting in higher circulating acylated ghrelin levels compared to their wild-type counterparts.<sup>64</sup> In contrast, mice in which there were higher BChE levels present and increased levels of circulating desacyl ghrelin displayed lower aggression levels (compared to wild-type mice).<sup>64</sup> The above studies support BChE as a ghrelin esterase in circulation, however, in BChE deficient human populations there have been no adverse side-effects on their health as long as they do not eat a high-fat diet.<sup>68-69</sup> This data suggests that there may be a compensation mechanism for ghrelin hydrolysis or there is a yet unidentified ghrelin esterase that is responsible for a major portion of ghrelin to desacyl ghrelin processing.<sup>68-69</sup>

In addition to lipoprotein complexes and esterases (Figure 1.3), ghrelin has also been found to interact with autoantibodies in circulation. Autoantibodies are antibodies that recognize self-antigens that are produced in germ-like B-cells as a part of native immunity.<sup>70</sup> These antigens may be found in all cell types or be highly specific for a specific cell types or organs.<sup>70</sup> Ghrelin-reactive autoantibodies were initially discovered in blood serum in both humans and rodents.<sup>71-72</sup> There is also evidence of desacyl ghrelin-reactive autoantibodies (Immunoglobulin G (IgG)) in the same species.<sup>71-73</sup> Ghrelin-reactive IgG was the first antibody detected revealing

that it may have a functional role in ghrelin signaling by protecting it from degradation in plasma.<sup>71</sup> In the same study, it was shown that depletion of IgG from the plasma resulted in loss of acylated ghrelin while titration back into plasma resulted in recovery, indicating that ghrelin-reactive autoantibodies also serve as a chaperone of ghrelin in a similar fashion to lipoproteins that protect ghrelin from hydrolysis.<sup>71</sup> There has been investigation into the relative affinity of IgG in different populations, with IgG from obese individuals exhibiting higher affinity for the ghrelin-IgG complexes.<sup>71</sup> This stronger interaction between ghrelin and its autoantibody extends the lifetime of ghrelin in circulation leading to higher acylated ghrelin concentrations and enhanced trafficking.<sup>71-72</sup> This observation is consistent with the finding that high levels of ghrelin-reactive antibodies lead to increased appetite and an elevated ability for ghrelin to signal hunger.<sup>71-72, 74</sup> In contrast, patients with anorexia nervosa were shown to have lower ghrelin-IgG plasma levels and lower affinity for ghrelin-IgG complex formation which leads to the opposite effect, less stable ghrelin and inefficient ghrelin signaling.<sup>73</sup> The ghrelin-IgG complexes provide another area for exploration into ghrelin trafficking throughout circulation and its ability to serve its biological functions.

The biological activity of ghrelin stems from its ability to bind and activate its GHS-R1a receptor.<sup>10, 75</sup> Initial investigations of this receptor were through expression and cloning analysis.<sup>27</sup> There was also investigation into ligand binding to the GHS-R1a to identify compounds or peptide sequences that would elevate growth hormone release from the anterior pituitary gland for disorders involving a lack of growth hormone release.<sup>27, 76-77</sup> GHS-R1a was confirmed as a GPCR (G-protein coupled receptor) through homology modeling as well as antibody-binding studies.<sup>27, 78</sup> The activation of signaling through GHS-R1a is indicated by increased intracellular calcium release, increased protein kinase C (PKC) activity, and inhibition

of GHS-R1a activity by guanosine triphosphate analogues.<sup>27</sup> The GHS-R1a receptor requires the first five amino acids of ghrelin for recognition and activation with equal efficiency to full length ghrelin (amino acids 1-28), however the receptor will weakly bind the first four amino acids of ghrelin with similar receptor activation to full length ghrelin (amino acids 1-28).<sup>26</sup> Receptor activation requires a lipid moiety at the S3 position for complete receptor activation which can be achieved using ligands bearing medium to long acyl chains (up to 16 carbons), however, there is a decreased affinity with acyl chains with less than 7 carbons.<sup>26</sup> After recognition and activation of the receptor the signaling transduction pathway indicative of GPCRs is initiated and PKA (protein kinase A)/cAMP (cyclic adenosine monophosphate) pathway is the proposed mechanism for GH secretion.<sup>79</sup> A majority of the studies investigating the effects of ghrelin on receptor activation have been based in pituitary cells; however, the result of activation can differ based upon the cell type. Hepatoma, hypothalamus, and colonic epithelial cells all induce varying cascades which are caused by GHS-R1a activation.<sup>80-82</sup> The different roles and receptor activation behavior is one of the proposed sources for the diversity in ghrelin's biological role.

**Bloodstream**

---

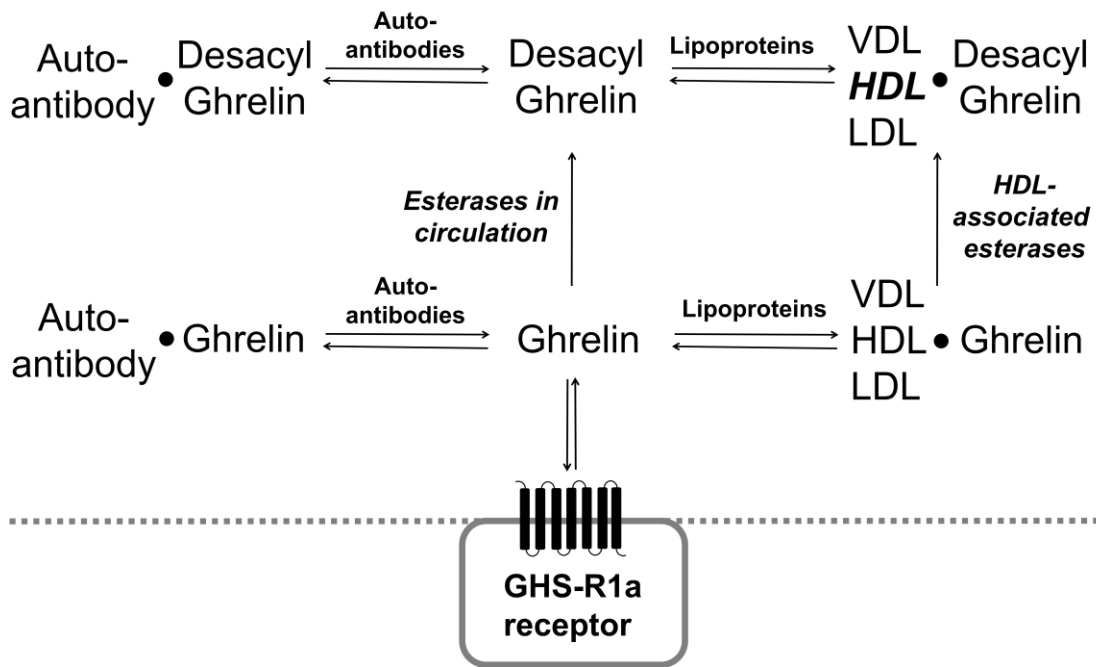


**Figure 1.3. Ghrelin interacts with multiple partners in circulation.** Ghrelin and desacyl ghrelin can interact with multiple binding partners in the bloodstream (equilibrium arrows), with esterases converting ghrelin to desacyl ghrelin by serine ester hydrolysis (single arrows). In interaction with lipoproteins (VLDL, HDL, and LDL), desacyl ghrelin shows a preference for binding to HDL (bold). Figure is reproduced with permission from Reference 46 (Appendix II). © 2016 Taylor and Francis.

### 1.2.5 Physiological effects

Since its discovery in 1999, ghrelin has been implicated in a variety of physiological processes and critical biological signaling pathways.<sup>10</sup> The initial role identified for ghrelin was to signal the release of growth hormone, then subsequently ghrelin was shown to control appetite signaling and the hunger response.<sup>10</sup> This diversified role increased the interest into ghrelin and ghrelin signaling, since the ability to control hunger is advantageous and critical for obesity therapeutics. Through additional investigations ghrelin has been implicated in food intake, reward-seeking behavior, body weight (adiposity), glucose homeostasis and insulin production, energy balance, and gastrointestinal mobility.<sup>83-95</sup> Ghrelin's effects are far-reaching with implications in learning and memory, psychological stress, mood and anxiety, depression, thymopoiesis (the production of thymocytes, which later become T cells), sleep/wake rhythm, and aging.<sup>96-111</sup>

Circulating ghrelin levels also play a role in a number of pathological conditions. It has been established that ghrelin levels have positive correlation with cachexia associated with chronic obstructive lung disease (COPD) or chronic heart failure (CHF).<sup>112-114</sup> There is a negative correlation between ghrelin levels with insulin resistance which has implications in the formation and progression of diabetes.<sup>112-114</sup> Ghrelin serum levels are low in obese patients and binge-eaters but very high in patients with Prader-Willi syndrome associated with hyperphagia, Hashimoto's Thyroiditis, or patients with anorexia nervosa and bulimia nervosa.<sup>40, 113-118</sup> Body weight alone is not an indication of circulating ghrelin levels, since ghrelin levels are not elevated in obese patients with Bardet-Biedl syndrome, Cushing's disease, or HIV-Lipodystrophy.<sup>118-122</sup> In non-obesity related illnesses such as Parkinson's disease, ghrelin has

been demonstrated to play a neuroprotective role.<sup>104, 106</sup> The ability to better understand and to control ghrelin signaling could potentially treat the diseases mentioned above, as well as, other ghrelin-linked disorders.

## **1.3 GOAT**

### **1.3.1 Discovery**

After the discovery of ghrelin in 1999,<sup>10</sup> there was a subsequent search for the acyl transferase that catalyzed the attachment of the 8 carbon chain lipid moiety to ghrelin. This enzyme, ghrelin *O*-acyltransferase (GOAT), was identified by two independent research groups in 2008.<sup>48-49</sup> The search for GOAT focused on a family of *O*-acyltransferases given the designation MBOAT (membrane-bound *O*-acyltransferase).<sup>24</sup> Proghrelin contains a signal sequence which traffics it to the endoplasmic reticulum, it was thought a membrane-bound enzyme such as a member of the MBOAT family (since members of this family are located in the membrane of the ER ) would be good a candidate for the ghrelin acyltransferase.<sup>44</sup> There are sixteen members of the MBOAT family of enzymes, three of which (including GOAT) act upon protein substrates with the other family members acting upon small molecules.<sup>24, 48-49</sup> Two examples of MBOATs in the family that modify non-protein substrates include ACATs which attach fatty acids to cholesterol and DGAT1 which acylates diacylglycerol.<sup>24</sup> Genome database searches using criteria such as similarity to known MBOAT members sequences, presence of a human homolog, and a known primary sequence of the gene of interest were necessary metrics for the uncharacterized pool of candidates to investigate.<sup>48-49</sup> Using mRNA silencing there was a candidate, MBOAT4, which when it was silenced lead to a lack of ghrelin acylation.<sup>48</sup> In side-by-side studies knockout comparisons in TT (thyroid carcinoma)<sup>48</sup> and INS-1 (pancreatic

insulin-secreting) cells<sup>49</sup> between MBOAT4 and other MBOAT family members demonstrated that this enzyme was required to acylate ghrelin.<sup>48-49</sup> After exogenous expression in endocrine cell lines GOAT was able to acylate proghrelin which demonstrates the ubiquity of GOAT/ghrelin in different tissue types.<sup>49</sup> There have also been two recent studies which indicate that there is ghrelin reacylation extracellularly in both the bone marrow and in the hippocampus which would indicate that GOAT is not necessarily located primarily in the ER membrane but also located in the plasma membrane.<sup>30-31</sup> These findings also possibly indicate that there is a cyclical nature to ghrelin signaling with deacylation and then selective reacylation of ghrelin.<sup>30-31</sup>

### **1.3.2 GOAT conservation across species**

GOAT is a topologically complex membrane bound protein containing the conserved residues asparagine-307 (N307) and histidine-338 (H338) which have been shown to be required for enzyme function.<sup>48-49, 123</sup> MBOAT family members that modify protein substrates include GOAT, PORCN and Hhat.<sup>24</sup> GOAT acylates using a medium chain fatty acid (8-carbon chain) instead of a long chain like PORCN and Hhat (16-carbon chain).<sup>37, 123-126</sup> The other differentiating factor between these enzymes is PORCN and Hhat acylate a cysteine or threonine residue (PORCN has been shown to acylate at a serine residue, though preferentially a cysteine) when GOAT is demonstrated to acylate a serine residue (although GOAT has been observed to acylate a threonine residue in bullfrog ghrelin).<sup>37, 123-128</sup> These protein-modifying MBOATs are ER integral membrane proteins which modify substrates within the ER lumen; however, the precise mechanism in which the acyl donor enters the ER lumen is still unclear.<sup>24, 123</sup> Purification and solubilization of these membrane-bound enzymes in an active form has been a

challenge, with success reported only for Hhat and ACAT1 (known as SOAT1).<sup>124, 126, 129-130</sup>

While there are no structural models available for any MBOAT family members, five MBOAT family members that have been topologically examined including human ACAT1 (Acyl-CoA:cholesterol acyltransferase, also known as Sterol *O*-acyltransferase, SOAT), ACAT2, Ghrelin *O*-acyltransferase (GOAT), Hedgehog acyltransferase (Hhat) and yeast Gup1.<sup>37, 123-124,</sup>

<sup>131-132</sup> To determine the topology of GOAT, Taylor and coworkers applied topological mapping programs (MemBrain and MEMSAT-SVM), and cross-species conservation analysis, modeling, and hydropathy mapping to separate the primary sequence into sections (helical, nonhelical, loop domains) (Figure 1.4).<sup>123</sup> Through the use of selective permeabilization and epitope tags, it was determined that GOAT contains 11 transmembrane domains and one re-entrant loop.<sup>123</sup> The topology and mutational studies found that N307 and H338 are required for activity and located in the C-terminus of the enzyme which is consistent with other MBOAT family members.<sup>123</sup>

Other than the described methodology, no other published data is available on the secondary (tertiary/quaternary) structure of this enzyme or how catalysis occurs to octanoylate ghrelin. The topology mapping is a good step in the right direction but does not provide enough information to model or locate the substrate binding site(s) or the active site.

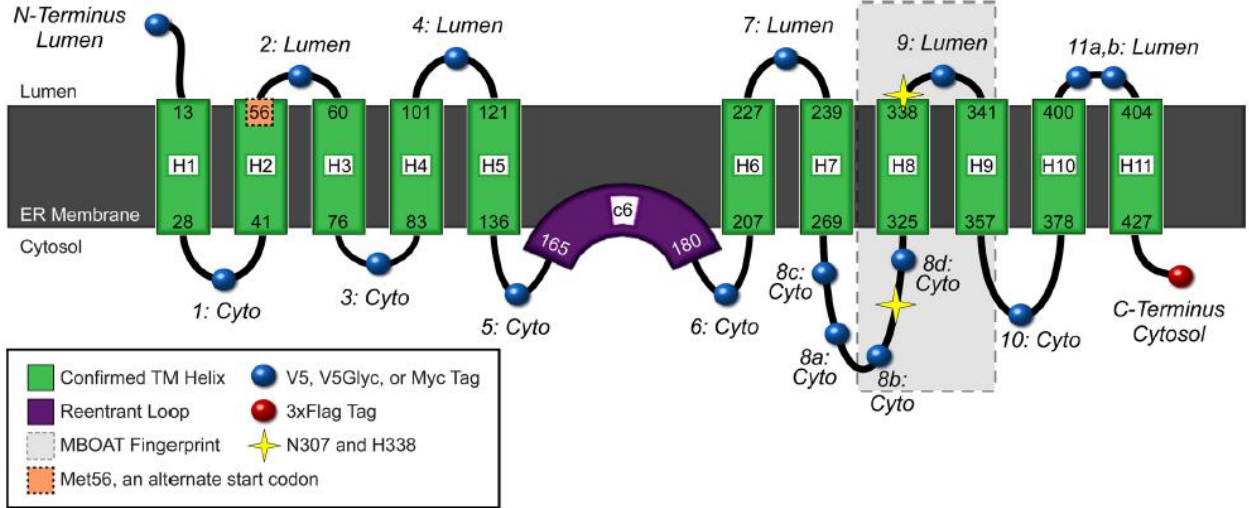


**Figure 1.4. The proposed membrane topology of GOAT.** This is the current topological mapping of the structure of GOAT as published by Taylor and coworkers of the enzyme in the endoplasmic reticulum membrane. GOAT contains two conserved residues N307 and H338 (starred) eleven transmembrane helices as well as one re-entrant loop. Figure reproduced with permission from Reference 123 (Appendix III). © 2013 American Society for Biochemistry and Molecular Biology.

## 1.4 GOAT inhibitors

Ghrelin has implications in a variety of disease states such as diabetes, Prader-Willi Syndrome and obesity, so the ability to control or modulate ghrelin signaling is an opportunity to treat a variety of ghrelin-linked diseases.<sup>117, 133-135</sup> Acylation of ghrelin by GOAT is a necessary step for GHS-R1a receptor activation, which makes this processing step an attractive target for inhibition.<sup>26</sup> There is also the possibility that there will be reduced off-target effects when targeting ghrelin acylation since GOAT only has one predicted substrate, ghrelin.<sup>136</sup> GOAT is a high-value target for controlling or modulating ghrelin signaling; however, there has been difficulty in inhibitor design since there has been no identification of the catalytic machinery or the residues that comprise the active site of GOAT.

### 1.4.1 Ghrelin product mimetics as GOAT inhibitors

The first reported class of GOAT inhibitors was peptide-based product mimetics of acylated ghrelin. There are four known inhibitors that contain a portion of ghrelin's N-terminal sequence as well as an acyl chain derivative: [Dap<sup>3</sup>]octanoyl-ghrelin(1–5)-NH<sub>2</sub>, [Dap<sup>3</sup>]octanoyl-ghrelin(1–28)-NH<sub>2</sub>, phenylalkyl triazole-linked acylated ghrelin and Go-CoA-Tat (Figure 1.5).<sup>137-139</sup> Of these inhibitors, Go-CoA-Tat has been shown to disrupt ghrelin signaling.<sup>137</sup>

Initially, a pentapeptide mimetic of ghrelin containing an amidated C-terminus was used as a human GOAT (hGOAT) inhibitor.<sup>138</sup> Through subsequent testing with attachment of an octanoyl group at the S3 position, this modification increased the inhibitory efficiency 50%.<sup>138</sup> The acyl chain length was also varied to find GOAT's preference; attachment of a 14-carbon myristoyl or a 16-carbon palmitoyl in place of the 8-carbon octanoyl group abolished all inhibitory activity.<sup>138</sup> The final resulting peptide inhibitor replaced the ester linkage of the acyl

group with an amide linkage to yield [Dap<sup>3</sup>]octanoyl-ghrelin(1–5)-NH<sub>2</sub>, which to date is one of the most potent peptide mimetic GOAT inhibitors reported in an *in vitro* enzyme assay to have an IC<sub>50</sub> value of 1 μM.<sup>138</sup> The longer full-length ghrelin mimetic, [Dap<sup>3</sup>]octanoyl-ghrelin(1–28)-NH<sub>2</sub> also acts as a potent GOAT inhibitor with a slightly lower measured *in vitro* IC<sub>50</sub> of 0.2 μM.<sup>138</sup> These inhibitors are structurally similar to octanoylated ghrelin and so may have unintended GHS-R1a receptor activation since peptide length (first four residues) and the octanoyl group are recognized by the receptor.<sup>26</sup>

In an effort to increase the low potency, biostability, and cell permeability of the current field of peptide mimetic inhibitors, a series of 1,2,3-triazole linked acylated peptides were designed (Figure 1.5).<sup>139</sup> These peptides used GSSFL-NH<sub>2</sub> as their starting peptide scaffold, replacing S3 with a Dap (2,3-diaminopropanoic acid, which is converted to an azide via a diazo transfer) residue which is the site of acylation in the parent peptide. The triazole linkage acts in a similar manner to an ester/amide bond, however, it increases the biostability and is more resistant to biological enzymatic degradation compared to [Dap<sup>3</sup>]octanoyl-ghrelin(1–5)-NH<sub>2</sub>.<sup>139</sup> After copper-catalyzed cycloaddition the peptide then has an alkylated triazole in place of the octanoyl ester.<sup>140</sup> A panel of triazole-linked side chains were incorporated including a range of aromatic groups to probe hGOAT tolerance instead of simple acyl chains.<sup>139</sup> The most potent inhibitor, phenylpropyl triazole, has an *in vitro* measured IC<sub>50</sub> of 0.7 μM.<sup>139</sup> There was a defined relationship between the inhibitory activity and the length of the side chain, extending or shortening the length of the acyl chain from phenylpropyl resulted in loss of inhibitory activity.<sup>139</sup> Like the above mentioned [Dap<sup>3</sup>]octanoyl-ghrelin(1–5)-NH<sub>2</sub>, the phenylalkyl triazole inhibitors are peptide mimetics containing the first five amino acids of ghrelin, the first four are required for receptor activation, and acyl chain stemming from the S3 position, so there is still

the possibility that these inhibitors would show low cell permeability and receptor activation as well.

Since previous inhibitor studies have identified that GOAT discriminates substrate length as well as the length of the acyl chain, there was an effort to combine both of these considerations into one bi-substrate inhibitor GO-CoA-Tat (Figure 1.5).<sup>137</sup> The first ten amino acids of ghrelin were selected in an effort to increase GOAT selectivity, octanoyl-CoA, and an 11-mer HIV Tat-derived peptide sequence to enhance cell penetration.<sup>137</sup> In cell studies using HeLa and HEK 293FT cell lines expressing mGOAT and preproghrelin, GO-CoA-Tat decreased acylated ghrelin levels with a measured IC<sub>50</sub> of 5 μM in their assay and had no effect on levels of desacyl ghrelin.<sup>137</sup> During cell studies there was delayed inhibition observed, with cells having to be incubated for 24 hours in the presence of Go-CoA-Tat, indicating a slow kinetic interaction.<sup>137</sup> In mice treated with GO-CoA-Tat, serum levels of acylated ghrelin decreased, they showed resistance to weight gain on a high fat diet and had a significant increase of insulin levels in a glucose challenge.<sup>137</sup> In other rodents GO-CoA-Tat treatment decreased fasting-induced food foraging and hoarding in hamsters and reduced meal frequency in rats.<sup>137, 141-142</sup> GO-CoA-Tat shows no evidence of cytotoxicity and when measured there was no observed GHS-R1a receptor activation.<sup>137</sup> GO-CoA-Tat is the first instance of an inhibitor having therapeutic potential for GOAT and ghrelin acylation as a drug target.

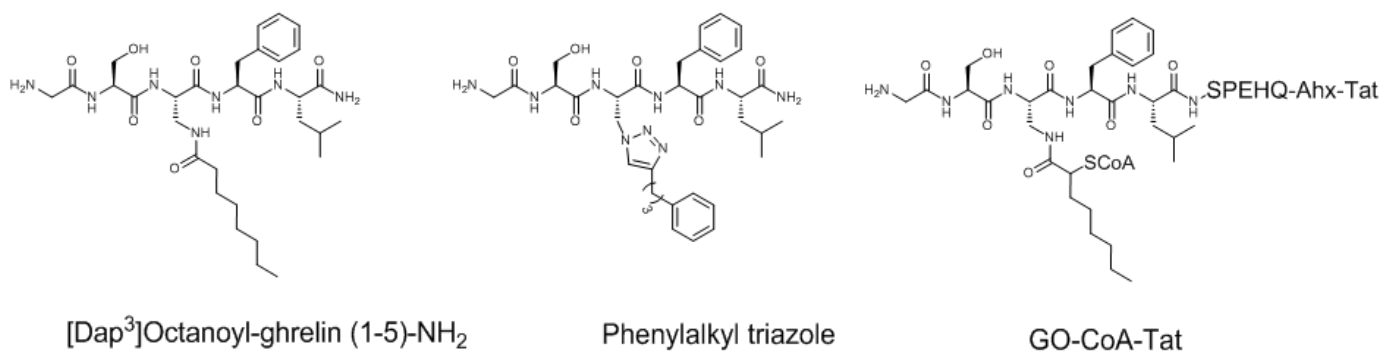


**Figure 1.5. Peptide mimetic inhibitors of GOAT.** Figure is reproduced with permission from Reference 46 (Appendix II). © 2016 Taylor and Francis.

### 1.4.2 Small molecule GOAT inhibitors

The first reported investigation into small molecule inhibitors of GOAT was performed by Garner and Janda in 2010 and 2011.<sup>143-144</sup> After a screen of small molecule library, a series of small molecule inhibitors containing small and medium acyl chains exhibited low micromolar IC<sub>50</sub> values (Figure 1.6).<sup>143-144</sup> The relative inhibitor effectiveness compared to acyl chain length is an indication that these small molecules might be targeting the octanoyl-CoA binding site. These lipidated small molecule inhibitors were the first step towards small molecule inhibitors; however, no cell or animal studies were conducted so their efficacy as therapeutics is unknown.

The next step in small molecule inhibitor design was to try and mimic the transition state of the GOAT octanoylation reaction by using aromatic groups that model peptide side chains. These aromatic groups would theoretically mimic ghrelin's N-terminal peptide side chain residues in the GOAT active site. In a series of reported inhibitors from Harran and coworkers, their small molecules mimic serine and phenylalanine residues which surround S3's octanoylation site.<sup>145</sup> However, their patented and most potent inhibitor BK1114 (Figure 1.6) does not contain those functionalities that were proposed to increase inhibitor affinity.<sup>145</sup>

In a more recent study, a screen of an NIH small molecule library identified two derivatives of 2-cyano-3,12-dioxooleana-1,9(11)-dien-28-oic acid (CDDO) as inhibitors of hGOAT in a microsomal enzyme assay with IC<sub>50</sub> values in the low micromolar range (Figure 1.6).<sup>146</sup> The GOAT inhibitors provide information about the potential mechanism for GOAT-catalyzed acylation, as structure activity relationship studies of these compounds demonstrate that compounds containing Michael addition electrophiles point to a covalent reversible

inhibition-based mechanism as their mechanism of action for GOAT inhibition.<sup>146</sup> This conclusion implies that there might be a functionally essential cysteine in the GOAT active site.

There are currently two industrial labs that are investigating possible small molecule inhibitors of GOAT for therapeutic use, Takeda Pharmaceuticals and Eli Lilly (Figure 1.6). Takeda has reported in the patent literature small molecule inhibitors containing a series of aromatic rings.<sup>147-148</sup> They have recently reported the most potent GOAT inhibitor to date using a screening of an internal small molecule library and from that lead compound, 4-chloro-6-{[2-methyl-6-(trifluoromethyl)pyridin-3-yl]methoxy}-1-benzothiophen-3-yl)acetic acid was synthesized.<sup>148</sup> In a microsomal enzyme assay, ELISA, and *in vivo* mouse studies this small molecule exhibited single nanomolar IC<sub>50</sub> values and decreased the total amount of acylated ghrelin.<sup>148</sup> The inhibitor still needs to be evaluated further *in vitro* and to investigate if there are possible off-target effects, however, there is indication from competition studies that this small molecule is targeting the octanoyl-CoA binding site. This is hypothesis supported by the use of the above mentioned small molecule inhibitor of GOAT (Figure 1.6, Takeda 2017 compound) in a lipid competition experiment.<sup>148</sup> The amount of octanoyl-CoA was varied in comparison to the inhibitor compound, which showed a shift in its IC<sub>50</sub> (higher) at increasing levels of octanoyl-CoA, indicating it was octanoyl-CoA substrate competitive.<sup>148</sup> The other pharmaceutical company with patented GOAT inhibitors, Eli Lilly, has reported two piperidyl-ethyl-pyrimidine derived GOAT inhibitors.<sup>149-150</sup> The supporting information in their patent applications indicates that these compounds (Figure 1.6) have potency in enzyme-, cell-, and animal studies. The lead compound in this class was discovered using a high-throughput GOAT activity screening assay. Through compound optimization both inhibitors have mid-nanomolar range in *in vitro* GOAT activity assays.<sup>149-150</sup> The published data on the Takeda GOAT inhibitors indicate that these

small molecules are targeting the octanoyl-CoA binding site within GOAT's active site. Further inhibitor testing for unintended effects, receptor activation, as well as, positive effects of blocking ghrelin signaling (body weight, glucose levels, insulin secretion) still need to be evaluated.

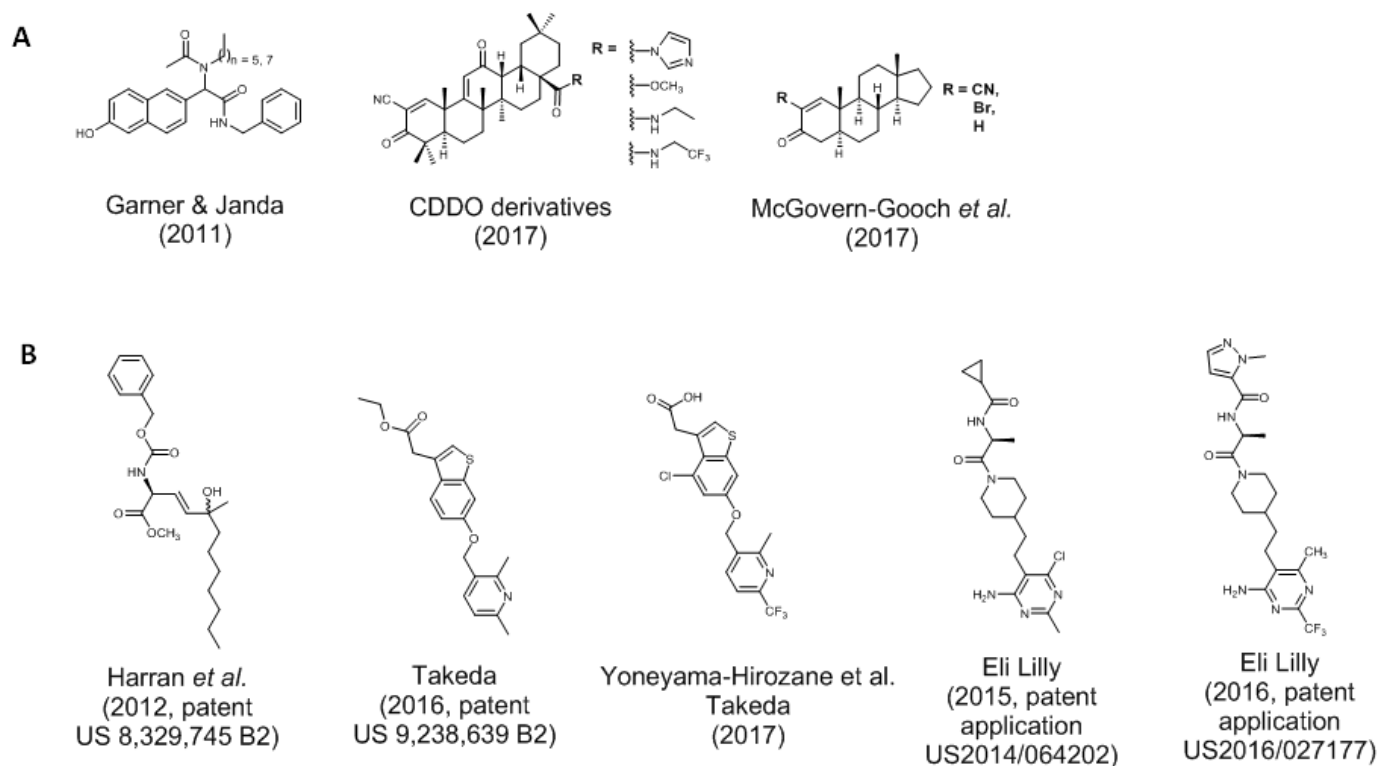


**Figure 1.6. Small molecule GOAT inhibitors.** A) The current field of academic-derived inhibitors published in peer-reviewed publication and B) is the current field of industrial-derived inhibitors reported in patent applications or issued patents. Figure was adapted with permission from Reference 46 (Appendix II). © 2016 Taylor and Francis.

## 1.5 GOAT recognition of ghrelin- the role of the N-terminal “GSSF” sequence and beyond

The active site and catalytic mechanism of GOAT remains to be revealed, the functional and structural recognition elements for GOAT recognition within ghrelin and ghrelin mimetic substrates have been characterized. After GOAT's initial discovery, Yang and coworkers utilized full-length proghrelin to evaluate GOAT's sequence selectivity near the site of acylation.<sup>138</sup> In these studies an [<sup>3</sup>H]octanoyl radiolabel-based assay was used to study mouse proghrelin acylation by mouse GOAT (mGOAT).<sup>138</sup> Mutation of S3 to alanine, G1 to serine, F4 to alanine, and addition of a serine-alanine dipeptide at the N-terminus all resulted in no acylation, indicating the N-terminal region's importance in GOAT recognition.<sup>138</sup> There was no noticeable decrease in the efficiency of substrate acylation in the presence of an S2 alanine mutation.<sup>138</sup> A less noticeable impact on proghrelin octanoylation was also observed when positions five through seven of proghrelin were mutated to alanine, indicating that the first five residues are of primary importance for recognition by GOAT.<sup>123, 138</sup>

Further analysis using fluorescently labeled peptides with the sequence GSSFLC<sub>AcDan</sub> and a microsomal enzyme assay was used to define a broad structure-activity relationship of substrate requirements for GOAT reactivity to occur.<sup>136, 151</sup> These studies indicated that the N-terminal glycine is important for recognition, with any loss of the N-terminal amine abrogating all catalysis.<sup>151</sup> There is a broad sequence tolerance at the S2 position with alanine, threonine, valine and phenylalanine all accepted.<sup>136, 151</sup> The mouse and human isoforms of GOAT can accept an amine substitution at S3 which reduces but does not eliminate acylation activity.<sup>136, 152</sup> The bullfrog form of ghrelin contains a threonine at the acylation site and has been demonstrated to be acylated, which supports the evidence that there can be substitution at this position

without loss of catalytic activity.<sup>127-128</sup> There was also broad tolerance at the F4 position with a variety of amino acid substitutions.<sup>136, 151</sup> These studies determined that the G1 position is absolutely necessary for acylation, as is a hydroxyl residue (serine or threonine) at the S3 position, with the S2 and F4 having broad tolerance for a variety of chemical group substitutions. Since the active site and catalytic residues of GOAT are still unknown, these structure-activity relationship studies helped to identify ghrelin substrate requirements which are necessary for GOAT catalysis to occur.

To determine if intermediate sequence lengths between full-length proghrelin (1-94) and small N-terminal peptides (1-5), there was an interest if longer sequences could bind and be efficiently bind to GOAT. Peptides with the sequences of ghrelin (1-5), (1-10), (1-18), and (1-28) were evaluated.<sup>136</sup> Their IC<sub>50</sub> values were measured in microsomal enzyme assay leading to the observation that there was tighter binding affinity (lower IC<sub>50</sub>) with the longer the ghrelin sequence, with a discrepancy with (1-10) exhibiting a higher IC<sub>50</sub> value than the other sequences.<sup>136</sup> There were also studies using Dap-incorporated peptides with longer ghrelin sequences, ghrelin (1-10) and (1-27), which also showed that the longer sequence had a tighter binding affinity than the shorter sequence.<sup>152</sup> These data indicate that there are possible substrate interactions occurring outside conventional ghrelin (1-5) sequence and is advantageous for GOAT binding.

## **1.6 Obestatin**

In 2005, bioinformatic analysis of the sequence of preproghrelin identified a conserved region that was surrounded by potential enzymatic cleavage sites that could result in cleavage and formation of a new peptide hormone (other than ghrelin).<sup>153</sup> This 23 amino acid peptide,

named obestatin, is derived from the C-terminus of proghrelin and contains a C-terminal amidated glycine residue.<sup>153</sup> The complete processing pathway of obestatin is unknown, including the enzyme(s) that cleave obestatin from proghrelin.<sup>50</sup> Obestatin is found in the same cell types as ghrelin, specifically several endocrine cell types.<sup>153-162</sup> The initial study describing obestatin reported that intraperitoneal/intracerebroventricular injection of obestatin decreased food intake and also reduced body weight in mice as well as inhibiting gastrointestinal mobility.<sup>153, 163-169</sup> Since this initial study, only a minority of other studies (25%) have replicated these findings such as evidence of an anorexigenic effect upon obestatin administration.<sup>170-185</sup> The large number of conflicting findings may be the result of differences in *in vitro* and *in vivo* methodology as well as the relatively short half-life and stability of the obestatin peptide.<sup>186-187</sup> Due to the varying experimental results, the exact role obestatin is involved in are undefined or at least ambiguous.

Since ghrelin activates the GHS-R1a receptor, it was thought that obestatin also acts as a receptor ligand. When measured in crude plasma membrane preparation of rat jejunum (the part of the small intestine between the duodenum and ileum), obestatin was found to bind jejunum with high affinity indicating it was binding to a receptor in the membrane.<sup>153</sup> It was hypothesized that obestatin was binding to an orphan GPCR (akin to GHS-R1a), with the receptor identified as GPR39.<sup>153, 167</sup> In CHO (chinese hamster ovary) cells expressing the GPR39 receptor, there was observed receptor activation in the presence of obestatin.<sup>153</sup> Subsequent studies failed to reproduce these initial findings, and the current consensus holds that obestatin is not an endogenous ligand for GPR39.<sup>171, 174-175</sup> Apart from GPR39, some studies have found that obestatin binds the GLP-1R and CRF receptors, although the reproducibility of these studies remains to be established.<sup>154, 185, 188-189</sup> There are still unanswered questions as to the processing

and biological role of obestatin; including what is the mechanism of cleavage from C-ghrelin, is obestatin activating a receptor and is it actually a hormone?

### **1.7 Aims of this work**

There are three main aims of this work described in this thesis. The first was to create an expression system for proghrelin to enable purification to homogeneity, allowing investigation of the secondary structure of the protein. This led to the second aim of my doctoral studies, investigating unique processing behavior of proghrelin and C-ghrelin that was observed during proghrelin purification. The final aim was to develop a structure activity relationship of small substrate mimetics of ghrelin with unnatural amino acid incorporation. There has been little investigation into the structure of proghrelin and its recognition as a substrate for GOAT-catalyzed octanoylation beyond the initial study by Yang and coworkers. In order to understand the effects of the C-terminus of proghrelin on enzymatic catalysis as well as any interactions that the enzyme has with proghrelin outside the active site, proghrelin needs to be further evaluated. The approach taken was to investigate secondary structural motifs present in proghrelin and the contribution of ghrelin and C-ghrelin to identify potential recognition elements for proghrelin-GOAT interactions. There was a unique cleavage behavior seen while purifying recombinantly expressed proghrelin which could indicate that under biological conditions proghrelin processes obestatin in the absence of an unknown proposed enzyme. In the same vein of understanding GOAT's acylation of proghrelin, small peptide mimetics were designed utilizing an unnatural amino acid at the S3 position in order to study purely binding instead of binding and catalysis of the enzyme. These unnatural amino acid incorporated peptides were designed to make a model peptide for future therapeutic development. The study of the biological substrate and trying to

understand the implications of its structural and processing behavior is fundamental to understanding the GOAT system and the eventual effects ghrelin has on the body.

## 1.8 References

1. Walsh, C. T.; Garneau-Tsodikova, S.; Gatto, G. J., Jr., Protein posttranslational modifications: the chemistry of proteome diversifications. *Angew Chem Int Ed Engl* **2005**, *44* (45), 7342-72.
2. Woodgett, J. R.; Hunter, T., Regulation of protein kinase C by activators, Ca<sup>2+</sup>, and phosphorylation. *Prog Clin Biol Res* **1987**, *249*, 237-47.
3. Zhang, K.; Williams, K. E.; Huang, L.; Yau, P.; Siino, J. S.; Bradbury, E. M.; Jones, P. R.; Minch, M. J.; Burlingame, A. L., Histone acetylation and deacetylation: identification of acetylation and methylation sites of HeLa histone H4 by mass spectrometry. *Mol Cell Proteomics* **2002**, *1* (7), 500-8.
4. Johnson, D. R.; Bhatnagar, R. S.; Knoll, L. J.; Gordon, J. I., Genetic and biochemical studies of protein N-myristoylation. *Annu Rev Biochem* **1994**, *63*, 869-914.
5. Bijlmakers, M. J.; Marsh, M., The on-off story of protein palmitoylation. *Trends Cell Biol* **2003**, *13* (1), 32-42.
6. Buglino, J. A.; Resh, M. D., Palmitoylation of Hedgehog proteins. *Vitam Horm* **2012**, *88*, 229-52.
7. Linder, M. E.; Deschenes, R. J., New insights into the mechanisms of protein palmitoylation. *Biochemistry* **2003**, *42* (15), 4311-20.
8. Pepinsky, R. B.; Zeng, C.; Wen, D.; Rayhorn, P.; Baker, D. P.; Williams, K. P.; Bixler, S. A.; Ambrose, C. M.; Garber, E. A.; Miatkowski, K.; Taylor, F. R.; Wang, E. A.; Galdes, A., Identification of a palmitic acid-modified form of human Sonic hedgehog. *J Biol Chem* **1998**, *273* (22), 14037-45.
9. Pickart, C. M., Ubiquitin enters the new millennium. *Mol Cell* **2001**, *8* (3), 499-504.

10. Kojima, M.; Hosoda, H.; Date, Y.; Nakazato, M.; Matsuo, H.; Kangawa, K., Ghrelin is a growth-hormone-releasing acylated peptide from stomach. *Nature* **1999**, *402* (6762), 656-60.
11. Casey, P. J.; Seabra, M. C., Protein prenyltransferases. *J Biol Chem* **1996**, *271* (10), 5289-92.
12. Jiang, H.; Zhang, X.; Chen, X.; Aramsangtienchai, P.; Tong, Z.; Lin, H., Protein Lipidation: Occurrence, Mechanisms, Biological Functions, and Enabling Technologies. *Chem Rev* **2018**, *118* (3), 919-988.
13. Zhang, F. L.; Casey, P. J., Protein prenylation: molecular mechanisms and functional consequences. *Annu Rev Biochem* **1996**, *65*, 241-69.
14. Furmanek, A.; Hofsteenge, J., Protein C-mannosylation: facts and questions. *Acta Biochim Pol* **2000**, *47* (3), 781-9.
15. Mechref, Y.; Novotny, M. V., Structural investigations of glycoconjugates at high sensitivity. *Chem Rev* **2002**, *102* (2), 321-69.
16. Wells, L.; Vosseller, K.; Cole, R. N.; Cronshaw, J. M.; Matunis, M. J.; Hart, G. W., Mapping sites of O-GlcNAc modification using affinity tags for serine and threonine post-translational modifications. *Mol Cell Proteomics* **2002**, *1* (10), 791-804.
17. Giles, N. M.; Watts, A. B.; Giles, G. I.; Fry, F. H.; Littlechild, J. A.; Jacob, C., Metal and redox modulation of cysteine protein function. *Chem Biol* **2003**, *10* (8), 677-93.
18. Jacob, C.; Giles, G. I.; Giles, N. M.; Sies, H., Sulfur and selenium: the role of oxidation state in protein structure and function. *Angew Chem Int Ed Engl* **2003**, *42* (39), 4742-58.
19. Nadolski, M. J.; Linder, M. E., Protein lipidation. *FEBS J* **2007**, *274* (20), 5202-10.
20. Thinon, E.; Hang, H. C., Chemical reporters for exploring protein acylation. *Biochem Soc Trans* **2015**, *43* (2), 253-61.

21. Towler, D. A.; Gordon, J. I.; Adams, S. P.; Glaser, L., The biology and enzymology of eukaryotic protein acylation. *Annu Rev Biochem* **1988**, *57*, 69-99.
22. Takada, R.; Satomi, Y.; Kurata, T.; Ueno, N.; Norioka, S.; Kondoh, H.; Takao, T.; Takada, S., Monounsaturated fatty acid modification of Wnt protein: its role in Wnt secretion. *Dev Cell* **2006**, *11* (6), 791-801.
23. Doubravska, L.; Krausova, M.; Gradl, D.; Vojtechova, M.; Tumova, L.; Lukas, J.; Valenta, T.; Pospichalova, V.; Fafilek, B.; Plachy, J.; Sebesta, O.; Korinek, V., Fatty acid modification of Wnt1 and Wnt3a at serine is prerequisite for lipidation at cysteine and is essential for Wnt signalling. *Cell Signal* **2011**, *23* (5), 837-48.
24. Hofmann, K., A superfamily of membrane-bound O-acyltransferases with implications for wnt signaling. *Trends Biochem Sci* **2000**, *25* (3), 111-2.
25. Avau, B.; Carbone, F.; Tack, J.; Depoortere, I., Ghrelin signaling in the gut, its physiological properties, and therapeutic potential. *Neurogastroenterol Motil* **2013**, *25* (9), 720-32.
26. Bednarek, M. A.; Feighner, S. D.; Pong, S. S.; McKee, K. K.; Hreniuk, D. L.; Silva, M. V.; Warren, V. A.; Howard, A. D.; Van Der Ploeg, L. H.; Heck, J. V., Structure-function studies on the new growth hormone-releasing peptide, ghrelin: minimal sequence of ghrelin necessary for activation of growth hormone secretagogue receptor 1a. *J Med Chem* **2000**, *43* (23), 4370-6.
27. Howard, A. D.; Feighner, S. D.; Cully, D. F.; Arena, J. P.; Liberators, P. A.; Rosenblum, C. I.; Hamelin, M.; Hreniuk, D. L.; Palyha, O. C.; Anderson, J.; Paress, P. S.; Diaz, C.; Chou, M.; Liu, K. K.; McKee, K. K.; Pong, S. S.; Chaung, L. Y.; Elbrecht, A.; Dashkevich, M.; Heavens, R.; Rigby, M.; Sirinathsinghji, D. J.; Dean, D. C.; Melillo, D. G.; Patchett, A. A.; Nargund, R.; Griffin, P. R.; DeMartino, J. A.; Gupta, S. K.; Schaeffer, J. M.; Smith, R. G.; Van der Ploeg, L.

- H., A receptor in pituitary and hypothalamus that functions in growth hormone release. *Science* **1996**, *273* (5277), 974-7.
28. Callaghan, B.; Furness, J. B., Novel and conventional receptors for ghrelin, desacyl-ghrelin, and pharmacologically related compounds. *Pharmacol Rev* **2014**, *66* (4), 984-1001.
29. Delhanty, P. J.; Sun, Y.; Visser, J. A.; van Kerkwijk, A.; Huisman, M.; van Ijcken, W. F.; Swagemakers, S.; Smith, R. G.; Themmen, A. P.; van der Lely, A. J., Unacylated ghrelin rapidly modulates lipogenic and insulin signaling pathway gene expression in metabolically active tissues of GHSR deleted mice. *PLoS One* **2010**, *5* (7), e11749.
30. Hopkins, A. L.; Nelson, T. A.; Guschina, I. A.; Parsons, L. C.; Lewis, C. L.; Brown, R. C.; Christian, H. C.; Davies, J. S.; Wells, T., Unacylated ghrelin promotes adipogenesis in rodent bone marrow via ghrelin O-acyl transferase and GHS-R1a activity: evidence for target cell-induced acylation. *Sci Rep* **2017**, *7*, 45541.
31. Murtuza, M. I.; Isokawa, M., Endogenous ghrelin-O-acyltransferase (GOAT) acylates local ghrelin in the hippocampus. *J Neurochem* **2018**, *144* (1), 58-67.
32. Date, Y.; Kojima, M.; Hosoda, H.; Sawaguchi, A.; Mondal, M. S.; Suganuma, T.; Matsukura, S.; Kangawa, K.; Nakazato, M., Ghrelin, a novel growth hormone-releasing acylated peptide, is synthesized in a distinct endocrine cell type in the gastrointestinal tracts of rats and humans. *Endocrinology* **2000**, *141* (11), 4255-61.
33. Stengel, A.; Tache, Y., Ghrelin - a pleiotropic hormone secreted from endocrine x/a-like cells of the stomach. *Front Neurosci* **2012**, *6*, 24.
34. Mizutani, M.; Atsuchi, K.; Asakawa, A.; Matsuda, N.; Fujimura, M.; Inui, A.; Kato, I.; Fujimiya, M., Localization of acyl ghrelin- and des-acyl ghrelin-immunoreactive cells in the rat

- stomach and their responses to intragastric pH. *Am J Physiol Gastrointest Liver Physiol* **2009**, 297 (5), G974-80.
35. Rindi, G.; Necchi, V.; Savio, A.; Torsello, A.; Zoli, M.; Locatelli, V.; Raimondo, F.; Cocchi, D.; Solcia, E., Characterisation of gastric ghrelin cells in man and other mammals: studies in adult and fetal tissues. *Histochem Cell Biol* **2002**, 117 (6), 511-9.
36. Date, Y.; Nakazato, M.; Hashiguchi, S.; Dezaki, K.; Mondal, M. S.; Hosoda, H.; Kojima, M.; Kangawa, K.; Arima, T.; Matsuo, H.; Yada, T.; Matsukura, S., Ghrelin is present in pancreatic alpha-cells of humans and rats and stimulates insulin secretion. *Diabetes* **2002**, 51 (1), 124-9.
37. Konitsiotis, A. D.; Jovanovic, B.; Ciepla, P.; Spitaler, M.; Lanyon-Hogg, T.; Tate, E. W.; Magee, A. I., Topological analysis of Hedgehog acyltransferase, a multipalmitoylated transmembrane protein. *J Biol Chem* **2015**, 290 (6), 3293-307.
38. Koussounadis, A.; Langdon, S. P.; Um, I. H.; Harrison, D. J.; Smith, V. A., Relationship between differentially expressed mRNA and mRNA-protein correlations in a xenograft model system. *Sci Rep* **2015**, 5, 10775.
39. McManus, J.; Cheng, Z.; Vogel, C., Next-generation analysis of gene expression regulation--comparing the roles of synthesis and degradation. *Mol Biosyst* **2015**, 11 (10), 2680-9.
40. Korbonits, M.; Bustin, S. A.; Kojima, M.; Jordan, S.; Adams, E. F.; Lowe, D. G.; Kangawa, K.; Grossman, A. B., The expression of the growth hormone secretagogue receptor ligand ghrelin in normal and abnormal human pituitary and other neuroendocrine tumors. *J Clin Endocrinol Metab* **2001**, 86 (2), 881-7.
41. Gnanapavan, S.; Kola, B.; Bustin, S. A.; Morris, D. G.; McGee, P.; Fairclough, P.; Bhattacharya, S.; Carpenter, R.; Grossman, A. B.; Korbonits, M., The tissue distribution of the

- mRNA of ghrelin and subtypes of its receptor, GHS-R, in humans. *J Clin Endocrinol Metab* **2002**, *87* (6), 2988.
42. Chen, C. Y.; Fujimiya, M.; Asakawa, A.; Chang, F. Y.; Cheng, J. T.; Lee, S. D.; Inui, A., At the cutting edge: ghrelin gene products in food intake and gut motility. *Neuroendocrinology* **2009**, *89* (1), 9-17.
43. Takahashi, T.; Ida, T.; Sato, T.; Nakashima, Y.; Nakamura, Y.; Tsuji, A.; Kojima, M., Production of n-octanoyl-modified ghrelin in cultured cells requires prohormone processing protease and ghrelin O-acyltransferase, as well as n-octanoic acid. *J Biochem* **2009**, *146* (5), 675-82.
44. Zhu, X.; Cao, Y.; Voogd, K.; Steiner, D. F., On the processing of proghrelin to ghrelin. *J Biol Chem* **2006**, *281* (50), 38867-70.
45. Romero, A.; Kirchner, H.; Heppner, K.; Pfluger, P. T.; Tschop, M. H.; Nogueiras, R., GOAT: the master switch for the ghrelin system? *Eur J Endocrinol* **2010**, *163* (1), 1-8.
46. Cleverdon, E. R.; McGovern-Gooch, K. R.; Hougland, J. L., The octanoylated energy regulating hormone ghrelin: An expanded view of ghrelin's biological interactions and avenues for controlling ghrelin signaling. *Mol Membr Biol* **2016**, *33* (6-8), 111-124.
47. Zhou, A.; Webb, G.; Zhu, X.; Steiner, D. F., Proteolytic processing in the secretory pathway. *J Biol Chem* **1999**, *274* (30), 20745-8.
48. Gutierrez, J. A.; Solenberg, P. J.; Perkins, D. R.; Willency, J. A.; Knierman, M. D.; Jin, Z.; Witcher, D. R.; Luo, S.; Onyia, J. E.; Hale, J. E., Ghrelin octanoylation mediated by an orphan lipid transferase. *Proc Natl Acad Sci U S A* **2008**, *105* (17), 6320-5.

49. Yang, J.; Brown, M. S.; Liang, G.; Grishin, N. V.; Goldstein, J. L., Identification of the acyltransferase that octanoylates ghrelin, an appetite-stimulating peptide hormone. *Cell* **2008**, *132* (3), 387-96.
50. Garg, A., The ongoing saga of obestatin: is it a hormone? *J Clin Endocrinol Metab* **2007**, *92* (9), 3396-8.
51. Berg, J. M.; Tymoczko, J. L.; Stryer, L.; Stryer, L., *Biochemistry*. 6th ed.; W.H. Freeman: New York, 2007.
52. Purnell, J. Q.; Weigle, D. S.; Breen, P.; Cummings, D. E., Ghrelin levels correlate with insulin levels, insulin resistance, and high-density lipoprotein cholesterol, but not with gender, menopausal status, or cortisol levels in humans. *J Clin Endocrinol Metab* **2003**, *88* (12), 5747-52.
53. De Vriese, C.; Hacquebard, M.; Gregoire, F.; Carpentier, Y.; Delporte, C., Ghrelin interacts with human plasma lipoproteins. *Endocrinology* **2007**, *148* (5), 2355-62.
54. Holmes, E.; Davies, I.; Lowe, G.; Ranganath, L. R., Circulating ghrelin exists in both lipoprotein bound and free forms. *Ann Clin Biochem* **2009**, *46* (Pt 6), 514-6.
55. Beaumont, N. J.; Skinner, V. O.; Tan, T. M.; Ramesh, B. S.; Byrne, D. J.; MacColl, G. S.; Keen, J. N.; Bouloux, P. M.; Mikhailidis, D. P.; Bruckdorfer, K. R.; Vanderpump, M. P.; Srai, K. S., Ghrelin can bind to a species of high density lipoprotein associated with paraoxonase. *J Biol Chem* **2003**, *278* (11), 8877-80.
56. De Vriese, C.; Gregoire, F.; Lema-Kisoka, R.; Waelbroeck, M.; Robberecht, P.; Delporte, C., Ghrelin degradation by serum and tissue homogenates: identification of the cleavage sites. *Endocrinology* **2004**, *145* (11), 4997-5005.

57. Delhanty, P. J.; Huisman, M.; Julien, M.; Mouchain, K.; Brune, P.; Themmen, A. P.; Abribat, T.; van der Lely, A. J., The acylated (AG) to unacylated (UAG) ghrelin ratio in esterase inhibitor-treated blood is higher than previously described. *Clin Endocrinol (Oxf)* **2015**, *82* (1), 142-6.
58. McGovern-Gooch, K. R.; Rodrigues, T.; Darling, J. E.; Sieburg, M. A.; Abizaid, A.; Hougland, J. L., Ghrelin Octanoylation Is Completely Stabilized in Biological Samples by Alkyl Fluorophosphonates. *Endocrinology* **2016**, *157* (11), 4330-4338.
59. Dantas, V. G.; Furtado-Alle, L.; Souza, R. L.; Chautard-Freire-Maia, E. A., Obesity and variants of the GHRL (ghrelin) and BCHE (butyrylcholinesterase) genes. *Genet Mol Biol* **2011**, *34* (2), 205-7.
60. Eubanks, L. M.; Stowe, G. N.; De Lamo Marin, S.; Mayorov, A. V.; Hixon, M. S.; Janda, K. D., Identification of alpha2 macroglobulin as a major serum ghrelin esterase. *Angew Chem Int Ed Engl* **2011**, *50* (45), 10699-702.
61. Satou, M.; Nishi, Y.; Yoh, J.; Hattori, Y.; Sugimoto, H., Identification and characterization of acyl-protein thioesterase 1/lysophospholipase I as a ghrelin deacylation/lysophospholipid hydrolyzing enzyme in fetal bovine serum and conditioned medium. *Endocrinology* **2010**, *151* (10), 4765-75.
62. Brimijoin, S.; Chen, V. P.; Pang, Y. P.; Geng, L.; Gao, Y., Physiological roles for butyrylcholinesterase: A BChE-ghrelin axis. *Chem Biol Interact* **2016**, *259* (Pt B), 271-275.
63. Chen, V. P.; Gao, Y.; Geng, L.; Brimijoin, S., Butyrylcholinesterase regulates central ghrelin signaling and has an impact on food intake and glucose homeostasis. *Int J Obes (Lond)* **2017**.

64. Chen, V. P.; Gao, Y.; Geng, L.; Parks, R. J.; Pang, Y. P.; Brimijoin, S., Plasma butyrylcholinesterase regulates ghrelin to control aggression. *Proc Natl Acad Sci U S A* **2015**, *112* (7), 2251-6.
65. Schopfer, L. M.; Lockridge, O.; Brimijoin, S., Pure human butyrylcholinesterase hydrolyzes octanoyl ghrelin to desacyl ghrelin. *Gen Comp Endocrinol* **2015**, *224*, 61-8.
66. Yao, J.; Yuan, Y.; Zheng, F.; Zhan, C. G., Unexpected Reaction Pathway for butyrylcholinesterase-catalyzed inactivation of "hunger hormone" ghrelin. *Sci Rep* **2016**, *6*, 22322.
67. Li, B.; Duysen, E. G.; Lockridge, O., The butyrylcholinesterase knockout mouse is obese on a high-fat diet. *Chem Biol Interact* **2008**, *175* (1-3), 88-91.
68. Manoharan, I.; Boopathy, R.; Darvesh, S.; Lockridge, O., A medical health report on individuals with silent butyrylcholinesterase in the Vysya community of India. *Clin Chim Acta* **2007**, *378* (1-2), 128-35.
69. Manoharan, I.; Wieseler, S.; Layer, P. G.; Lockridge, O.; Boopathy, R., Naturally occurring mutation Leu307Pro of human butyrylcholinesterase in the Vysya community of India. *Pharmacogenet Genomics* **2006**, *16* (7), 461-8.
70. Elkon, K.; Casali, P., Nature and functions of autoantibodies. *Nat Clin Pract Rheumatol* **2008**, *4* (9), 491-8.
71. Takagi, K.; Legrand, R.; Asakawa, A.; Amitani, H.; Francois, M.; Tennoune, N.; Coeffier, M.; Claeysens, S.; do Rego, J. C.; Dechelotte, P.; Inui, A.; Fetissov, S. O., Anti-ghrelin immunoglobulins modulate ghrelin stability and its orexigenic effect in obese mice and humans. *Nat Commun* **2013**, *4*, 2685.

72. Francois, M.; Takagi, K.; Legrand, R.; Lucas, N.; Beutheu, S.; Bole-Feysot, C.; Cravezic, A.; Tennoune, N.; do Rego, J. C.; Coeffier, M.; Inui, A.; Dechelotte, P.; Fetissof, S. O., Increased Ghrelin but Low Ghrelin-Reactive Immunoglobulins in a Rat Model of Methotrexate Chemotherapy-Induced Anorexia. *Front Nutr* **2016**, *3*, 23.
73. Terashi, M.; Asakawa, A.; Harada, T.; Ushikai, M.; Coquerel, Q.; Sinno, M. H.; Dechelotte, P.; Inui, A.; Fetissof, S. O., Ghrelin reactive autoantibodies in restrictive anorexia nervosa. *Nutrition* **2011**, *27* (4), 407-13.
74. Francois, M.; Barde, S.; Legrand, R.; Lucas, N.; Azhar, S.; el Dhaybi, M.; Guerin, C.; Hokfelt, T.; Dechelotte, P.; Coeffier, M.; Fetissof, S. O., High-fat diet increases ghrelin-expressing cells in stomach, contributing to obesity. *Nutrition* **2016**, *32* (6), 709-715.
75. Kojima, M.; Hosoda, H.; Matsuo, H.; Kangawa, K., Ghrelin: discovery of the natural endogenous ligand for the growth hormone secretagogue receptor. *Trends Endocrinol Metab* **2001**, *12* (3), 118-22.
76. Bowers, C. Y.; Reynolds, G. A.; Chang, D.; Hong, A.; Chang, K.; Momany, F., A study on the regulation of growth hormone release from the pituitaries of rats in vitro. *Endocrinology* **1981**, *108* (3), 1071-80.
77. Bowers, C. Y.; Sartor, A. O.; Reynolds, G. A.; Badger, T. M., On the actions of the growth hormone-releasing hexapeptide, GHRP. *Endocrinology* **1991**, *128* (4), 2027-35.
78. Pedretti, A.; Villa, M.; Pallavicini, M.; Valoti, E.; Vistoli, G., Construction of human ghrelin receptor (hGHS-R1a) model using a fragmental prediction approach and validation through docking analysis. *J Med Chem* **2006**, *49* (11), 3077-85.
79. Root, A. W.; Root, M. J., Clinical pharmacology of human growth hormone and its secretagogues. *Curr Drug Targets Immune Endocr Metabol Disord* **2002**, *2* (1), 27-52.

80. Murata, M.; Okimura, Y.; Iida, K.; Matsumoto, M.; Sowa, H.; Kaji, H.; Kojima, M.; Kangawa, K.; Chihara, K., Ghrelin modulates the downstream molecules of insulin signaling in hepatoma cells. *J Biol Chem* **2002**, *277* (7), 5667-74.
81. Kohno, D.; Gao, H. Z.; Muroya, S.; Kikuyama, S.; Yada, T., Ghrelin directly interacts with neuropeptide-Y-containing neurons in the rat arcuate nucleus: Ca<sup>2+</sup> signaling via protein kinase A and N-type channel-dependent mechanisms and cross-talk with leptin and orexin. *Diabetes* **2003**, *52* (4), 948-56.
82. Mousseaux, D.; Le Gallic, L.; Ryan, J.; Oiry, C.; Gagne, D.; Fehrentz, J. A.; Galleyrand, J. C.; Martinez, J., Regulation of ERK1/2 activity by ghrelin-activated growth hormone secretagogue receptor 1A involves a PLC/PKCvarepsilon pathway. *Br J Pharmacol* **2006**, *148* (3), 350-65.
83. Tschop, M.; Smiley, D. L.; Heiman, M. L., Ghrelin induces adiposity in rodents. *Nature* **2000**, *407* (6806), 908-13.
84. Cowley, M. A.; Smith, R. G.; Diano, S.; Tschop, M.; Pronchuk, N.; Grove, K. L.; Strasburger, C. J.; Bidlingmaier, M.; Esterman, M.; Heiman, M. L.; Garcia-Segura, L. M.; Nillni, E. A.; Mendez, P.; Low, M. J.; Sotonyi, P.; Friedman, J. M.; Liu, H.; Pinto, S.; Colmers, W. F.; Cone, R. D.; Horvath, T. L., The distribution and mechanism of action of ghrelin in the CNS demonstrates a novel hypothalamic circuit regulating energy homeostasis. *Neuron* **2003**, *37* (4), 649-61.
85. Cummings, D. E., Ghrelin and the short- and long-term regulation of appetite and body weight. *Physiol Behav* **2006**, *89* (1), 71-84.

86. Cummings, D. E.; Frayo, R. S.; Marmonier, C.; Aubert, R.; Chapelot, D., Plasma ghrelin levels and hunger scores in humans initiating meals voluntarily without time- and food-related cues. *Am J Physiol Endocrinol Metab* **2004**, *287* (2), E297-304.
87. Cummings, D. E.; Purnell, J. Q.; Frayo, R. S.; Schmidova, K.; Wisse, B. E.; Weigle, D. S., A preprandial rise in plasma ghrelin levels suggests a role in meal initiation in humans. *Diabetes* **2001**, *50* (8), 1714-9.
88. Wortley, K. E.; del Rincon, J. P.; Murray, J. D.; Garcia, K.; Iida, K.; Thorner, M. O.; Sleeman, M. W., Absence of ghrelin protects against early-onset obesity. *J Clin Invest* **2005**, *115* (12), 3573-8.
89. Sun, Y.; Asnicar, M.; Saha, P. K.; Chan, L.; Smith, R. G., Ablation of ghrelin improves the diabetic but not obese phenotype of ob/ob mice. *Cell Metab* **2006**, *3* (5), 379-86.
90. Broglio, F.; Arvat, E.; Benso, A.; Gottero, C.; Muccioli, G.; Papotti, M.; van der Lely, A. J.; Deghenghi, R.; Ghigo, E., Ghrelin, a natural GH secretagogue produced by the stomach, induces hyperglycemia and reduces insulin secretion in humans. *J Clin Endocrinol Metab* **2001**, *86* (10), 5083-6.
91. Broglio, F.; Gottero, C.; Benso, A.; Prodam, F.; Destefanis, S.; Gauna, C.; Maccario, M.; Deghenghi, R.; van der Lely, A. J.; Ghigo, E., Effects of ghrelin on the insulin and glycemic responses to glucose, arginine, or free fatty acids load in humans. *J Clin Endocrinol Metab* **2003**, *88* (9), 4268-72.
92. Egido, E. M.; Rodriguez-Gallardo, J.; Silvestre, R. A.; Marco, J., Inhibitory effect of ghrelin on insulin and pancreatic somatostatin secretion. *Eur J Endocrinol* **2002**, *146* (2), 241-4.

93. Falken, Y.; Hellstrom, P. M.; Sanger, G. J.; Dewit, O.; Dukes, G.; Gryback, P.; Holst, J. J.; Naslund, E., Actions of prolonged ghrelin infusion on gastrointestinal transit and glucose homeostasis in humans. *Neurogastroenterol Motil* **2010**, *22* (6), e192-200.
94. Murray, C. D.; Martin, N. M.; Patterson, M.; Taylor, S. A.; Ghatei, M. A.; Kamm, M. A.; Johnston, C.; Bloom, S. R.; Emmanuel, A. V., Ghrelin enhances gastric emptying in diabetic gastroparesis: a double blind, placebo controlled, crossover study. *Gut* **2005**, *54* (12), 1693-8.
95. Tack, J.; Depoortere, I.; Bisschops, R.; Delporte, C.; Coulie, B.; Meulemans, A.; Janssens, J.; Peeters, T., Influence of ghrelin on interdigestive gastrointestinal motility in humans. *Gut* **2006**, *55* (3), 327-33.
96. Chuang, J. C.; Zigman, J. M., Ghrelin's Roles in Stress, Mood, and Anxiety Regulation. *Int J Pept* **2010**, *2010*.
97. Diano, S.; Farr, S. A.; Benoit, S. C.; McNay, E. C.; da Silva, I.; Horvath, B.; Gaskin, F. S.; Nonaka, N.; Jaeger, L. B.; Banks, W. A.; Morley, J. E.; Pinto, S.; Sherwin, R. S.; Xu, L.; Yamada, K. A.; Sleeman, M. W.; Tschop, M. H.; Horvath, T. L., Ghrelin controls hippocampal spine synapse density and memory performance. *Nat Neurosci* **2006**, *9* (3), 381-8.
98. Spencer, S. J.; Emmerzaal, T. L.; Kozicz, T.; Andrews, Z. B., Ghrelin's Role in the Hypothalamic-Pituitary-Adrenal Axis Stress Response: Implications for Mood Disorders. *Biol Psychiatry* **2015**, *78* (1), 19-27.
99. Kanoski, S. E.; Fortin, S. M.; Ricks, K. M.; Grill, H. J., Ghrelin signaling in the ventral hippocampus stimulates learned and motivational aspects of feeding via PI3K-Akt signaling. *Biol Psychiatry* **2013**, *73* (9), 915-23.

100. Kanoski, S. E.; Hayes, M. R.; Greenwald, H. S.; Fortin, S. M.; Gianessi, C. A.; Gilbert, J. R.; Grill, H. J., Hippocampal leptin signaling reduces food intake and modulates food-related memory processing. *Neuropsychopharmacology* **2011**, *36* (9), 1859-70.
101. Lutter, M.; Sakata, I.; Osborne-Lawrence, S.; Rovinsky, S. A.; Anderson, J. G.; Jung, S.; Birnbaum, S.; Yanagisawa, M.; Elmquist, J. K.; Nestler, E. J.; Zigman, J. M., The orexigenic hormone ghrelin defends against depressive symptoms of chronic stress. *Nat Neurosci* **2008**, *11* (7), 752-3.
102. Barim, A. O.; Aydin, S.; Colak, R.; Dag, E.; Deniz, O.; Sahin, I., Ghrelin, paraoxonase and arylesterase levels in depressive patients before and after citalopram treatment. *Clin Biochem* **2009**, *42* (10-11), 1076-81.
103. Kurt, E.; Guler, O.; Serteser, M.; Cansel, N.; Ozbulut, O.; Altinbas, K.; Alatas, G.; Savas, H.; Gecici, O., The effects of electroconvulsive therapy on ghrelin, leptin and cholesterol levels in patients with mood disorders. *Neurosci Lett* **2007**, *426* (1), 49-53.
104. Andrews, Z. B.; Erion, D.; Beiler, R.; Liu, Z. W.; Abizaid, A.; Zigman, J.; Elsworth, J. D.; Savitt, J. M.; DiMarchi, R.; Tschoep, M.; Roth, R. H.; Gao, X. B.; Horvath, T. L., Ghrelin promotes and protects nigrostriatal dopamine function via a UCP2-dependent mitochondrial mechanism. *J Neurosci* **2009**, *29* (45), 14057-65.
105. Dixit, V. D.; Yang, H.; Sun, Y.; Weeraratna, A. T.; Youm, Y. H.; Smith, R. G.; Taub, D. D., Ghrelin promotes thymopoiesis during aging. *J Clin Invest* **2007**, *117* (10), 2778-90.
106. Moon, M.; Kim, H. G.; Hwang, L.; Seo, J. H.; Kim, S.; Hwang, S.; Kim, S.; Lee, D.; Chung, H.; Oh, M. S.; Lee, K. T.; Park, S., Neuroprotective effect of ghrelin in the 1-methyl-4-phenyl-1,2,3,6-tetrahydropyridine mouse model of Parkinson's disease by blocking microglial activation. *Neurotox Res* **2009**, *15* (4), 332-47.

107. Szentirmai, E.; Kapas, L.; Krueger, J. M., Ghrelin microinjection into forebrain sites induces wakefulness and feeding in rats. *Am J Physiol Regul Integr Comp Physiol* **2007**, *292* (1), R575-85.
108. Szentirmai, E.; Kapas, L.; Sun, Y.; Smith, R. G.; Krueger, J. M., Spontaneous sleep and homeostatic sleep regulation in ghrelin knockout mice. *Am J Physiol Regul Integr Comp Physiol* **2007**, *293* (1), R510-7.
109. Szentirmai, E.; Hajdu, I.; Obal, F., Jr.; Krueger, J. M., Ghrelin-induced sleep responses in ad libitum fed and food-restricted rats. *Brain Res* **2006**, *1088* (1), 131-40.
110. Tolle, V.; Bassant, M. H.; Zizzari, P.; Poindessous-Jazat, F.; Tomasetto, C.; Epelbaum, J.; Bluet-Pajot, M. T., Ultradian rhythmicity of ghrelin secretion in relation with GH, feeding behavior, and sleep-wake patterns in rats. *Endocrinology* **2002**, *143* (4), 1353-61.
111. Weikel, J. C.; Wichniak, A.; Ising, M.; Brunner, H.; Friess, E.; Held, K.; Mathias, S.; Schmid, D. A.; Uhr, M.; Steiger, A., Ghrelin promotes slow-wave sleep in humans. *Am J Physiol Endocrinol Metab* **2003**, *284* (2), E407-15.
112. Nagaya, N.; Kojima, M.; Uematsu, M.; Yamagishi, M.; Hosoda, H.; Oya, H.; Hayashi, Y.; Kangawa, K., Hemodynamic and hormonal effects of human ghrelin in healthy volunteers. *Am J Physiol Regul Integr Comp Physiol* **2001**, *280* (5), R1483-7.
113. Cummings, D. E.; Weigle, D. S.; Frayo, R. S.; Breen, P. A.; Ma, M. K.; Dellinger, E. P.; Purnell, J. Q., Plasma ghrelin levels after diet-induced weight loss or gastric bypass surgery. *N Engl J Med* **2002**, *346* (21), 1623-30.
114. Muller, T. D.; Perez-Tilve, D.; Tong, J.; Pfluger, P. T.; Tschop, M. H., Ghrelin and its potential in the treatment of eating/wasting disorders and cachexia. *J Cachexia Sarcopenia Muscle* **2010**, *1* (2), 159-167.

115. Shiiya, T.; Nakazato, M.; Mizuta, M.; Date, Y.; Mondal, M. S.; Tanaka, M.; Nozoe, S.; Hosoda, H.; Kangawa, K.; Matsukura, S., Plasma ghrelin levels in lean and obese humans and the effect of glucose on ghrelin secretion. *J Clin Endocrinol Metab* **2002**, *87* (1), 240-4.
116. Geliebter, A.; Gluck, M. E.; Hashim, S. A., Plasma ghrelin concentrations are lower in binge-eating disorder. *J Nutr* **2005**, *135* (5), 1326-30.
117. DelParigi, A.; Tschop, M.; Heiman, M. L.; Salbe, A. D.; Vozarova, B.; Sell, S. M.; Bunt, J. C.; Tataranni, P. A., High circulating ghrelin: a potential cause for hyperphagia and obesity in prader-willi syndrome. *J Clin Endocrinol Metab* **2002**, *87* (12), 5461-4.
118. Malandrino, N.; Miceli, A.; Leggio, L.; Mingrone, G.; Capristo, E., High ghrelin levels in post-treatment euthyroid patients with Hashimoto's thyroiditis: a case-control preliminary study. *Exp Clin Endocrinol Diabetes* **2014**, *122* (9), 540-3.
119. Buscher, A. K.; Cetiner, M.; Buscher, R.; Wingen, A. M.; Hauffa, B. P.; Hoyer, P. F., Obesity in patients with Bardet-Biedl syndrome: influence of appetite-regulating hormones. *Pediatr Nephrol* **2012**, *27* (11), 2065-2071.
120. Giordano, R.; Picu, A.; Pagotto, U.; De Iasio, R.; Bonelli, L.; Prodam, F.; Broglio, F.; Marafetti, L.; Pasquali, R.; Maccario, M.; Ghigo, E.; Arvat, E., The negative association between total ghrelin levels, body mass and insulin secretion is lost in hypercortisolemic patients with Cushing's disease. *Eur J Endocrinol* **2005**, *153* (4), 535-43.
121. Koutkia, P.; Meininger, G.; Canavan, B.; Breu, J.; Grinspoon, S., Metabolic regulation of growth hormone by free fatty acids, somatostatin, and ghrelin in HIV-lipodystrophy. *Am J Physiol Endocrinol Metab* **2004**, *286* (2), E296-303.
122. Libe, R.; Morpurgo, P. S.; Cappiello, V.; Maffini, A.; Bondioni, S.; Locatelli, M.; Zavanone, M.; Beck-Peccoz, P.; Spada, A., Ghrelin and adiponectin in patients with Cushing's

- disease before and after successful transsphenoidal surgery. *Clin Endocrinol (Oxf)* **2005**, *62* (1), 30-6.
123. Taylor, M. S.; Ruch, T. R.; Hsiao, P. Y.; Hwang, Y.; Zhang, P.; Dai, L.; Huang, C. R.; Berndsen, C. E.; Kim, M. S.; Pandey, A.; Wolberger, C.; Marmorstein, R.; Machamer, C.; Boeke, J. D.; Cole, P. A., Architectural organization of the metabolic regulatory enzyme ghrelin O-acyltransferase. *J Biol Chem* **2013**, *288* (45), 32211-28.
124. Matevossian, A.; Resh, M. D., Membrane topology of hedgehog acyltransferase. *J Biol Chem* **2015**, *290* (4), 2235-43.
125. Gao, X.; Hannoush, R. N., Single-cell imaging of Wnt palmitoylation by the acyltransferase porcupine. *Nat Chem Biol* **2014**, *10* (1), 61-8.
126. Buglino, J. A.; Resh, M. D., Hhat is a palmitoylacyltransferase with specificity for N-palmitoylation of Sonic Hedgehog. *J Biol Chem* **2008**, *283* (32), 22076-88.
127. Kaiya, H.; Kojima, M.; Hosoda, H.; Koda, A.; Yamamoto, K.; Kitajima, Y.; Matsumoto, M.; Minamitake, Y.; Kikuyama, S.; Kangawa, K., Bullfrog ghrelin is modified by n-octanoic acid at its third threonine residue. *J Biol Chem* **2001**, *276* (44), 40441-8.
128. Kaiya, H.; Sakata, I.; Yamamoto, K.; Koda, A.; Sakai, T.; Kangawa, K.; Kikuyama, S., Identification of immunoreactive plasma and stomach ghrelin, and expression of stomach ghrelin mRNA in the bullfrog, *Rana catesbeiana*. *Gen Comp Endocrinol* **2006**, *148* (2), 236-44.
129. Chang, S. C.; Magee, A. I., Acyltransferases for secreted signalling proteins (Review). *Mol Membr Biol* **2009**, *26* (1), 104-13.
130. Buglino, J. A.; Resh, M. D., Identification of conserved regions and residues within Hedgehog acyltransferase critical for palmitoylation of Sonic Hedgehog. *PLoS One* **2010**, *5* (6), e11195.

131. Chen, M. H.; Li, Y. J.; Kawakami, T.; Xu, S. M.; Chuang, P. T., Palmitoylation is required for the production of a soluble multimeric Hedgehog protein complex and long-range signaling in vertebrates. *Genes Dev* **2004**, *18* (6), 641-59.
132. Guo, Z. Y.; Lin, S.; Heinen, J. A.; Chang, C. C.; Chang, T. Y., The active site His-460 of human acyl-coenzyme A:cholesterol acyltransferase 1 resides in a hitherto undisclosed transmembrane domain. *J Biol Chem* **2005**, *280* (45), 37814-26.
133. Delhanty, P. J.; Huisman, M.; Baldeon-Rojas, L. Y.; van den Berge, I.; Grefhorst, A.; Aribat, T.; Leenen, P. J.; Themmen, A. P.; van der Lely, A. J., Des-acyl ghrelin analogs prevent high-fat-diet-induced dysregulation of glucose homeostasis. *FASEB J* **2013**, *27* (4), 1690-700.
134. Francois, M.; Barde, S.; Legrand, R.; Lucas, N.; Azhar, S.; El Dhaybi, M.; Guerin, C.; Hokfelt, T.; Dechelotte, P.; Coeffier, M.; Fetissof, S. O., High-fat diet increases ghrelin-expressing cells in stomach, contributing to obesity. *Nutrition* **2016**, *32* (6), 709-15.
135. Heppner, K. M.; Muller, T. D.; Tong, J.; Tschop, M. H., Ghrelin in the control of energy, lipid, and glucose metabolism. *Methods Enzymol* **2012**, *514*, 249-60.
136. Darling, J. E.; Zhao, F.; Loftus, R. J.; Patton, L. M.; Gibbs, R. A.; Hougland, J. L., Structure-activity analysis of human ghrelin O-acyltransferase reveals chemical determinants of ghrelin selectivity and acyl group recognition. *Biochemistry* **2015**, *54* (4), 1100-10.
137. Barnett, B. P.; Hwang, Y.; Taylor, M. S.; Kirchner, H.; Pfluger, P. T.; Bernard, V.; Lin, Y. Y.; Bowers, E. M.; Mukherjee, C.; Song, W. J.; Longo, P. A.; Leahy, D. J.; Hussain, M. A.; Tschop, M. H.; Boeke, J. D.; Cole, P. A., Glucose and weight control in mice with a designed ghrelin O-acyltransferase inhibitor. *Science* **2010**, *330* (6011), 1689-92.
138. Yang, J.; Zhao, T. J.; Goldstein, J. L.; Brown, M. S., Inhibition of ghrelin O-acyltransferase (GOAT) by octanoylated pentapeptides. *Proc Natl Acad Sci U S A* **2008**, *105* (31), 10750-5.

139. Zhao, F.; Darling, J. E.; Gibbs, R. A.; Hougland, J. L., A new class of ghrelin O-acyltransferase inhibitors incorporating triazole-linked lipid mimetic groups. *Bioorg Med Chem Lett* **2015**, *25* (14), 2800-3.
140. Holub, J. M.; Kirshenbaum, K., Tricks with clicks: modification of peptidomimetic oligomers via copper-catalyzed azide-alkyne [3+2] cycloaddition. *Chem Soc Rev* **2010**, *39* (4), 1325-1337.
141. Teubner, B. J.; Garretson, J. T.; Hwang, Y.; Cole, P. A.; Bartness, T. J., Inhibition of ghrelin O-acyltransferase attenuates food deprivation-induced increases in ingestive behavior. *Horm Behav* **2013**, *63* (4), 667-73.
142. Teuffel, P.; Wang, L.; Prinz, P.; Goebel-Stengel, M.; Scharner, S.; Kobelt, P.; Hofmann, T.; Rose, M.; Klapp, B. F.; Reeve, J. R., Jr.; Stengel, A., Treatment with the ghrelin-O-acyltransferase (GOAT) inhibitor GO-CoA-Tat reduces food intake by reducing meal frequency in rats. *J Physiol Pharmacol* **2015**, *66* (4), 493-503.
143. Garner, A. L.; Janda, K. D., cat-ELCCA: a robust method to monitor the fatty acid acyltransferase activity of ghrelin O-acyltransferase (GOAT). *Angew Chem Int Ed Engl* **2010**, *49* (50), 9630-4.
144. Garner, A. L.; Janda, K. D., A small molecule antagonist of ghrelin O-acyltransferase (GOAT). *Chem Commun (Camb)* **2011**, *47* (26), 7512-4.
145. Harran, P. G.; Brown, M. S.; Goldstein, J. L.; Yang, J.; Zhao, T. J., Small Molecule Inhibitors of Ghrelin O-Acyltransferase. Google Patents: 2010.
146. McGovern-Gooch, K. R.; Mahajani, N. S.; Garagozzo, A.; Schramm, A. J.; Hannah, L. G.; Sieburg, M. A.; Chisholm, J. D.; Hougland, J. L., Synthetic Triterpenoid Inhibition of Human

Ghrelin O-Acyltransferase: The Involvement of a Functionally Required Cysteine Provides Mechanistic Insight into Ghrelin Acylation. *Biochemistry* **2017**, *56* (7), 919-931.

147. Takakura, N.; Banno, Y.; Terao, Y.; OCHIDA, A.; Morimoto, S.; Kitamura, S.; Tomata, Y.; Yasuma, T.; IKOMA, M.; Masuda, K., Aromatic ring compound. Google Patents: 2013.

148. Yoneyama-Hirozane, M.; Deguchi, K.; Hirakawa, T.; Ishii, T.; Odani, T.; Matsui, J.; Nakano, Y.; Imahashi, K.; Takakura, N.; Chisaki, I.; Takekawa, S.; Sakamoto, J., Identification and Characterization of a New Series of Ghrelin O-Acyl Transferase Inhibitors. *SLAS Discov* **2017**, 2472555217727097.

149. Galka, C. S.; Hembre, E. J.; Honigschmidt, N. A.; Martinez-Grau, M. A.; PLAZA, G. R.; RUBIO, A., Ghrelin o-acyl transferase inhibitors. Google Patents: 2016.

150. Martinez-Grau, M. A., Substituted piperidyl-ethyl-pyrimidine as ghrelin o-acyl transferase inhibitor. Google Patents: 2015.

151. Darling, J. E.; Prybolsky, E. P.; Sieburg, M.; Houglund, J. L., A fluorescent peptide substrate facilitates investigation of ghrelin recognition and acylation by ghrelin O-acyltransferase. *Anal Biochem* **2013**, *437* (1), 68-76.

152. Taylor, M. S.; Dempsey, D. R.; Hwang, Y.; Chen, Z.; Chu, N.; Boeke, J. D.; Cole, P. A., Mechanistic analysis of ghrelin-O-acyltransferase using substrate analogs. *Bioorg Chem* **2015**, *62*, 64-73.

153. Zhang, J. V.; Ren, P. G.; Avsian-Kretchmer, O.; Luo, C. W.; Rauch, R.; Klein, C.; Hsueh, A. J., Obestatin, a peptide encoded by the ghrelin gene, opposes ghrelin's effects on food intake. *Science* **2005**, *310* (5750), 996-9.

154. Granata, R.; Settanni, F.; Gallo, D.; Trovato, L.; Biancone, L.; Cantaluppi, V.; Nano, R.; Annunziata, M.; Campiglia, P.; Arnoletti, E.; Ghe, C.; Volante, M.; Papotti, M.; Muccioli, G.;

Ghigo, E., Obestatin promotes survival of pancreatic beta-cells and human islets and induces expression of genes involved in the regulation of beta-cell mass and function. *Diabetes* **2008**, *57* (4), 967-79.

155. Gronberg, M.; Tsolakis, A. V.; Magnusson, L.; Janson, E. T.; Saras, J., Distribution of obestatin and ghrelin in human tissues: immunoreactive cells in the gastrointestinal tract, pancreas, and mammary glands. *J Histochem Cytochem* **2008**, *56* (9), 793-801.

156. Guo, Z. F.; Ren, A. J.; Zheng, X.; Qin, Y. W.; Cheng, F.; Zhang, J.; Wu, H.; Yuan, W. J.; Zou, L., Different responses of circulating ghrelin, obestatin levels to fasting, re-feeding and different food compositions, and their local expressions in rats. *Peptides* **2008**, *29* (7), 1247-54.

157. Kellokoski, E.; Kunnari, A.; Jokela, M.; Makela, S.; Kesaniemi, Y. A.; Horkko, S., Ghrelin and obestatin modulate early atherogenic processes on cells: enhancement of monocyte adhesion and oxidized low-density lipoprotein binding. *Metabolism* **2009**, *58* (11), 1572-80.

158. Pradhan, G.; Wu, C. S.; Han Lee, J.; Kanikarla, P.; Guo, S.; Yechoor, V. K.; Samson, S. L.; Sun, Y., Obestatin stimulates glucose-induced insulin secretion through ghrelin receptor GHS-R. *Sci Rep* **2017**, *7* (1), 979.

159. Tsolakis, A. V.; Grimelius, L.; Stridsberg, M.; Falkmer, S. E.; Waldum, H. L.; Saras, J.; Janson, E. T., Obestatin/ghrelin cells in normal mucosa and endocrine tumours of the stomach. *Eur J Endocrinol* **2009**, *160* (6), 941-9.

160. Volante, M.; Rosas, R.; Ceppi, P.; Rapa, I.; Cassoni, P.; Wiedenmann, B.; Settanni, F.; Granata, R.; Papotti, M., Obestatin in human neuroendocrine tissues and tumours: expression and effect on tumour growth. *J Pathol* **2009**, *218* (4), 458-66.

161. Zhao, C. M.; Furnes, M. W.; Stenstrom, B.; Kulseng, B.; Chen, D., Characterization of obestatin- and ghrelin-producing cells in the gastrointestinal tract and pancreas of rats: an immunohistochemical and electron-microscopic study. *Cell Tissue Res* **2008**, *331* (3), 575-87.
162. Morash, M. G.; Gagnon, J.; Nelson, S.; Anini, Y., Tissue distribution and effects of fasting and obesity on the ghrelin axis in mice. *Regul Pept* **2010**, *163* (1-3), 62-73.
163. Bresciani, E.; Rapetti, D.; Dona, F.; Bulgarelli, I.; Tamiazzo, L.; Locatelli, V.; Torsello, A., Obestatin inhibits feeding but does not modulate GH and corticosterone secretion in the rat. *J Endocrinol Invest* **2006**, *29* (8), RC16-8.
164. Green, B. D.; Irwin, N.; Flatt, P. R., Direct and indirect effects of obestatin peptides on food intake and the regulation of glucose homeostasis and insulin secretion in mice. *Peptides* **2007**, *28* (5), 981-7.
165. Nagaraj, S.; Peddha, M. S.; Manjappara, U. V., Fragments of obestatin as modulators of feed intake, circulating lipids, and stored fat. *Biochem Biophys Res Commun* **2008**, *366* (3), 731-7.
166. Nagaraj, S.; Peddha, M. S.; Manjappara, U. V., Fragment analogs as better mimics of obestatin. *Regul Pept* **2009**, *158* (1-3), 143-8.
167. Zhang, J. V.; Jahr, H.; Luo, C. W.; Klein, C.; Van Kolen, K.; Ver Donck, L.; De, A.; Baart, E.; Li, J.; Moechars, D.; Hsueh, A. J., Obestatin induction of early-response gene expression in gastrointestinal and adipose tissues and the mediatory role of G protein-coupled receptor, GPR39. *Mol Endocrinol* **2008**, *22* (6), 1464-75.
168. Brunetti, L.; Leone, S.; Orlando, G.; Recinella, L.; Ferrante, C.; Chiavaroli, A.; Di Nisio, C.; Di Michele, P.; Vacca, M., Effects of obestatin on feeding and body weight after standard or cafeteria diet in the rat. *Peptides* **2009**, *30* (7), 1323-7.

169. Brunetti, L.; Di Nisio, C.; Recinella, L.; Orlando, G.; Ferrante, C.; Chiavaroli, A.; Leone, S.; Di Michele, P.; Shohreh, R.; Vacca, M., Obestatin inhibits dopamine release in rat hypothalamus. *Eur J Pharmacol* **2010**, *641* (2-3), 142-7.
170. Bassil, A. K.; Haglund, Y.; Brown, J.; Rudholm, T.; Hellstrom, P. M.; Naslund, E.; Lee, K.; Sanger, G. J., Little or no ability of obestatin to interact with ghrelin or modify motility in the rat gastrointestinal tract. *Br J Pharmacol* **2007**, *150* (1), 58-64.
171. Chartrel, N.; Alvear-Perez, R.; Leprince, J.; Iturrioz, X.; Reaux-Le Goazigo, A.; Audinot, V.; Chomarar, P.; Coge, F.; Nosjean, O.; Rodriguez, M.; Galizzi, J. P.; Boutin, J. A.; Vaudry, H.; Llorens-Cortes, C., Comment on "Obestatin, a peptide encoded by the ghrelin gene, opposes ghrelin's effects on food intake". *Science* **2007**, *315* (5813), 766; author reply 766.
172. De Smet, D.; Jochmans, K.; Neyns, B., Development of thrombotic thrombocytopenic purpura after a single dose of gemcitabine. *Ann Hematol* **2008**, *87* (6), 495-6.
173. Gourcerol, G.; Million, M.; Adelson, D. W.; Wang, Y.; Wang, L.; Rivier, J.; St-Pierre, D. H.; Tache, Y., Lack of interaction between peripheral injection of CCK and obestatin in the regulation of gastric satiety signaling in rodents. *Peptides* **2006**, *27* (11), 2811-9.
174. Holst, B.; Egerod, K. L.; Schild, E.; Vickers, S. P.; Cheetham, S.; Gerlach, L. O.; Storjohann, L.; Stidsen, C. E.; Jones, R.; Beck-Sickinger, A. G.; Schwartz, T. W., GPR39 signaling is stimulated by zinc ions but not by obestatin. *Endocrinology* **2007**, *148* (1), 13-20.
175. Lauwers, E.; Landuyt, B.; Arckens, L.; Schoofs, L.; Luyten, W., Obestatin does not activate orphan G protein-coupled receptor GPR39. *Biochem Biophys Res Commun* **2006**, *351* (1), 21-5.
176. Nogueiras, R.; Pfluger, P.; Tovar, S.; Arnold, M.; Mitchell, S.; Morris, A.; Perez-Tilve, D.; Vazquez, M. J.; Wiedmer, P.; Castaneda, T. R.; DiMarchi, R.; Tschop, M.; Schurmann, A.;

Joost, H. G.; Williams, L. M.; Langhans, W.; Dieguez, C., Effects of obestatin on energy balance and growth hormone secretion in rodents. *Endocrinology* **2007**, *148* (1), 21-6.

177. Samson, W. K.; White, M. M.; Price, C.; Ferguson, A. V., Obestatin acts in brain to inhibit thirst. *Am J Physiol Regul Integr Comp Physiol* **2007**, *292* (1), R637-43.

178. Sibilgia, V.; Bresciani, E.; Lattuada, N.; Rapetti, D.; Locatelli, V.; De Luca, V.; Dona, F.; Netti, C.; Torsello, A.; Guidobono, F., Intracerebroventricular acute and chronic administration of obestatin minimally affect food intake but not weight gain in the rat. *J Endocrinol Invest* **2006**, *29* (11), RC31-4.

179. Tremblay, F.; Perreault, M.; Klaman, L. D.; Tobin, J. F.; Smith, E.; Gimeno, R. E., Normal food intake and body weight in mice lacking the G protein-coupled receptor GPR39. *Endocrinology* **2007**, *148* (2), 501-6.

180. Van Dijck, A.; Van Dam, D.; Vergote, V.; De Spiegeleer, B.; Luyten, W.; Schoofs, L.; De Deyn, P. P., Central administration of obestatin fails to show inhibitory effects on food and water intake in mice. *Regul Pept* **2009**, *156* (1-3), 77-82.

181. Yamamoto, D.; Ikeshita, N.; Daito, R.; Herningtyas, E. H.; Toda, K.; Takahashi, K.; Iida, K.; Takahashi, Y.; Kaji, H.; Chihara, K.; Okimura, Y., Neither intravenous nor intracerebroventricular administration of obestatin affects the secretion of GH, PRL, TSH and ACTH in rats. *Regul Pept* **2007**, *138* (2-3), 141-4.

182. Zizzari, P.; Longchamps, R.; Epelbaum, J.; Bluet-Pajot, M. T., Obestatin partially affects ghrelin stimulation of food intake and growth hormone secretion in rodents. *Endocrinology* **2007**, *148* (4), 1648-53.

183. Kobelt, P.; Wisser, A. S.; Stengel, A.; Goebel, M.; Bannert, N.; Gourcerol, G.; Inhoff, T.; Noetzel, S.; Wiedenmann, B.; Klapp, B. F.; Tache, Y.; Monnikes, H., Peripheral obestatin has no effect on feeding behavior and brain Fos expression in rodents. *Peptides* **2008**, *29* (6), 1018-27.
184. Mondal, M. S.; Toshinai, K.; Ueno, H.; Koshinaka, K.; Nakazato, M., Characterization of obestatin in rat and human stomach and plasma, and its lack of acute effect on feeding behavior in rodents. *J Endocrinol* **2008**, *198* (2), 339-46.
185. Unniappan, S.; Speck, M.; Kieffer, T. J., Metabolic effects of chronic obestatin infusion in rats. *Peptides* **2008**, *29* (8), 1354-61.
186. Gao, X. Y.; Kuang, H. Y.; Liu, X. M.; Ma, Z. B.; Nie, H. J.; Guo, H., Plasma obestatin levels in men with chronic atrophic gastritis. *Peptides* **2008**, *29* (10), 1749-54.
187. Seim, I.; Walpole, C.; Amorim, L.; Josh, P.; Herington, A.; Chopin, L., The expanding roles of the ghrelin-gene derived peptide obestatin in health and disease. *Mol Cell Endocrinol* **2011**, *340* (1), 111-7.
188. Ataka, K.; Inui, A.; Asakawa, A.; Kato, I.; Fujimiya, M., Obestatin inhibits motor activity in the antrum and duodenum in the fed state of conscious rats. *Am J Physiol Gastrointest Liver Physiol* **2008**, *294* (5), G1210-8.
189. Fujimiya, M.; Asakawa, A.; Ataka, K.; Kato, I.; Inui, A., Different effects of ghrelin, des-acyl ghrelin and obestatin on gastroduodenal motility in conscious rats. *World J Gastroenterol* **2008**, *14* (41), 6318-26.

## **Chapter 2: Proghrelin and C-ghrelin: Expression, purification and structural analysis**

The work presented in this chapter is unpublished. In this chapter, there was experimental contribution from Carlos A. Castañeda (Syracuse University), performed the nuclear magnetic resonance analysis and interpretation for structural characterization of proghrelin.

## 2.1 Introduction

Following the initial discovery of GOAT and its role in ghrelin maturation,<sup>1-2</sup> there was interest in the mechanism by which this enzyme modifies its biological substrate proghrelin.<sup>3</sup> In a second study from the Brown and Goldstein laboratory following their initial discovery of GOAT,<sup>2</sup> recombinantly expressed mouse proghrelin-His<sub>8</sub> was utilized for GOAT octanoylation assays. They used a GST-TEV-mouse-proghrelin-His<sub>8</sub> fusion construct to express the gene in *E. coli*.<sup>3</sup> It was purified using glutathione-agarose beads and proghrelin-His<sub>8</sub> was liberated using a TEV protease. After the TEV cleavage; nickel affinity chromatography, dialysis, and concentration were all used to yield purified proghrelin-His<sub>8</sub>.<sup>3</sup> Their substrate selectivity studies used proghrelin-His<sub>8</sub> to study GOAT octanoylation by incubating recombinantly expressed proghrelin-His<sub>8</sub> with mouse GOAT (mGOAT)-containing membrane fraction in the presence of [<sup>3</sup>H]octanoyl-CoA.<sup>3</sup> Following the octanoylation reaction, the proghrelin-His<sub>8</sub> was isolated utilizing nickel-coated beads and octanoylation was detected by liquid scintillation counting.<sup>3</sup> This study was the first instance of recombinant expression and purification of mouse proghrelin. This investigation also focused on the N-terminal region and alanine mutations and looked at no other factors influencing proghrelin GOAT interactions.<sup>3</sup> Subsequent studies used small peptides to investigate GOAT octanoylation, with the longest sequence being full-length ghrelin (1-28), with the first five N-terminal amino acids to be the predominant motif for GOAT recognition.<sup>4-7</sup> In contrast, the C-terminal sequence of proghrelin or the full-length protein has not been extensively studied.

Moving forward from biochemical and functional studies, there has been no investigation into the structure of full-length proghrelin but a small number into the hormones produced from

proghrelin, ghrelin and obestatin.<sup>8-10</sup> After the initial discovery of ghrelin, there was investigation into the necessary recognition motifs of acylated ghrelin to its cognate receptor GHS-R1a.<sup>11</sup> Knowing the requirements for receptor binding was of interest since GHS-R1a recognition is necessary for ghrelin's biological effects.<sup>11-14</sup> There have been two studies using molecular dynamics to investigate ghrelin's structure in relation to its receptor.<sup>15-16</sup> Their studies indicated that ghrelin (acylated) has secondary structural in the form of an alpha helix from residues P7 to E17 and a backwards folding loop from E17 to K20. This helix was present in either simply water or when a lipid membrane was introduced.<sup>15-16</sup> There was also a conclusion that the octanoylated S3 and residue F4 form a rigid structure that acts as an anchor in the plasma membrane.<sup>15-16</sup> To study the environment of the GHS-R1a located in the plasma membrane and its relation to ghrelin structure, further structural studies employing circular dichroism (CD) used the addition of sodium dodecyl sulfate (SDS) micelles and trifluoroethanol (TFE) which act to induce structure in proteins.<sup>15</sup> For both desacyl and acylated ghrelin, the presence of SDS or TFE lead to the formation of an alpha helix from P7 to S18.<sup>17</sup> There has also been investigation into the secondary structure of desacyl and acylated ghrelin using <sup>1</sup>H NMR (nuclear magnetic resonance) to identify structural features.<sup>17-20</sup> Using CD and NMR there was a similar structure found in previous studies, in which they concluded that there is formation of a small alpha helix between P7 and Q14 only if SDS (40-80 mM, CMC for SDS is 7-10 mM) or a structure-stabilizing agent such as hexafluoroacetone (HFA) (25-80% v/v) was present.<sup>18</sup> There was no concentration dependence of SDS in relation to ghrelin structure but there was concentration dependency in relation with HFA addition.<sup>18</sup> Based upon these analytical methods and structural modeling, there was a conclusion that there is a small helical core in ghrelin in the presence of lipids (structural agents) but it is a mostly flexible peptide that goes through multiple

conformations.<sup>20</sup> In juxtaposition to the previously reported studies which used the addition of structuring agents, CD spectra were measured for both acylated ghrelin (1-28) and acylated ghrelin (1-5), in a purely aqueous environment. Both ghrelin sequences exhibited features consistent with random coil conformation and lack of a defined secondary structure.<sup>19</sup> This data was supported by <sup>1</sup>H NMR studies indicating a lack of structure present in acylated ghrelin. Further analysis using 2D NMR, TOCSY (total correlation spectroscopy) and NOESY (nuclear Overhauser effect spectroscopy), demonstrated that the chemical shifts were not greatly dispersed which indicates that both desacyl and acylated ghrelin are mostly random coil and unstructured.<sup>19</sup> These studies were all non-buffered and in an aqueous solution in the absence of any lipids or detergent. The sample environment could impact any potential structural elements and is probably why these results are different from other published results. The structural investigation including the use of molecular dynamics, CD, and NMR conclude that ghrelin has a flexible structure that is random coil in an aqueous solution. This conformation changes when a membrane-like domain is present (including SDS) or a fluorinated structuring agent such as TFE or HFA. There was no indication that ghrelin's structure impacted binding to its receptor but simulations with GOAT or implication to GOAT-ghrelin binding was not evaluated in any study.

The interest in obestatin and the initial evidence that it plays a role in human health motivated structural studies of this peptide.<sup>21-23</sup> Similar to ghrelin, CD spectra of obestatin in pure water indicates that little secondary structure is present.<sup>23</sup> When TFE, up to 70%, was added there was some formation of helical characteristics.<sup>23</sup> NMR analysis of obestatin using the fingerprint region of NOESY (correlations between backbone NH signals and backbone CHα signals) in the presence of 33% TFE showed secondary structure, mainly single turn helix conformation between residues P4 and Q15 and H19 and A22 respectively.<sup>23</sup> The majority of the

secondary structural elements were mapped in the C-terminal half of this 23 amino acid peptide from peak shifts during NMR analysis, with the first 10 residues having no structural characteristics. Other studies of obestatin (or obestatin (11-23)) structure included lipids solution with obestatin based on the hypothesis that contact with a membrane or membrane-like lipid/detergent aggregate was essential for obestatin structure formation.<sup>21-22, 24</sup> This model was supported by circular dichroism studies with detection of secondary structure (alpha helix) in the presence of SDS that was not observed in buffer alone.<sup>21-22</sup> In NMR studies, inclusion of lipids resulted in peak dispersion reflecting the presence of stable secondary structure (alpha helix) with both TOCSY and NOESY.<sup>21</sup> Chemical shift values from this study agree with previously mentioned ones that indicated that a majority of peaks associated with secondary structure were present in the C-terminal region of obestatin.

In contrast to ghrelin and obestatin as described above, there has been a limited effort to further explore the potential for proghrelin structure to impact proghrelin recognition, binding and modification by GOAT. The study of human proghrelin and human GOAT has more therapeutic and biological relevancy since the goal of any work is to relate it to human subjects. The only characterization of GOAT's substrate has been in its mouse form. Sequence alignment between mouse and human proghrelin showed that they share 86% conservation and 100% similarity (Figure 2.1), differences mainly arriving from differences in their C-terminal portions. Characterizing the structure of human proghrelin is crucial to understanding the enzyme-substrate relationship between proghrelin and GOAT, which will inform inhibitor design and aid in the identification of potential substrate-enzyme contact points outside of the active site.

```

BAA89371.1 human proghrelin 1 GSSFLSPEHQRVQQRKESKKPPAKLQPRALAGWLRPEDGGQAEGAEDELEVRFNAPFDVG
AAI32231.1 mouse proghrelin 1 GSSFLSPEHQKAQQRKESKKPPAKLQPRALEGWLHPEDRGQAEEETEELEIRFNAPFDVG
*****  *****  ***  ***  ***  *  ***  *****

BAA89371.1 human proghrelin 61 IKLSGVQYQQHSQALGKFLQDILWEEAKEAPADK
AAI32231.1 mouse proghrelin 61 IKLSGAQYQQHGRALGKFLQDILWEEVKEAPADK
*****  *****  *****  *****

```

**Figure 2.1. Human and mouse proghrelin (1-94) protein sequence alignment.** Sequence alignment was done using Clustal W. Stars under the sequences indicate the residue is conserved across the two species, gaps indicate that the residue is not conserved.

## 2.2 Results

### 2.2.1 Human proghrelin expression system

To facilitate structural and functional investigations of human proghrelin, a bacterial expression system was designed for expressing proghrelin in the context of a fusion protein construct. The proghrelin gene was designed to include an N-terminal Glutathione *S*-transferase tag (GST-tag) to improve solubility and provide the capability for GST affinity purification, a TEV protease site for removal of GST from proghrelin, and a C-terminal His<sub>6</sub> tag for affinity purification and Western blotting.<sup>25</sup> This gene design mirrors the proghrelin expression system that Yang and coworkers used to express mouse proghrelin in their studies.<sup>2-3</sup> The complete fusion protein encoded by the GThPH (GST-TEV-human Proghrelin-His6) gene would be 328 amino acids (38.02 kDa), with TEV cleavage liberating the 100- amino acid proghrelin-His<sub>6</sub> (11.3 kDa). The gene insert was synthesized commercially (Genewiz) and provided in a pUC57 vector, with the GThPH insert then subcloned into the pET23a plasmid for protein expression using BL21 (DE3) *E. coli*.<sup>26</sup> In a similar effort to explore the impact of the processing products of proghrelin, a gene construct for the C-terminal portion of proghrelin, which remains following ghrelin excision (C-ghrelin), was designed with the same affinity tags as proghrelin. This gene used the same parent plasmid, GThPH, with an enzymatic restriction site inserted so C-ghrelin could be inserted and ligated. The GThCgH (GST-TEV-human C-ghrelin-His6) gene would be 303 amino acids (35.1 kDa), with TEV cleavage liberating a 74 amino acid (including 2 extra amino acids added during *HINDIII* restriction site insertion) C-ghrelin-His<sub>6</sub> (8.3 kDa).

### 2.2.2 Induction method optimization for proghrelin-His<sub>6</sub>

The classical method for protein expression using the T7-lac induction system uses a lactose analog, isopropyl  $\beta$ -D-1-thiogalactopyranoside (IPTG), to induce gene expression.<sup>27</sup> When IPTG induction (0.4 mM) was used to express GThPH (Figure 2.1A) there was protein detected during lysis only in the presence of a denaturing lysis buffer (3XSB, 3X SDS sample buffer, which shows full protein content of the cell) instead of in the non-denaturing lysis buffer (BPER (Thermo scientific), bacterial protein extraction reagent, which extracts only soluble protein during lysis). This result indicated that insoluble inclusion bodies had formed which often reflects protein misfolding and aggregation (Figure 2.2A). In light of insoluble GThPH expression with IPTG induction, protein expression using autoinduction media was explored to attempt to increase the production of soluble protein. Autoinduction media, which contains a mixture of glucose, glycerol and lactose, results in a more gradual induction of recombinant protein expression.<sup>28</sup> When GThPH was expressed using this method in BL21 (DE3) *E. coli*, the fusion protein expressed was observed in the soluble protein fraction of the bacterial lysate (Figure 2.2B). Expression of GThPH was further confirmed with both Anti-GST and Anti-His Western blotting (Figure 2.3 A-B). There was the appearance of lower molecular weight proteins between 25-35 kDa which were GST-tagged, based upon the Anti-GST western blot (Figure 2.3B). This behavior is likely the result of protein cleavage and is discussed in detail in Chapter 3. Optimization of the growth conditions including time, temperature and culture size all contributed to the level of protein expression observed.

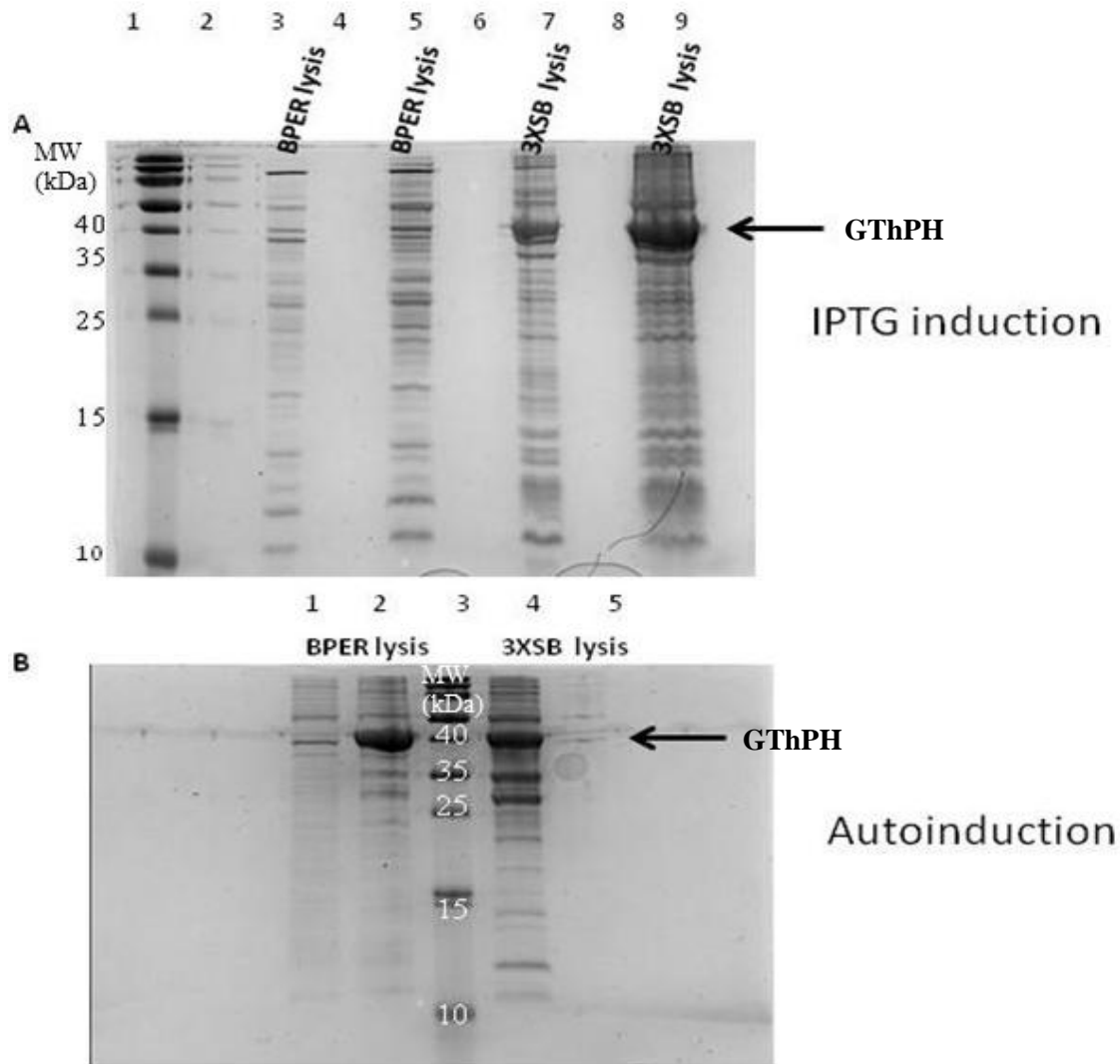


**Figure 2.2. Expression analysis of recombinantly expressed GThPH. A) Expression analysis of IPTG-induced GThPH.** 1mL bacterial pellets from two growths were lysed using BPER reagent or 3XSB. The gel is 12% polyacrylamide. Lane 1, protein ladder (Thermo scientific); Lane 3, BPER lysis; Lane 5, BPER lysis of growth 2; Lane, 7 3XSB lysis; Lane 9, 3XSB lysis of growth 2. **B) Autoinduction expression analysis of GThPH.** 1mL bacterial pellets were lysed using BPER reagent or 3XSB from one growth. The gel is 12% polyacrylamide. Lane 1, pET23a lysed with B-PER; Lane 2, GThPH lysed with B-PER; Lane 3, protein ladder (Thermo scientific); Lane 4, GThPH lysed with 3XSB; Lane5, pET23a lysed with 3XSB.

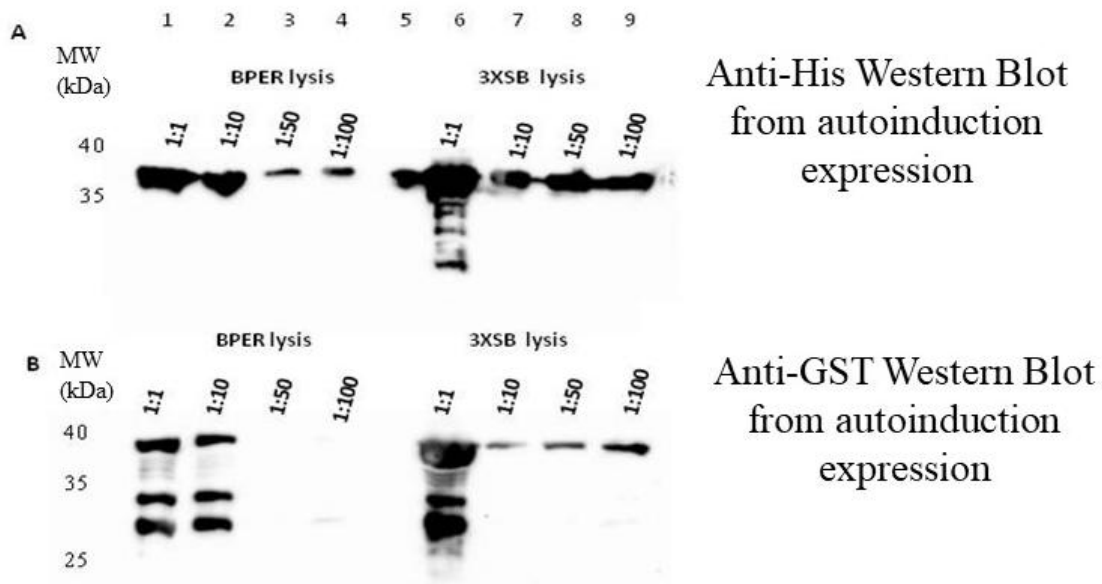


**Figure 2.3. Western blot analysis of recombinantly expressed GThPH. A) Anti-His western of the autoinduction expression of GThPH.** The membrane was blotted with Anti-His-HRP conjugated antibody. The gel is 12% polyacrylamide. Molecular weight marker is to the left of lane 1. Lane 1, BPER lysis 1x; Lane 2, BPER lysis 1/10x; Lane 3, BPER lysis 1/50x; Lane 4, BPER lysis 1/100x; Lane 6, 3X sample buffer lysis 1x; Lane 7, 3X sample buffer lysis 1/10x; Lane 8, 3X sample buffer 1/50x; Lane 9, 3X sample buffer lysis 1/100x. **B) Anti-GST western of the autoinduction expression of GThPH.** The membrane was blotted with Anti-GST-HRP conjugated antibody. The gel is 12% polyacrylamide. Molecular weight marker is to the left of Lane 1. Lane 1, BPER lysis 1x; Lane 2, BPER lysis 1/10x; Lane 3, BPER lysis 1/50x; Lane 4, BPER lysis 1/100x; Lane 5, Space; Lane 6, 3XSB lysis 1x; Lane 7, 3XSB lysis 1/10x; Lane 8, 3XSB 1/50x; Lane 9, 3XSB lysis 1/100x.

### **2.2.3 C-ghrelin insolubility utilizing autoinduction**

The efforts to induce GThCgH in the same manner as proghrelin (GThPH) did not yield soluble protein. When GThCgH was expressed using autoinduction media, very little soluble protein expression was observed with the majority of protein present in the insoluble fraction (Figure 2.4A). Further analysis of the cell pellet remaining after non-denaturing bacterial lysis indicated that the majority of GThCgH was in inclusion bodies (Figure 2.4B). This loss of soluble expression for GThCgH compared to the proghrelin construct GThPH was unexpected and potentially reflects differences in protein structure and an increase in instability between proghrelin and C-ghrelin. Attempts to increase GThCgH solubility by autoinduction expression at a lower temperature were unsuccessful.

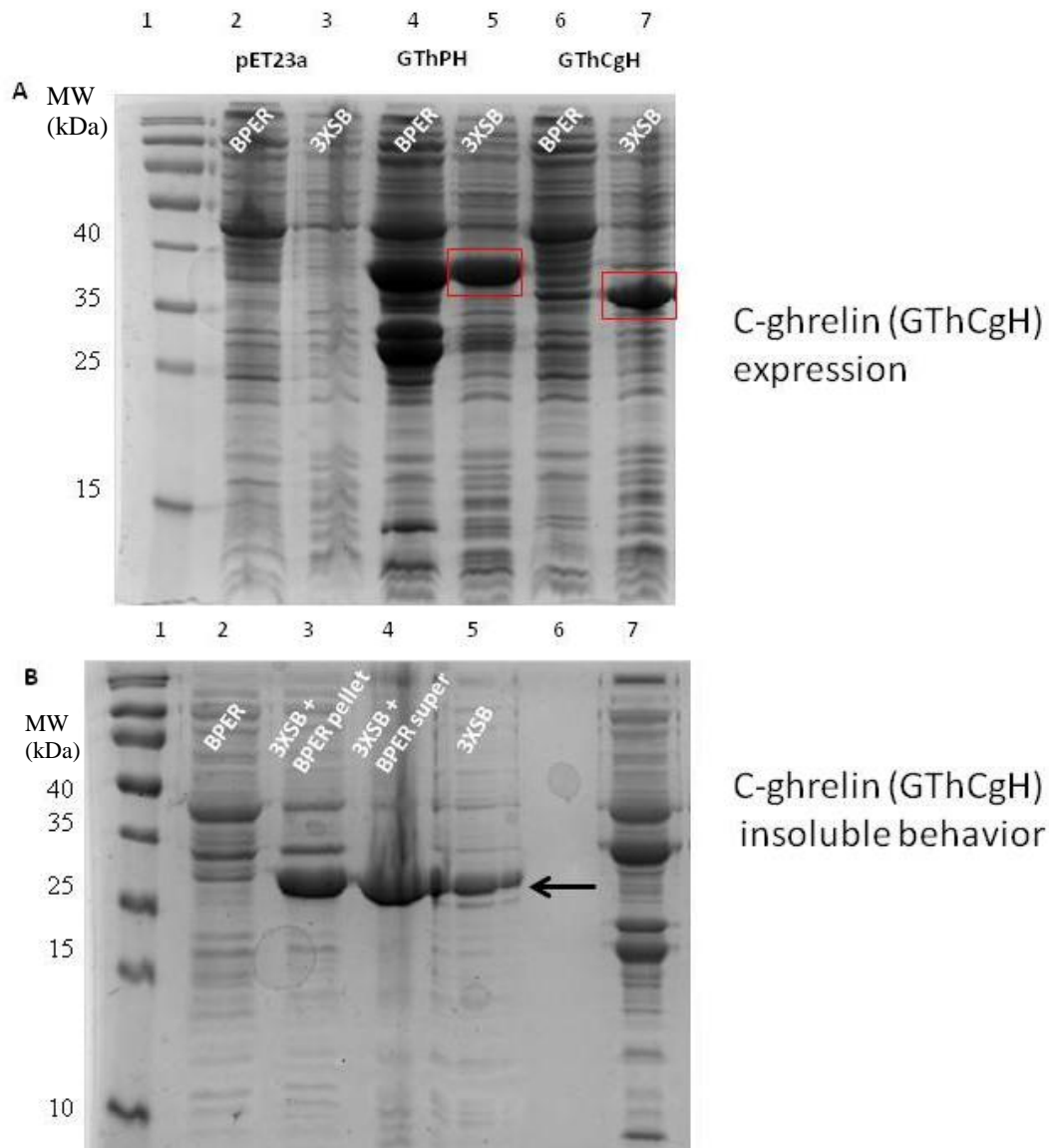


**Figure 2.4. GThCgH autoinduction expression analysis. A) GThCgH autoinduction expression.** 1mL bacterial pellets are lysed using BPER and 3X sample buffer, parental proteins are boxed in red. The gel is 12% polyacrylamide. Lane 1, protein ladder (Thermo scientific); Lane 2, pET23a BPER lysis; Lane 3, pET23a 3XSB lysis; Lane 4, GThPH BPER lysis; Lane 5, GThPH 3XSB lysis; Lane 6, GThCgH BPER lysis; Lane 7, GThCgH 3XSB lysis. **B) GThCgH insoluble expression characterized.** Bacterial pellets lysed using BPER reagent, the supernatant removed, and the pellet was subsequently lysed using 3XSB; to confirm insoluble behavior another pellet was lysed using only 3XSB. The gel is 12% polyacrylamide. Lane 1, protein ladder (Thermo scientific); Lane 2, GThCgH BPER lysed pellet; Lane 3, BPER'd pellet lysed using 3XSB; Lane 4, GThCgH 3XSB lysis; Lane 5, GThCgH BPER lysis vortex then 3X SDS sample buffer was added; Lane 7, GThPH BPER lysis.

#### 2.2.4 C-ghrelin expression optimization

As autoinduction methods were not efficient in producing soluble GThCgH (Figure 2.5), IPTG-based induction (0.4 mM IPTG) was explored for GThCgH expression using a temperature range used from 16-28 °C. A low but detectable level of soluble C-ghrelin expression was observed at 16 °C. To attempt to further increase the expression of soluble GThCgH, the expression host was changed from BL21 (DE3) *E. coli* to LEMO-21 *E. coli*, which have been shown to facilitate expression of insoluble proteins through concurrent induction of lysozyme expression using rhamnose induction.<sup>29</sup> This change to another cell line as well as the optimization of time, temperature, and the concentration of rhamnose (1 mM was optimal) during protein induction lead to an increase in the yield of GThCgH expression.

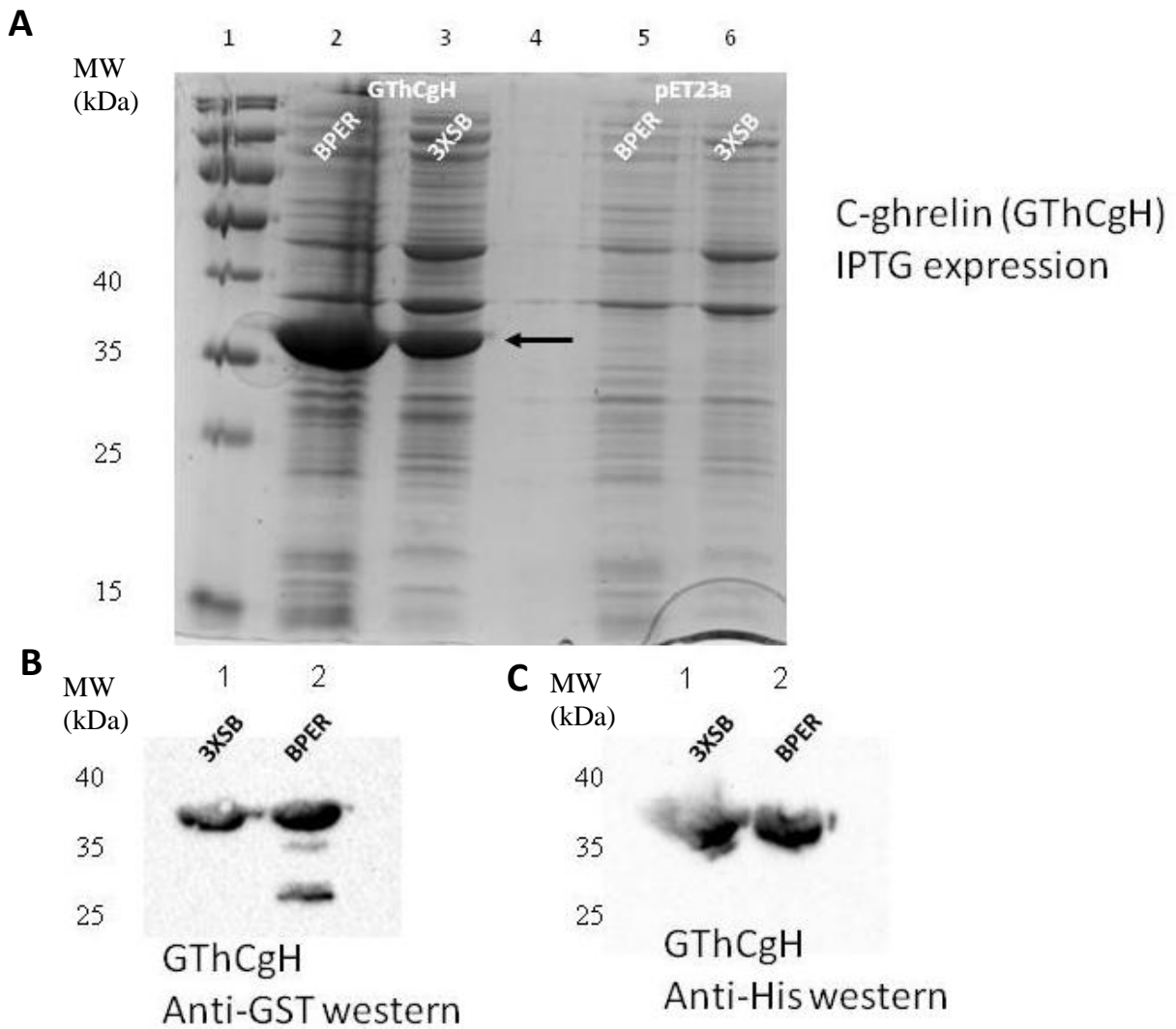


**Figure 2.5. IPTG induction of GThCgH expression. A) GThCgH expression analysis.**

Bacterial pellets of IPTG-induced cultures (0.4 mM IPTG) were lysed using BPER and 3XSB.

The gel is 12% polyacrylamide. Lane 1, protein ladder (Thermo scientific); Lane 2, GThCgH

3XSB lysis; Lane 3, GThCgH BPER lysis; Lane 5, pET23a 3XSB lysis; Lane 6, pET23a BPER

lysis. **B) Expression analysis Anti-GST western blot.** Bacterial proteins were detected using an

Anti-GST-HRP conjugated antibody. The gel is 12% polyacrylamide. Molecular weight marker

is to the left of Lane 1. Lane 1, GThCgH 3XSB lysis; Lane 2, GThCgH BPER lysis. **C)**

**Expression analysis Anti-His western blot.** Bacterial proteins were detected using an Anti-His-

HRP conjugated antibody. Molecular weight marker is to the left of Lane 1. The gel is 12%

polyacrylamide. Molecular weight marker is to the left of Lane 1. Lane 1, GThCgH 3XSB lysis;

Lane 2, GThCgH BPER lysis.

## 2.2.5 Purification method for proghrelin-His<sub>6</sub>

### 2.2.5.1 Ni<sup>2+</sup>-Sephacrose Purifications

To obtain purified proghrelin-His<sub>6</sub>, an initial proposed scheme was to affinity purify GThPH from bacterial lysate, perform a TEV protease digestion, to cleave GST from GThPH, and affinity purify proghrelin-His<sub>6</sub> away from GST and the TEV protease. The first method attempted to purify GThPH from bacterial lysate utilized the His<sub>6</sub> tag present in the C-terminus of the protein. Following preparative-scale GThPH expression, the bacterial pellet was lysed by sonication and GThPH was purified from the bacterial lysate utilizing a HisTrap Fast Flow (FF) Ni<sup>2+</sup>-Sephacrose High Performance column (GE). Purifications utilized two different elution methods, stepwise elution in which the elution starts at 20 mM imidazole and then directly increases to 250 mM imidazole and a gradient elution in which the elution starts at 20 mM imidazole and gradually increases over a given volume to 250 mM imidazole. The length of the gradient was modified from a short to a longer time course; however, none of these efforts improved the purity directly out of the lysate (Figure 2.6A). The stepwise elution resulted in better purity than the gradient elution, but there were still contaminant proteins that persisted throughout the initial Ni<sup>2+</sup>-IMAC purification. In the first attempts at purifying GThPH from bacterial lysate there were appearances of lower molecular weight proteins (proteins between 35-25 kDa) in the sample which impeded homogeneity.

Since there were a plethora of impurities present in the eluted fractions after Ni<sup>2+</sup>-Sephacrose column, another IMAC column was substituted to investigate whether it would improve purity. The Co<sup>2+</sup>-HiTrap TALON crude column (GE) yielded no improvement in

purification of GThPH using stepwise elution. In both cases, Ni<sup>2+</sup>-Sephrose and Co<sup>2+</sup>-Agarose based columns produced the same result heterogeneity in eluted fractions (Figure 2.6B).

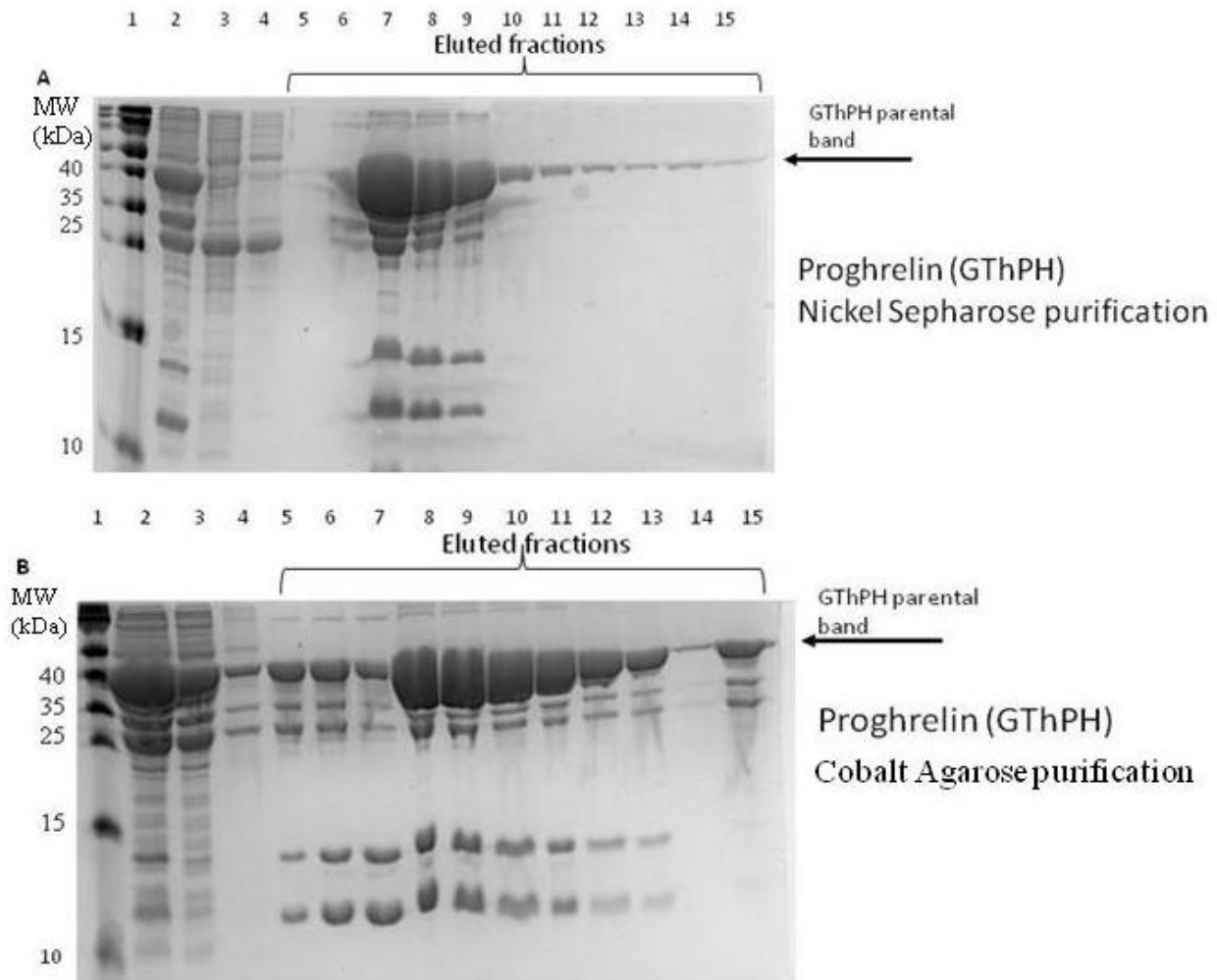


**Figure 2.6. FPLC purification of GThPH from bacterial lysate. A)  $\text{Ni}^{2+}$ -IMAC FPLC purification.** Bacterial lysate after sonication was loaded onto a HisTrap FF column. Eluted fractions were collected from under the A280 peak using a Step-wise elution method. The gel is 12% polyacrylamide. Lane 1, protein ladder (Thermo scientific); Lane 2, Loaded crude lysate of GThPH; Lane 3, flow-through; Lane 4, wash with lysis buffer; Lane 5, fraction #10; Lane 6, fraction # 12; Lane 7, fraction #14; Lane 8, fraction #16; Lane 9, fraction #17; Lane 10, fraction #18; Lane 11, fraction #20; Lane 12, fraction #22; Lane 13, fraction #24; Lane 14, fraction #26; Lane 15, fraction #30. **B)  $\text{Co}^{2+}$ -HiTrap TALON (IMAC) FPLC purification.** Bacterial lysate after sonication was loaded onto a  $\text{Co}^{2+}$ -TALON column. Eluted fractions were collected from under the A280 peak using a Step-wise elution method. The gel is 12% polyacrylamide. Lane 1, protein ladder (Thermo scientific); Lane 2, Loaded crude lysate of GThPH; Lane 3, flow-through; Lane 4, wash with lysis buffer; Lane 5, fraction #24; Lane 6, fraction #25; Lane 7, fraction #26; Lane 8, fraction #27; Lane 9, fraction #28; Lane 10, fraction #29; Lane 11, fraction #30; Lane 12, fraction #31; Lane 13, fraction #32; Lane 14, fraction #33; Lane 15, fraction #34.

The next step in the proghrelin-His<sub>6</sub> purification was a TEV digestion using TEV-His<sub>6</sub> protease (prepared from bacterial lysate using a HisTrap FF Ni<sup>2+</sup>-Sepharose High Performance column (GE)) which cleaves the GST tag from GThPH yielding proghrelin-His<sub>6</sub>. Cleavage by TEV-His<sub>6</sub> protease is observable via the loss of the parental GThPH band and the appearance of a 25 kDa band equivalent to GST and an approximately 12 kDa band which is proghrelin-His<sub>6</sub> (Figure 2.7A). The most efficient GThPH: TEV-His<sub>6</sub> ratio was determined to be 2000:1, which was observed to digest completely over 48 hours (Figure 2.7B). However, a ratio of 200:1(GThPH: TEV-His<sub>6</sub> protease) was used throughout purifications since this ratio digested GThPH in a shorter time compared to a 2000:1 ratio and resulted in reduced lower molecular weight impurities. Western blot analysis confirmed TEV-His<sub>6</sub> cleavage with production of cleavage products at the appropriate molecular weights, confirmation of the fragment containing the GST tag using an Anti-GST antibody and proghrelin-His<sub>6</sub> and TEV-His<sub>6</sub> detected using an Anti-His antibody. There was also a number of lower molecular weight protein bands observed in the digestion reaction which were not bound by either Anti-GST or Anti-His antibodies.

Purification of the TEV digestion reaction utilizing a Ni<sup>2+</sup>-IMAC column should afford the two His<sub>6</sub>-tagged proteins in the reaction, proghrelin-His<sub>6</sub> and TEV-His<sub>6</sub>. However, this second Ni<sup>2+</sup>-IMAC purification proved ineffective for generating the desired level of proghrelin-His<sub>6</sub> purity with the presence of lower molecular weight protein impurities (Figure 2.8).

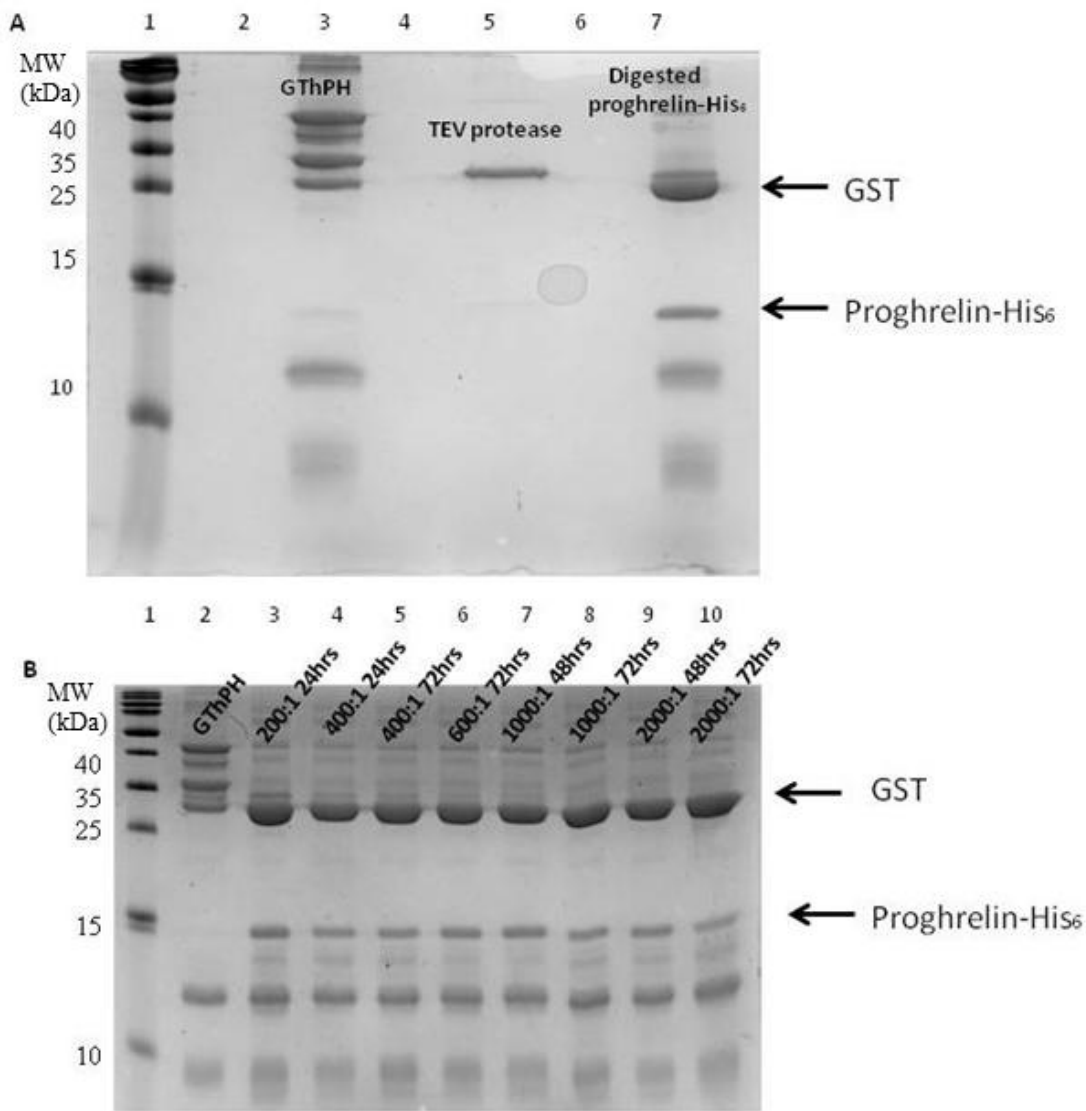


**Figure 2.7. TEV digestion analysis of GThPH** **A) TEV digestion of GThPH.** GThPH after a Ni<sup>2+</sup>-IMAC purification was incubated with TEV-His<sub>6</sub> protease and the digestion was analyzed. The 38 kDa band is GThPH, 26 kDa band is GST, and 12 kDa band is proghrelin-His<sub>6</sub>. The gel is 12% polyacrylamide. Lane 1, protein ladder (Thermo scientific); Lane 3, GThPH without TEV protease; Lane 5, TEV protease; Lane 7, GThPH with TEV protease. **B) TEV protease digestion of GThPH with varying reaction conditions.** GThPH after a Ni<sup>2+</sup>-IMAC purification was incubated with TEV-His<sub>6</sub> protease under varying conditions, GThPH: TEV ratio and time (hrs), rxn indicates reaction. The 38 kDa band is GThPH, 26 kDa band is GST, and 12 kDa band is proghrelin-His<sub>6</sub>. The gel is 12% polyacrylamide. Lane 1, protein ladder (Thermo scientific); Lane 2, GThPH without TEV; Lane 3, 200:1 rxn 24hrs (positive control); Lane 4, 400:1 rxn; 24hrs; Lane 5, 400:1 rxn 72hrs; Lane 6, 600:1 rxn 72 hrs; Lane 7, 1000:1 48 hrs; Lane 8, 1000:1 rxn 72hrs; Lane 9, 2000:1 rxn 48hrs; Lane 10, 2000:1 rxn 72hrs.

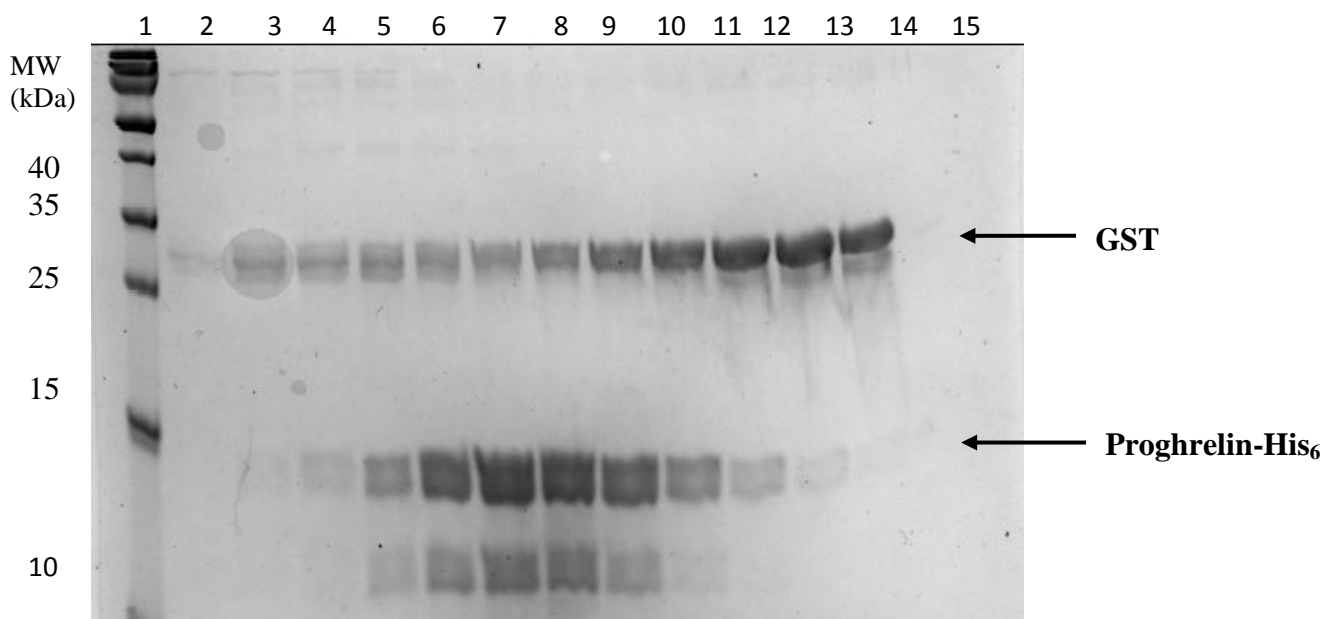


**Figure 2.8. Ni<sup>2+</sup>-IMAC purification following TEV digestion of GThPH.** The fusion protein GThPH (193 mg) was digested using TEV-His<sub>6</sub> protease (1930 µg). After digestion the GThPH mixture was purified using Ni<sup>2+</sup>-IMAC column and fractions were collected from the second A280 peak using a step-wise elution method. The gel is 15% polyacrylamide. Lane 1, protein ladder (Thermo scientific); Lane 2, Fraction # 17; Lane 3 Fraction #18; Lane 4, Fraction #19; Lane 5, Fraction #20; Lane 6, Fraction #21; Lane 7, Fraction #22; Lane 8, Fraction #23; Lane 9, Fraction #24; Lane 10, Fraction #25; Lane 11, Fraction # 26; Lane 12, Fraction #27; Lane 13, Fraction # 28.

### 2.2.5.2 Proghrelin purity improved after GST-Sepharose added to purification

In light of this lack of homogeneity, the purification procedure for GThPH and proghrelin-His<sub>6</sub> was redesigned by introducing a GST affinity purification step using a GSTrap FF (fast flow) High Performance GST-Sepharose affinity column (GE) into the purification, as well as the introduction of a GST-tagged TEV-His<sub>6</sub> protease provided as a gift by Dr. Michael Cosgrove (SUNY Upstate Medical University).

For GST affinity purification of GThPH, the same lysis procedure was used for GThPH from BL21 (DE3) *E. coli* as was described above, followed by purification using a GST-Sepharose column which utilizes the attraction of the GST-tag to immobilized glutathione. The GThPH fusion protein was effectively enriched from the cell lysate using the GST-Sepharose column (Figure 2.9A). This method was optimized using a gradient-based elution and glutathione as the competitor, with flow rate is much lower compared to a HisTrap FF column (0.5 mL/min compared to 5 mL/min) and sample/volume size are markedly larger since the binding kinetics appeared slower with GST-Sepharose compared to Ni<sup>2+</sup>-Sepharose resin. Compared to purification using the His<sub>6</sub> tag, GST affinity purification as the first step of the purification method markedly increased the purity of the protein sample from bacterial lysate. Following the GSTrap purification, TEV protease digestion was performed using a GST-TEV-His<sub>6</sub> protease which allows for removal of both the cleaved GST tag and GST-TEV-His<sub>6</sub> protease by another GST-Sepharose column. However, this second GST-Sepharose column was inefficient in depleting sufficient GST-containing from the digestion reaction to allow the desired level of purification of proghrelin-His<sub>6</sub>.

With tandem GST affinity purifications proving ineffective, the His<sub>6</sub> affinity tag of proghrelin-His<sub>6</sub> provides an orthogonal affinity purification option for post-digestion purification of proghrelin-His<sub>6</sub>. The GST-TEV-His<sub>6</sub> protease, as well as, the GST cleavage products all lack a metal affinity tag making it was less likely that these proteins would be retained on the Ni<sup>2+</sup>-IMAC column. After digestion with the GST-TEV-His<sub>6</sub> protease, the digestion reaction was purified using a Ni<sup>2+</sup>-IMAC column. The eluted fractions containing proghrelin-His<sub>6</sub> were depleted of GST-containing proteins and an overall improvement in proteins purity was obtained compared to previous approaches (Figure 2.9B). However, the small molecular weight protein impurities persisted through the Ni<sup>2+</sup>-IMAC purification. The molecular weight differences between the protein impurities and proghrelin-His<sub>6</sub> suggest that size exclusion chromatography would serve as an appropriate final purification step. Size exclusion chromatography (SEC) was integrated into the procedure to obtain purified proghrelin-His<sub>6</sub>.

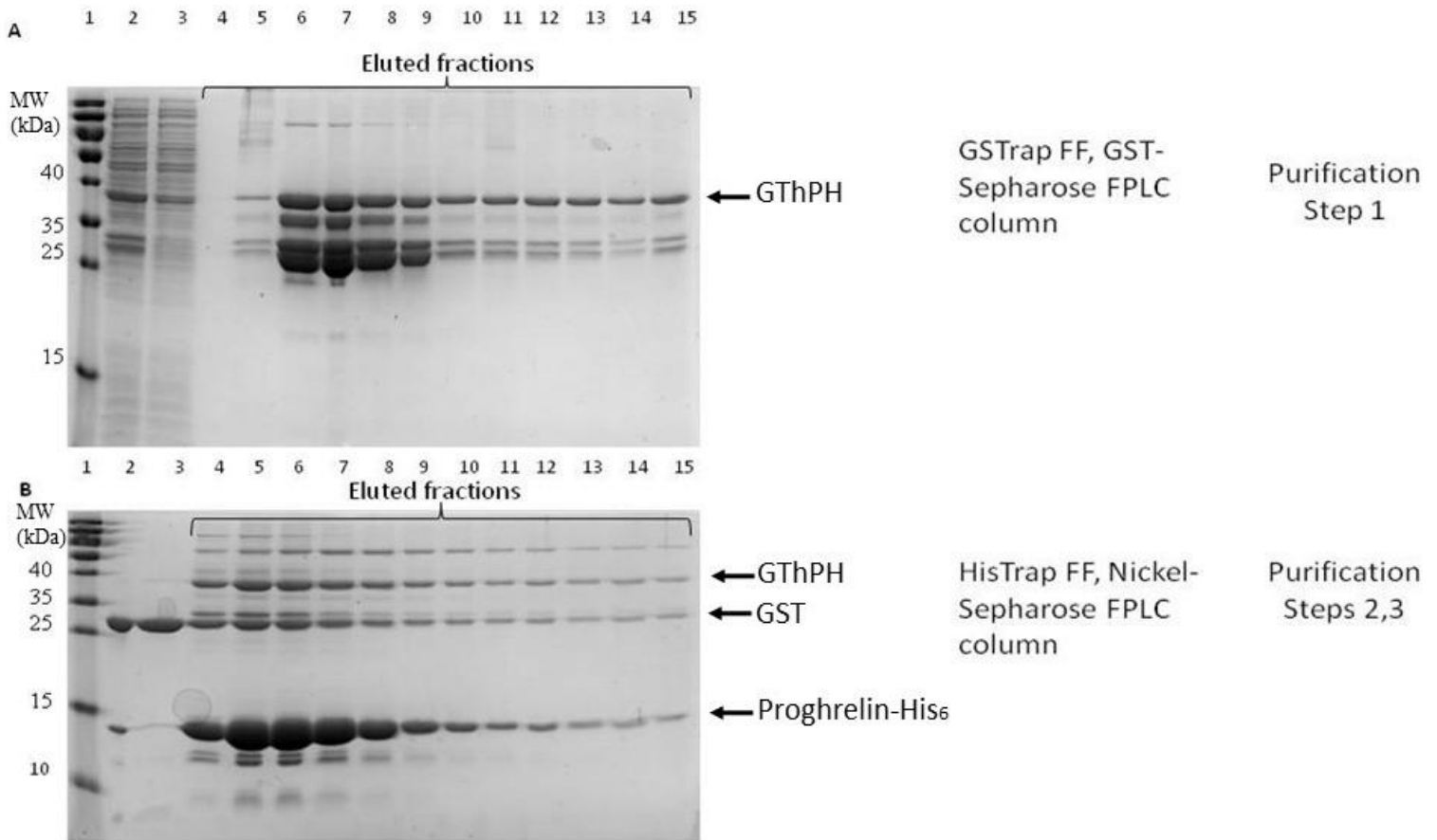


**Figure 2.9. GThPH purification using tandem GST and His<sub>6</sub> affinity purifications. A) FPLC fractions from gradient purification of GThPH using a GSTrap FF column.** Bacterial pellet was lysed using sonication and loaded onto a GSTrap FF column. Fractions were collected from the A280 peak using a gradient elution method. The gel is 12% polyacrylamide. Lane 1, protein ladder (Thermo scientific); Lane 2, crude lysate of GThPH; Lane 3, flow-through; Lane 4, fraction #12; Lane 5 fraction #13; Lane 6, fraction #17; Lane 7, fraction # 18; Lane 8, fraction #19; Lane 9, fraction #20 Lane 10, fraction #22; Lane 11, fraction #24; Lane 12, fraction #25; Lane 13 fraction #26; Lane 14, fraction #30; Lane 15, fraction #40. **B) FPLC fractions from gradient purification of GThPH TEV digestion using a HisTrap FF column following TEV digestion.** The TEV digestion was loaded onto a HisTrap FF column. Fractions were collected from the A280 peak using a step-wise elution method. The gel is 15% polyacrylamide. Lane 1, protein ladder (Thermo scientific); Lane 2, TEV digest of GThPH; Lane 3, column flow-through; Lane 4, fraction #2; Lane 5, fraction #4; Lane 6, fraction #6; Lane 7, fraction # 7; Lane 8, fraction # 8; Lane 9, fraction # 9; Lane 10, fraction #10; Lane 11, fraction # 12; Lane 12, fraction # 14; Lane 13, fraction # 15; Lane 14, fraction # 16; Lane 15, fraction # 17.

### **2.2.5.3 Size exclusion chromatography affords purified proghrelin-His<sub>6</sub>**

Incorporation of size exclusion chromatography (SEC) using either a HiLoad 16/60 Superdex 75 or a HiPrep 16/60 Sephacryl S-100 HR size exclusion column (GE) dramatically improved the purity of proghrelin-His<sub>6</sub> and yielded homogeneous proghrelin-His<sub>6</sub> (Figure 2.10). To maximize proghrelin-His<sub>6</sub> yield and minimize degradation/cleavage leading to lower molecular weight impurities, the complete purification protocol (bacterial cell lysis, GST-Sepharose column, TEV digestion, Ni<sup>2+</sup>-IMAC column, size exclusion chromatography, proghrelin-His<sub>6</sub> concentration) was completed in the minimal time possible (roughly 26-30 hours). Delays in completing the purification protocol were found to increase the amount of lower-molecular weight bands which impacted the efficiency of the SEC purification. Over several purifications, it was also found that avoiding free-thaw cycles during and after the purification, concentrating the samples quickly, and protein lyophilization as soon as possible reduced the appearance of the lower molecular weight impurities.

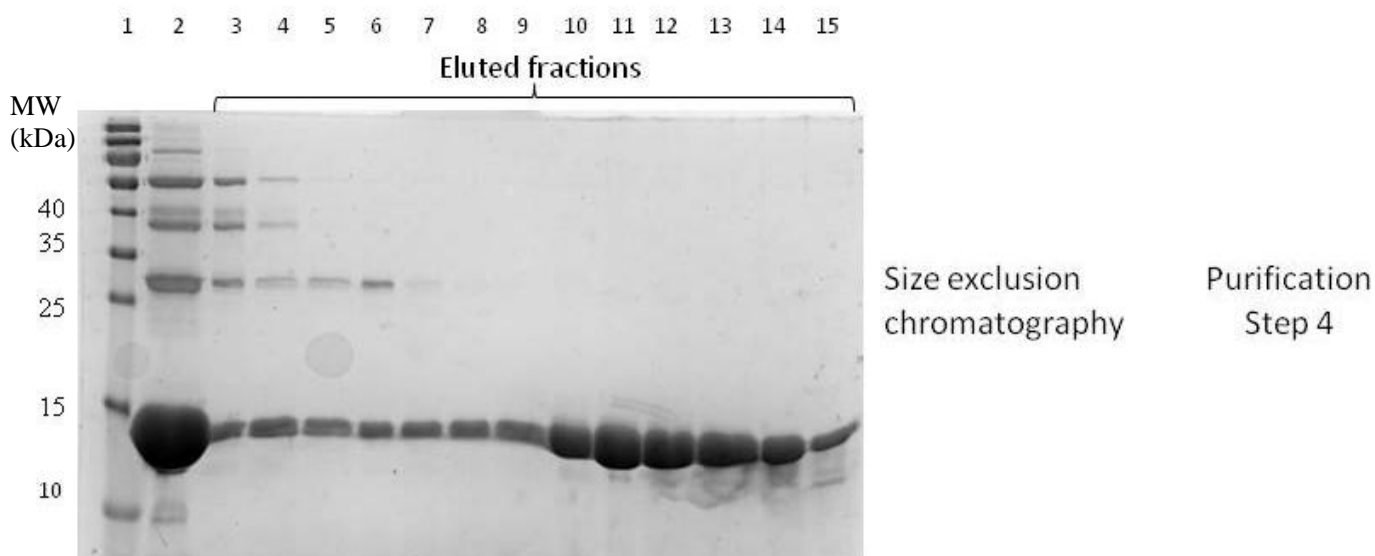


**Figure 2.10. Size exclusion chromatography purification of proghelin-His<sub>6</sub> using a HiLoad16/60 Superdex 75pg size exclusion column.** Fractions from the HisTrap FF column in Figure 2.9B were pooled and loaded onto a HiLoad16/60 Superdex 75pg size exclusion column. Fractions were collected from the A280 peak(s). The gel is 15% polyacrylamide. Lane 1, protein ladder (Thermo scientific); Lane 2, Loaded nickel column concentrate; Lane 3, Fraction #7; Lane 4, Fraction #10; Lane 5, Fraction #12; Lane 6, Fraction #14; Lane 7, Fraction #16; Lane 8, Fraction #18; Lane 9, Fraction #20; Lane 10, Fraction #22; Lane 11, Fraction #24; Lane 12, Fraction #25; Lane 13, Fraction #26; Lane 14, Fraction #29; Lane 15, Fraction #30.

## 2.2.6 Purification approaches for C-ghrelin

### 2.2.6.1 Ni<sup>2+</sup>-Sephacrose based purifications

As mentioned previously, C-ghrelin in the construct GThCgH initially expressed as an insoluble protein but with expression optimization soluble expression of this protein was improved. Prior to exploring IPTG-based induction, GThCgH from expression in autoinduction media was purified under denaturing conditions using Ni<sup>2+</sup>-IMAC resin by batch purification rather than flow purification described for GThPH. This purification method uses the presence of urea and guanidine hydrochloride (GuHCl) throughout the purification to increase the solubility of protein that express as insoluble aggregates. The purification of GThCgH under these conditions led to protein enrichment from bacterial lysate with little appearance of other impurities. However, during refolding following purification where the concentration of GuHCl is lowered, the GThCgH protein denatured and formed an insoluble aggregate in solution with less than 500 mM GuHCl present. A variety of approaches for protein refolding were attempted, including gradient elution with stepping down of denaturant concentration and step-wise dialysis, but none of these approaches improved the production of soluble GThCgH. Given these limitations, we investigated the efficiency of TEV digestion in the presence of sufficient GuHCl to allow GThCgH solubilization, but TEV digestion was not able to proceed under these conditions with little to no evidence of GST cleavage (similar to Figure 2.12). Since, GThCgH was unable to be purified successfully and solubly using this method, it was abandoned when the final expression optimization using LEMO-21 *E. coli* cells were used.

### 2.2.6.2 C-ghrelin purification using established GThPH protocol

GThCgH was expressed under conditions described above using IPTG-based induction (0.4 mM IPTG) in LEMO-21 *E. coli* and then initially purified in the exact same manner as GThCgH using GST-Sepharose FPLC purification. In the analysis of the eluted fractions from this purification, the banding pattern mirrored what was observed during GThPH purification but with the corresponding mass differences (Figure 2.11). This was both encouraging and also interesting, as this indicates that both proteins show the same cleavage/banding pattern after lysis and column purification with their similarity located in the C-terminal ghrelin sequence. Following GST affinity purification, GThCgH was subjected to TEV protease digestion using the same procedure as with GThPH. However, the GST-TEV-His<sub>6</sub> protease was unable to cleave GST from GThCgH (Figure 2.12). The lack of cleavage using TEV protease blocks the generation and purification of C-ghrelin-His<sub>6</sub>, and subsequent studies of C-ghrelin utilized the non-proteolyzed GThCgH fusion protein.

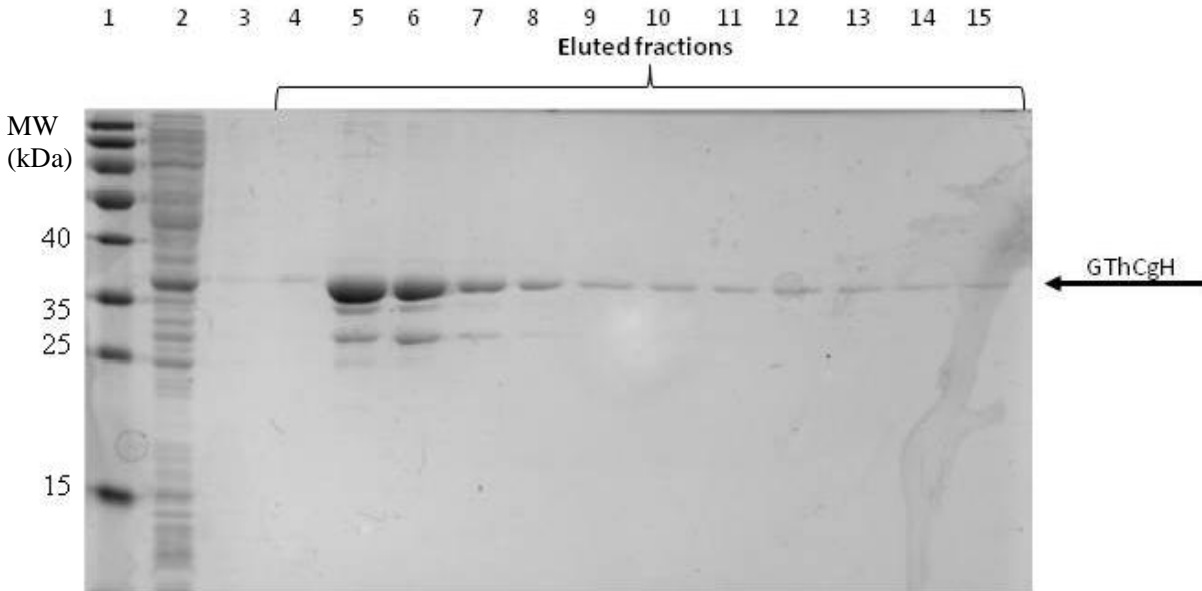


**Figure 2.11. GST-Sepharose FPLC purification of GThCgH.** A bacterial pellet was lysed using sonication and was loaded onto a GStrap FF column. Fractions were collected under the A280 peak from gradient elution method. The gel is 12% polyacrylamide. Lane 1, protein ladder (Thermo scientific); Lane 2, crude lysate of GThCgH; Lane 3, column flow-through; Lane 4, fraction #12; Lane 5, fraction #14; Lane 6, fraction #17; Lane 7, fraction #18; Lane 8, fraction #19; Lane 9, fraction #20; Lane 10, fraction #22; Lane 11, fraction #23; Lane 12, fraction #24; Lane 13, fraction #22; Lane 14, fraction #26; Lane 15, fraction #40.

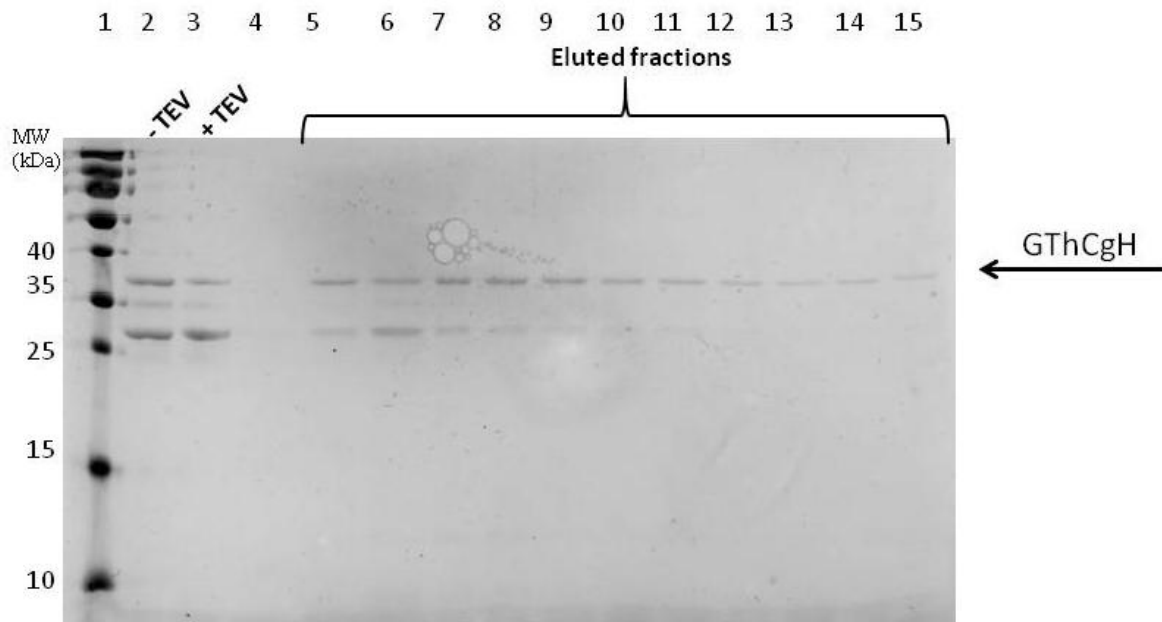


**Figure 2.12 TEV protease is unable to cleave C-ghrelin from GThCgH.** The eluted fractions from Figure 2.11 were pooled and GST-TEV-His<sub>6</sub> protease was added and the digestion was allowed to proceed. The digestion was then loaded onto a HisTrap FF column. Fractions were collected from the A280 peak using a step-wise elution method. Compare lanes 2 and 3 to see the inability of the TEV protease to digest GThCgH. The gel is 12% polyacrylamide. Lane 1, protein ladder (Thermo scientific); Lane 2, GThCgH in absence of GST-TEV-His<sub>6</sub> protease ; Lane 3, GThCgH in presence of GST-TEV-His<sub>6</sub> protease; Lane 4, fraction #4; Lane 5, fraction #5; Lane 6, fraction # 6; Lane 7, fraction #7; Lane 8, fraction #8; Lane 9, fraction #9; Lane 10, fraction #10; Lane 11, fraction #11; Lane 12, fraction #12; Lane 13, fraction #13; Lane 14, fraction #14; Lane 15, fraction #15.

### **2.2.7 Analysis of purified proghrelin-His<sub>6</sub>**

The product of purification of GThPH, proghrelin-His<sub>6</sub>, was confirmed with by a variety of methods. Anti-His Western blot analysis confirm the presence of the C-terminal His<sub>6</sub> tag on a protein of appropriate molecular weight (Figure 2.13). Analysis of purified proghrelin-His<sub>6</sub> by gel electrophoresis followed by both Coomassie and silver staining confirmed purification to >95% purity (Figure 2.14).<sup>30</sup> The mass of purified proghrelin-His<sub>6</sub> was verified by mass spectrometry with a Thermo LTQ Orbitrap mass spectrometer spectrum as representative data (Figure 2.15 and 2.16). All analytical data are consistent with purification of proghrelin-His<sub>6</sub> to homogeneity.

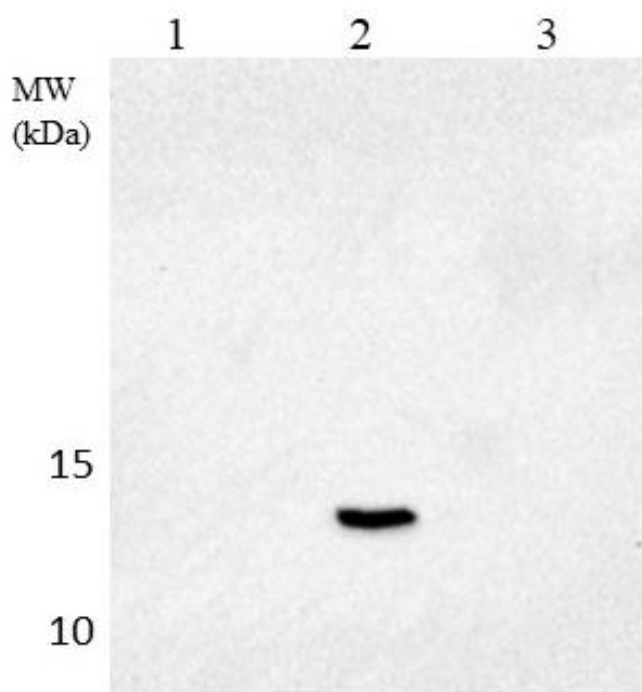


**Figure 2.13. Anti-His Western Blot of purified proghrelin-His<sub>6</sub>.** After size exclusion chromatography fractions were pooled and concentrated. A purified sample of proghrelin-His<sub>6</sub> was run on an SDS-PAGE gel and detected using an Anti-His-HRP conjugated antibody. The gel is 15% polyacrylamide. The molecular weight marker is indicated to the left of lane 1. Lane 2 contains the proghrelin-His<sub>6</sub> sample.

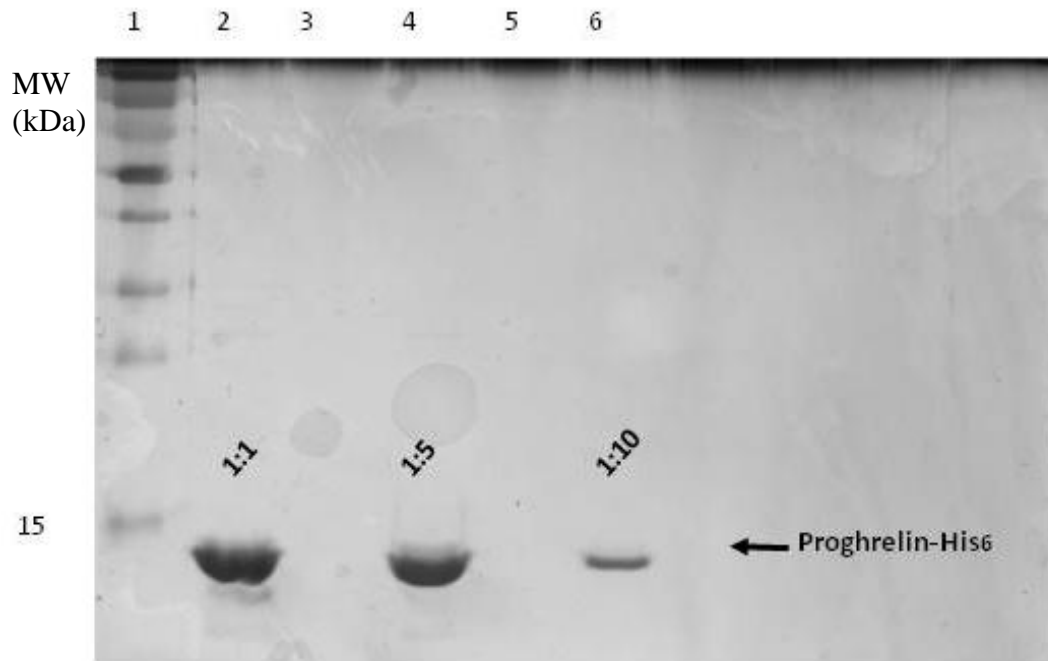


**Figure 2.14. Verification of proghrelin-His<sub>6</sub> using silver staining of purified proghrelin.** After size exclusion chromatography eluted fractions were pooled and concentrated, and diluted to either 1:5 or 1:10 for gel loading. A 15% polyacrylamide gel, the gel was subjected to gel electrophoresis and then silver stained using manufacturer's specifications (Bio Rad). Lane 1, protein ladder (Thermo scientific); Lane 2, proghrelin-His<sub>6</sub>; Lane 4, proghrelin-His<sub>6</sub> 1:5 dilution; Lane 6, proghrelin-His<sub>6</sub> 1:10 dilution.

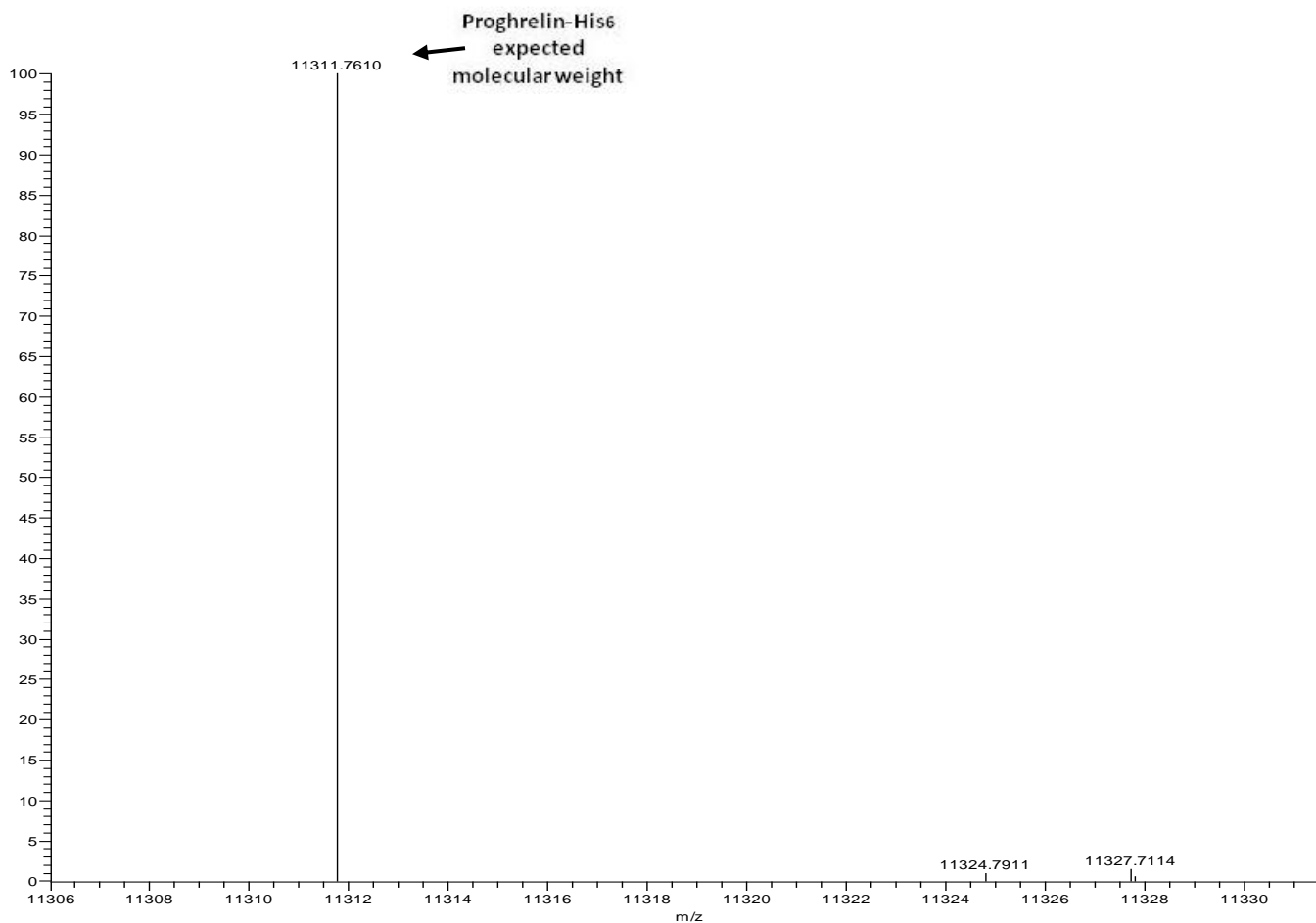


**Figure 2.15. Verification of proghrelin-His<sub>6</sub> mass by ESI-MS (monoisotopic).** The spectrum was obtained utilizing Monoisotopic analysis using a Thermo LTQ Orbitrap mass spectrometer. Monoisotopic spectrum for proghrelin-His<sub>6</sub>.

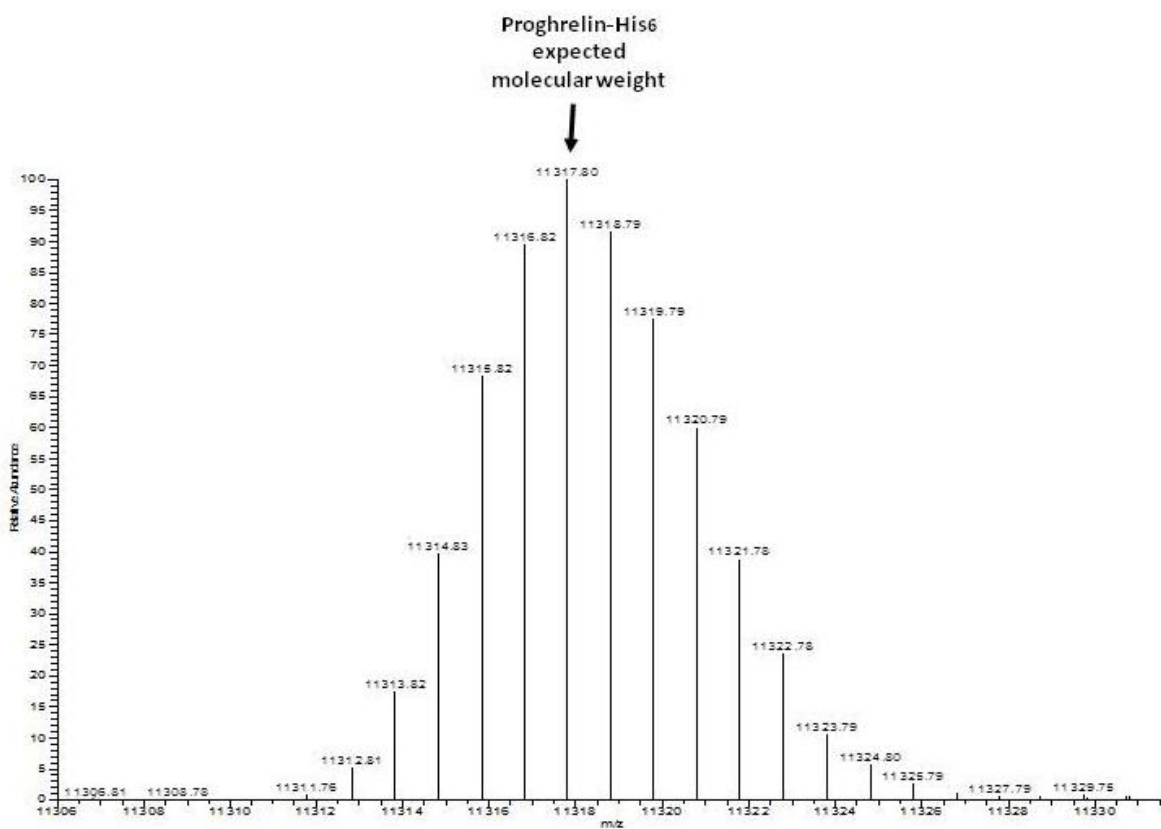


**Figure 2.16. Verification of proghrelin-His<sub>6</sub> mass by ESI-MS (isotopic envelope).** The spectrum was obtained utilizing Extracted Isotopic Envelope analysis using a Thermo LTQ Orbitrap mass spectrometer. Extracted isotopic envelope spectrum for proghrelin-His<sub>6</sub>.

## **2.2.8 Circular dichroism analysis of proghrelin-His<sub>6</sub>**

Circular dichroism (CD) of obestatin and ghrelin peptides has been used to study their structure in aqueous buffers and also in micelle and detergent solutions.<sup>15-21, 23-24</sup> To commence the investigation of potential secondary structure within human proghrelin, the circular dichroism spectrum of proghrelin was measured under a variety of conditions including different buffers and detergents.

### **2.2.8.1 pH and buffer effects on proghrelin CD spectrum**

Initial investigations of the proghrelin CD included buffer pH and buffer composition optimization. There was no observed effect of pH in 25 mM phosphate buffer (ranging from pH of 5.5 to 7.3) on the secondary structure of proghrelin structure as monitored by CD (Figure 2.17). Two other buffers were explored for CD measurements, 25 mM Tris-HCl (2-amino-2-(hydroxymethyl)propane-1,3-diol) and 50 mM HEPES ((4-(2-hydroxyethyl)-1-piperazineethanesulfonic acid)), with buffer pH maintained at 7.3. Compared to phosphate buffer, 25 mM Tris-HCl (pH 7.3) enhanced formation of secondary structure (alpha helix) compared to either 25 mM phosphate buffer or 50 mM HEPES as reflected by a ~2-3-fold enhancement of ellipticity at 222 nm (Figure 2.19A). Increased background signal and an associated decrease in signal to noise ratio in the presence of 50 mM HEPES buffer rendered this buffer non-useful for further CD studies. The proghrelin concentration dependence was also determined, with 20 and 40  $\mu$ M proghrelin providing similar CD spectra (Figure 2.18). Accordingly, 20  $\mu$ M proghrelin was used in subsequent analyses.

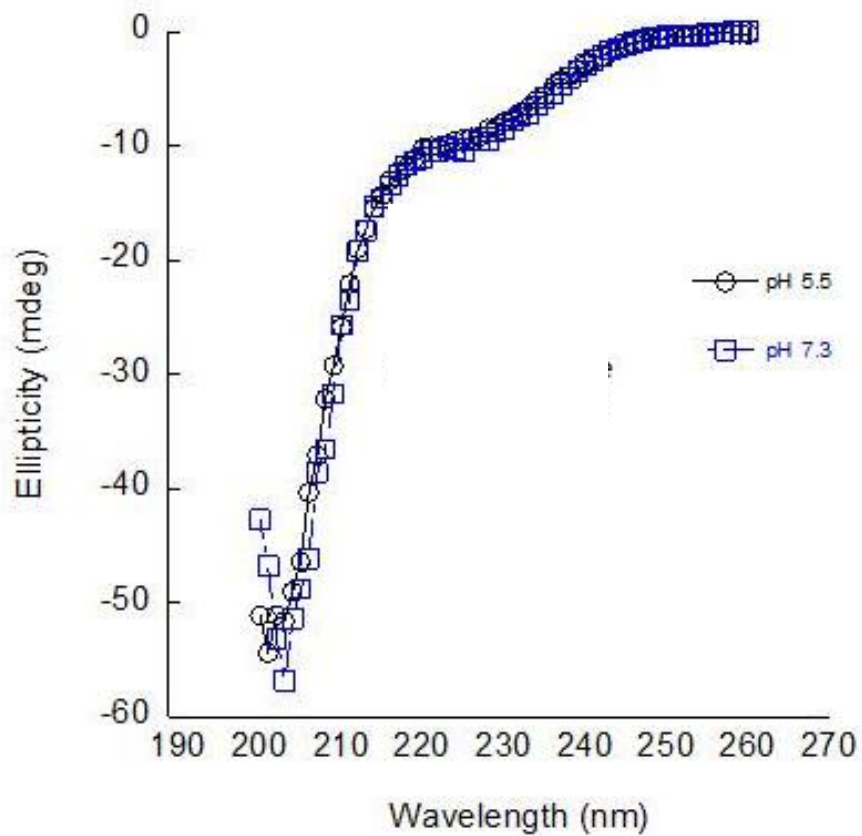


**Figure 2.17. pH dependence of proghrelin-His<sub>6</sub> CD spectrum in 25 mM phosphate buffer.** Proghrelin samples (40  $\mu$ M) were prepared in 300  $\mu$ L of 25 mM Na<sub>2</sub>HPO<sub>4</sub>/NaH<sub>2</sub>PO<sub>4</sub> containing 1 mM EDTA. Spectra were collected over the range 200-260 nm. Pathlength of the quartz cuvette was 0.1 cm and three accumulations were collected for each spectrum.

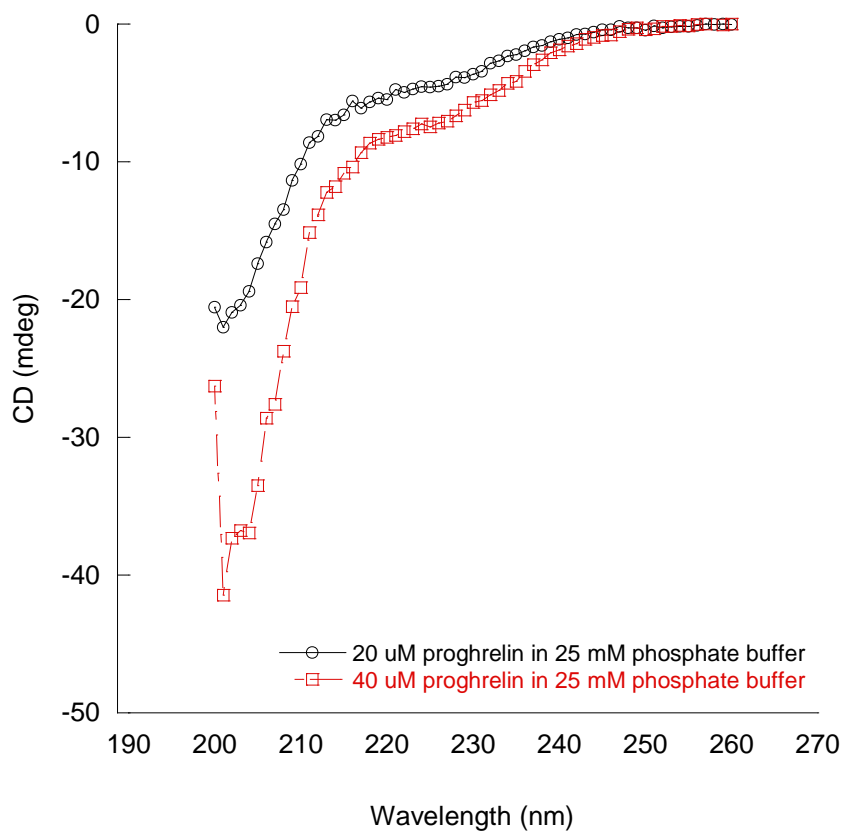


**Figure 2.18. Concentration dependence of proghrelin-His<sub>6</sub> CD spectrum in 25 mM phosphate buffer.** Starting proghrelin sample (50  $\mu$ M) were prepared in 300  $\mu$ L of 25 mM Na<sub>2</sub>HPO<sub>4</sub>/NaH<sub>2</sub>PO<sub>4</sub> then subsequently diluted for 40 and 20  $\mu$ M. Spectra were collected over the range 200-260 nm. Pathlength of the quartz cuvette was 0.1 cm and three accumulations were collected for each spectrum.

### 2.2.8.2 Proghrelin secondary structure enhancement with detergents

CD spectra of proghrelin suggest the presence of alpha helical structure in buffer alone. Based on literature reports that detergents such as SDS can enhance secondary structure in obestatin and ghrelin,<sup>15-16, 18, 20-21</sup> the CD spectra of proghrelin was examined in the presence of detergents to determine if similar enhancement of secondary structure is observed. A titration of SDS in either 25 mM phosphate or 25 mM Tris-HCl buffer led to an increase in helical character as reflected by increased ellipticity at 222 nm (Figure 2.19B). The increase in ellipticity reaches a maximum concentration at 2 mM SDS in 25 mM phosphate buffer and 1 mM SDS in 25 mM Tris-HCl, which compares favorably to the concentration of 2.8 mM SDS used in studies on obestatin<sup>21</sup> and lies below the critical micelle concentration for SDS (7-10 mM). This behavior indicates that the detergent is stabilizing formation of secondary structure within proghrelin. A number of non-ionic detergents ((3-((3-cholamidopropyl) dimethylammonio)-1-propanesulfonate) (CHAPS), octa- $\beta$ -D -glucopyranoside (OBD), n-decyl- $\beta$ -D-maltoside (DM), Tergitol and Triton X-100) were also examined for their ability to enhance the secondary structure of proghrelin as well as investigate more physiological detergents. All of these detergents were added at 0.1 and 1 mM, modeled from the SDS titration (Figure 2.20). Of the non-ionic detergents, Triton X-100 exhibited the largest increase in proghrelin secondary structure. In comparison between Triton X-100 and SDS, SDS was the better choice to aide in the secondary structure in both 25 mM phosphate buffer and Tris-HCl.

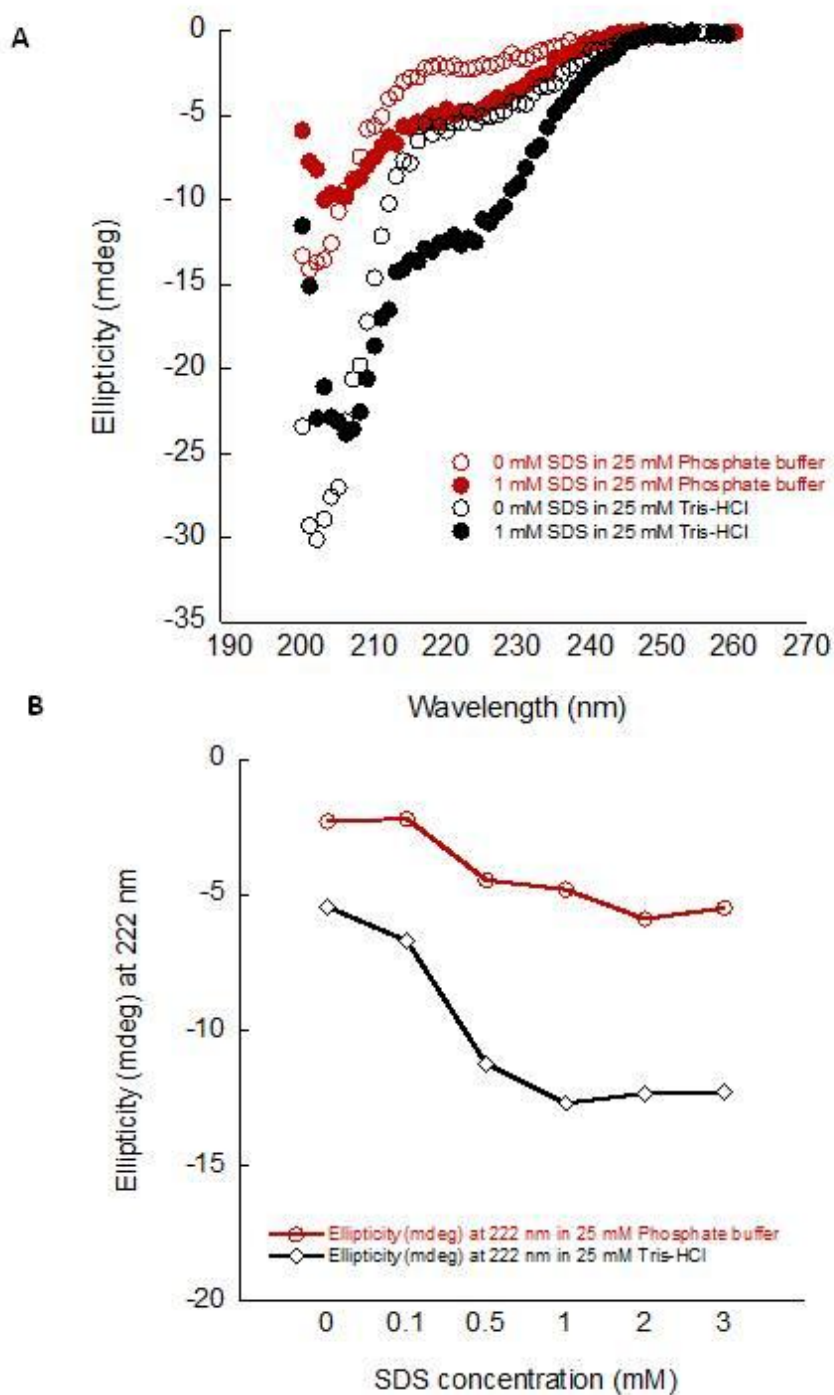


**Figure 2.19. Impact of SDS on the CD spectrum of proghrelin-His<sub>6</sub>.** Proghrelin-His<sub>6</sub> samples (20  $\mu$ M) were prepared in 300  $\mu$ L of 25 mM Na<sub>2</sub>HPO<sub>4</sub>/NaH<sub>2</sub>PO<sub>4</sub> or 25 mM Tris-HCl. A) CD spectra spectra of proghrelin-His<sub>6</sub> in 25 mM phosphate and 25 mM Tris-HCl buffer in the absence and presence of 1 mM SDS. B) The dependence of ellipticity at 222 nm on SDS concentration (0, 0.1, 0.5, 1, 2, and 3 mM SDS) in 25 mM phosphate and Tris-HCl buffer. Spectra were collected over the range 200-260 nm. Pathlength of the quartz cuvette was 0.1 cm and three accumulations were collected for each spectrum.

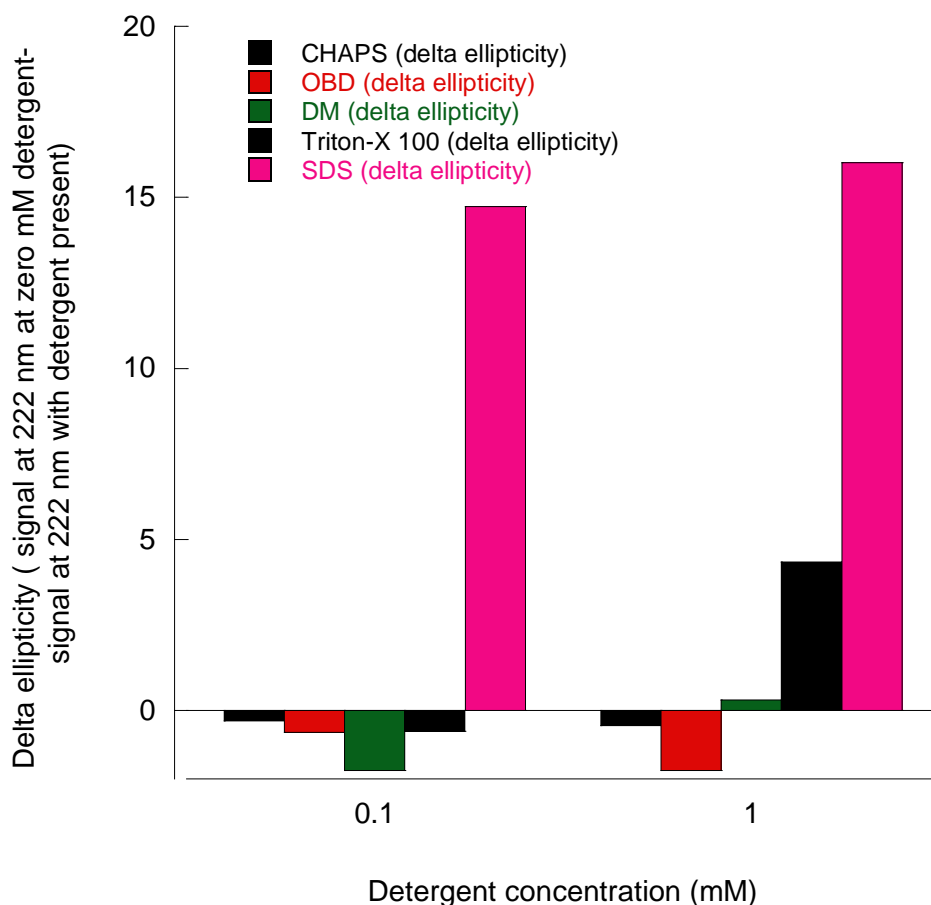


**Figure 2.20. Impact of detergents on the CD spectra of proghrelin-His<sub>6</sub>.** Proghrelin-His<sub>6</sub> samples (40  $\mu$ M) were prepared in 300  $\mu$ L of 25 mM Na<sub>2</sub>HPO<sub>4</sub>/NaH<sub>2</sub>PO<sub>4</sub>. The signals were buffer corrected and then delta ellipticity was calculated by subtracting the 0 mM detergent point signal at 222 nm from either the 0.1 or 1 mM detergent signal at 222 nm. A positive delta ellipticity indicates that there is more secondary structure present. Spectra were collected over the range 200-260 nm. Pathlength of the quartz cuvette was 0.1 cm and three accumulations were collected for each spectrum.

### **2.2.8.3 Comparison of ghrelin and proghrelin isolates the secondary structure contribution of C-ghrelin**

Ghrelin structural studies indicate that ghrelin is very flexible and there is little to no secondary structure present,<sup>19-20</sup> suggesting that the secondary structure observed in proghrelin can be localized to the C-terminal region of the ghrelin precursor. The relative contribution of C-ghrelin, not just obestatin, compared to ghrelin is important to identify the residues involved in alpha helix formation. A circular dichroism spectrum of ghrelin shows no evidence for secondary structure which is consistent with the previously reported data (Figure 2.21).<sup>19-20</sup> However, when comparison of ellipticity per residue for proghrelin and ghrelin indicates that the mean residue ellipticity is nearly identical between these two proteins (Figure 2.21B). This is consistent with the secondary structure within proghrelin not spread equally across the protein and instead involving a small number of residues, most likely in the C-terminus of proghrelin.

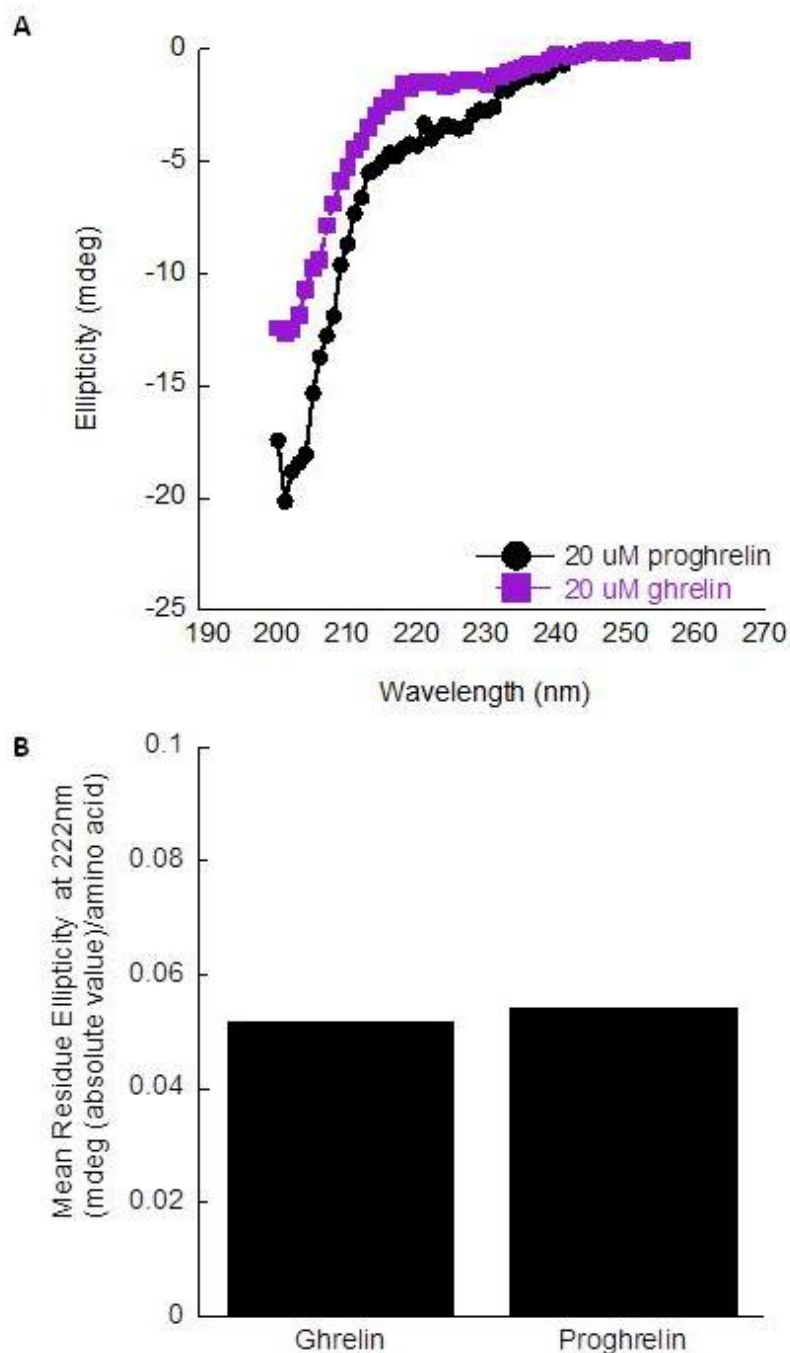


**Figure 2.21. Comparison of CD spectra between ghrelin and proghrelin in aqueous environment.** Ghrelin and proghrelin samples (20  $\mu\text{M}$ ) were prepared in 300  $\mu\text{L}$  of 25 mM  $\text{Na}_2\text{HPO}_4/\text{NaH}_2\text{PO}_4$  (proghrelin) or water (ghrelin). **A**) CD spectra of proghrelin (black) and ghrelin (purple) overlaid. **B**) **Mean residue ellipticity comparison.** Signal at 222 nm (absolute value) divided by the total number of amino acid residues (100 aa for proghrelin-His<sub>6</sub>, 28 aa for ghrelin). Spectra were collected over the range 200-260 nm. Pathlength of the quartz cuvet was 0.1 cm and three accumulations were collected for each spectrum.

### 2.2.9 Nuclear magnetic resonance studies of proghrelin-His<sub>6</sub>

The NMR analysis detailed below is with the assistance of Carlos A. Castañeda who ran the NMR experiments and helped to interpret the data obtained. Upon purification of proghrelin-His<sub>6</sub> a preliminary nuclear magnetic resonance study was completed using natural abundance <sup>1</sup>H-<sup>15</sup>N SOFAST-HMQC to evaluate the potential for structural elements within proghrelin (Figure 2.22). The NMR spectrum from this study showed multiple dispersed peaks suggesting the presence of folded secondary structure in proghrelin. To facilitate further NMR characterization of proghrelin structure, <sup>15</sup>N labeled proghrelin-His<sub>6</sub> was expressed and purified. <sup>15</sup>N labeled proghrelin-His<sub>6</sub> was purified by the same protocol as unlabeled proghrelin-His<sub>6</sub> (a GST-Sepharose Fast Flow column, digestion using a GST- tagged TEV-His<sub>6</sub> protease, a HisTrap Ni-Sepharose High Performance column, and SEC using a HiLoad 16/60 Superdex 75 pg size exclusion column). Eluted proghrelin-His<sub>6</sub> fractions were pooled and concentrated to a minimum concentration of 250-300 μM for NMR studies. Initial NMR experiments included a pH-dependence study at pH 7.3 and pH 5.5, with the lower pH slowing the hydrogen-deuterium exchange in the sample leading to enhancement of the NMR spectrum (Figure 2.23).

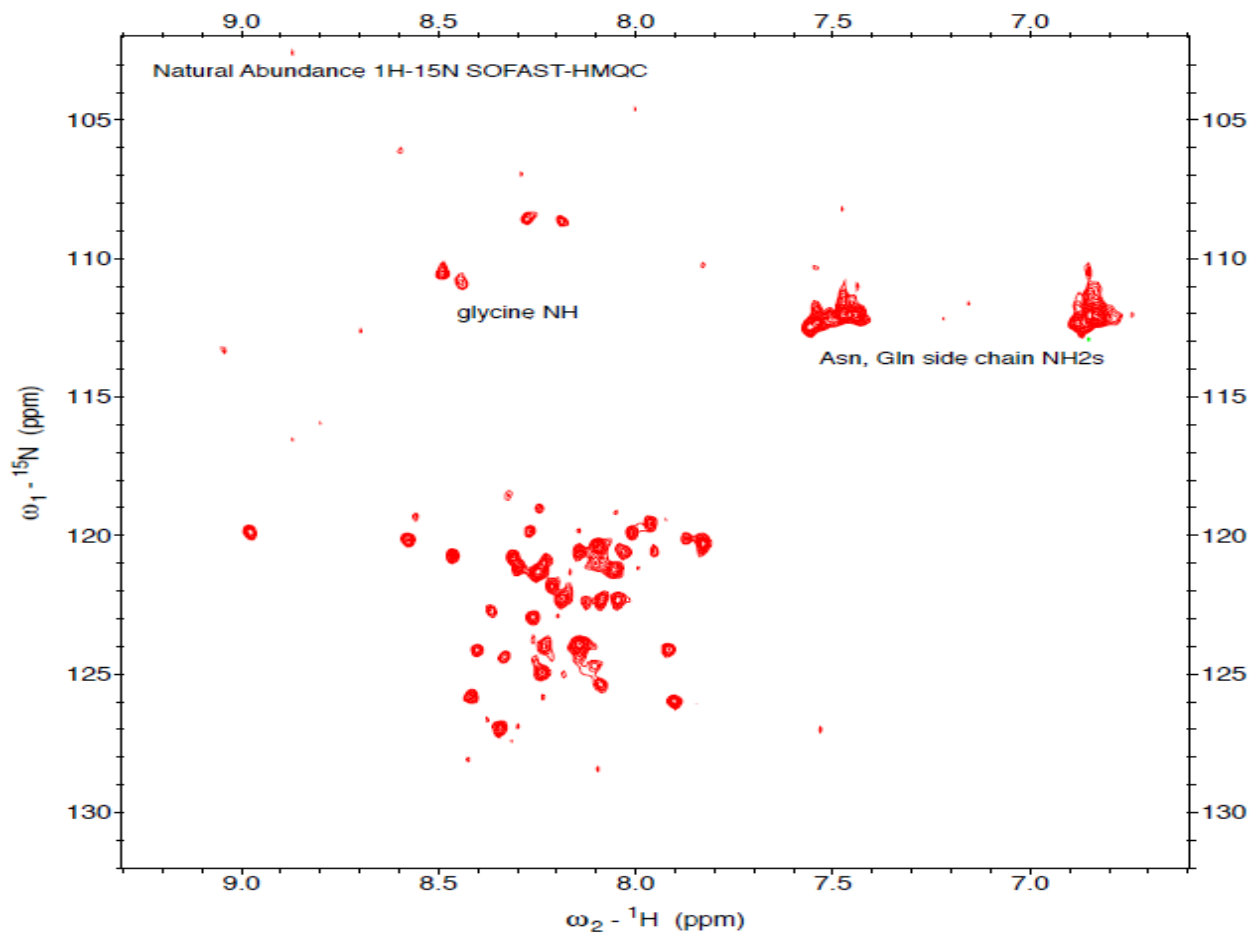


**Figure 2.22. Natural abundance NMR of proghrelin-His<sub>6</sub>.** Purified proghrelin (<sup>14</sup>N) 300μM in 20 mM NaH<sub>2</sub>PO<sub>4</sub>, 50mM Na Cl, 1mM TCEP and 1mM EDTA containing 5% D<sub>2</sub>O. The SOFAST experiment identifies interactions with <sup>1</sup>H-<sup>15</sup>N backbone amides. The NMR experiment lasted 12-hours with 1024 scans and was run on an 800 MHz NMR.

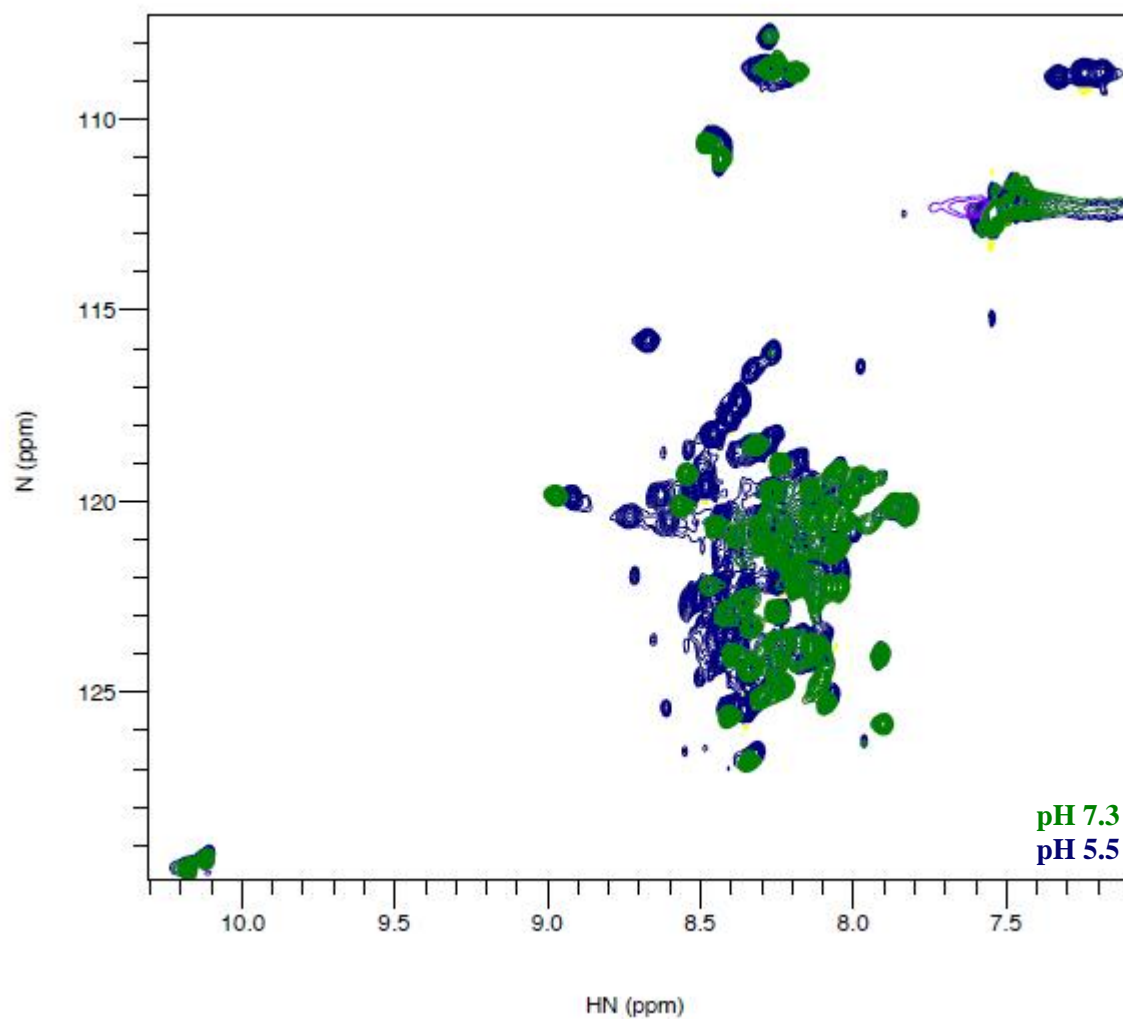


**Figure 2.23. pH dependence of proghrelin-His<sub>6</sub> NMR spectrum.** An HSQC spectrum was collected for 250  $\mu$ M proghrelin in 20 mM NaH<sub>2</sub>PO<sub>4</sub>, 50 mM NaCl, 1mM TCEP and 1 mM EDTA containing 5% D<sub>2</sub>O at pH 7.3 (500  $\mu$ L total volume), followed addition of 10  $\mu$ L of 1 M HCl to drop the pH from 7.3 to 5.5. The spectrum in green is pH 7.3, a spectrum in blue is pH 5.5., and samples were analyzed on the 800 MHz NMR.

Subsequent efforts to pursue additional 2-D NMR analyses such as COSY and NOESY scans were handicapped by low levels of proghrelin-His<sub>6</sub> expression. The amount of protein produced from <sup>15</sup>N-labeling is decreased due to the minimal media used in these expressions to ensure that expressed protein is exclusively transcribed with <sup>15</sup>N-containing amino acids.<sup>31</sup> Extensive attempts to improve the expression of <sup>15</sup>N-labeled GThPH, including changing culture volumes and <sup>15</sup>NH<sub>4</sub>Cl concentration, were unsuccessful. Furthermore, this low level of proghrelin expression appeared to lead to a higher fraction of lower molecular weight impurities and consequently a lower amount of purified proghrelin. While these initial NMR studies of proghrelin are promising and supported the presence of secondary structure within proghrelin, the residues involved and overall molecular architecture remain to be determined.

## 2.3 Conclusions

The expression and purification of GThPH and GThCgH resulted in varying patterns of protein expression, with GThPH exhibiting a high level of soluble expression while GThCgH required complete optimization in order to obtain a small quantity of soluble protein. In terms of expression and purification, these two fusion protein constructs exhibit very little similarity. This behavior is very interesting since the only difference between them consists of the 28 amino acids residues of the ghrelin sequence. Both constructs exhibited cleavage behavior during expression and purification, which will be explored in more detail in Chapter 3.

Purification of proghrelin-His<sub>6</sub> from the GThPH fusion protein was accomplished using a four-step purification process including two affinity purifications, a protease digestion, and a final size-exclusion purification step. However, subsequent to purification to homogeneity, the lower molecular weight impurities observed during purification of proghrelin reappear in purified fractions following incubation in solution. Since these lower molecular weight proteins were a constant partner to proghrelin-His<sub>6</sub> from lysis through multiple column purifications, these proteins may result of self-cleavage or degradation of proghrelin itself. This behavior is unusual for proteins, but is intriguing and makes a possible case for C-terminal ghrelin processing. This cleavage behavior is discussed further in Chapter 3. To avoid formation of these lower molecular weight impurities, based on observations during repeated proghrelin purifications proghrelin was aliquoted to avoid freeze-thaw cycles, concentrated occurred directly after size exclusion chromatography, and the concentration of protein samples were kept below 100  $\mu$ M to avoid appearance of cleaved proghrelin-His<sub>6</sub>.

Studies of purified proghrelin-His<sub>6</sub> using circular dichroism support the presence of alpha helical secondary structure in this small protein. Inclusion of detergents to proghrelin, specifically SDS, increases the secondary structure of the protein which is consistent with the literature.<sup>15, 17, 20-21</sup> It was determined that detergents (especially SDS) enhance the secondary structure of proghrelin. The behavior demonstrated by this protein is of interest since proghrelin is located in the ER, is modified by an enzyme located in the ER membrane and then is trafficked and excreted via endosomes.<sup>10</sup> This protein is in contact with lipids throughout its residence inside the cell and during processing, which could be necessary for secondary structure formation. Such structure formation could impact proghrelin recognition and acylation by GOAT through enzyme substrate interactions outside the N-terminal sequence of ghrelin that so far has been shown to be essential for modification by GOAT.<sup>3, 5-6</sup>

The secondary structure within proghrelin appears to be localized within the C-terminal sequence of proghrelin by comparison of CD spectra for ghrelin and proghrelin. Investigations of ghrelin and obestatin's secondary structure in the literature also supports this model, with ghrelin was shown to be mostly random coil but obestatin possessing more defined alpha helical character.<sup>19-21</sup> It remains to be determined if the secondary structure in proghrelin is localized to the obestatin sequence or extends to other residues.

NMR analysis of unlabeled proghrelin supports the presence of secondary structure suggested by circular dichroism. While these initial NMR experiments support further investigation into proghrelin structure, the yield of <sup>15</sup>N proghrelin was not a high enough to support further NMR analysis. The low yielding expression also lead to higher appearance of lower molecular weight impurities and thus less homogeneous size exclusion chromatography fractions. All of these data are encouraging and interesting as to the secondary structure of

proghrelin and its implications in GOAT acylation and proghrelin processing. However, the exact residues and secondary structure of proghrelin has yet to be determined and is a future goal of this research.

## 2.4 Materials and Methods

### 2.4.1 Transformation of pET23a/24a and pUC57-GST-TEV-proghrelin-His<sub>6</sub> into DH5a *E. coli*.

200 ng of DNA was added to 100  $\mu$ L of Z-competent DH5a *E. coli* and incubated for 30 min on ice. The transformation mixture was then plated on prewarmed LB agar plates containing either ampicillin (100  $\mu$ g/mL) or and kanamycin (50  $\mu$ g/mL) as appropriate and incubated at 37 °C overnight (~17 hr). Two colonies were picked from each plate and inoculated into 5 mL cultures containing 1X LB (5 mL) and either ampicillin (100  $\mu$ g/mL, pET23a) or kanamycin (50  $\mu$ g/mL, pET24a, pUC57). Cultures were incubated with shaking (225 rpm) at 37 °C for 17 hr. Cultures were pelleted and purified using manufacturer's specifications of EZ 10 spin column plasmid DNA gel extraction kit (Bio Basic Inc.).

**2.4.2 Analytical gel procedure.** The uncut vector controls were performed under the following conditions: pUC57 (20  $\mu$ L total volume), pUC57 (400 ng), NEB 10x Buffer 4 (2  $\mu$ L), and ultrapure H<sub>2</sub>O; pET23a (20  $\mu$ L total volume), pET23a (400 ng), NEB 10x Buffer 4 (2  $\mu$ L), and ultrapure H<sub>2</sub>O. The single digest was performed under the following conditions: pUC57 (20  $\mu$ L total volume), pUC57 (400 ng), *NotI* (0.5  $\mu$ L, 10,000 units/mL) or *NdeI* (0.5  $\mu$ L, 10,000 units/mL), NEB 10x Buffer 4 (2  $\mu$ L), and ultrapure H<sub>2</sub>O; pET23a (20  $\mu$ L total volume), pET23a (400 ng), *NotI* (0.5  $\mu$ L, 10,000 units/mL) or *NdeI* (.0.5  $\mu$ L, 10,000 units/mL), NEB 10x Buffer 4 (2  $\mu$ L), and ultrapure H<sub>2</sub>O; pET24a (20  $\mu$ L total volume ), pUC57 (400 ng), *NotI* (0.5  $\mu$ L, 10,000 units/mL) or *NdeI* (0.5  $\mu$ L, 10,000 units/mL), NEB 10x Buffer 4 (2  $\mu$ L), and ultrapure H<sub>2</sub>O. The double digest was performed under the following conditions: pUC57 (20  $\mu$ L total volume ), pUC57 (400 ng), *NotI* (0.5  $\mu$ L, 10,000 units/mL), *NdeI* (0.5  $\mu$ L, 10,000 units/mL), NEB 10x Buffer 4 (2  $\mu$ L), and ultrapure H<sub>2</sub>O; pET23a (20  $\mu$ L total volume), pET23a (400 ng), *NotI* (0.5

μL, 10,000 units/mL), *NdeI* (0.5 μL, 10,000 units/mL), NEB 10x Buffer 4 (2 μL), and ultrapure H<sub>2</sub>O; pET24a (20 μL total volume), pUC57 (400 ng), *NotI* (0.5 μL, 10,000 units/mL), *NdeI* (0.5 μL, 10,000 units/mL), NEB 10x Buffer 4 (2 μL), and ultrapure H<sub>2</sub>O. Reactions were incubated for 2 hr at 37 °C, followed by analysis and purification of the vector digestion by agarose gel electrophoresis (0.8% agarose, 1X TAE buffer); the size of the insert and linearized vector were verified by comparison to a DNA standards ladder (1kB PLUS ladder, GoldBio).

**2.4.3 Double digest procedure.** pUC57 and pET vectors were digested with *NotI* and *NdeI* prior to ligation. The double digest reactions were performed under the following conditions: pUC57 (30 μL total volume), pUC57 (2 μg), *NotI* (1 μL, 10,000 units/mL), *NdeI* (1 μL, 10,000 units/mL), 100x BSA (0.3 μL), NEB 10x Buffer 4 (3 μL), and ultrapure H<sub>2</sub>O (14.7 μL); pET23a (60 μL total volume), pET23a (2 μg), *NotI* (1 μL, 10,000 units/mL), *NdeI* (1 μL, 10,000 units/mL), 100x BSA (0.4 μL), NEB 10x Buffer 4 (4 μL), and ultrapure H<sub>2</sub>O (7.6 μL); pET24a (60 μL total volume), pET24a (2 μg), *NotI* (1 μL, 10,000 units/mL), *NdeI* (1 μL, 10,000 units/mL), 100x BSA (0.4 μL), NEB 10x Buffer 4 (4 μL), and ultrapure H<sub>2</sub>O (4.6 μL). Reactions were incubated for 2 hr at 37 °C, followed by analysis and purification of the vector digestion by agarose gel electrophoresis (0.8% agarose, 1X TAE buffer); the size of the insert and linearized vector were verified by comparison to a DNA standards ladder.

**2.4.4 Ligation of GST-TEV-proghrelin-His<sub>6</sub> into pET24a and pET23a.** Ligations were performed using a 1:3 molar ratio of vector to insert. Ligation reactions were performed under the following conditions: pET23a GThPH (21 μL total volume), *NotI-NdeI* double digested pET23a (50 ng), *NotI-NdeI* double digested pUC57 (41.9 ng), ultrapure H<sub>2</sub>O (6 μL), 2x Quick Ligase buffer (10 μL), and T4 Quick Ligase (New England Biolabs, 1 μL). Following addition of

Quick Ligase, reactions were incubated at room temperature for 5 min. Ligation mixtures (5  $\mu$ L) were then transformed into a 50  $\mu$ L aliquot of chemically competent Z-competent DH5 $\alpha$  *E.coli* (Zymo Research) followed by incubation on ice for 30 min. Transformed bacteria were spread on a LB-ampicillin plate (100  $\mu$ g/mL) for pET23a ligation and incubated at 37 °C overnight. Following overnight incubation at 37 °C, single colonies were inoculated into LB media (5 mL) containing appropriate antibiotic in sterile culture tubes. These cultures were incubated overnight at 37 °C with shaking (225 rpm). Following overnight growth, plasmids were purified from the saturated cultures using EZ-10 Spin Column Plasmid DNA kit (Bio Basic Inc.) per manufacturer's instructions. Ligation was verified by double digestion with *NotI* and *NdeI* to excise the ligated insert followed by agarose gel electrophoresis and DNA sequencing (Genewiz Inc.).

**2.4.5 Transformation of ligated GThPH into Z-competent BL21(DE3) *E. coli*.** Plasmid of pET23a GThPH was transformed into Z-competent BL21 (DE3) *E. coli*. Plasmids (100 ng) were transformed into a 100  $\mu$ L aliquot of chemically competent Z-competent BL21 (DE3) cells (Zymo Research) followed by incubation on ice for 30 min. Transformed bacteria were spread on LB-ampicillin plates (100  $\mu$ g/mL) and incubated at 37 °C overnight.

Following overnight incubation, single colonies were used plucked and a 5mL culture of LB media was grown for 4 hr at 37°C then this was used to inoculate cultures of autoinduction media (1% tryptone, 0.5% yeast extract, 25 mM Na<sub>2</sub>HPO<sub>4</sub>, 25 mM KH<sub>2</sub>PO<sub>4</sub>, 50 mM NH<sub>4</sub>Cl, 5 mM Na<sub>2</sub>SO<sub>4</sub>, 2 mM MgSO<sub>4</sub>, 0.5% glycerol, 0.05% glucose, 0.2%  $\alpha$ -D-lactose, and 100  $\mu$ g/mL ampicillin). The shaken for 24 hr at 400 rpm at 28 °C. Following growth, bacteria were harvested by centrifugation (6000 x g, 15 min) and the supernatant removed. The bacterial pellet was

resuspended in B-PER lysis reagent (Thermo Scientific, 100  $\mu$ L), vortexed on high for 1 min, and cell debris was removed by centrifugation (15,000 x *g*, 5 min). Proteins in the resulting supernatant were then analyzed 12% acrylamide gel electrophoresis and Coomassie staining.

**2.4.6 Auto-Induction media conditions.** pET23a GThPH or pET23a GThCgH was transformed into *Z*-competent BL21 (DE3) *E. coli* cells. Plasmids (100 ng) were transformed into a 50  $\mu$ L aliquot of chemically competent *Z*-competent BL21 (DE3) cells (Zymo Research) followed by incubation on ice for 30 min. Transformed bacteria were spread on LB-ampicillin plates (100  $\mu$ g/mL) and incubated at 37°C overnight.

Following overnight incubation, single colony was used to inoculate a 5 mL culture of LB media. The culture was shaken for 4 hr at 225 rpm at 37°C. The 5 mL culture was then inoculated into 1 L of autoinduction media (1% tryptone, 0.5% yeast extract, 25 mM Na<sub>2</sub>HPO<sub>4</sub>, 25 mM KH<sub>2</sub>PO<sub>4</sub>, 50 mM NH<sub>4</sub>Cl, 5 mM Na<sub>2</sub>SO<sub>4</sub>, 2 mM MgSO<sub>4</sub>, 0.5% glycerol, 0.05% glucose, 0.2%  $\alpha$ -D-lactose, and 100  $\mu$ g/mL ampicillin). The culture was shaken for 24 hr at 225 rpm at 28°C. Following growth, bacteria were harvested by centrifugation (6000 x *g*, 15 min) and the supernatant removed. Four 1 mL bacterial pellets were also prepared from the larger culture. One of the 1 mL bacterial pellets was resuspended in BPER lysis reagent (Thermo Scientific, 150  $\mu$ L), vortexed on high for 1 min, and cell debris was removed by centrifugation (15,000 x *g*, 5 min). A second 1 mL bacterial pellet was resuspended in 3XSB (Thermo Scientific, 50  $\mu$ L), heated at 95 °C for 5 min, and cell debris was removed by centrifugation (15,000 x *g*, 5 min). Protein in the resulting supernatant were then analyzed 12% acrylamide gel electrophoresis and Coomassie staining.

**2.4.7 IPTG induction growth conditions.** Plasmid of pET23a+GThPH or pET23a+GThCgH was transformed into *Z*-competent BL21 (DE3) *E. coli* cells. Plasmids (100 ng) were transformed into a 50  $\mu$ L aliquot of chemically competent *Z*-competent BL21 (DE3) *E. coli* cells (Zymo Research) followed by incubation on ice for 30 min. Transformed bacteria were spread on LB-ampicillin plates (100  $\mu$ g/mL) and incubated at 37 °C overnight.

Following overnight incubation, single colony was used to inoculate a 5 mL culture of LB media. The culture was shaken for 4 hr at 225 rpm at 37 °C. The 5 mL culture was then inoculated into 1 L of IPTG base media (20 g/L tryptone, 10 g/L yeast extract, 5 g/L NaCl, 1% glucose, 100  $\mu$ g/mL ampicillin) and shaken at 37 °C 225 rpm until the culture reached an optical density at 600 nm of 0.6 then induced by addition of IPTG (0.4 mM), shake at 225 rpm (25 °C for GThPH, 16 °C for GThCgH) overnight (~16 hr). Following growth, bacteria were harvested by centrifugation (6000 x *g*, 15 min) and the supernatant removed. Four 1 mL bacterial pellets were also prepared from the larger culture. One of the 1 mL bacterial pellets was resuspended in B-PER lysis reagent (Thermo Scientific, 100  $\mu$ L), vortexed on high for 1 min, and cell debris was removed by centrifugation (15,000 x *g*, 5 min). A second 1 mL bacterial pellet was resuspended in 3XSB (Thermo Scientific, 50  $\mu$ L), heated at 95 °C for 5 min, and cell debris was removed by centrifugation (15,000 x *g*, 5 mins) Protein in the resulting supernatant were then analyzed 12% acrylamide gel electrophoresis and Coomassie staining.

**2.4.8 GThGgH IPTG induction using LEMO-21 *E. coli* cells growth conditions.** Plasmid of pET23a GThCgH was transformed into LEMO 21 *E. coli* cells. Plasmids (100 ng) were transformed into a 50  $\mu$ L aliquot of chemically competent *Z*-competent LEMO 21 *E. coli* cells (Zymo Research) followed by incubation on ice for 30 min. Transformed bacteria were spread

on LB-ampicillin/chloramphenicol plates (100 µg/mL, 30 µg/mL respectively) and incubated at 37 °C overnight.

Following overnight incubation, single colony was used to inoculate a 5 mL culture of LB media. The culture was shaken for 16-18 hr at 225 rpm at 37 °C. The 5 mL culture was then inoculated into 300 mL of media Terrific broth (Bio Basic) containing 100 µg/mL ampicillin, 34 µg/mL chloramphenicol and shaken at 37 °C 225 rpm until the culture reached an optical density at 600 nm of 0.6 then induced by addition of IPTG (0.4 mM) and rhamnose (1 mM), shake at 16 °C overnight (~17 hr). Following growth, bacteria were harvested by centrifugation (6000 x g, 15 min) and the supernatant removed. Four 1 mL bacterial pellets were also prepared from the larger culture. One of the 1 mL bacterial pellets was resuspended in B-PER lysis reagent (Thermo Scientific, 100 µL), vortexed on high for 1 min, and cell debris was removed by centrifugation (15,000 x g, 5 min). A second 1 mL bacterial pellet was resuspended in 3XSB (Thermo Scientific, 50 µL), heated at 95 °C for 5 min, and cell debris was removed by centrifugation (15,000 x g, 5 min) Protein in the resulting supernatant were then analyzed 12% polyacrylamide gel electrophoresis and Coomassie staining.

**2.4.9 SDS-PAGE analysis.** 3XSB lysis was performed by using cell lysate (50 µL) was mixed with 25 µL of 3X SDS sample buffer and heated to 95 °C for 5 min, followed by centrifugation (10,000 x g, 5 min) to pellet insoluble material. B-PER lysis was performed using BPER lysis reagent (Thermo Scientific, 150 µL), vortexed on high for 1 min, and cell debris was removed by centrifugation (15,000 x g, 5 mins). 25 µL of 3XSB was added and heated to 95 °C for 5 min, followed by centrifugation (10,000 x g, 5 min) to pellet insoluble material. Protein standards ladder (Thermo Scientific) and samples were loaded onto a 12% polyacrylamide gel and run at

150 V for 1 hr 30 min, until the dye band had migrated to the bottom of the gel. Total protein in cell lysate samples was visualized by staining with Coomassie Blue stain and imaged on a ChemiDoc XRS+ BioRad gel imager.

**2.4.10 Coomassie Blue staining procedure.** Each 12% polyacrylamide gel was rinsed with ultra pure water and covered in approximately 50 mL of destain solution (stock: 2 L water, 1.6 L methanol, 0.4 L acetic acid). The gel was microwaved for 18 sec, at which point the destain solution was removed and approximately 50 mL of Coomassie blue stain was added (stock: 0.25 g Coomassie Blue dye, 500 mL methanol, 75 mL acetic acid). The gel was microwaved for 30 sec and rocked for 5 min. The stain solution was removed, destain solution was added and rocked for 15 min, followed by another round of destain addition and rocking for 15 min. The gel was then placed into ultra pure water rocked overnight. Protein gels were then imaged using BioRad XRS+ gel imager.

**2.4.11 Western blot procedure.** Cell lysates were run on a 12% polyacrylamide gel as described above. A polyvinylidene fluoride (PVDF) membrane was activated by immersion in methanol for 30 seconds, followed by equilibration in transfer buffer (20% v/v methanol, 48 mM Tris Base, 39 mM glycine and 0.034% v/v SDS) for 10 min. Filter papers and sponges were also soaked in transfer buffer. The gel was assembled into a transfer cassette and proteins were transferred to the PVDF membrane for 20 min at 350 mA, using a BioRad TransBlot Turbo RTA Transfer kit per manufacturer's instructions.

Following electroblotting, the PVDF membrane was washed in tris buffered saline (TBS, 0.05 M Tris and 0.14 M NaCl), TBST (TBS with 0.1% v/v Tween 20) and blocked for 4 hr in 10% v/v nonfat milk in TBST. The membrane was then probed with an HRP- $\alpha$ -antiHis primary

antibody (1:500 dilution, Rockland) or HRP-- $\alpha$ -antiGST primary antibody (1:500 dilution, Rockland) in 10% milk TBST under parafilm overnight. Following washing in TBST, the membrane was treated with the West Pico Chemiluminescent substrate imaging reagent (Thermo Scientific) and imaged on a ChemiDoc XRS+ BioRad gel documentation system.

**2.4.12 TEV digestion.** TEV-His<sub>6</sub> protease was expressed and purified using the pMHT238 – TEV gp1 plasmid following a published procedure.<sup>32</sup> For TEV cleavage of the GThPH fusion protein, initial reaction conditions were GThPH fusion protein (100  $\mu$ g), TEV protease (10  $\mu$ g) in 120  $\mu$ L total reaction volume at room temperature for 18 hr. The cleavage reaction was analyzed using SDS-PAGE, Coomassie staining and Western blotting (described above). A reaction time course was conducted using the same conditions using various time points (5min, 30 min, 1hr, 2 hr, 3 hr, 4 hr, and 18 hr). Following time course analysis, new reaction conditions were investigated: 3hr at room temperature, 3hr at 34 °C, 24 hr at room temperature, and 18 hr at 34 °C. Reaction analysis revealed that cleavage at 34 °C for 24 hr as the optimal conditions. The reaction scale was increased to 11 mL for 48 mg GThPH protein, using the same conditions stated above. The reaction was then purified using FPLC purification. Following incorporation of GST-TEV-His<sub>6</sub>, TEV digestions proceeded using a 200:1 ratio of GThPH and TEV protease in 300 mM NaCl, 50 mM Tris-HCl, 10 mM glutathione (GSTrap elution buffer) for 8-10 hr at 34 °C. After digestion the mixture was then purified using a HisTrap FF column (GE).

**2.4.13 TEV protease ratio reaction.** The ratio of GThPH and TEV protease were varied per the following: A 193 mg TEV protease digest of GThPH fusion protein 100:1 ratio was performed using the following conditions: GThPH fusion protein (193 mg), TEV protease (1930  $\mu$ g), DTT (1mM), and EDTA (0.5 mM, pH 7.8) in 2.2 mL reaction volume at 34 °C for 18 hr. The

digestion reaction purified using FPLC gradient elution purification as described in 2.4.17 and analyzed using SDS-PAGE and Anti-His western. The fractions were combined, concentrated to a volume of 5mL and desalted using Tris-HCl (pH 7.3). A series of ratio reactions were performed using 200:1, 400:1, 600:1, 1000:1, 2000:1 ratios of GThPH to TEV protease. TEV protease digest of GThPH fusion protein 200:1 ratio using the following conditions: GThPH fusion protein (6 mg), TEV protease (30  $\mu$ g), DTT (1 mM), and EDTA (0.5 mM, pH 7.8) in 1.12 mL reaction volume at 34 °C for 18 hr; 400:1 ratio using the following conditions: GThPH fusion protein (6 mg), TEV protease (15  $\mu$ g), DTT (1 mM), and EDTA (0.5 mM, pH 7.8) in 1.12 mL reaction volume at 34 °C for 18 hr; 600:1 ratio using the following conditions: GThPH fusion protein (6 mg), TEV protease (10  $\mu$ g), DTT (1 mM), and EDTA (0.5 mM, pH 7.8) in 1.12 mL reaction volume at 34 °C for 18 hr; 1000:1 ratio using the following conditions: GThPH fusion protein (6 mg), TEV protease (6  $\mu$ g), DTT (1 mM), and EDTA (0.5 mM, pH 7.8) in 1.12 mL reaction volume at 34 °C for 18 hr; 2000:1 ratio using the following conditions: GThPH fusion protein (6 mg), TEV protease (3  $\mu$ g), DTT (1 mM), and EDTA (0.5 mM, pH 7.8) in 1.12 mL reaction volume at 34 °C for 18 hr. Reactions were then analyzed by SDS-PAGE and Coomassie staining. The series of ratio reactions (200:1, 400:1, 600:1, 1000:1, and 2000:1) were repeated, however, a reaction time course was conducted using the same conditions using various time points (24, 48, and 72 hr). The longer reaction time was concluded to make no visible difference in the digest.

**2.4.14 Circular dichroism.** Size- exclusion purified samples were pooled and then buffer exchanged into 25 mM Na<sub>2</sub>HPO<sub>4</sub>/NaH<sub>2</sub>PO<sub>4</sub> or 25 mM Tris-HCl using 5 kDa molecular weight cutoff concentrators (SpinX UF, Corning, Corning, NY). Fractions were concentrated to ¼ of their initial volume, supplemented with buffer to original volume, spun down (2,500 x g, 4° C) to

¼ of the volume, repeated until three volumes worth of buffer have been added. After buffer exchanging an A280 was taken ( $\epsilon=12490 \text{ M}^{-1}\text{cm}^{-1}$ ). CD solutions contained proghrelin-His<sub>6</sub> (40  $\mu\text{M}$  or 20  $\mu\text{M}$ ). Spectra were collected using 1mm Suprasil High Resolution Quartz cuvet (Hellma Analytics, Müllheim, Germany). Three accumulations were used for each spectra collection. There were five minute incubations after addition of detergents, before a spectrum was collected.

**2.4.15 <sup>15</sup>N labeling of proghrelin-His<sub>6</sub>.** pET23a GThPH was transformed into Z-competent BL21 (DE3) *E. coli* cells. Plasmids (100 ng) were transformed into a 50  $\mu\text{L}$  aliquot of chemically competent Z-competent BL21 (DE3) *E. coli* cells (Zymo Research) followed by incubation on ice for 30 min. Transformed bacteria were spread on LB-ampicillin plates (100  $\mu\text{g}/\text{mL}$ ) and incubated at 37 °C overnight.

Following overnight incubation, single colony was used to inoculate a 5 mL culture of LB media. The culture was shaken for 4 hr at 225 rpm at 37 °C. The 5 mL culture was then inoculated into 1 L of autoinduction media (section 2.4.6). Initially 2.5 mM FeCl<sub>3</sub> was added to the autoinduction media; however, it was not included after first initial growths because of degradation it caused. The culture was shaken for 24 hr at 225 rpm at 28 °C. Following growth, bacteria were harvested by centrifugation (6,000 x g, 15 min) and the supernatant removed. Four 1 mL bacterial pellets were also prepared from the larger culture. One of the 1 mL bacterial pellets was resuspended in B-PER lysis reagent (Thermo Scientific, 100  $\mu\text{L}$ ), vortexed on high for 1 min, and cell debris was removed by centrifugation (10,000 x g, 5 min). A second 1 mL bacterial pellet was resuspended in 3X sample buffer (Thermo Scientific, 50  $\mu\text{L}$ ), heated at 95°C for 5 min, and cell debris was removed by centrifugation (10,000 x g, 5 min). Protein in the

resulting supernatant were then analyzed 12% acrylamide gel electrophoresis and Coomassie staining.

The protein was then purified using standard GThPH protocol, concentrated to as high of a concentration as possible (ideally 100-300  $\mu\text{M}$ ) and NMR studies were conducted by Carlos A Castañeda.

**2.4.16 GThCgH cloning.** A *HINDIII* restriction site was inserted after the TEV cleavage site in pET23a GThPH – primers were synthesized by Integrated DNA Technologies.

Primers: Forward 5' CTGTA CTTCCAGGGTAAGCTTTTTCTGAGTCCG 3'

Reverse 3' CGGACTCAGAAAAAGCTTACCCTGGAAGTACAG 5'

Primers were dissolved in purified water and concentrations were determined by UV absorbance at 260 nm. PCR mutagenesis reactions (50  $\mu\text{L}$ ) contained the following components: 1x Pfu reaction buffer; 10 ng pET23a GST-TEV-proghrelin-His<sub>6</sub>; 125 ng forward primer; 125 ng reverse primer, 20  $\mu\text{M}$  dNTPs, and 1  $\mu\text{L}$  Pfu Turbo DNA polymerase (Agilent). The thermocycler program for PCR mutagenesis proceeded as follows: initial denaturation (94 °C, 5 min); 30 cycles of denaturation (94 °C, 30 sec), annealing (56 °C, 1 min), and extension (68 °C, 2 min); final extension (68 °C, 5 min). *DpnI* (1  $\mu\text{L}$ , 20,000 units/mL) was added and reactions were incubated at 37 °C for 1 hr. After *DpnI* digestion, 5  $\mu\text{L}$  of the PCR reaction mixture was transformed into 50  $\mu\text{L}$  of Z-competent DH5 $\alpha$  cells (Zymo Research) followed by incubation on ice for 30 min. Transformed bacteria were spread on LB-ampicillin (100  $\mu\text{g}/\text{mL}$ ) plates and incubated at 37 °C overnight. Single colonies were then inoculated into 5 ml LB media containing 100  $\mu\text{g}/\text{mL}$  ampicillin in sterile culture tubes, which were incubated at 37°C overnight with shaking (225 rpm). Following overnight growth, plasmids were purified from cultures using

EZ-10 Spin Column Plasmid DNA kit (BioBasic) per manufacturer's instructions. The product was verified by DNA sequencing (Genewiz).

PCR mutagenesis was also performed to insert a 5' HINDIII, C-terminal His<sub>6</sub> tag and a 3' *NotI* restriction site in c-ghrelin.

Primers: Forward 5' TATAGCAA AACTGCAA AAGCTTGCACTGGCCGGTTGG 3'

Reverse 3' CTCGAGTGCGGCCGCTTAATGGTGGTGATGGTGATGTATA 5'

Primers were synthesized by Integrated DNA Technologies. Primers were dissolved in purified water and concentrations were determined by UV absorbance at 260 nm. PCR mutagenesis reactions (50  $\mu$ L) contained the following components: 1x One Taq standard reaction buffer; 40 ng pET23a GST-TEV-proghrelin-His<sub>6</sub> template; 125 ng forward primer; 125 ng reverse primer, 20  $\mu$ M dNTPs, and One Taq DNA polymerase (1  $\mu$ L, 5,000 units/mL) (Agilent). The thermocycler program for PCR mutagenesis proceeded as follows: initial denaturation (94 °C, 1 min); 33 cycles of denaturation (94°C, 30 sec), annealing (59°C, 1 min), and extension (68 °C, 2 min); final extension (68 °C, 5 min). Following PCR mutagenesis the PCR product was run on a 0.8% agarose gel at 110 V for ~1.5 hr, then DNA was gel extracted using EZ-10 Gel Extraction kit (BioBasic) per manufacturer's instructions, and concentrations were measured by UV absorbance at 260 nm. The c-ghrelin gene was ligated into pET23a GST-TEV-X-His<sub>6</sub>. 3  $\mu$ g pET23a GST-TEV proghrelin-His<sub>6</sub> and C-ghrelin insert DNA was digested with *HINDIII* (1  $\mu$ L, 20,000 units/mL), *NotI* (1  $\mu$ L, 20,000 units/mL), 3  $\mu$ l cutsmart buffer (30  $\mu$ L total volume), and incubated at 37°C for 2 hr. Samples were then run on a 0.8% agarose gel at 110 V for ~1 hr. The bands for the pET23a vector and the C-ghrelin insert were each cut out and DNA was purified using EZ-10 Gel Extraction kit (BioBasic) per manufacturer's instructions, and concentrations were measured by UV absorbance at 260 nm.

Ligations were performed with 50 ng of vector DNA, 40 ng insert DNA, 10  $\mu$ L quick ligase buffer, and 1  $\mu$ L Quick Ligase (total volume 10  $\mu$ L) and incubated on ice for 5 m. 5  $\mu$ L of ligation reaction was added to 100  $\mu$ L Z-competent DH5 $\alpha$  cells, followed by 30 min incubation on ice. Cells were spread on LB- ampicillin (100  $\mu$ g/mL) plates and incubated at 37  $^{\circ}$ C overnight. Single colonies were inoculated into 5 ml LB cultures containing 100  $\mu$ g/ml ampicillin and grown overnight at 37 $^{\circ}$ C with shaking (225 rpm). Following overnight growth, plasmids were purified from cultures using EZ-10 Spin Column Plasmid DNA kit (BioBasic) per manufacturer's instructions and successful ligation was confirmed by DNA sequencing (Genewiz).

**2.4.17 GThPH Purification.** The resuspended cell pellet was stored at 4  $^{\circ}$  C overnight. Cells were placed on ice, and a protease cocktail was added to the resuspended pellet before sonication, composed of PMSF (10  $\mu$ g /mL) in 15mL of lysis buffer. Bacteria were lysed using a sonicator per the following protocol: power setting of 12; 8 cycles of sonication for 30 sec followed by 30 sec rest. The lysis solution was centrifuged (20, 000 x g, 30 min) at 4  $^{\circ}$  C, with the resulting supernatant removed and filtered using a 10 mL syringe and 0.45 micron syringe tip filter. The supernatant was then volume up to 250 mL in lysis buffer and purified using a GSTrap FF GST sepharose High Performance column. Buffers for GSTrap FPLC were prepared as follows: lysis (300 mM NaCl, 50 mM Tris, 10% glycerol); elution buffer (300 mM NaCl, 50 mM Tris, 10 % glycerol, and 10 mM glutathione). A gradient elution was performed using GSTrap column (0.5 mL/min) with the following method: 250 mL of lysis buffer containing 0 mM glutathione followed by load of the filtered bacterial lysate, 50 mL wash with lysis buffer and a gradient elution over 100 mL, 0-100% of elution buffer containing 10 mM glutathione. The desired fractions (2 mL) containing the GThPH fusion protein were combined

to final volume of 45 mL. Protein content was determined via Bradford assay in  $\mu\text{g/mL}$  then the corresponding amount of TEV protease was added (1:50-1:200) to the combined fractions in a 50 mL conical tube and was placed in a 34 °C water bath for 8-10 hr. Following the TEV digestion the sample was then loaded onto a primed a HisTrap FF  $\text{Ni}^{2+}$  Sepharose High Performance column (2 x 5 mL) column using a step-wise elution. The following method: 15 mL of lysis buffer, 45 mL of TEV digestion mixture, 25 mL of wash buffer and a step-wise elution over 75 mL of elution buffer. After HisTrap column proghrelin- His<sub>6</sub> selected fractions were buffer exchanged by two cycles of adding an equal volume of 20 mM  $\text{NaH}_2\text{PO}_4$ , 50 mM NaCl or 100 mM NaCl, 50 mM Tris-HCl, (pH 7.3) to sample and concentration, yielding a final volume of 2 mL. The 2 mL concentrate was then run on HiLoad 16/60 Superdex 75 pg size exclusion column (GE) or HiPrep 16/60 Sephacryl S-100 High Resolution size exclusion column (GE). Buffer for size exclusion column was prepared as follows: lysis buffer (20 mM  $\text{NaH}_2\text{PO}_4$ , 50 mM NaCl or 100 mM NaCl, 50 mM Tris-HCl, pH 7.3). Buffer was continuously run through the column for 120 mL (1 column volume) after injection of 2 mL of sample and an elution profile was obtained. Fractions (1 mL each) were then analyzed by SDS-PAGE and Coomassie staining. Fractions containing a homogenous product were combined and concentrated, stored at -80 °C.

**2.4.18 GST-TEV-His<sub>6</sub> protease preparation.** Transform Z-competent Rosetta 2 *E. coli* cells with 100 ng of GST-TEV-His<sub>6</sub> and plate onto an LB ampicillin/chloramphenicol (100  $\mu\text{g/mL}$ , 34  $\mu\text{g/mL}$ ) selection plate. Grow at 37 °C overnight. One colony was used to inoculate a 50 mL culture of Terrific broth (Thermo Fischer) containing 50  $\mu\text{g/mL}$  ampicillin and 34  $\mu\text{g/mL}$  chloramphenicol. Grow overnight at 30 °C shaking at 210 rpm. Inoculate 1L Terrific broth with 15 mL each of the seed 50 mL culture. Grow cultures at 37°C, shaking at 210 rpm until  $\text{OD}_{600} =$

1.0 (check every ½ hour). Once optical density reached 1.0, cool cultures for 1 hr at 4 °C. After OD has been met turn the shaking incubator down 16 °C. After 1 hr, add 1 mL of 1M IPTG to each culture and grow cultures for 20-26 hr at 16 °C, shaking 210 rpm.

Purification of GST-TEV-His<sub>6</sub> utilizes the GSTrap FF column purification from section 2.4.17.

**2.4.19 GThCgH resin purification.** The resuspended cell pellet was thawed at 4 °C overnight. Cells were cooled on ice, followed by addition a protease cocktail composed of PMSF (10 µg /mL) in 15 mL of lysis buffer. (For denaturing conditions the pellet was resuspended in resuspension buffer (20 mL) and lysed using a sonicator per the following protocol: power setting of 12; 8 cycles of sonication for 30 sec followed by 30 sec rest. The lysis solution was centrifuged (20,000 x g, 20 min) at 4 °C, the supernatant was poured off and the pellet was resuspended in resuspension buffer again and centrifuged, the supernatant was poured off and finally resuspended in binding buffer which was filtered using a 10 mL syringe and 0.45 micron syringe tip filter). The pellet was lysed using using a sonicator per the following protocol: power setting of 12; 8 cycles of sonication for 30 sec followed by 30 sec rest. The lysis solution was centrifuged (20,000 x g, 20 min) at 4 °C, the supernatant was poured off filtered using a 10 mL syringe and 0.45 micron syringe tip filter. His60 Ni<sup>2+</sup> resin was equilibrated with 2 column volumes of lysis buffer, spun down 700 x g, 10 min, 4 °C, bacterial lysate was added to resin rocked 18 hr spun down 700 x g, 10 min, 4 °C, 3 column volumes of wash buffer 1 then 2 were added to resin in three increments with resin spun down 700 x g, 10 min, 4 °C between each addition, 1.5 column volumes of elution buffer was then added rocked 1 hr at 4 °C, then spun down 700 x g, 10 min, 4 °C. At each step the supernatant was collected. Buffers (pH 7.3) for His60 Ni<sup>2+</sup> resin (Clonotech) were prepared as follows: resuspension buffer (20 mM Tris-HCl,

500 mM NaCl, 2 M GuHCl, 2% Triton-100), binding buffer (20 mM Tris-HCl, 500 mM NaCl, 6 M GuHCl, 5mM imidazole), wash buffer 1 (20 mM Tris-HCl, 500 mM NaCl, 6 M Urea, 10 mM imidazole); wash buffer 2 (20 mM Tris-HCl, 500 mM NaCl, 3 M Urea, 100mM imidazole); refolding buffer (20 mM Tris-HCl, 500 mM NaCl, 20 mM imidazole), elution buffer (20 mM Tris-HCl, 500 mM NaCl, 500 mM imidazole).

For non-denaturing purification of GThCgH, the resin conditions were the same as described above with a change in buffers. The buffers (pH 7.3) were prepared as follows: lysis buffer (20 mM NaH<sub>2</sub>PO<sub>4</sub>, 300 mM NaCl, 10 mM imidazole), wash buffer 1 (20 mM NaH<sub>2</sub>PO<sub>4</sub>, 300 mM NaCl, 20 mM imidazole), wash buffer 2 (20 mM NaH<sub>2</sub>PO<sub>4</sub>, 300 mM NaCl, 50 mM imidazole) and elution buffer (20 mM NaH<sub>2</sub>PO<sub>4</sub>, 300 mM NaCl, 250 mM imidazole).

## 2.5 References

1. Gutierrez, J. A.; Solenberg, P. J.; Perkins, D. R.; Willency, J. A.; Knierman, M. D.; Jin, Z.; Witcher, D. R.; Luo, S.; Onyia, J. E.; Hale, J. E., Ghrelin octanoylation mediated by an orphan lipid transferase. *Proc Natl Acad Sci U S A* **2008**, *105* (17), 6320-5.
2. Yang, J.; Brown, M. S.; Liang, G.; Grishin, N. V.; Goldstein, J. L., Identification of the acyltransferase that octanoylates ghrelin, an appetite-stimulating peptide hormone. *Cell* **2008**, *132* (3), 387-96.
3. Yang, J.; Zhao, T. J.; Goldstein, J. L.; Brown, M. S., Inhibition of ghrelin O-acyltransferase (GOAT) by octanoylated pentapeptides. *Proc Natl Acad Sci U S A* **2008**, *105* (31), 10750-5.
4. Darling, J. E.; Prybolsky, E. P.; Sieburg, M.; Hougland, J. L., A fluorescent peptide substrate facilitates investigation of ghrelin recognition and acylation by ghrelin O-acyltransferase. *Anal Biochem* **2013**, *437* (1), 68-76.
5. Darling, J. E.; Zhao, F.; Loftus, R. J.; Patton, L. M.; Gibbs, R. A.; Hougland, J. L., Structure-activity analysis of human ghrelin O-acyltransferase reveals chemical determinants of ghrelin selectivity and acyl group recognition. *Biochemistry* **2015**, *54* (4), 1100-10.
6. Taylor, M. S.; Dempsey, D. R.; Hwang, Y.; Chen, Z.; Chu, N.; Boeke, J. D.; Cole, P. A., Mechanistic analysis of ghrelin-O-acyltransferase using substrate analogs. *Bioorg Chem* **2015**, *62*, 64-73.
7. Taylor, M. S.; Hwang, Y.; Hsiao, P. Y.; Boeke, J. D.; Cole, P. A., Ghrelin O-acyltransferase assays and inhibition. *Methods Enzymol* **2012**, *514*, 205-28.
8. Kojima, M.; Hosoda, H.; Date, Y.; Nakazato, M.; Matsuo, H.; Kangawa, K., Ghrelin is a growth-hormone-releasing acylated peptide from stomach. *Nature* **1999**, *402* (6762), 656-60.

9. Zhang, J. V.; Ren, P. G.; Avsian-Kretchmer, O.; Luo, C. W.; Rauch, R.; Klein, C.; Hsueh, A. J., Obestatin, a peptide encoded by the ghrelin gene, opposes ghrelin's effects on food intake. *Science* **2005**, *310* (5750), 996-9.
10. Zhu, X.; Cao, Y.; Voogd, K.; Steiner, D. F., On the processing of proghrelin to ghrelin. *J Biol Chem* **2006**, *281* (50), 38867-70.
11. Bednarek, M. A.; Feighner, S. D.; Pong, S. S.; McKee, K. K.; Hreniuk, D. L.; Silva, M. V.; Warren, V. A.; Howard, A. D.; Van Der Ploeg, L. H.; Heck, J. V., Structure-function studies on the new growth hormone-releasing peptide, ghrelin: minimal sequence of ghrelin necessary for activation of growth hormone secretagogue receptor 1a. *J Med Chem* **2000**, *43* (23), 4370-6.
12. Lim, C. T.; Kola, B.; Korbonits, M., The ghrelin/GOAT/GHS-R system and energy metabolism. *Rev Endocr Metab Disord* **2011**, *12* (3), 173-86.
13. Mear, Y.; Enjalbert, A.; Thirion, S., GHS-R1a constitutive activity and its physiological relevance. *Front Neurosci* **2013**, *7*, 87.
14. Yada, T.; Damdindorj, B.; Rita, R. S.; Kurashina, T.; Ando, A.; Taguchi, M.; Koizumi, M.; Sone, H.; Nakata, M.; Kakei, M.; Dezaki, K., Ghrelin signalling in beta-cells regulates insulin secretion and blood glucose. *Diabetes Obes Metab* **2014**, *16 Suppl 1*, 111-7.
15. Beevers, A. J.; Kukol, A., Conformational flexibility of the peptide hormone ghrelin in solution and lipid membrane bound: a molecular dynamics study. *J Biomol Struct Dyn* **2006**, *23* (4), 357-64.
16. Kukol, A., The structure of ghrelin. *Vitam Horm* **2008**, *77*, 1-12.
17. Staes, E.; Absil, P. A.; Lins, L.; Brasseur, R.; Deleu, M.; Lecouturier, N.; Fievez, V.; Rieux, A.; Mingeot-Leclercq, M. P.; Raussens, V.; Preat, V., Acylated and unacylated ghrelin binding to

- membranes and to ghrelin receptor: towards a better understanding of the underlying mechanisms. *Biochim Biophys Acta* **2010**, *1798* (11), 2102-13.
18. De Ricco, R.; Valensin, D.; Gaggelli, E.; Valensin, G., Conformation propensities of des-acyl-ghrelin as probed by CD and NMR. *Peptides* **2013**, *43*, 62-7.
19. Silva Elipe, M. V.; Bednarek, M. A.; Gao, Y. D., <sup>1</sup>H NMR structural analysis of human ghrelin and its six truncated analogs. *Biopolymers* **2001**, *59* (7), 489-501.
20. Vortmeier, G.; DeLuca, S. H.; Els-Heindl, S.; Chollet, C.; Scheidt, H. A.; Beck-Sickinger, A. G.; Meiler, J.; Huster, D., Integrating solid-state NMR and computational modeling to investigate the structure and dynamics of membrane-associated ghrelin. *PLoS One* **2015**, *10* (3), e0122444.
21. Alen, B. O.; Nieto, L.; Gurriaran-Rodriguez, U.; Mosteiro, C. S.; Alvarez-Perez, J. C.; Otero-Alen, M.; Camina, J. P.; Gallego, R.; Garcia-Caballero, T.; Martin-Pastor, M.; Casanueva, F. F.; Jimenez-Barbero, J.; Pazos, Y., The NMR structure of human obestatin in membrane-like environments: insights into the structure-bioactivity relationship of obestatin. *PLoS One* **2012**, *7* (10), e45434.
22. Scrima, M.; Campiglia, P.; Esposito, C.; Gomez-Monterrey, I.; Novellino, E.; D'Ursi, A. M., Obestatin conformational features: a strategy to unveil obestatin's biological role? *Biochem Biophys Res Commun* **2007**, *363* (3), 500-5.
23. Subasinghage, A. P.; Green, B. D.; Flatt, P. R.; Irwin, N.; Hewage, C. M., Metabolic and structural properties of human obestatin {1-23} and two fragment peptides. *Peptides* **2010**, *31* (9), 1697-705.
24. Schwyzer, R., In search of the 'bio-active conformation'--is it induced by the target cell membrane? *J Mol Recognit* **1995**, *8* (1-2), 3-8.

25. Esposito, D.; Chatterjee, D. K., Enhancement of soluble protein expression through the use of fusion tags. *Curr Opin Biotechnol* **2006**, *17* (4), 353-8.
26. Wood, W. B., Host specificity of DNA produced by Escherichia coli: bacterial mutations affecting the restriction and modification of DNA. *J Mol Biol* **1966**, *16* (1), 118-33.
27. Studier, F. W.; Moffatt, B. A., Use of bacteriophage T7 RNA polymerase to direct selective high-level expression of cloned genes. *J Mol Biol* **1986**, *189* (1), 113-30.
28. Studier, F. W., Protein production by auto-induction in high density shaking cultures. *Protein Expr Purif* **2005**, *41* (1), 207-34.
29. Schlegel, S.; Lofblom, J.; Lee, C.; Hjelm, A.; Klepsch, M.; Strous, M.; Drew, D.; Slotboom, D. J.; de Gier, J. W., Optimizing membrane protein overexpression in the Escherichia coli strain Lemo21(DE3). *J Mol Biol* **2012**, *423* (4), 648-59.
30. Irie, S., [A highly sensitive silver staining for detection of proteins in polyacrylamide gels (author's transl)]. *Seikagaku* **1980**, *52* (6), 411-3.
31. Paliy, O.; Gunasekera, T. S., Growth of E. coli BL21 in minimal media with different gluconeogenic carbon sources and salt contents. *Appl Microbiol Biotechnol* **2007**, *73* (5), 1169-72.
32. Blommel, P. G.; Fox, B. G., A combined approach to improving large-scale production of tobacco etch virus protease. *Protein Expr Purif* **2007**, *55* (1), 53-68.

### **Chapter 3: Processing behavior of proghrelin and C-ghrelin**

The work in this chapter is unpublished. In this chapter, there was an experimental contribution from Casey L. Cabrinha (Syracuse University summer REU undergraduate) who assisted with construction and expression of proghrelin variants containing alanine mutations and Terry Watt and Tasha Toro (Xavier University of Louisiana) who performed mass spectrometry analysis of proghrelin cleavage products.

### 3.1 Introduction

As mentioned in Chapter 1, there are multiple products derived from proghrelin after acylation by GOAT. The two major products are ghrelin and C-ghrelin, which is then further processed to obestatin (Figure 3.1).<sup>1-6</sup> Ghrelin processing from proghrelin is well characterized, and knockout studies targeting prohormone convertases/furins show an absence of mature ghrelin in those cells indicating a loss of processing of proghrelin to ghrelin.<sup>4-5, 7-9</sup> However, C-ghrelin processing leading to the peptide hormone obestatin has not been characterized to the same extent. There is a general consensus based upon sequence and gene splicing that obestatin is a processing product from proghrelin, specifically C-ghrelin.<sup>10-12</sup> The exact enzymes or mechanism in which obestatin is cleaved from C-ghrelin is unknown. Similarly the processing pathway for a newly identified splicing variant produced from obestatin (1-23), obestatin (11-23), is also undefined (Figure 3.1).<sup>13</sup> With obestatin determined to contain an amidated C-terminus, the processing of the C-terminus of obestatin is presumed to proceed through carboxypeptidase which cleaves the C-terminal lysine followed by modification by peptidyl glycine  $\alpha$ -amidating monooxygenase (PAM) to yield C-terminal amidation.<sup>1, 5, 9-10, 14</sup> The lack of information surrounding the obestatin processing pathway from C-ghrelin, leading to production of two independent hormones from the same proghrelin prohormone, marks this pathway as a system worthy of investigation.

Throughout both the expression and purification of proghrelin described in Chapter 2, loss of the parent protein and concurrent observation of small protein bands indicate that cleavage of the proghrelin construct was occurring. The cleavage behavior which results in an observed heterogeneity was also observed throughout protein purification and in homogeneous proghrelin samples verified by silver staining and mass spectrometry. Cleavage of homogeneous

proghrelin-His<sub>6</sub> is consistent with proghrelin cleaving itself, rather than another protein being responsible for the observed cleavage behavior. This systematic and continuous cleavage of proghrelin-His<sub>6</sub> was challenging to avoid and has been consistent since proghrelin was first expressed. In order to further understand the protein and determine how best to avoid this cleavage during purification, the processing behavior was characterized and explored. In this chapter the cleavage of proghrelin is analyzed and this role in C-ghrelin processing is assessed.

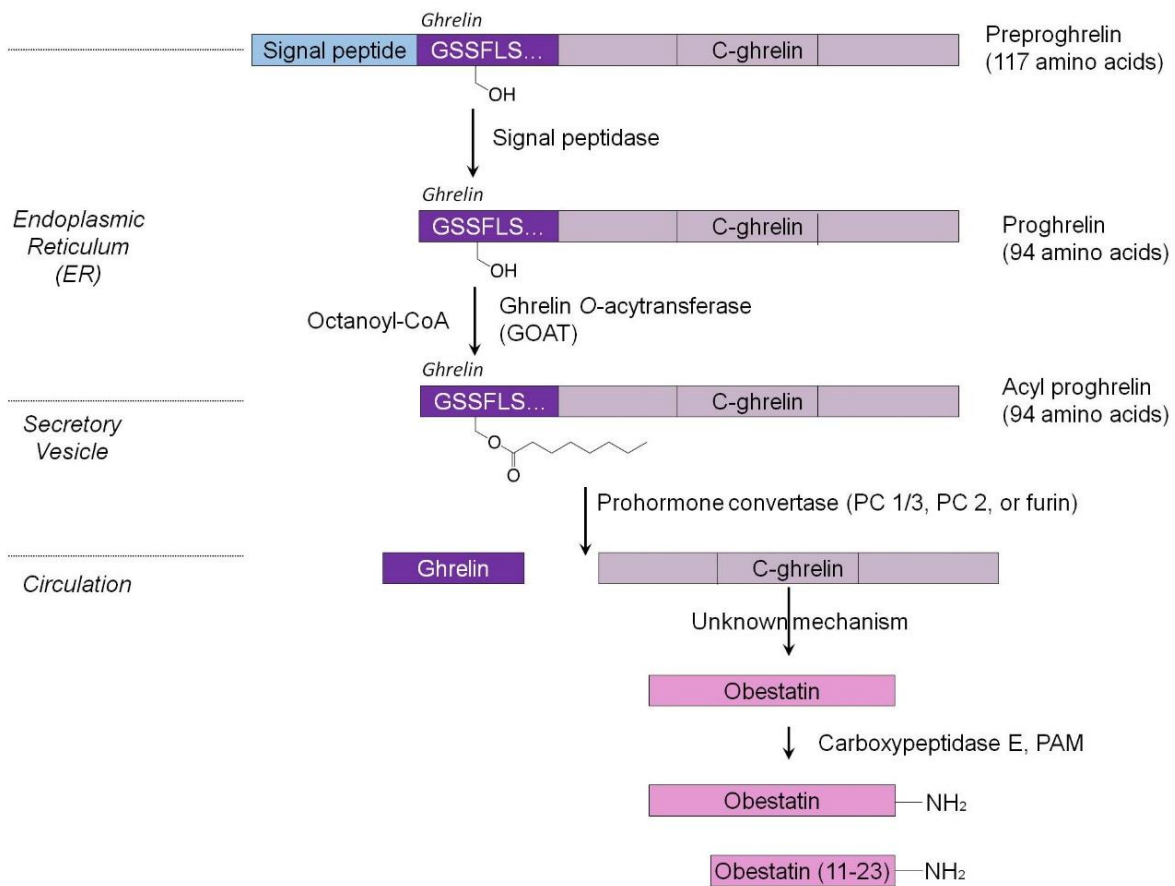


**Figure 3.1. The proghrelin processing pathway.** Portions of this figure are adapted and reprinted with permission from Reference 6 (Appendix II). © 2016 Taylor and Francis.

## 3.2 Results

### 3.2.1 Proghrelin cleavage behavior in bacterial lysate

The first observation of the cleavage of proghrelin and C-ghrelin followed bacterial cell lysis during protein expression. This behavior was observed in lysis conditions using a mild non-denaturing detergent (BPER (Thermo scientific), bacterial protein extraction reagent) compared to harsher denaturing lysis using sample buffer including SDS (3XSB, 3X sample buffer) (Chapter 2). The lower molecular weight bands contain a GST-tag as verified by Western blotting but appear to lack the C-terminal His<sub>6</sub>-tag (Chapter 2, Figure 2.2). To attempt to block GThPH cleavage by endogenous proteases, bacterial lysis buffers were treated with protease inhibitor cocktails including phenylmethylsulfonyl fluoride (PMSF, serine protease inhibitor), benzamidine (trypsin-like enzymes, serine protease inhibitor), pepstatin A (aspartyl protease inhibitor), and leupeptin (cysteine, serine and threonine protease inhibitor). However, protease inhibitor addition did not eliminate the cleavage of GThPH during bacterial lysis with a non-denaturing detergent based reagent such as BPER reagent or during sonication (Figure 3.2). The same cleavage behavior was observed plus or minus a protease cocktail.

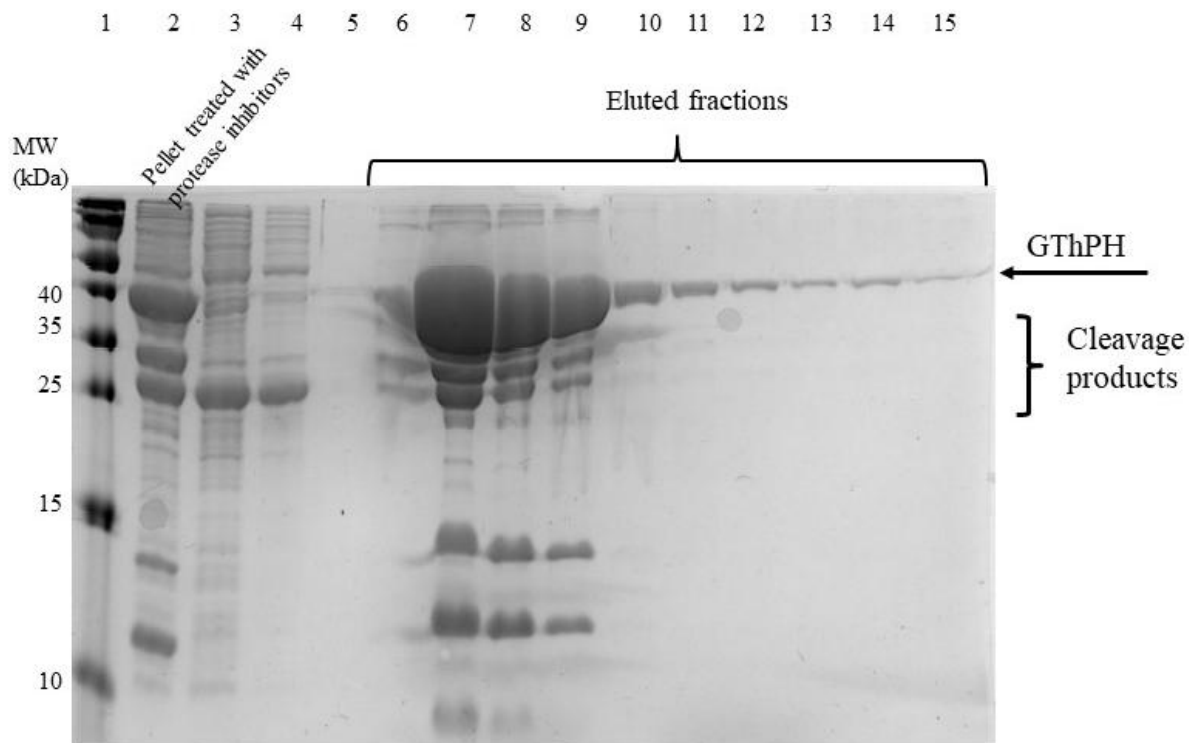


**Figure 3.2. Addition of a protease cocktail during bacterial lysis and purification does not inhibit cleavage.** A 300 mL bacterial pellet of GThPH was sonicated in the presence of a protease cocktail (10  $\mu\text{g}/\text{mL}$  PMSF, 50  $\mu\text{g}/\text{mL}$  benzamidine, 10  $\mu\text{g}/\text{mL}$  leupeptin, and 0.7  $\mu\text{g}/\text{mL}$  pepstatin A) and was loaded onto a HisTrap FF column using a step-wise elution method. Fractions were collected from under the A280 peak. No difference in cleavage was observed with a protease cocktail present. The gel is 12% polyacrylamide. Lane 1, protein ladder (Thermo scientific); Lane 2, post-sonicated GThPH (in the presence of protease cocktail); Lane 3, column flow-through; Lane 4, column wash; Lane 6, fraction 1; Lane 7 fraction 2; Lane 8, fraction 3; Lane 9, fraction 5; Lane 10, fraction 7; Lane 11, fraction 9; Lane 12, fraction 12; Lane 13, fraction 15; Lane 14, fraction 18; Lane 15, fraction 20.

The observed cleavage of proghrelin occurs within a short time scale during bacterial lysis using non-denaturing conditions. The time frame of GThPH cleavage is approximately 6-15 minutes after the initial bacterial pellet is lysed before the addition of denaturing sample loading buffer for polyacrylamide gel analysis. The lower molecular weight proteins including GST-tagged proteins were not present during bacterial lysis when bacterial pellets were lysed using denaturing conditions (3XSB). The loss of GThPH cleavage under denaturing conditions indicates that a folded protein structure is likely important for cleavage behavior and/or the presence of the denaturant blocks GThPH from interacting with lipids or other proteins in the bacterial cytosol that enhance cleavage.

In light of the reproducible cleavage of GThPH in bacterial lysate on relatively short time scales (<10-20 minutes), we investigated this behavior to determine the solution conditions accelerate or inhibit GThPH cleavage. The first avenue was to ascertain if this cleavage can either be halted or enhanced by addition of metal ions into the bacterial lysate and the metal dependency of GThPH cleavage in lysate. However, the behavior observed during multiple studies with metal ion addition was unclear and not reproducible from experiment to experiment. Since bacterial lysate contains many molecular species including unidentified *E. coli* proteins and lipids, studies in lysate were limited and instead the focus switched to study proghrelin's cleavage behavior in its purified form. In future studies of proghrelin cleavage, incubation with fractionated bacterial lysates may be pursued to explore the impact (if any) of bacterially derived proteins or small molecules.

To inhibit the cleavage behavior observed in bacterial lysate and purified samples, a denaturing purification protocol was utilized since addition of a denaturing bacterial lysis limited GThPH cleavage. As bacterial lysis by denaturing gel loading sample buffer including SDS

completely inhibited cleavage of GThPH, we reasoned GThPH purification under denaturing conditions may have allowed for proghrelin purification without cleavage. Supporting this approach was the denaturing purification protocol that was used for C-ghrelin (Chapter 2) with some success. For the GThPH purification under denaturing conditions, guanidine hydrochloride (GuHCl, 6 M) was included in all buffers from bacterial pellet resuspension, sonication and resin purification. In the presence of GuHCl, the GThPH fusion protein did not exhibit cleavage as reflected by a single predominant band by SDS-PAGE analysis, compared to the three predominant bands observed in the absence of GuHCl (Figure 3.3). The suppression of GThPH cleavage upon bacterial lysis in the presence of 6 M GuHCl was encouraging. After elution during buffer exchange decreasing the concentration of GuHCl there was aggregation of the fusion protein, this same behavior was observed using both dialysis and a gradient elution to lower the concentration of GuHCl over a greater period of time. This aggregation behavior was also observed with C-ghrelin's denaturing purification. While the suppression of proghrelin cleavage under denaturing conditions supports the requirement for a folded protein or an unidentified protein-protein interaction for the cleavage behavior observed with this protein, the aggregation observed upon removal of GuHCl precluded further development of a denaturing protocol for proghrelin purification.

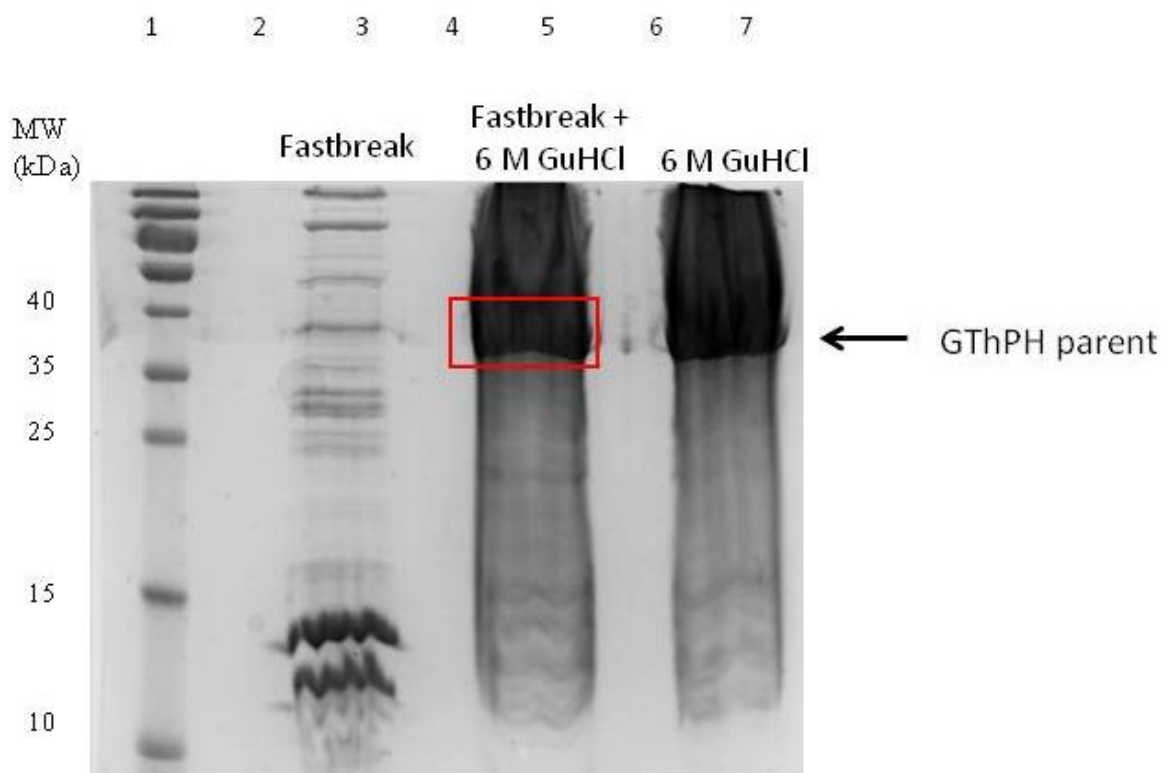


**Figure 3.3. Bacterial pellet lysis in the presence of 6 M GuHCl.** 1 mL bacterial pellets were resuspended in buffer containing either 0 or 6 M GuHCl then lysed using FastBreak cell lysis reagent (Promega), a non-denaturing cell lysis reagent. Lane 7 is the result of growth of a 300 mL bacterial pellet which was lysed in 6 M GuHCl. The red box indicates GThPH which appears as a single band. The gel is 12% polyacrylamide. Lane 1 protein ladder (Thermo scientific) Lane 3, 1 mL bacterial pellet lysed using FastBreak; Lane 5, 1 mL bacterial pellet lysed using FastBreak in presence of 6 M GuHCl; Lane 7, A sample from a 300 mL bacterial pellet resuspended and sonicated in presence of 6 M GuHCl.

### 3.2.2 Proghrelin cleavage in purified samples

The cleavage behavior observed in bacterial lysate was also observed in purified proghrelin-His<sub>6</sub> samples, which was discussed briefly in Chapter 2. Homogeneous proghrelin-His<sub>6</sub> purified by size exclusion chromatography was stored at 4 °C and over a time span of 24 hours lower molecular weight cleavage products were observed. Upon further examination, it became apparent that purified proghrelin-His<sub>6</sub> would degrade when stored in solution, with protein remaining intact only if frozen or lyophilized. Freeze-thaw cycles in solution added to the appearance of cleavage of proghrelin, so these cycles were avoided as much as possible. There was also an observable increase in lower molecular weight cleavage products as a result of centrifugation during protein concentration and buffer exchanging with centrifugation. This was demonstrated in a side-by-side comparison of a sample in which half was either concentrated or left dilute and then analyzed by gel electrophoresis (Figure 3.4). This behavior may suggest a potential for protein-protein interactions between proghrelin molecules to contribute to the observed cleavage of proghrelin since a higher concentration would increase the relative number of these interactions occurring.

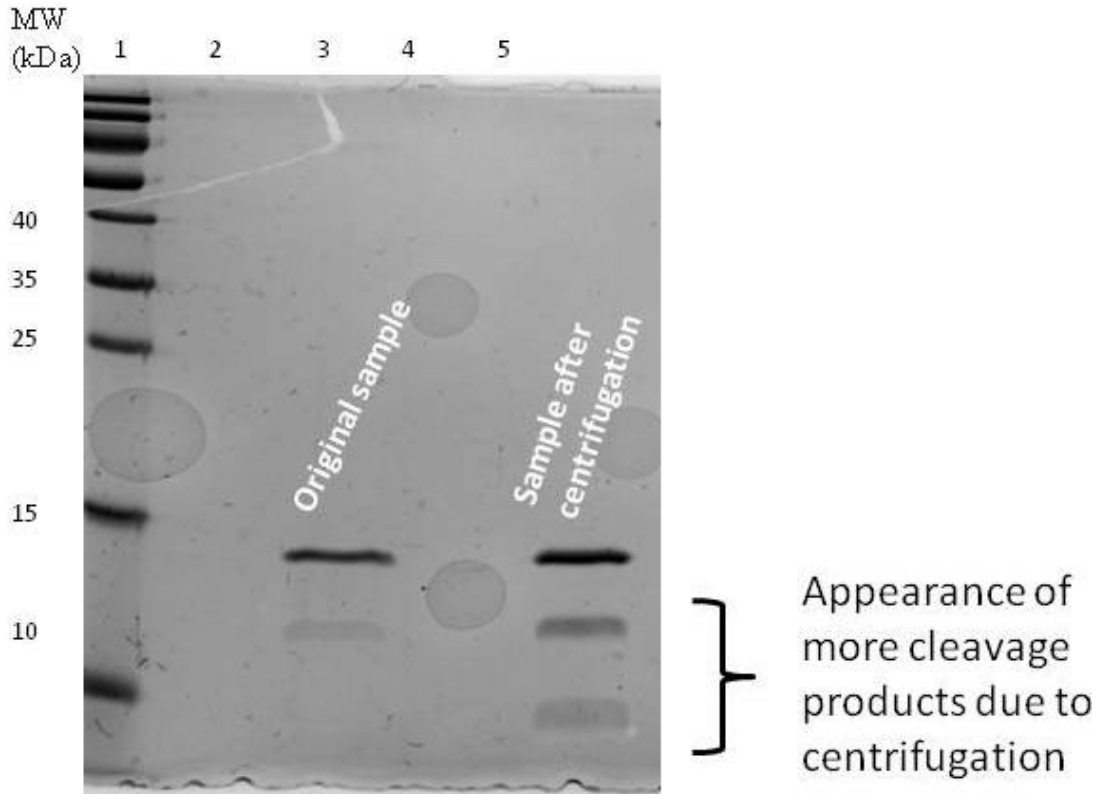


**Figure 3.4. Increased proghrelin-His<sub>6</sub> cleavage observed following protein concentration.** After purification using size exclusion chromatography, fractions were pooled, half were left unconcentrated and the other half were concentrated to a tenth of their original volume. The concentrated sample was corrected for protein concentration before gel loading. The gel is 15% polyacrylamide. Lane 1, protein ladder (Thermo scientific); Lane 3, unconcentrated purified proghrelin-His<sub>6</sub> sample; Lane 5, concentrated purified proghrelin-His<sub>6</sub> sample.

In an attempt to stabilize purified proghrelin, ethylenediaminetetraacetic acid (EDTA) was added to purified samples to chelate any metals that may contribute to proghrelin cleavage (Figure 3.5). The rationale for EDTA addition was the behavior with metal addition to bacterial lysate having some effect but not reproducibly increasing proghrelin cleavage. While proghrelin cleavage was observed in samples that were EDTA-free, addition of EDTA (1 or 5 mM) appears to suppress proghrelin degradation over the time course monitored (Figure 3.5). Moving forward, this finding supported that inclusion of EDTA in proghrelin storage buffers would stabilize proghrelin against cleavage.

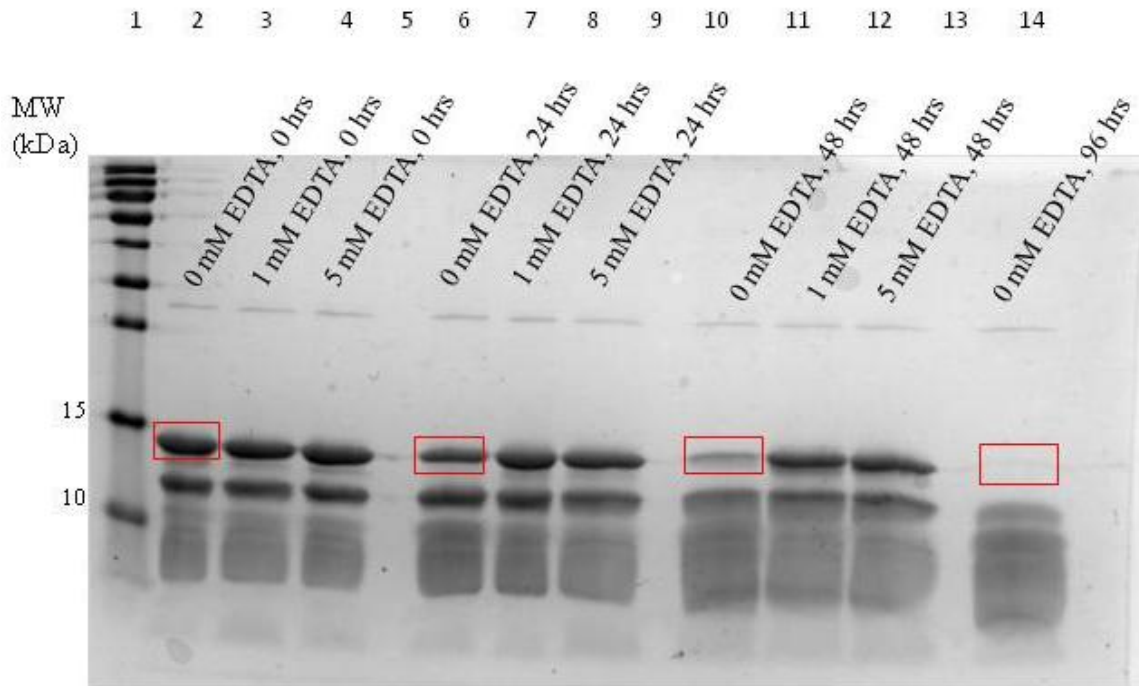


**Figure 3.5. Addition of EDTA stabilized proghrelin-His<sub>6</sub> against cleavage.** Purified proghrelin-His<sub>6</sub> was incubated at room temperature for up to 96 hours with varying concentration of EDTA added. Red boxes indicate proghrelin-His<sub>6</sub> at each time point (0, 24, 48, 96 hours) in the absence of EDTA (0 mM). The gel is 15% polyacrylamide. Lane 1, protein ladder (Thermo scientific); Lane 2, 0mM EDTA/0 hrs; Lane 3, 1 mM EDTA/ 0 hrs; Lane 4, 5 mM EDTA/ 0 hrs; Lane 6 0 mM EDTA / 24 hrs; Lane 7, 1 mM EDTA/ 24 hrs; Lane 8, 5 mM EDTA/ 24 hrs; Lane 10, 0 mM EDTA/ 48 hrs; Lane 11, 1 mM EDTA/48 hrs; Lane 12, 5 mM EDTA/ 48 hrs; Lane 14, 0 mM EDTA/96 hrs.

### 3.2.3 Mass spectrometry analysis of proghrelin cleavage

To determine the location of the cleavage site(s) within purified proghrelin, the proghrelin cleavage products were analyzed by our collaborator Prof. Terry Watt at Xavier University of Louisiana using MALDI-TOF (matrix-assisted laser desorption/ionization-time of flight) mass spectrometry (Figure 3.6, Table 3.1). To generate samples for MALDI-TOF analysis, purified proghrelin was incubated at room temperature in 50 mM Tris-HCl, pH 7.3 for a series of time points over a span of six days. Following this incubation, the proghrelin-derived peptides were analyzed and cleavage sites assigned based on the mass of the peptide products. Proghrelin cleavages were observed at several sites in a short stretch of sequence, with this fragmentation occurring over time in an ordered process (Table 3.1, Figure 3.7). The cleavages occur at a high concentration towards the C-terminus of obestatin (proghrelin amino acid residues 53-77 and the obestatin splice variant amino acids 63-77), with the first observable cleavages at Q73 and K77 by 48hrs, following longer incubation cuts at A74, Y68, and H71 were also detected. The C-terminal fragments with their corresponding N-terminal fragments for the cleavage sites listed above (1-68 and 69-100, 1-71 and 72-100, 1-73 and 74-100, 1-74 and 75-100, 1-77 and 78-100) were detected (Table 3.1, Figure 3.7). This analysis confirms that purified proghrelin cleaves itself at a small set of potential sites in a time-dependent manner.

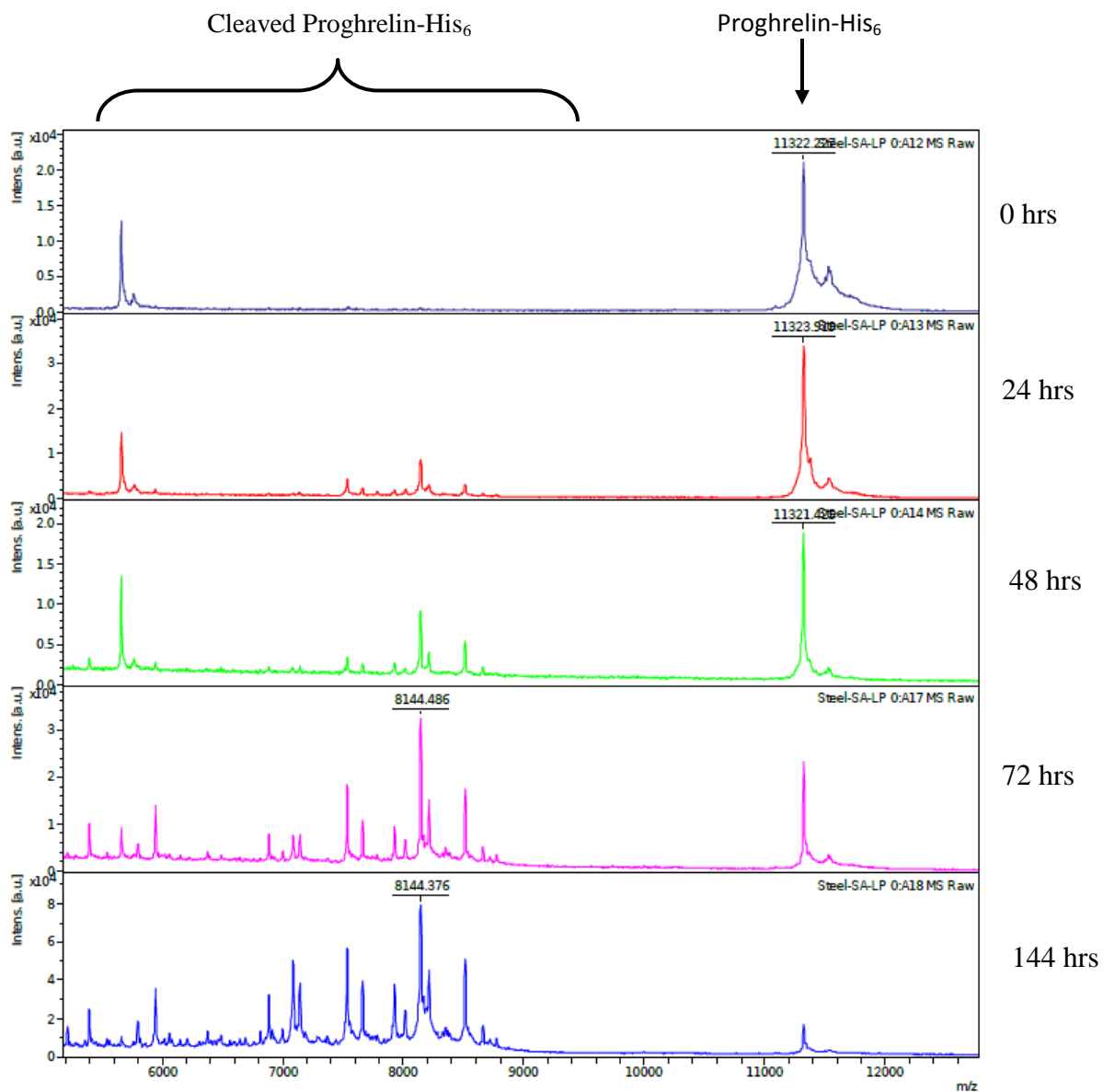


**Figure 3.6. MALDI-TOF mass spectrometry analysis of time-dependent proghrelin-His<sub>6</sub> cleavage.** The amount of uncleaved proghrelin (11,322 Da) gradually decreases consistent with cleavage of the protein over 144 hours. Proghrelin was prepared in 50 mM Tris-HCl, pH 8.0 and allowed to sit at room temperature. Each panel is indicated by the hour the sample was taken, the parental protein is indicated with a black arrow at the top right of the figure, small peptides derived from cleavage are under the black bracket at the top left of the figure.

| Mass (m/z)<br>observed | Time fragment occurred (hrs) |       |       |       |        | Sequence fragment (proghrelin-His <sub>6</sub> length<br>1-100) |
|------------------------|------------------------------|-------|-------|-------|--------|---|
|                        | 0hrs                         | 24hrs | 48hrs | 72hrs | 144hrs |   |
|                        |                              |       |       |       |        | <b>N-terminal fragment</b>                                      |
| 11322                  | x                            | x     | x     | x     | x      | 1 - 100   |
| 8514                   |                              |       | x     | x     | x      | 1 - 77  |
| 8216                   |                              |       |       | x     | x      | 1 - 74  |
| 8144                   |                              | x     | x     | x     | x      | 1 - 73  |
| 8016                   |                              |       |       |       | x      | 1 - 72  |
| 7929                   |                              |       |       | x     | x      | 1 - 71  |
| 7664                   |                              |       |       | x     | x      | 1 - 69  |
| 7535                   |                              |       |       | x     | x      | 1 - 68  |
| 7144                   |                              |       |       |       | x      | 1 - 65  |
| 7088                   |                              |       |       |       | x      | 1 - 64  |
| 6887                   |                              |       |       |       | x      | 1 - 62  |
|                        | 0hrs                         | 24hrs | 48hrs | 72hrs | 144hrs | <b>C-terminal fragment</b>                                      |
| 3803.1                 |                              |       |       | x     | x      | 69 - 100  |
| 3410.1                 |                              |       |       |       | x      | 72 - 100  |
| 3194.8                 |                              | x     |       | x     | x      | 74 - 100  |
| 3123.8                 |                              |       |       | x     | x      | 75 - 100  |
| 2825.6                 |                              |       |       | x     | x      | 78 - 100  |

**Table 3.1. Fragmentation analysis of proghrelin-His<sub>6</sub> cleavage.** The table displays fragment sizes (m/z) and their corresponding sequence from the cleavage of proghrelin-His<sub>6</sub>. The time points at which each fragment at detected are indicated by an “x”.

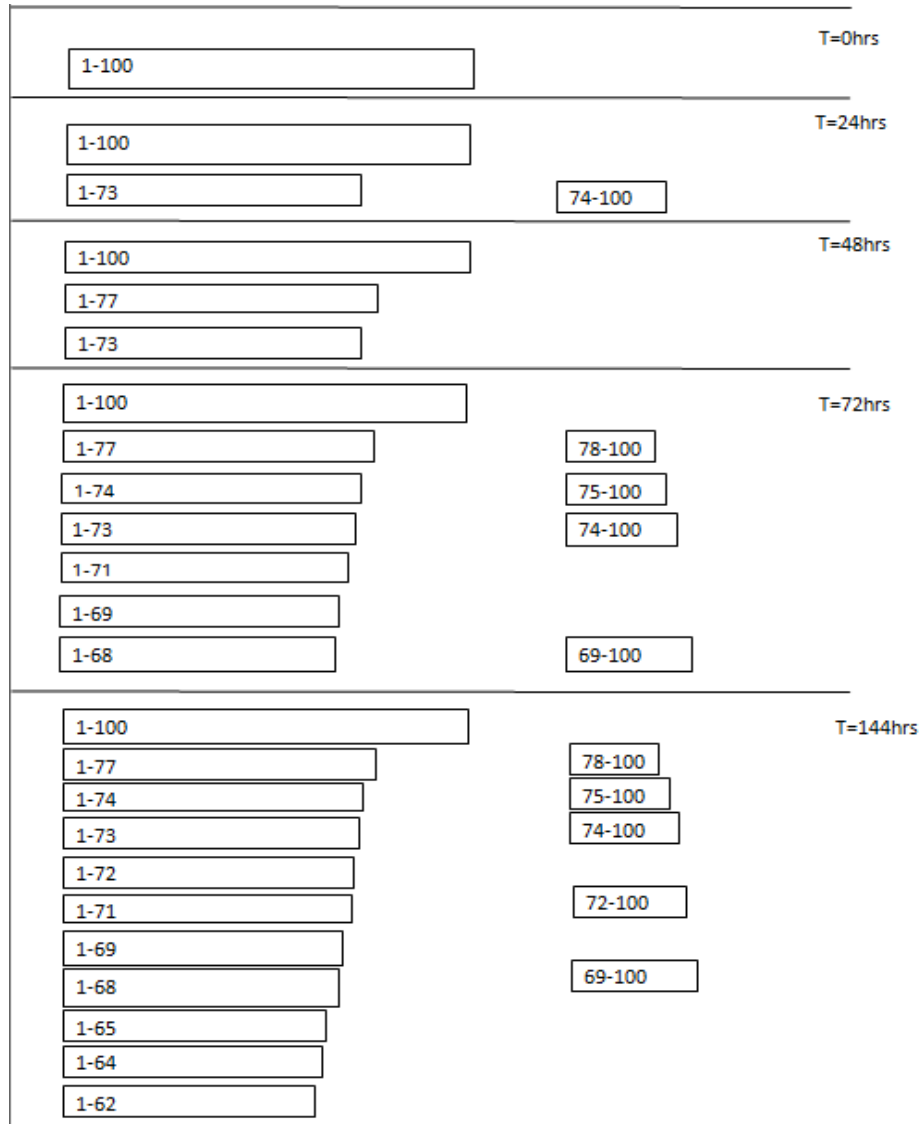


**Figure 3.7. Proghrelin-derived peptides observed by mass spectrometry analysis of a 144 hour time course.** Fragments of proghrelin-His<sub>6</sub>'s sequence observed during the 144 hour time course in Figure 3.6 and Table 3.1. The m/z values were analyzed and the fragmentation was plotted onto proghrelin-His<sub>6</sub>'s sequence. The boxes correspond with the size of the sequence displayed and the time the fragments started to occur T= x hours.

### 3.2.4 Alanine mutagenesis studies towards inhibition of proghrelin cleavage

The mass spectrometry analysis of proghrelin indicated a small set of cleavage sites in the C-terminal portion of the protein. There was a two-fold effort to inhibit the cleavage behavior informed by the mass spectrometry; the first was to mutate amino acids at the cut sites near C-terminal obestatin. This was done in order to try to block proghrelin's cleavage by mutating the cleavage site. This approach is under the assumption that the individual amino acids at the cleavage sites and their distinct functionalities are important for a motif recognition or mechanistically for cleavage to occur. If this is so, mutating the required residue(s) should inhibit or slow the cleavage. The second approach was to mutate a series of amino acids near the beginning of obestatin (N-terminal C-ghrelin) where there is a high concentration of amino acids that can serve to chelate metal ions or act as general bases, generally associated with a catalytic core in proteases such as chymotrypsin (Figure 3.9A).<sup>15-16</sup> This approach takes a mechanistic route in trying to eliminate the residues that contribute to or are responsible for cleavage. Each amino acid in this two-pronged approach was mutated to alanine to remove side chain functionality which may contribute to residue recognition or catalysis of protein cleavage (a representative alanine mutant expression analysis shown Figure 3.8). The amino acids at the cleavage sites identified by mass spectrometry (Q73, K77, and F78) were individually mutated to alanine without an observable change in cleavage behavior. Double and triple alanine mutants were also examined (Q73A-K77A, Q73A-F78A, and Q73A-K77A-F78A) but their behavior was similarly unchanged relative to non-mutated proghrelin (wild-type proghrelin). Focusing on potential catalytic residues (specifically, glutamic acid (E) and aspartic acid (D)), amino acids from E37 to E50 were mutated to alanine but no difference in the cleavage pattern with the alanine mutants compared to non-mutated proghrelin (E43A expression shown in Figure 3.8).

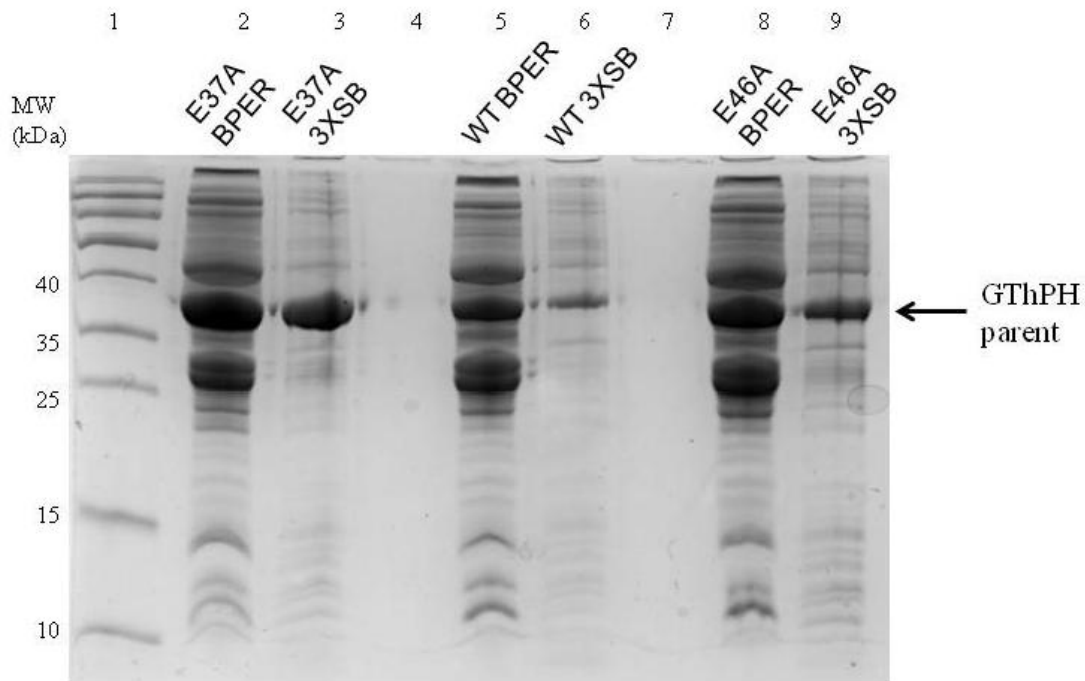


**Figure 3.8. Alanine mutations of GThPH lead to no change in protein cleavage.** This is representative data for all alanine mutations made in proghrelin's sequence. 1 mL bacterial pellets from E37A, E46A or wild-type (WT) growths of GThPH were lysed using either BPER reagent or 3XSB then analyzed by SDS-PAGE and Coomassie staining. There is no discernable difference between the alanine mutants and WT GThPH cleavage pattern. The gel is 12% polyacrylamide. Lane 1, protein ladder (Thermo scientific); Lane 2, E37A BPER lysis; Lane 3, E37A 3XSB lysis; Lane 5, WT GThPH BPER lysis; Lane 6, WT GThPH 3XSB lysis; Lane 8, E46A BPER lysis; Lane 9, E46A 3XSB.

The residues that were targeted for mutation in the stretch from 30-50 are highly conserved across all mammalian species in which proghrelin has been found and sequenced (Figure 3.9B). This conservation suggests these residues may be important for proghrelin interactions with GOAT, the ghrelin receptor GHS-R1a and/or that this cleavage behavior is also present in proghrelin across species. Since, none of the individual alanine mutations resulted in delayed or inhibited cleavage there is the possibility that multiple residues are involved or the residues targeted for mutation play no role in proghrelin's cleavage behavior.

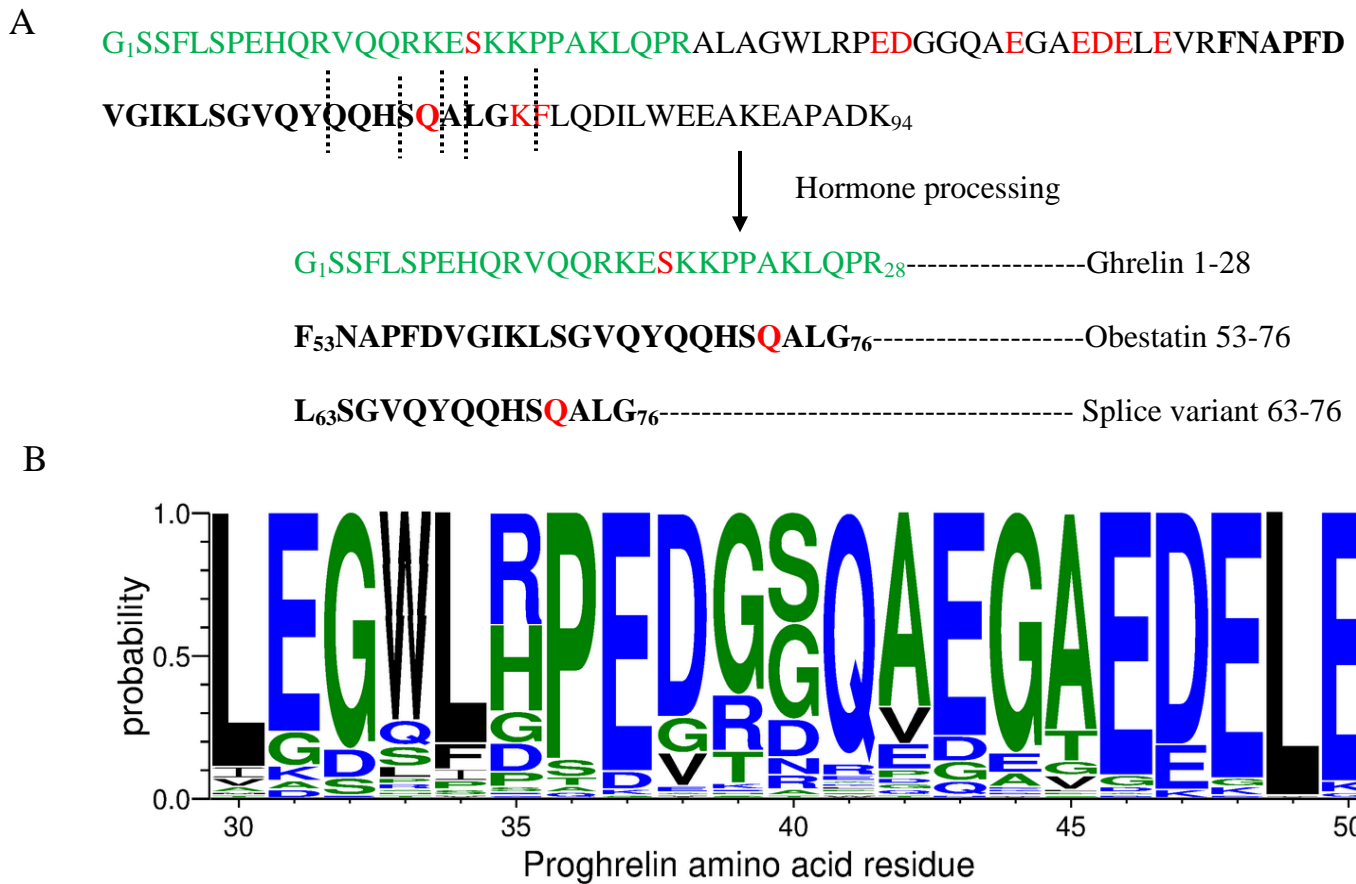


**Figure 3.9. Hormone products from proghrelin processing.** A) Cleavage sites from MALDI-TOF fragmentation analysis. Cut sites are indicated with black dotted lines in proghrelin's sequence, amino acid residues that were mutated to alanine indicated in red. The individual products from biological hormone processing are indicated (ghrelin, obestatin and obestatin's splicing variant) and their lengths are in terms of proghrelin's sequence. Ghrelin is in green text, obestatin in bold text in proghrelin's sequence. **B) Homology alignment of amino acid probability for proghrelin residues 30-50.** This is the range which contains the necessary residues for cleavage. The figure is a result of all known mammalian proghrelin sequences input into WebLogo. Residues that are more conserved are larger at their position.

### **3.2.5 Development of a fluorescence-based system to investigate proghrelin cleavage**

The cleavage of proghrelin, both in bacterial lysate and purified samples, has been observed continuously throughout expression and purification of proghrelin. Proghrelin cleavages had been detected using SDS-PAGE followed by either Coomassie staining and /or Western blotting. Mass spectrometry was also used but only indicated the sites of cleavage not the sequence or residues needed for it to occur. With these methods not conducive to a complete characterization of proghrelin cleavage behavior, another analytical technique was needed to analyze proghrelin cleavage.

Work done by Brian Callahan and coworkers created a system that utilized cyan fluorescent protein (CFP) and yellow fluorescent protein (YFP) in a Förster resonance energy transfer (FRET) system to study the intein splicing.<sup>17-19</sup> Callahan then modified this system to monitor cleavage of the protein Hedgehog which is induced by cholesterol (Figure 3.10).<sup>17-21</sup> Since, this FRET system has been previously used to study protein splicing, it could be potentially used to study proghrelin's unique cleavage behavior. A fluorescent protein construct was created to substitute proghrelin into CFP-X-YFP (CXY, where X is a small linker sequence) FRET construct yielding CFP-proghrelin-YFP (CpgY) (Figure 3.11).

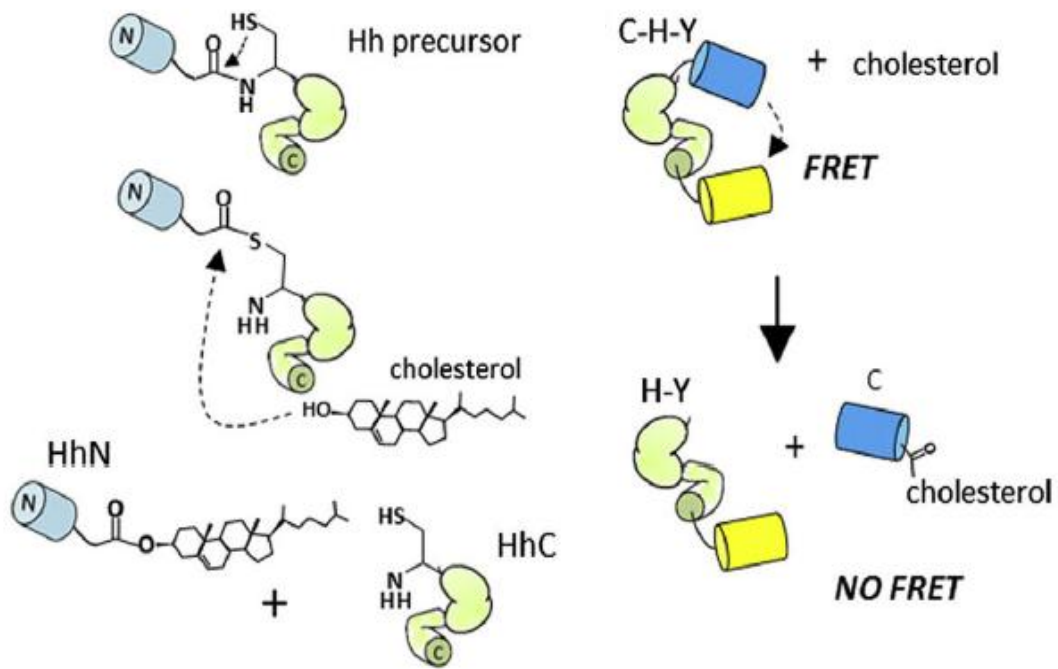


**Figure 3.10. Schematic of hedgehog cholesterolysis and the FRET construct used to study it, developed by Brian Callahan.** This figure is reproduced with permission of reference 21 (Appendix IV). © 2015 Elsevier.

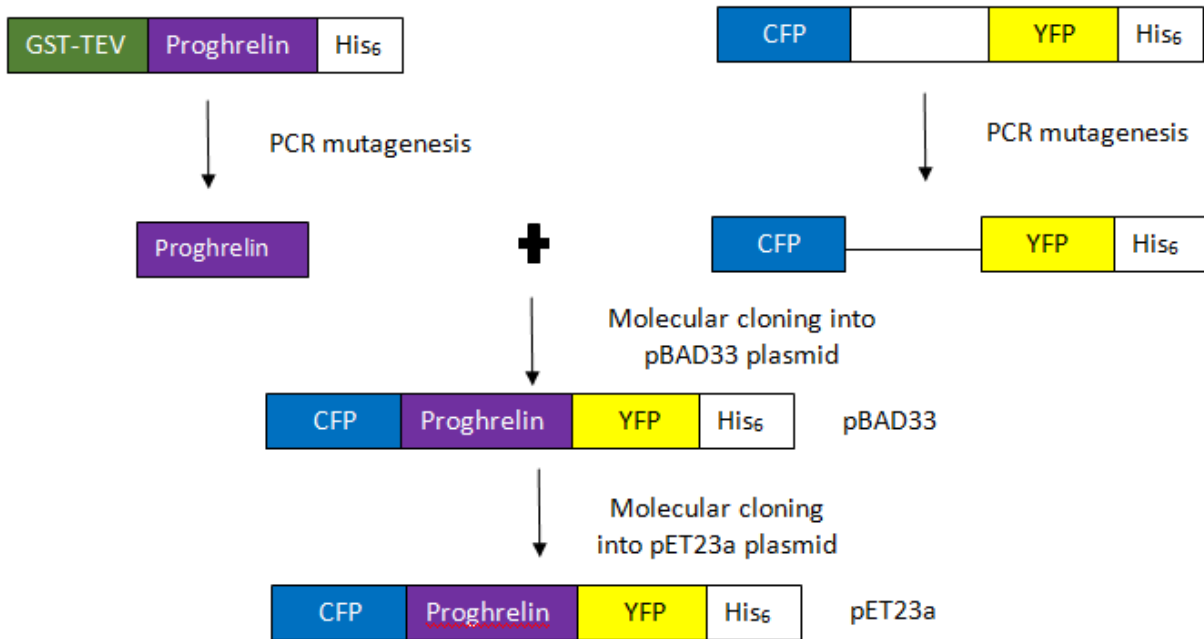


**Figure 3.11. Cloning schematic of obtaining CpgY from the GST-based GThPH.**

The CpgY construct allows investigation of proghrelin self-cleavage by both gel analysis and fluorescence-based measurements. The CpgY fusion construct was created by inserting restriction sites on either end of the proghrelin sequence in the GThPH vector by PCR. The proghrelin sequence was then ligated into the pBAD33 CXY vector. After ligation into the pBAD33 plasmid was complete it was then subcloned in a pET23a plasmid since previous work with proghrelin in its GST-fusion construct high expression and was easily inducible (Figure 3.11).<sup>22</sup> The design of this plasmid provided the opportunity to study proghrelin cleavage utilizing fluorescence/FRET measurements and places proghrelin in another fusion protein construct to ascertain if the cleavage observed in GThPH occurs in another structural/sequence context.

CpgY was expressed utilizing the standard autoinduction protocol.<sup>22</sup> The expression was analyzed via Coomassie staining and Anti-His Western blotting to confirm that the presence of CpgY which has a C-terminal His<sub>6</sub>-tag (Figure 3.12). Following gel analysis using non-reducing conditions (no dithiothreitol or heating), CpgY lysate was fluorescently analyzed and initial FRET readings were compared to CXY and CY (CFP-YFP, with no X linker region) in bacterial lysate (Figure 3.13). CpgY had a similar FRET signature to that observed for CXY and CY, indicating that FRET was occurring in the protein.

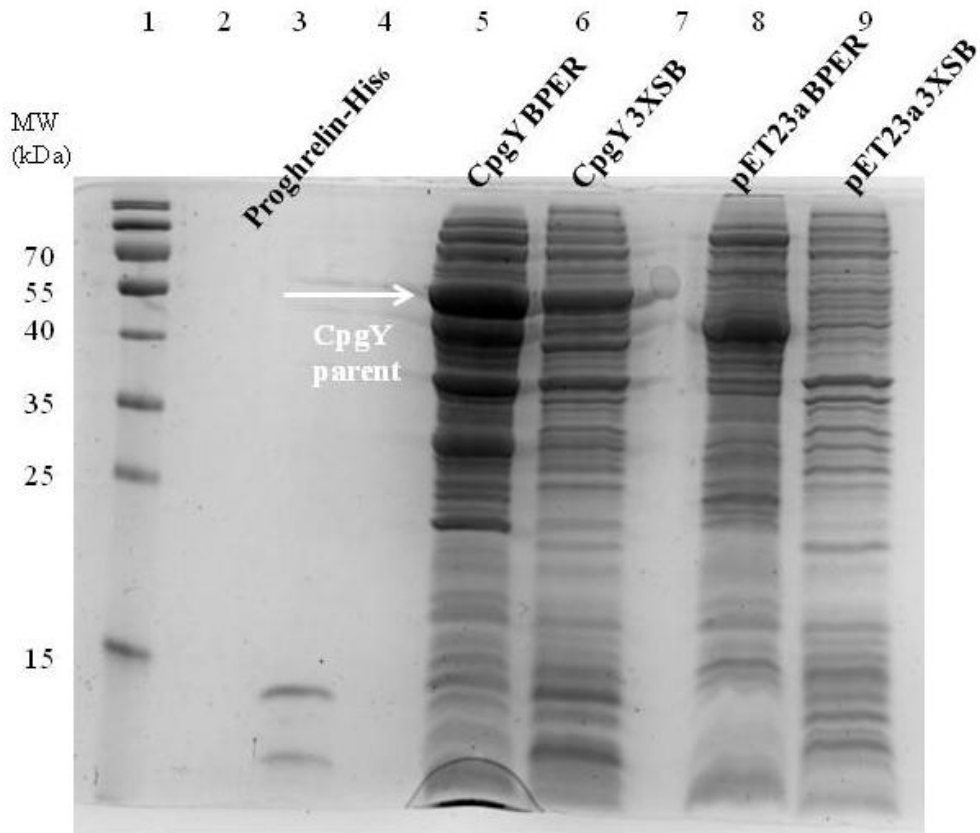


**Figure 3.12. Expression of bacterially expressed pET23a CpgY.** 1 mL bacterial pellets, either CpgY or pET23a (empty vector), were lysed with BPER cell extraction reagent or 3XSB then loaded onto an SDS-PAGE gel. CpgY parental protein is a 63 kDa and runs closer to 70 kDa than 55 kDa. The gel is 12% polyacrylamide. Lane 1, protein ladder (Thermo scientific); Lane 3, purified proghrelin-His<sub>6</sub>; Lane 5, CpgY BPER bacterial pellet lysis; Lane 6, CpgY 3XSB bacterial pellet lysis; Lane 8, pET23a BPER bacterial pellet lysis; Lane 9, pET23a 3XSB bacterial pellet lysis.

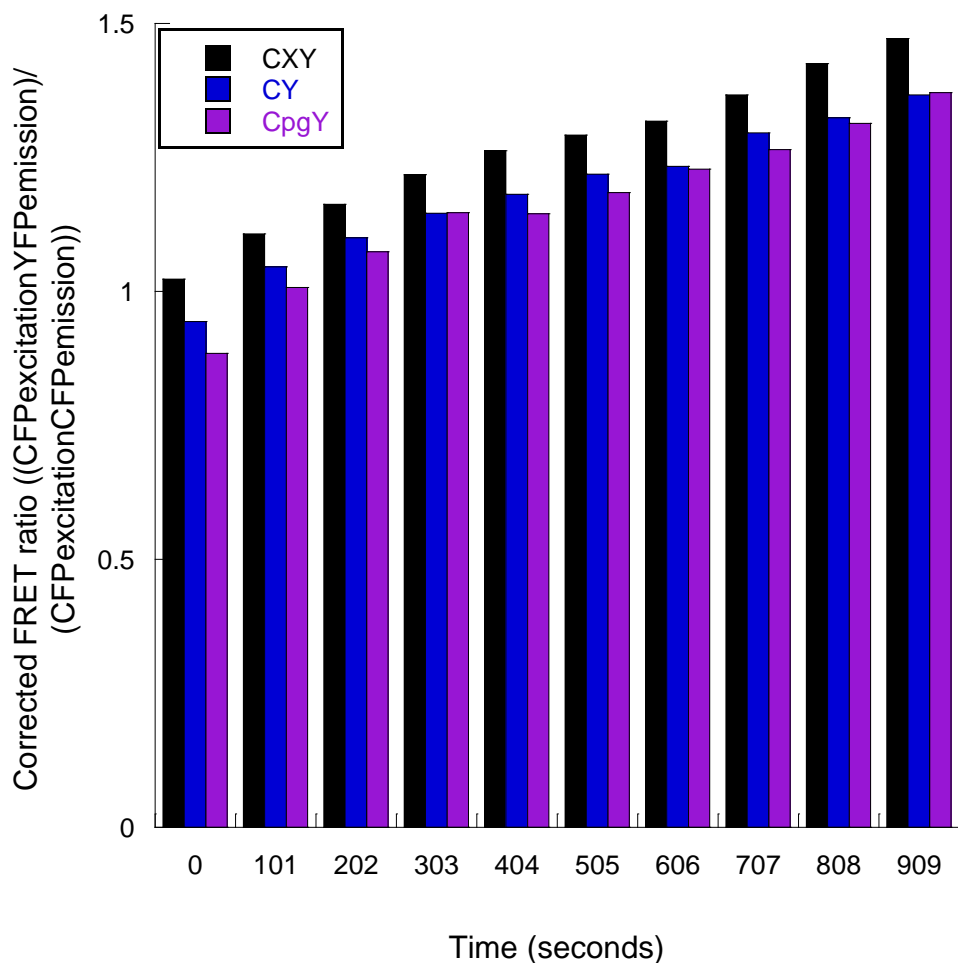


**Figure 3.13. Initial FRET readings of CpgY in bacterial lysate.** Bacterial pellets were lysed using BPER reagent and diluted into 50 mM Tris-HCl, pH 7.3 in a 96-well polystyrene black coated microplate (Thermo fischer). Fluorescence readings were taken for  $YFP_{excitation} YFP_{emission}$  (488, 580 nm),  $CFP_{excitation} CFP_{emission}$  (400, 485 nm),  $CFP_{excitation} YFP_{emission}$  (400, 540 nm). The corrected FRET ratio is  $CFP_{excitation} YFP_{emission} / CFP_{excitation} CFP_{emission}$ . Readings were taken every 1:41 minutes (101 seconds) for each CpgY, CXY, and CY.

CpgY was purified utilizing the His<sub>6</sub> tag on the C-terminal YFP using Ni<sup>2+</sup>-IMAC resin and a batch method purification, such as in Chapter 2 for C-ghrelin.<sup>23</sup> This sample was concentrated and stored under foil at 4 °C. The purified sample was visualized both using Coomassie staining and fluorescence monitoring using the FRET signal as a result of CFP<sub>excitation</sub>YFP<sub>emission</sub>. If proghrelin cleaves itself there should be a loss of FRET signal due to the lack of transfer of energy from CFP to YFP (Figure 3.14). The time course demonstrated that there is indeed a loss of FRET due to cleavage of the CpgY construct in a purified sample over the time course (Figure 3.15A). There was also support of this using gel analysis of the cleavage samples (Figure 3.15B).

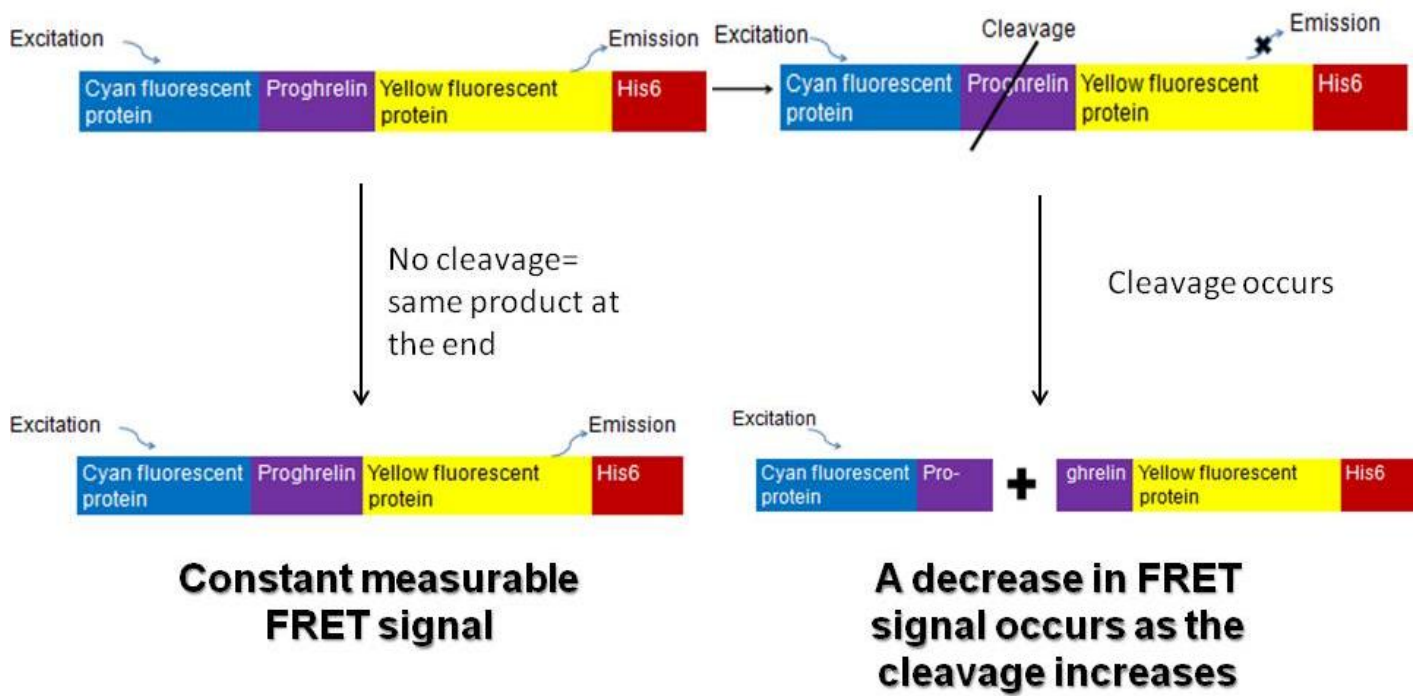


**Figure 3.14. Proghrelin cleavage using FRET signal.** Schematic displaying the expected results from the CpgY FRET construct in the case that there is (right) or if cleavage does not occur (left).

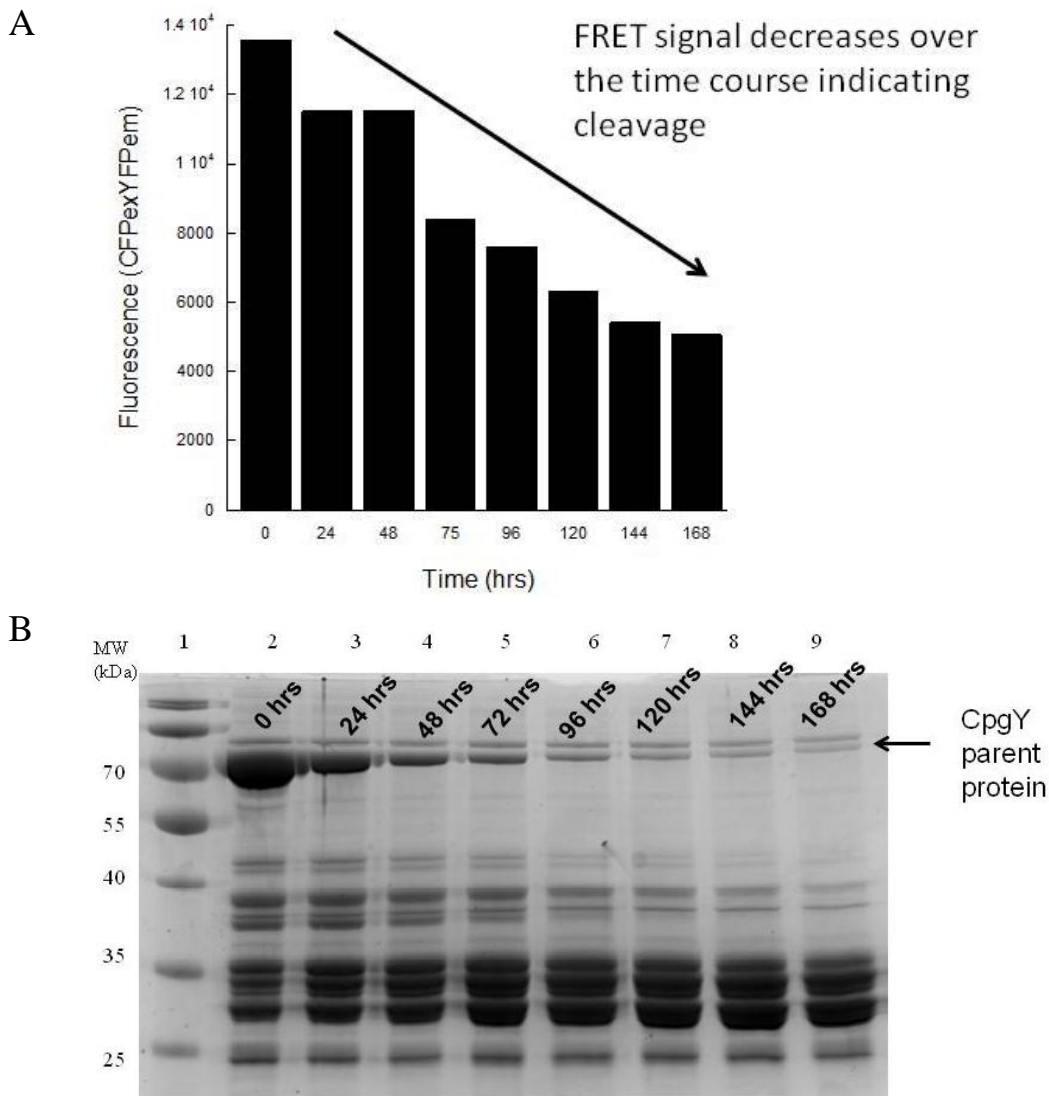
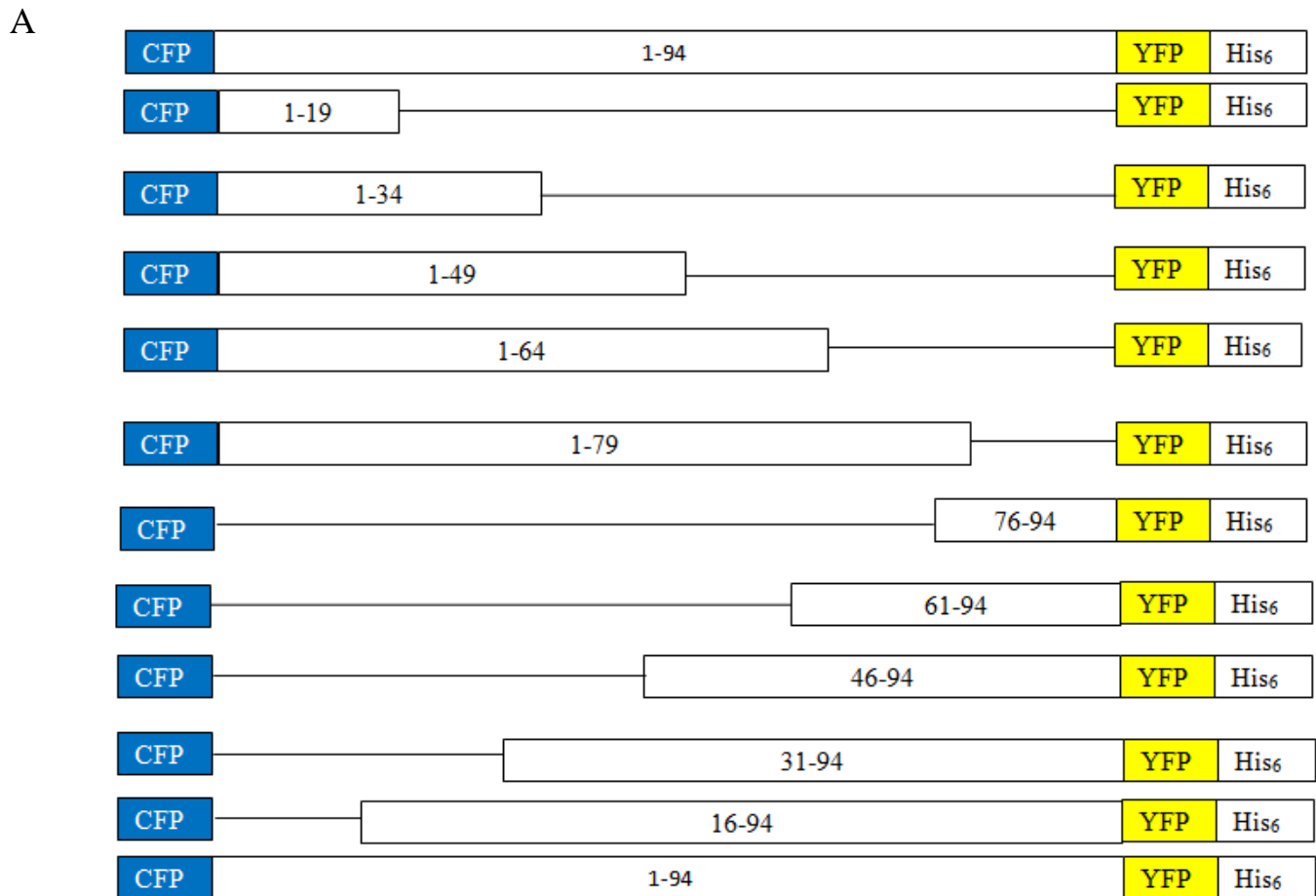


**Figure 3.15. Cleavage of purified CpgY.** The purified FRET construct CpgY was incubated at 4 °C under foil for the allotted times (0, 24, 48, 72, 96, 120, 144, and 168 hours). A sample from the incubation was taken for fluorescence reading and gel analysis. **A) FRET readings for CpgY cleavage time course.** The fluorescence readings were at  $\lambda_{\text{excitation}}$  400 nm  $\lambda_{\text{emission}}$  540 nm, exciting CFP and emitting YFP. Samples were diluted into 50 mM Tris-HCl pH 7.3 in a 96-well polystyrene black coated microplate (Thermo fischer). The FRET signal decreases over the allotted time due to the cleavage of proghrelin and the loss of energy transfer from CFP to YFP, shown in bar chart. **B) Gel analysis of CpgY cleavage.** CpgY was purified using  $\text{Ni}^{2+}$ -IMAC resin and concentrated yielding Lane 1. Samples taken from the same time points used for fluorescence readings were analyzed by SDS-PAGE and Coomassie staining. The gel is 12% polyacrylamide. Lane 1, protein ladder (Thermo scientific); Lane 2, 0 hrs incubation of CpgY; Lane 3, 24 hrs incubation; Lane 4, 48 hrs incubation; Lane 5, 72 hrs incubation; Lane 6, 96 hrs incubation; Lane 7, 120 hrs incubation; Lane 8, 144 hrs incubation; Lane 9, 168 hrs incubation.

With the cleavage observed in the CpgY construct, proghrelin has been shown to cleave in two different protein fusion constructs and as purified proghrelin-His<sub>6</sub>. In addition to enabling detection of proghrelin cleavage by FRET, the CpgY construct provides the ability to detect CpgY protein cleavage by in-gel fluorescent imaging of crude bacterial lysates or purified samples. To leverage this capability, a series of CpgY constructs containing truncations of proghrelin were designed to determine which parts of proghrelin are either required for cleavage or susceptible to cleavage. In these constructs, successive 15 amino acid deletions were introduced proceeding both from the N- to C-terminus and the C- to N-terminus to yield a total 10 proghrelin truncations (Figure 3.16).



**B**

**Sequence of the truncation (proghrelin only)**

| Sequence   | Truncation length |
|--|-------------------|
| GSSFLSPEHQRVQQRKESKPPAKLQPRALAGWLRPEDGGQAEGAEDELEVRFNAPFDVGIKLSGVYQQHSQALGKFLQDILWEEAKEAPADK | (1-94)            |
| GSSFLSPEHQRVQQRKESKPPAKLQPRALAGWLRPEDGGQAEGAEDELEVRFNAPFDVGIKLSGVYQQHSQALGKFL                | (1-79)            |
| GSSFLSPEHQRVQQRKESKPPAKLQPRALAGWLRPEDGGQAEGAEDELEVRFNAPFDVGIKLS                              | (1-64)            |
| GSSFLSPEHQRVQQRKESKPPAKLQPRALAGWLRPEDGGQAEGADEL  | (1-49)            |
| GSSFLSPEHQRVQQRKESKPPAKLQPRALAGWL  | (1-34)            |
| GSSFLSPEHQRVQQRKESK  | (1-19)            |
| KESKPPAKLQPRALAGWLRPEDGGQAEGADEL   | (16-49)           |
| KESKPPAKLQPRALAGWLRPEDGGQAEGAEDELEVRFNAPFDVGIKLSGVYQQHSQALGKFLQDILWEEAKEAPADK                | (16-94)           |
| AGWLRPEDGGQAEGAEDELEVRFNAPFDVGIKLSGVYQQHSQALGKFLQDILWEEAKEAPADK                              | (31-94)           |
| EDELEVRFNAPFDVGIKLSGVYQQHSQALGKFLQDILWEEAKEAPADK   | (46-94)           |
| IKLSGVYQQHSQALGKFLQDILWEEAKEAPADK  | (61-94)           |
| GKFLQDILWEEAKEAPADK  | (76-94)           |

**Figure 3.16. Proghrelin N- and C-terminal truncation constructs. A) Proghrelin truncation sequence from N- or C-terminal CpgY. The lines in the figure are to indicate the missing sequence; there is no linker region in each fluorescent fusion protein. B) The sequence of proghrelin in each of the FRET constructs shown in A. Actual amino acid composition of proghrelin in each fusion construct. Ghrelin indicated in green text and obestatin in bold.**

The CpgY truncation constructs were expressed in Z-competent BL21 (DE3) *E. coli*, with all constructs producing soluble proteins and Anti-His Western blotting confirming the correct size for the intact protein. FRET readings were taken both demonstrated that the protein is the correct size and that they all have FRET signals. To try and identify if cleavages were occurring and in which direction N to C or C to N-terminal the constructs were fluorescently imaged using in-gel fluorescence using both CFP<sub>excitation</sub>YFP<sub>emission</sub> and YFP<sub>excitation</sub>YFP<sub>emission</sub> (Figure 3.17 and 3.18, both the result of YFP<sub>excitation</sub>YFP<sub>emission</sub> imaging). In comparison to the control constructs CXY and YFP, there were distinct banding patterns for each of the CpgY constructs (Figure 3.17).

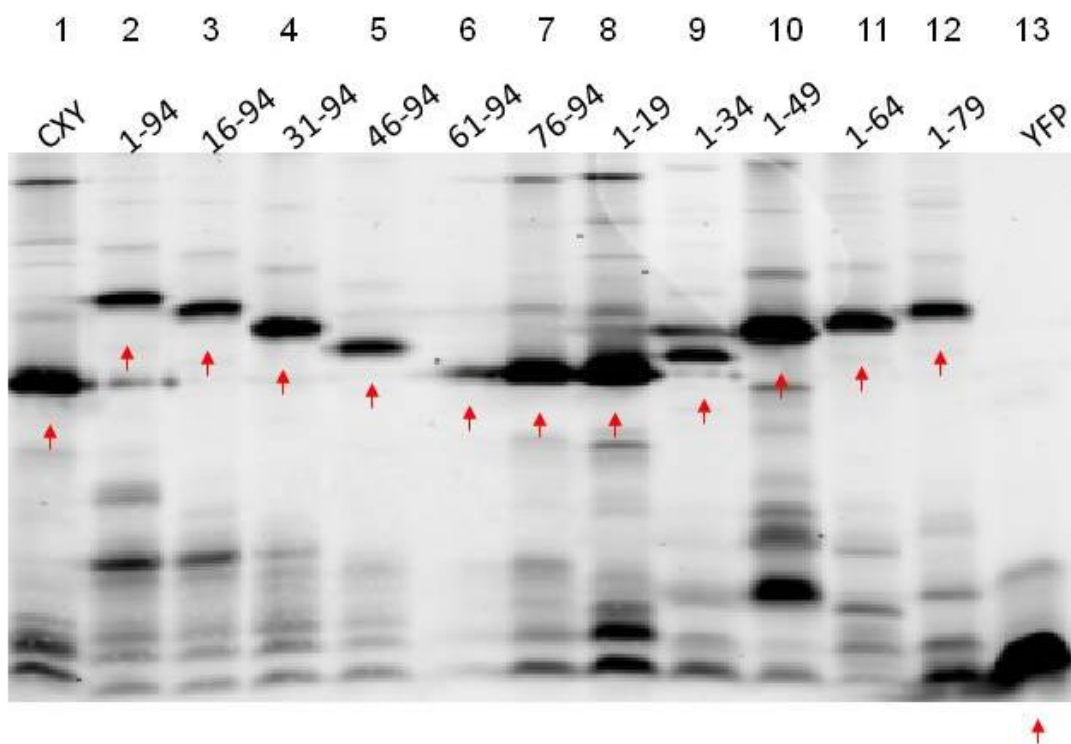


**Figure 3.17. Fluorescent imaging of CpgY proghrelin truncation constructs.** 1 mL bacterial pellets were lysed using BPER bacterial extraction reagent, non-reducing sample buffer (does not contain dithiothreitol and no boiling of the sample) and loaded onto a 12% polyacrylamide gel. The gel was imaged  $\lambda_{\text{excitation}}$  488 nm  $\lambda_{\text{emission}}$  580 nm for YFP<sub>excitation</sub> YFP<sub>emission</sub>. Red arrows indicate the parent protein in the fluorescent protein construct. The constructs are indicated by CpgY to indicate the construct and then the length of the truncation 1-X or X-94. Bands not present in either CXY or YFP are likely the result of construct cleavage. Lane 1, CXY; Lane 2, CpgY 1-94; Lane 3, CpgY 16-94; Lane 4, CpgY 31-94; Lane 5, CpgY 46-94; Lane 6, CpgY 61-94; Lane 7, CpgY 76-94; Lane 8, CpgY 1-19; Lane 9, CpgY 1-34; Lane 10, CpgY 1-49; Lane 11, CpgY 1-64; Lane 12, CpgY 1-79; Lane 13, YFP.

Comparison of the patterns for the truncation constructs supports that the cleavage behavior requires specific portions of the proghrelin sequence. From these observations it was determined that constructs 1-49, 16-94, 31-94, 1-64, and 1-79 show distinct proghrelin cleavage. The stable sequences were 1-34, 1-19, 46-94, 61-94 and 76-49 in which there was no observable proghrelin cleavage. Analysis of the FRET constructs indicated that the core sequence required for cleavage was the sequence from 30-49, since those lacking that sequence do not cleave. The fluorescent gel imaging used the YFP fluorescent signal of CpgY so it is likely that the C-terminal fragments from any cleavages were being observed. However, it was unclear from the in-gel imaging whether the cleavages were occurring N to C or C to N-terminally.

The constructs with the most prominent cleavage patterns were CpgY 1-49 and 16-94 which showed multiple distinct cleavage products. Specifically, the sequence from 16-49 was a highly unstable region based upon fluorescence gel imaging of the N- and C-terminal FRET constructs. This indicates that 16-49 is the minimal sequence required for protein construct cleavage (Figure 3.17 and 3.18, lane 8), and so, a FRET protein containing this sequence was also constructed and imaged and it showed a similar banding pattern to the 1-49 construct (Figure 3.18) which indicates that this region is essential for FRET protein cleavage to be observed.

The relative time scale of cleavage in the FRET construct was much slower than that of the GST construct, GThPH, possibly due to the fact that CFP and YFP are relatively large molecules compared to small molecule fluorophores which lead to stabilization of the proghrelin fusion protein. The observed relative time scale of cleavage in purified and in lysate of CpgY demonstrates that having CFP and YFP on either end of proghrelin increases stability and lifetime of the protein. In the GST-construct there is only one large protein bound to proghrelin

which leaves the C-terminus unbound and available to fold and interact with itself or other adjacent proteins. To determine whether proghrelin was being stabilized by the presence of both CFP and YFP a two-fold approach was taken the first being a series of X-94-YFP protein constructs. This approach will indicate whether incorporation of two large fluorophores are necessary for protein stability, as well as, to determine if the position of the large protein (N- or C-terminal) is important for proghrelin stability. The second approach was to generate a number of the truncated proghrelin sequences in the GST-TEV-X-His<sub>6</sub> fusion protein construct. Truncations were chosen for either their instability or the opposite; their sequence did not cleave in the FRET construct. Based upon the behavior observed with GThPH, ideally the truncated sequences will cleave on a faster time scale and could be purified using established methods (Chapter 2).

The CFP portion of CpgY was excised from the protein leaving pgY in a series of constructs containing the following N-terminal proghrelin sequence: 16-94, 31-94, 46-94, 61-94, and 76-94. When these YFP constructs were expressed and analyzed there was a greater losses of parental protein and the appearance of a greater number of distinct protein cleavage products compared to their observed behavior during their CpgY fluorescence imaging (Figure 3.18). All of the constructs except for 16-94 and 31-94 were completely stable in CpgY but in the pgY this behavior changed as did all of the five constructs. All of the pgY constructs were observed to have protein cleavage. This reaffirms that the presence of both CFP and YFP stabilized the parental protein and the proghrelin sequence.

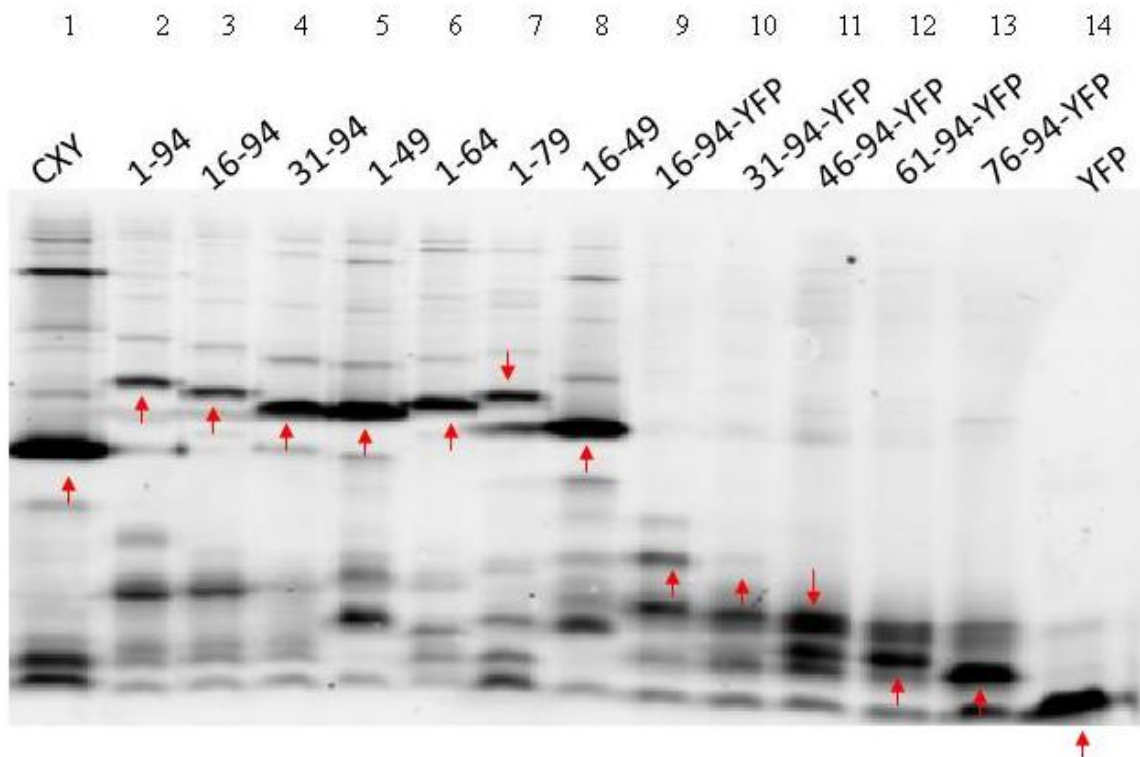


**Figure 3.18. Fluorescent imaging of proghrelin fluorescent protein constructs.** 1 mL bacterial pellets were lysed using BPER bacterial extraction reagent, non-reducing sample buffer (does not contain dithiothreitol and no boiling of the sample) and loaded onto a 12% polyacrylamide gel. The gel was imaged  $\lambda_{\text{excitation}}$  488 nm  $\lambda_{\text{emission}}$  580 nm for YFP<sub>excitation</sub> YFP<sub>emission</sub>. Red arrows indicate the parental protein in each of the fluorescent protein constructs. For comparison of CFP contribution look to Lane 3 compared to Lane 9 and Lane 4 compared to Lane 10. The constructs are indicated by CpgY to indicate the construct and then the length of the truncation 1-X or X-94. Lane 1, CXY; Lane 2, CpgY 1-94; Lane 3, CpgY 16-94; Lane 4, CpgY 31-94; Lane 5, CpgY 1-49; Lane 6, CpgY 1-64; Lane 7, CpgY 1-79; Lane 8, CpgY 16-49; Lane 9, 16-94-YFP; Lane 10, 31-94-YFP; Lane 11, CpgY 46-94-YFP; Lane 12, 61-94-YFP; Lane 13, 76-94-YFP; Lane 14, YFP.

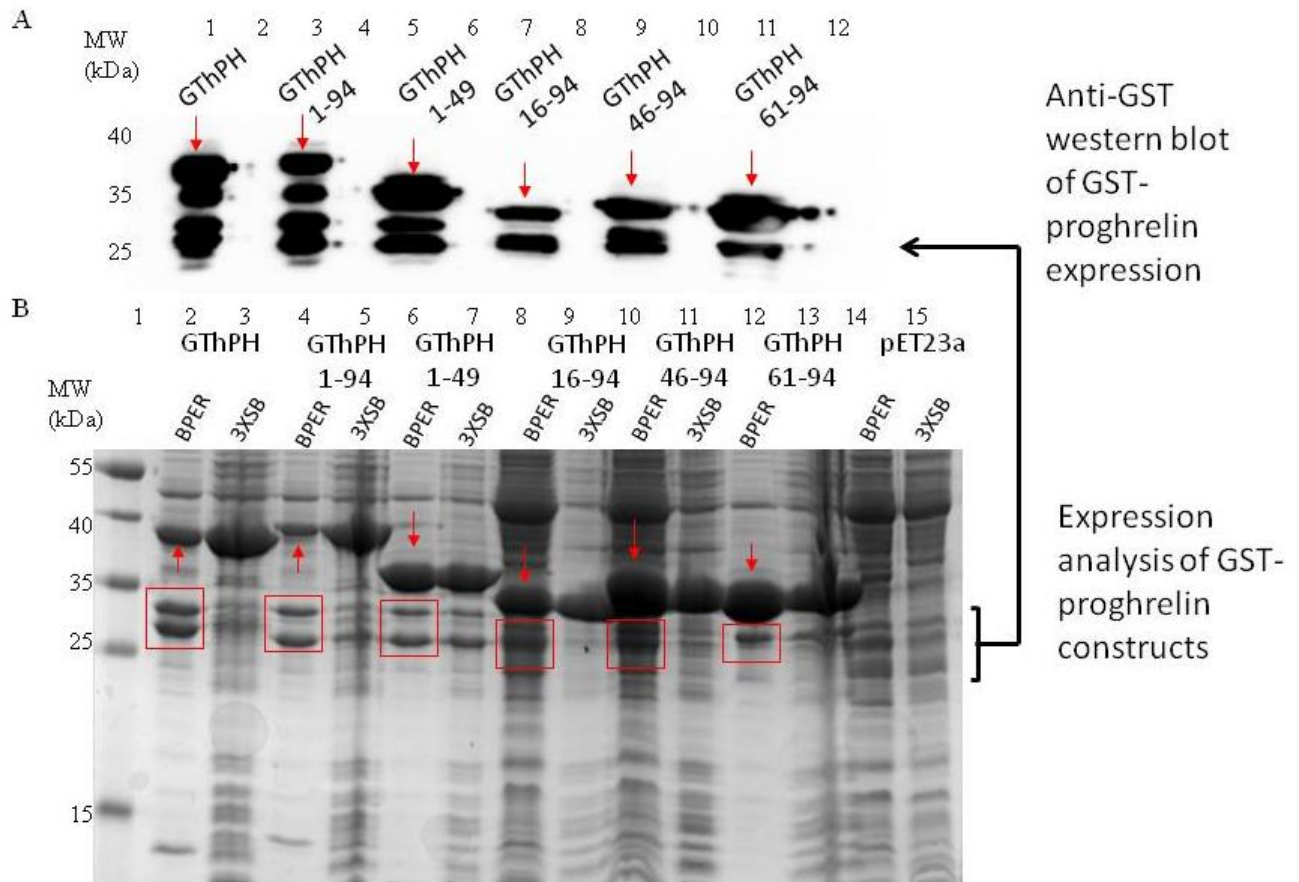


**Figure 3.19. GST-based proghrelin truncation expression analysis.** A) Anti-GST Western blot of the BPER lysed expression pellets in Figure 3.19B. The protein ladder is indicated to the left of Lane 1. The gel is 12% polyacrylamide. Lane 1, GThPH; Lane 3, GThPH 1-94; Lane 5, GThPH 1-49; Lane 7, GThPH 16-49; Lane 9, GThPH 46-94; Lane 11, GThPH 61-94; Lane 12, pET23a (empty vector). **B) Expression analysis of GST-truncated proghrelin fusion proteins.** 1 mL bacterial pellets were either lysed using BPER reagent or 3XSB and Coomassie stained. The red boxes correspond to the GST-tagged cleavage products in A. Parental GST-fusion proteins are indicated with red arrows. The gel is 12% polyacrylamide. Lane 1, protein ladder (Thermo scientific); Lane 2, GThPH BPER lysed; Lane 3, GThPH 3XSB; Lane 4, GThPH 1-94 BPER lysed; Lane 5, GThPH 1-94 3XSB; Lane 6, GThPH 1-49 BPER lysed; Lane 7, GThPH 1-49 3XSB; Lane 8, GThPH 16-49 BPER lysed; Lane 9, GThPH 16-49 3XSB; Lane 10, GThPH 46-94 BPER lysed; Lane 11, GThPH 46-94 3XSB; Lane 12, GThPH 61-94 BPER lysed; Lane 13, GThPH 61-94 3XSB; Lane 14, GThCgH BPER lysed; Lane 15, pET23 (empty vector) BPER lysed.

The GST-based proghrelin truncations allow investigation of proghrelin cleavage sequence dependency in a context in which has been characterized in full-length proghrelin, analysis by both N- and C-terminal Western blotting, time scale comparison (full length already studied to new truncated constructs) and investigate C-terminal stability. The sequences chosen in this study were from both sequences that lead to protein cleavage: 1-94, 1-49, and 16-49 or were stable in their FRET constructs: 46-94 and 61-94 (Figure 3.17). The trend was the same as in the FRET constructs in which constructs that were more prone to protein cleavage were observed to have more cleavage products in their GST-based constructs (Figure 3.19). The time scale of protein cleavage and overall lower molecular weight cleavage products from this GST-based study did not provide any additional information about the sequences, their contribution to proghrelin cleavage, or the individual residues responsible for cleavage and are overall inconclusive.

The proghrelin cleavage behavior in the proghrelin fusion proteins GThPH and CpgY constructs were observed as a result of expression in bacteria. To determine if the same behavior is observed in proteins expressed in mammalian cells, the CpgY construct was transferred into a mammalian plasmid containing a CMV promoter,<sup>24</sup> a pCAF vector, and transfected into HEK 293FT cells. Following transfection and fluorescent imaging, comparison to CpgY expressed in bacteria showed a similar banding pattern (Figure 3.20). The lower signal in mammalian samples is likely due to lower overall protein content and low transfection efficiency. These data are consistent with cleavage of proghrelin reflecting an intrinsic property of the protein rather than an artifact arising from expression in and purification from bacteria.

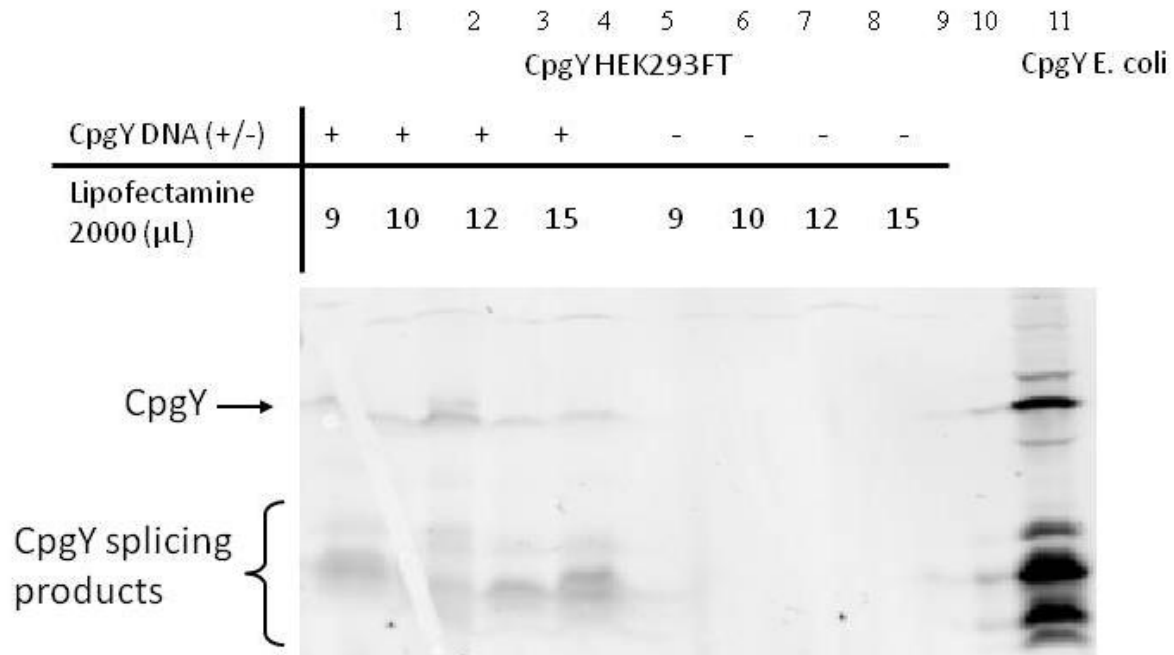


**Figure 3.20. Fluorescent imaging of CpgY transfected in HEK 293FT cells.** pCAF CpgY was transfected into  $1 \times 10^6$  cells/well in a 6-well plate using Lipofectamine 2000 transfection reagent (Thermo fischer), cells were harvested and lysed using RIPA buffer (containing a mini Roche tablet). Lane 11 is CpgY expressed in *E. coli*, a 1 mL pellet was lysed using BPER reagent. Non-reducing sample buffer (does not contain dithiothreitol and no boiling of the sample) was added to samples and loaded onto a 12% polyacrylamide gel. The gel was imaged  $\lambda_{excitation}$  488 nm  $\lambda_{emission}$  580 nm for YFP<sub>excitation</sub> YFP<sub>emission</sub>. The black arrow indicates the parental CpgY protein and the black bracket indicates the cleavage products observed. Lane 1, 9 μL Lipofectamine 2000 + 4 μg CpgY DNA; Lane 2, 10 μL Lipofectamine 2000 + 4 μg CpgY DNA; Lane 3, 12 μL Lipofectamine 2000 + 4 μg CpgY DNA; Lane 4, 15 μL Lipofectamine 2000 + 4 μg CpgY DNA; Lane 6, 9 μL Lipofectamine 2000; Lane 7, 10 μL Lipofectamine 2000; Lane 8, 12 μL Lipofectamine 2000; Lane 9, 15 μL Lipofectamine 2000; Lane 11, CpgY grown in from *E. coli*. and lysed using BPER .

### 3.2.6 Cleavage behavior of GST-C-ghrelin fusion protein

The studies above show proghrelin cleaves into discrete products, with the required residues and cleavage site both located within the C-ghrelin portion of proghrelin (Figure 3.9 and 3.21). Following bacterial expression, GThPH and GThCgH were analyzed for cleavage behavior. The C-ghrelin fusion expressed as a soluble protein under optimized conditions (Chapter 2), although less efficiently than the proghrelin construct. When bacterial pellets were lysed and analyzed by gel electrophoresis, a similar banding pattern appeared in both the proghrelin and C-ghrelin constructs and Anti-GST Western confirmed that as previously shown these bands are GST-tagged (Chapter 2, Figure 2.3 and 2.4). The bacterial lysis demonstrates that the GST-C-ghrelin fusion cleaves in a similar fashion to GST-proghrelin.

To further characterize C-ghrelin cleavage, mass spectrometry studies were pursued to identify the cleavage sites within the C-ghrelin sequence. Due to an inability of TEV protease to cleave C-ghrelin from GST, MALDI-TOF mass spectrometry was performed on purified GST-TEV-human C-ghrelin-His<sub>6</sub> samples. The same time course was repeated using the same conditions as the analysis for proghrelin-His<sub>6</sub> and resulted in mass spectra with a definitive cleavage pattern similar to proghrelin and similar fragmentation and cut sites as reflected by the C-terminal peptides detected (Figure 3.21).

A **GThCgH sequence**

MSPILGYWKI KGLVQPTRL L LEYLEEKYEE HLYERDEGDK WRNKKFELGL EFPNLPYYID  
 GDVKLTQSMA IIRYIADKHN MLGGCPKERA EISMLEGAVL DIRYGVSRIA YSKDFETLKV  
 DFLSKLP EML KMFEDRLCHK TYLNGDHVTH PDFMLYDALD VVLYMDPMCL DAFPKLVCFK  
 KRIEAIQID KYLKSSKYIA WPLQG WQATF GGGDHPPKID T**TENLYFQ**GKLA<sub>29</sub>LAG  
**WLRPEDGGQA EGAEDELEVR FNAPFDVGIK LSGVQYQQHS QALGKFLQDI**  
**LWEEAKEAPADKHHHHHH**

B

| C-ghrelin fragment sequence (in terms of proghrelin 1-100) | Amino acid sequence of fragment         | Mass (m/z) observed |
|--|---|---------------------|
| 72-100   | S QALGKFLQDI LWEEAKEAPA DKHHHHHHH       | 3409.6936           |
| 80-100   | QDI LWEEAKEAPA DKHHHHHHH                | 2565.2130           |
| 76-100   | GKFLQDILWE EAKEAPADKH HHHHHH            | 3010.4818           |
| 65-100   | GVQYQQHSQA LGKFLQDILW EEAKEAPADK HHHHHH | 4250.0815           |

**Figure 3.21. Fragments from MALDI-TOF analysis of GThCgH fusion protein. A) The amino acid of the fusion protein GST-TEV-C-ghrelin-His6 (GThCgH). TEV site is highlighted in blue, C-ghrelin sequence is in bold text. The first amino acid of C-ghrelin is indicated as A<sub>29</sub> (proghrelin residue 29). B) Mass spectrometry analysis of GThCgH cleavage. The m/z values observed were analyzed and compared to C-ghrelin's sequence for sequence identification. All of the fragments observed using MALDI-TOF are C-terminal.**

### 3.3 Conclusions

The behavior of proghrelin during bacterial expression and purification, followed by studies of purified proghrelin, are consistent with proghrelin exhibiting self-cleaving proteolytic activity. This self-cleavage is initially observed following non-denaturing lysis of bacterial cells and continues throughout the purification and after purification. Characterization in both bacterial lysate and purified samples has helped to identify behaviors that accelerate it, such as increased concentration of the protein sample. The unique cleavage behavior seen with proghrelin both purified and in its fusion protein construct (GThPH) has been characterized by SDS-PAGE using Coomassie staining and Western blotting.

The fluorescent proghrelin constructs (FRET, CpgY) were created and used in order to determine the residues that are required for proghrelin cleavage. This also provided another avenue to observe the cleavage in full-length proghrelin using fluorescence detection and fluorescent gel imaging. The FRET construct results further support that the cleavage observed is a property of proghrelin and not due to external interference from another protein or small molecule, since the same behavior was not seen with the control construct CXY. The cleavage behavior of proghrelin was also observed in different species (HEK 293FT mammalian cells and BL21 (DE3) *E. coli.*). The truncation constructs indicate that there is a region of proghrelin from amino acid residues 30-50 that is required for cleavage. This specific sequence was based upon the protein cleavage behavior of the N- and C-terminal sequence fluorescent gel imaging. To slow or completely inhibit proghrelin's cleavage behavior, amino acids within this range were mutated to alanine. The amino acids targeted for mutagenesis were those that can chelate metals or are commonly apart of a catalytic triad which could be responsible for proghrelin cleavage. The alanine mutants behaved exactly like the parent protein; possibly due to the fact that

multiple residues are responsible for this behavior and that if one residue is mutated another will take its place. This mutagenesis was not very informative and did not aid in identifying specific essential residues.

Amongst the CpgY proghrelin truncation constructs, the 1-49 and 16-49 sequences exhibited the most prominent cleavage of all constructs tested. This behavior was unexpected because, while these constructs contain the X-49 residues implicated for proghrelin cleavage activity by truncation analysis, they do not contain the downstream sequence region of proghrelin that has been identified as the cleavage site(s) within proghrelin by mass spectrometry. This could be the result of cleavage occurring within the N-terminal portion of YFP in a length-dependent cleavage site model instead of a model where specific amino acid residues are necessary for cleavage. This approach to identifying the necessary residues for proghrelin cleavage was informative and allowed comparison of residues between multiple different constructs. This methodology and analytical technique is useful for proteins that show splicing or unique processing behavior and should be pursued to probe for necessary residues or sequence.

Informed only by the sequence, FRET behavior and alanine mutations it was unclear where the exact cut sites are occurring. To determine the location of the cleavage sites within proghrelin, mass spectrometry was employed to unambiguously determine the identities of the fragments from these cleavages. The FRET constructs and conservation analysis indicated what region is necessary for cleavage to occur which then leads to the residues identified during mass spectrometry fragmentation analysis.

C-ghrelin cleavage was also characterized using mass spectrometry; C-ghrelin by itself has cleavage behavior as well as similar fragmentation as full-length proghrelin which indicates

that C-ghrelin's sequence is responsible for the cleavage behavior. This was interesting since there is no known mechanism/enzyme/actor that is responsible for the cleavage of obestatin,<sup>10</sup> suggesting that proghrelin and C-ghrelin could be self-processing. It is still unclear to the exact nature of the cleavage of proghrelin and whether structure or a multi-partner system is needed for cleavage, but the data indicates that ghrelin (1-28) is not needed for cleavage to occur and that the cuts are occurring near the cleavage sites of obestatin. The proximity to the cleavage sites of obestatin could just be coincidental or could provide the missing step in C-ghrelin processing.

The future of the research within this chapter is to further characterize proghrelin cleavage by identifying the residues/mechanism in which this process occurs. This will help to define whether the behavior that was observed during work with human proghrelin is biologically relevant and an intrinsic property of this small protein. It would also be advantageous to compare other species' full-length proghrelin to define if the cleavage behavior occurs solely in humans or in multiple species as the conservation analysis suggests.

### 3.4 Materials and Methods

**3.4.1 Cloning of proghrelin into pBAD33.** PCR mutagenesis was performed to insert a 5' *XhoI* and a 3' *PstI* restriction cut site on either end of proghrelin. Primers were synthesized by Integrated DNA Technologies. Primers were dissolved in purified water and concentrations were determined by UV absorbance at 260 nm.

Primer to insert *XhoI* site at the 5' end of proghrelin:

5'TATAGGCTCGAGCAAATTTGCGGAATATGGTAGCAGCTTTCTG 3'

Primer to insert *PstI* site at 3' end of proghrelin:

5'GCACCGGCCGATAAATGCTTTAACCTGCAGTATA 3'

PCR mutagenesis reactions (50  $\mu$ L) contained the following components: 1x One Taq standard reaction buffer; 40 ng pET23a GST-TEV-human proghrelin-His<sub>6</sub> template; 125 ng forward primer; 125 ng reverse primer, 20  $\mu$ M dNTPs, and One Taq DNA polymerase (1  $\mu$ L, 5,000 units/mL) (Agilent). The PCR thermocycler program proceeded as follows: initial denaturation (94 °C, 1 min); 33 cycles of denaturation (94 °C, 30 sec), annealing (59 °C, 1 min), and extension (68 °C, 2 min); final extension (68 °C, 5 min). The PCR product was run on a 0.8% agarose gel at 110 V for ~1.5 hr, then DNA was gel extracted using EZ-10 Gel Extraction kit (BioBasic) per manufacturer's instructions, and concentrations were measured by UV absorbance at 260 nm.

The proghrelin gene was ligated into pBAD33 CXY vector. 3  $\mu$ g pBAD33 CXY and the proghrelin PCR product DNA was digested with *XhoI* (1  $\mu$ L, 20,000 units/mL), *PstI* (1  $\mu$ L, 20,000 units/mL), 3  $\mu$ L Cutsmart buffer (30  $\mu$ L total volume), and incubated at 37 °C for 2 hr. Samples were then run on a 0.8% agarose gel at 110 V for ~1 hr. The bands for the pBAD33 vector and the proghrelin insert were each cut out and DNA was purified using EZ-10 Gel

Extraction kit (BioBasic) per manufacturer's instructions, and concentrations were measured by UV absorbance at 260 nm.

Ligations were performed with 250 ng of vector DNA, 12 ng insert DNA, 10  $\mu$ L quick ligase buffer, and 1  $\mu$ L Quick Ligase (total volume 20  $\mu$ L) and incubated on ice for 5 min. 5  $\mu$ L of ligation reaction was added to 100  $\mu$ L Z-competent DH5 $\alpha$  *E. coli*. cells followed by 30 min incubation on ice. Cells were spread on LB-chloramphenicol (34  $\mu$ g/mL) plates and incubated at 37  $^{\circ}$ C overnight. Single colonies were inoculated into 5 mL LB cultures containing 34  $\mu$ g/mL chloramphenicol and grown overnight at 37  $^{\circ}$ C with shaking (225 rpm).

Following overnight growth, plasmids were purified from cultures using EZ-10 Spin Column Plasmid DNA kit (BioBasic) per manufacturer's instructions. Sequencing of the gene was done by utilizing internal sequencing primers which were synthesized by Integrated DNA Technologies. Primers were dissolved in purified water and concentrations were determined by UV absorbance at 260 nm. The sequencing samples sent to Genewiz contained 1,000 ng of ligated DNA, 25 pmol of sequencing primer and H<sub>2</sub>O (10  $\mu$ L total volume).

Forward sequencing primer: 5' GCTAACTTCAAAGCCAGACACAAC 3'

Reverse sequencing primer: 5' GGTA AATTGACCTTAAAATTACTCTGTACT 3'.

**3.4.2 Cloning CpgY into pET23a.** The CFP-proghrelin-YFP gene was ligated into pET23a. 3  $\mu$ g pBAD33 CpgY and pET23a DNA was digested with *Sac*I (1  $\mu$ L, 20,000 units/mL), *Hind*III (1  $\mu$ L, 20,000 units/mL), 3  $\mu$ L Cutsmart buffer (30  $\mu$ L total volume), and incubated at 37  $^{\circ}$ C for 2 hr. Samples were then run on a 0.8% agarose gel at 110 V for ~1 hr. The bands for the pET23a vector and the proghrelin insert were each cut out and DNA was purified using EZ-10 Gel

Extraction kit (BioBasic) per manufacturer's instructions, and concentrations were measured by UV absorbance at 260 nm.

Ligations were performed with 30 ng of vector DNA, 42 ng insert DNA, 10  $\mu$ L quick ligase buffer, and 1  $\mu$ L Quick Ligase (total volume 10  $\mu$ L) and incubated on ice for 5 min. 5  $\mu$ L of ligation reaction was added to 100  $\mu$ L Z-competent DH5 $\alpha$  *E. coli* cells, followed by 30 min incubation on ice. Cells were spread on LB- ampicillin (100  $\mu$ g/mL) plates and incubated at 37  $^{\circ}$ C overnight. Single colonies were inoculated into 5 mL LB cultures containing 100  $\mu$ g/mL ampicillin and grown overnight at 37  $^{\circ}$ C with shaking (225 rpm). Following overnight growth, plasmids were purified from cultures using EZ-10 Spin Column Plasmid DNA kit (BioBasic) per manufacturer's instructions and successful ligation was confirmed by DNA sequencing (Genewiz).

**3.4.3 Removal of duplicate restriction site.** There were two *SacI* and *XhoI* sites in order to successfully clone the truncations each additional site was mutated (forward primers located below, their reverse complement were also ordered). PCR mutagenesis primers were designed to mutate out either an extra *XhoI* or *PstI* restriction site in pET23a CpgY and were synthesized by Integrated DNA Technologies. Primers were dissolved in purified water and concentrations were determined by UV absorbance at 260 nm.

*PstI* knockout 5' GACACCACGATGCCTGCTGCAATGGCAACAACG 3'

*XhoI* knockout 5' CACTAAAAGCTTGCGGCCGCACAGGAGCACCACCAC 3'

PCR mutagenesis reactions (50  $\mu$ L) contained the following components: 1x Pfu reaction buffer; 10 ng pET23a CpgY; 125 ng forward primer; 125 ng reverse primer, 20  $\mu$ M dNTPs, and 1  $\mu$ L Pfu Turbo DNA polymerase (Agilent). The thermocycler program for PCR mutagenesis

proceeded as follows: initial denaturation (94 °C, 5 min); 30 cycles of denaturation (94 °C, 30 sec), annealing (56 °C, 1 min), and extension (68 °C, 2 min); final extension (68 °C, 5 min).

*DpnI* (1 µL, 20,000 units/mL) was added and reactions were incubated at 37 °C for 1 hr. After *DpnI* digestion, 5 µL of the PCR reaction mixture was transformed into 50 µL of Z-competent DH5α *E. coli* cells (Zymo Research) followed by incubation on ice for 30 min. Transformed bacteria were spread on LB-ampicillin (100 µg/mL) plates and incubated at 37 °C overnight.

Single colonies were then inoculated into 5 mL LB media containing 100 µg/mL ampicillin in sterile culture tubes, which were incubated at 37 °C overnight with shaking (225 rpm). Following overnight growth, plasmids were purified from cultures using EZ-10 Spin Column Plasmid DNA kit (BioBasic) per manufacturer's instructions. The product was verified by DNA sequencing (Genewiz).

**3.4.4 Proghrelin truncation cloning.** PCR reactions was also performed to create proghrelin truncations 1-19, 1-34,1-49,1-64, 1-79, 16-94,31-94,46-94,61-94, and 76-94. Primers were synthesized by Integrated DNA Technologies. Primers were dissolved in purified water and concentrations were determined by UV absorbance at 260 nm.

The primer sequences were as follows (forward sequences are listed below, the reverse compliment was ordered for 1-X constructs):

1-79 5' GCACTGGGCAAGTTCCTGTGCTTTAACCTGCAGTATA 3'

1-64 5' GTGGGCATCAAGCTGAGTTGCTTTAACCTGCAGTATA 3'

1-49 5' GCCGAAGACGAGCTGTGCTTTAAGCTGCAGTATA 3'

1-34 5' GCACTGGCCGGTTGGTTATGCTTTAAGCTGCAGTATA 3'

1-19 5' GTTCAGCAGCGCAAGGAAAGTAAGTGCTTTAAGCTGCAGTATA 3'

16-94 5' TATAGGCTCGAGCAAATTTGCGGAATATAAGGAAAGTAAG 3'

31-94 5' TATAGGCTCGAGCAAATTTGCGGAATATGCCGGTTGGTTACGT 3'

46-94 5' TATAGGCTCGAGCAAATTTGCGGAATATGAAGACGAGCTGGAG 3'

61-94 5' TATAGGCTCGAGCAAATTTGCGGAATATATCAAGCTGAGT 5'

76-94 5' TATAGGCTCGAGCAAATTTGCGGAATATGGCAAGTTCCTG 3'

*Xho*I site at the 5' end

5'TATAGGCTCGAGCAAATTTGCGGAATATGGTAGCAGCTTTCTG3'

*Pst*I site at 3' end

5'GCACCGGCCGATAAATGCTTTAACCTGCAGTATA3'

For construct 16-49 the forward primer 16-94 and reverse 1-49 were used in PCR mutagenesis reaction.

PCR reactions (50  $\mu$ L) contained the following components: 1x One Taq standard reaction buffer; 40 ng pET23a CpgY (with corresponding *Sac*I or *Xho*I knockout) template; 125 ng forward primer; 125 ng reverse primer, 20  $\mu$ M dNTPs, and One Taq DNA polymerase (1  $\mu$ L, 5,000 units/mL) (Agilent). The thermocycler program for PCR mutagenesis proceeded as follows: initial denaturation (94  $^{\circ}$ C, 1 min); 33 cycles of denaturation (94  $^{\circ}$ C, 30 sec), annealing (59  $^{\circ}$ C, 1 min), and extension (68  $^{\circ}$ C, 2 min); final extension (68  $^{\circ}$ C, 5 min). Following PCR mutagenesis the PCR product was run on a 0.8% agarose gel at 110 V for ~1.5 hr, then DNA was gel extracted using EZ-10 Gel Extraction kit (BioBasic) per manufacturer's instructions, and concentrations were measured by UV absorbance at 260 nm.

The proghrelin truncated genes were ligated into pET23a CFP-proghrelin-YFP. 3  $\mu$ g pET23a CFP-proghrelin-YFP-His<sub>6</sub> and proghrelin truncation insert DNA was digested with *Sac*I (1  $\mu$ L, 20,000 units/mL), *Pst*I (1  $\mu$ L, 20,000 units/mL), 3  $\mu$ L cutsmart buffer (30  $\mu$ L total

volume), or digested with *Xho*I (1  $\mu$ L, 20,000 units/mL), *Hind*III (1  $\mu$ L, 20,000 units/mL), 3  $\mu$ L cutsmart buffer (30  $\mu$ L total volume) and incubated at 37 °C for 2 hr. Samples were then run on a 0.8% agarose gel at 110 V for ~1 hr. The bands for the pET23a vector and the insert were each cut out and DNA was purified using EZ-10 Gel Extraction kit (BioBasic) per manufacturer's instructions, and concentrations were measured by UV absorbance at 260 nm.

Ligations were performed with 50 ng of vector DNA, 40 ng insert DNA, 10  $\mu$ L quick ligase buffer, and 1  $\mu$ L Quick Ligase (total volume 10  $\mu$ L) and incubated on ice for 5 min. 5  $\mu$ L of ligation reaction was added to 100  $\mu$ L Z-competent DH5 $\alpha$  *E. coli* cells, followed by 30 min incubation on ice. Cells were spread on LB- ampicillin (100  $\mu$ g/mL) plates and incubated at 37 °C overnight. Single colonies were inoculated into 5 mL LB cultures containing 100  $\mu$ g/mL ampicillin and grown overnight at 37 °C with shaking (225 rpm). Following overnight growth, plasmids were purified from cultures using EZ-10 Spin Column Plasmid DNA kit (BioBasic) per manufacturer's instructions and successful ligation was confirmed by DNA sequencing (Genewiz).

**3.4.5 C-ghrelin GST-fusion cloning.** PCR primers were designed to insert a *Hind*III restriction site at the beginning of proghrelin's sequence and were synthesized by Integrated DNA Technologies.

PCR primers:

5' CTGTA~~CT~~TCCAGGGTAAGCTTTTTCTGAGTCCG 3'

3' GACATGAAGGTCCCATTTCGAAAAAGACTCAGGC 5'

Primers were dissolved in purified water and concentrations were determined by UV absorbance at 260 nm. PCR mutagenesis reactions (50  $\mu$ L) contained the following components:



ng reverse primer, 20  $\mu$ M dNTPs, and One Taq DNA polymerase (1  $\mu$ L, 5,000 units/mL) (Agilent). The thermocycler program for PCR mutagenesis proceeded as follows: initial denaturation (94 °C, 1 min); 33 cycles of denaturation (94 °C, 30 sec), annealing (59 °C, 1 min), and extension (68 °C, 2 min); final extension (68 °C, 5 min). Following PCR mutagenesis the PCR product was run on a 0.8% agarose gel at 110 V for ~1.5 hr, then DNA was gel extracted using EZ-10 Gel Extraction kit (BioBasic) per manufacturer's instructions, and concentrations were measured by UV absorbance at 260 nm.

The C-ghrelin gene was ligated into pET23a GST-TEV (*HindIII*)-X-His<sub>6</sub>. 3  $\mu$ g pET23a GST-TEV(*HindIII*)-proghrelin-His<sub>6</sub> and C-ghrelin insert DNA was digested with *HindIII* (1  $\mu$ L, 20,000 units/mL), *NotI* (1  $\mu$ L, 20,000 units/mL), 3  $\mu$ L cutsmart buffer (30  $\mu$ L total volume), and incubated at 37 °C for 2 hr. Samples were then run on a 0.8% agarose gel at 110 V for ~1 hr. The bands for the pET23a vector and the C-ghrelin insert were each cut out and DNA was purified using EZ-10 Gel Extraction kit (BioBasic) per manufacturer's instructions, and concentrations were measured by UV absorbance at 260 nm.

Ligations were performed with 50 ng of vector DNA, 40 ng insert DNA, 10  $\mu$ L quick ligase buffer, and 1  $\mu$ L Quick Ligase (total volume 10  $\mu$ L) and incubated on ice for 5 min. 5  $\mu$ L of ligation reaction was added to 100  $\mu$ L Z-competent DH5 $\alpha$  *E. coli* cells, followed by 30 min incubation on ice. Cells were spread on LB- ampicillin (100  $\mu$ g/mL) plates and incubated at 37 °C overnight. Single colonies were inoculated into 5 ml LB cultures containing 100  $\mu$ g/mL ampicillin and grown overnight at 37 °C with shaking (225 rpm). Following overnight growth, plasmids were purified from cultures using EZ-10 Spin Column Plasmid DNA kit (BioBasic) per manufacturer's instructions and successful ligation was confirmed by DNA sequencing (Genewiz).

**3.4.6 CpgY FRET assay.** Purified CpgY (purified same manner as Materials and Methods Chapter 2, section 2.4.19 non-denaturing conditions), CFP-X-YFP in a buffered solution (200 mM NaCl, 20 mM Tris-HCl, pH 7.3 or 50 mM Tris-HCl, pH 7.3) or bacterial lysate (10  $\mu$ L) were added to either 20 mM Tris-HCl, 10 mM EDTA or to the same buffer the sample was in to a total volume of 100  $\mu$ L. This protein sample was added to a black polystyrene 96-well plate (Costar) in the dark and kept under foil until it was read. The wavelength for excitation and emission were 488, 555 nm for YFP<sub>excitation</sub>YFP<sub>emission</sub>, 400, 485 nm for CFP<sub>excitation</sub>CFP<sub>emission</sub>, and 400, 540 nm for CFP<sub>excitation</sub>YFP<sub>emission</sub>. The plate was read three times, with the reads 10 min apart unless otherwise stated.

**3.4.7 Fluorescent gel imaging.** Protein constructs, either in bacterial lysate or purified protein were loaded onto a 12% SDS-PAGE gel using non-reducing sample buffer (no dithiothreitol present) immediately (no boiling of the sample). After the gel was finished running it was transferred to a blotting container filled with ultrapure H<sub>2</sub>O. The gel was then imaged using a Typhoon 9410 fluorescent gel imager (GE) (Upstate Medical School in Dr. Thomas Duncan's laboratory). The gel was scanned using  $\lambda_{ex}$  457 nm,  $\lambda_{em}$  526 nm for CFP<sub>excitation</sub>YFP<sub>emission</sub> and  $\lambda_{ex}$  488 nm,  $\lambda_{em}$  580 nm for YFP<sub>excitation</sub>YFP<sub>emission</sub>, each wavelength reading had a 20 nm bandpass, PMT no more than 600V, scan resolution 50 dots/cm, and pixel size 200. All images were analyzed using ImageQuant 5.1 software (GE).

**3.4.8 SDS-PAGE analysis.** 3XSB lysis was performed by using cell lysate (50  $\mu$ L) was mixed with 25  $\mu$ L of 3x SDS sample buffer and heated to 95 °C for 5 min, followed by centrifugation (10,000 x g, 5 min) to pellet insoluble material. B-PER lysis was

performed using B-PER lysis reagent (Thermo Scientific, 150  $\mu$ L), vortexed on high for 1 min, and cell debris was removed by centrifugation (10,000  $\times$   $g$ , 5 min). 25  $\mu$ L of 3X SDS sample buffer was added and heated to 95°C for 5 min, followed by centrifugation (10,000  $\times$   $g$ , 5 min) to pellet insoluble material. Samples and a protein standards ladder (Precision Plus Dual Color Standards, Bio Basic) were loaded onto a 12% polyacrylamide gel and run at 150V for 1 hr 30 min or until the dye band had migrated to the bottom of the gel. Total protein in cell lysate samples was visualized by staining with Coomassie Blue stain and imaged on a ChemiDoc XRS+ BioRad gel imager.

**3.4.9 Coomassie Blue staining procedure.** Each acrylamide gel was rinsed with ultra pure water and covered in approximately 50 mL of destain solution (stock: 2 L water, 1.6 L methanol, .4 L acetic acid). The gel was microwaved for 18 sec, at which point the destain solution was removed and approximately 50 mL of Coomassie blue stain was added (stock: 0.25 g Coomassie Blue dye, 500 mL methanol, 75 mL acetic acid). The gel was microwaved for 30 sec and rocked for 5 min. The stain solution was removed, destain solution was added and rocked for 15 min, followed by another round of destain addition and rocking for 15 min. The gel was then placed into ultra pure water and rocked overnight. Protein gels were then imaged using BioRad XRS+ gel imager.

**3.4.10 Western blot procedure.** Cell lysates or purified protein samples were run on a polyacrylamide gel as described above. A polyvinylidene fluoride (PVDF) membrane was activated by immersion in methanol for 30 sec, followed by equilibration in transfer buffer (20% v/v methanol, 48 mM Tris Base, 39 mM glycine and 0.034% v/v SDS) for 10 min. Filter papers

and sponges were also soaked in transfer buffer. The gel was assembled into a transfer cassette and proteins were transferred to the PVDF membrane for 20 min at 350 mA, using a BioRad TransBlot Turbo RTA Transfer kit per manufacturer's instructions.

Following electroblotting, the PVDF membrane was washed in Tris-buffered saline (TBS, 0.05 M Tris and 0.14 M NaCl), TBST (TBS with 0.1% v/v Tween 20) and blocked for 4 hr in 10% v/v nonfat milk in TBST. The membrane was then probed with an HRP- $\alpha$ -antiHis primary antibody (1:500 dilution, Rockland) or HRP- $\alpha$ -antiGST primary antibody (1:500 dilution, Rockland) in 10% milk TBST overnight under parafilm. Following washing in TBST, the membrane was treated with the West Pico Chemiluminescent substrate imaging reagent (Thermo Scientific) and imaged on a ChemiDoc XRS+ BioRad gel documentation system.

**3.4.11 Mass spectrometry of proghrelin and C-ghrelin cleavage.** Proghrelin was purified using its purification protocol (Chapter 2). Fractions were pooled; buffer exchanged into 50 mM Tris-HCL, pH 8.0 and concentrated to 28  $\mu$ M. A time course was conducted over 144 hr, a time point (20  $\mu$ L for mass spectrometry, 24  $\mu$ L for gel analysis) was taken from the stock every 24 hr and frozen at -80°C. After completion of the time course an SDS-PAGE gel was run and the mass spectrometry samples were sent on dry ice to Xavier University in New Orelans, LA.

**3.4.12 Alanine mutations of proghrelin-His<sub>6</sub>.** All primers were synthesized by Integrated DNA Technologies. Primers were dissolved in purified water and concentrations were determined by UV absorbance at 260 nm.

Forward primers (reverse compliment sequences were also ordered):

Q73A 5' CAGCAGCACAGTGCGGCACTGGGCAAGTTC 3'

K77A 5' CACAGTCAGGCACTGGGCGCGTTCCTGCAAGACATC 3'

F78A 5' CAGGCACTGGGCAAGGCCCTGCAAGACATCCTG 3'

Q73AK77A 5' CAGTATCAGCAGCACAGTGCGGCACTGGGCGCGTTCCTGCAAGAC 3'

Q73AF78A 5' CAGCAGCACAGTGCGGCACTGGGCAAGGCCGTGCAAGACATC 3'

S18A 5' CAGCGCAAGGAAGCCAAGAAGCCGCCG 3'

D38A 5' TTAGGTCCGGAAGCTGGCGGCCCAAGC 3'

D47A 5' GGCGCCGAAGCCGAGCTGGAG 3'

E43A 5' GGCCAAGCAGCAGGCGCCGAAGAC 3'

E48A 5' GCCGAAGACGCGCTGGAGGTTTCGC 3'

E50A 5' GCCGAAGACGAGCTGGCCGTTTCGCTTCAAC 3'

E37A 5' TGGTTACGTCCGGCAGATGGCGGCCCA 3'

E46A 5' GAAGGCGCCGCAGACGAGCTGGAG 3'

PCR mutagenesis reactions (50  $\mu$ L) contained the following components: 1x Pfu reaction buffer; 10 ng pET23a GST-TEV-human proghrelin-His<sub>6</sub>; 125 ng forward primer; 125 ng reverse primer, 20  $\mu$ M dNTPs, and 1  $\mu$ L Pfu Turbo DNA polymerase (Agilent). For double mutants the GThPH Q73A sequence was used as the template. The thermocycler program for PCR mutagenesis proceeded as follows: initial denaturation (94 °C, 5 min); 30 cycles of denaturation (94 °C, 30 sec), annealing (56 °C, 1 min), and extension (68 °C, 2 min); final extension (68 °C, 5 min). *DpnI* (1  $\mu$ L, 20,000 units/mL) was added and reactions were incubated at 37 °C for 1 hr. After *DpnI* digestion, 5  $\mu$ L of the PCR reaction mixture was transformed into 50  $\mu$ L of Z-competent DH5 $\alpha$  *E. coli* cells (Zymo Research) followed by incubation on ice for 30 min. Transformed bacteria were spread on LB-ampicillin (100  $\mu$ g/mL) plates and incubated at 37 °C overnight.

Single colonies were then inoculated into 5 ml LB media containing 100 µg/mL ampicillin in sterile culture tubes, which were incubated at 37 °C overnight with shaking (225 rpm). Following overnight growth, plasmids were purified from cultures using EZ-10 Spin Column Plasmid DNA kit (BioBasic) per manufacturer's instructions. The product was verified by DNA sequencing (Genewiz).

**3.4.13 GST-TEV-X-His<sub>6</sub> constructs.** Primers were synthesized by Integrated DNA Technologies. Primers were dissolved in purified water and concentrations were determined by UV absorbance at 260 nm.

1-X 5' TATACTGTA CTTC CAGGGTAAGCTTGGTAGCAGCTTTCTG 3'

16-49 5' TATACTGTA CTTC CAGGGTAAGCTTAAGGAAAGTAAGAAGCCG 3'

46-94 5' TATACTGTA CTTC CAGGGTAAGCTTGAAGACGAGCTGGAG 3'

61-94 5' TATACTGTA CTTC CAGGGTAAGCTTATCAAGCTGAGTGGTGTG 3'

X-94 5' GCGAAGGAAGCACCGGCCGATAAAGCGGCCGCACTATATA 5'

X-49 5' CAAGCAGAAGGCGCCGAAGACGAGCTGGCGGCCGC 3'

PCR mutagenesis reactions (50 µL) contained the following components: 1x One Taq standard reaction buffer; 40 ng pET23a CpgY template; 125 ng forward primer; 125 ng reverse primer, 20 µM dNTPs, and One Taq DNA polymerase (1 µL, 5,000 units/mL) (Agilent). The thermocycler program for PCR mutagenesis proceeded as follows: initial denaturation (94 °C, 1 min); 33 cycles of denaturation (94 °C, 30 sec), annealing (59 °C, 1 min), and extension (68 °C, 2 min); final extension (68 °C, 5 min). Following PCR mutagenesis the PCR product was run on a 0.8% agarose gel at 110 V for ~1.5 hr, then DNA was gel extracted using EZ-10 Gel Extraction

kit (BioBasic) per manufacturer's instructions, and concentrations were measured by UV absorbance at 260 nm.

The proghrelin truncated genes were ligated into pET23a GST-TEV-X-His<sub>6</sub>. 3 µg pET23a GST-TEV-proghrelin-His<sub>6</sub> and proghrelin truncation insert DNA was digested with *SacI* (1 µL, 20,000 units/mL), *PstI* (1 µL, 20,000 units/mL), 3 µL cutsmart buffer (30 µL total volume), or digested with *NotI* (1 µL, 20,000 units/mL), *HindIII* (1 µL, 20,000 units/mL), 3 µL cutsmart buffer (30 µL total volume) and incubated at 37 °C for 2 hr. Samples were then run on a 0.8% agarose gel at 110 V for ~1 hr. The bands for the pET23a vector and the insert were each cut out and DNA was purified using EZ-10 Gel Extraction kit (BioBasic) per manufacturer's instructions, and concentrations were measured by UV absorbance at 260 nm.

Ligations were performed with 50 ng of vector DNA, 40 ng insert DNA, 10 µL quick ligase buffer, and 1 µL Quick Ligase (total volume 10 µL) and incubated on ice for 5 min. 5 µL of ligation reaction was added to 100 µL Z-competent DH5α *E. coli* cells, followed by 30 min incubation on ice. Cells were spread on LB- ampicillin (100 µg/mL) plates and incubated at 37 °C overnight.

Single colonies were inoculated into 5 ml LB cultures containing 100 µg/mL ampicillin and grown overnight at 37 °C with shaking (225 rpm). Following overnight growth, plasmids were purified from cultures using EZ-10 Spin Column Plasmid DNA kit (BioBasic) per manufacturer's instructions and successful ligation was confirmed by DNA sequencing (Genewiz).

**3.4.14 Oligo annealing for construction of X-YFP proghrelin truncations.** DNA oligomers were constructed by Integrated DNA Technologies. Oligomers were dissolved in purified water

and concentrations were determined by UV absorbance at 260 nm. They utilized *SacI*, *XhoI* restriction sites.

Oligomers:

1. CGGCCACGAAGGCCAGGAGTGAAT GGGC
2. TCGAGCCCATTCACTCCTGGCCTTCGTGGCCGA

Anneal the oligomers together (200  $\mu$ M of each) using PCR protocol: 1 cycle (94°C, 5 min), 2 cycles (94°C, 30 sec), 2 cycles (94°C, 5 min), 2 cycles (80°C, 5 min), 1 cycle (72°C, 7 min), 1 cycle (66°C, 7 min), 5 cycles (60°C, 3 min), 6 cycles (52°C, 3 min), 7 cycles (46°C, 3 min), and finally 8 cycles (37°C, 20 min).

Ligations were performed with 100 ng of parent plasmid DNA either pET23a CpgY 16-94, 31-94, 46-94, 61-94, and 76-94 (already digested using *SacI* and *XhoI* to cut out CFP, gel extracted and purified), 1  $\mu$ L of the annealed oligomers from the PCR reaction, 2  $\mu$ L quick ligase buffer, and 1  $\mu$ L Quick Ligase (total volume 20  $\mu$ L) and incubated on ice for 5 min. 5  $\mu$ L of ligation reaction was added to 100  $\mu$ L Z-competent DH5 $\alpha$  *E. coli* cells, followed by 30 min incubation on ice. Cells were spread on LB- ampicillin (100  $\mu$ g/mL) plates and incubated at 37 °C overnight. Single colonies were inoculated into 5 mL LB cultures containing 100  $\mu$ g/mL ampicillin and grown overnight at 37 °C with shaking (225 rpm). Following overnight growth, plasmids were purified from cultures using EZ-10 Spin Column Plasmid DNA kit (BioBasic) per manufacturer's instructions and successful ligation was confirmed by DNA sequencing (Genewiz).

The only positive result was 16-94-YFP so this construct was used for the remaining constructs. This construct was then digested alongside CpgY 31-94, 46-94, 61-94, 76-94. 3  $\mu$ g pET23a 16-64-YFP and proghrelin truncation insert DNA was digested with *HINDIII* (1  $\mu$ L,

20,000 units/mL), *XhoI* (1  $\mu$ L, 20,000 units/mL), 3  $\mu$ L cutsmart buffer (30  $\mu$ L total volume) and incubated at 37 °C for 2 hr. Samples were then run on a 0.8% agarose gel at 110 V for ~1 hr. The bands for the pET23a vector and the insert were each cut out and DNA was purified using EZ-10 Gel Extraction kit (BioBasic) per manufacturer's instructions, and concentrations were measured by UV absorbance at 260 nm.

Ligations were performed with 50 ng of vector DNA, 40 ng insert DNA, 10  $\mu$ L quick ligase buffer, and 1  $\mu$ L Quick Ligase (total volume 10  $\mu$ L) and incubated on ice for 5 min. 5  $\mu$ L of ligation reaction was added to 100  $\mu$ L Z-competent DH5 $\alpha$  *E. coli* cells, followed by 30 min incubation on ice. Cells were spread on LB- ampicillin (100  $\mu$ g/mL) plates and incubated at 37°C overnight. Single colonies were inoculated into 5 mL LB cultures containing 100  $\mu$ g/mL ampicillin and grown overnight at 37°C with shaking (225 rpm). Following overnight growth, plasmids were purified from cultures using EZ-10 Spin Column Plasmid DNA kit (BioBasic) per manufacturer's instructions and successful ligation was confirmed by DNA sequencing (Genewiz).

**3.4.15 Cloning CpgY into pCAF.** The CpgY gene was ligated into pCAF. 3  $\mu$ g pET23a CpgY and pCAF DNA was digested with *NotI* (1  $\mu$ L, 10,000 units/mL), *EcoRI* (1  $\mu$ L, 20,000 units/mL), 3  $\mu$ L Cutsmart buffer (30  $\mu$ L total volume), and incubated at 37 °C for 2 hr. Samples were then run on a 0.8% agarose gel at 110 V for ~1 hr. The bands for the pCAF vector and the CpgY insert were each cut out and DNA was purified using EZ-10 Gel Extraction kit (BioBasic) per manufacturer's instructions, and concentrations were measured by UV absorbance at 260 nm.

Ligations were performed with 50 ng of vector DNA, 51 ng insert DNA, 10  $\mu$ L quick ligase buffer, and 1  $\mu$ L Quick Ligase (total volume 10  $\mu$ L) and incubated on ice for 5 min. 5  $\mu$ L

of ligation reaction was added to 100  $\mu$ L Z-competent DH5 $\alpha$  *E. coli* cells, followed by 30 min incubation on ice. Cells were spread on LB- ampicillin (100  $\mu$ g/mL) plates and incubated at 37  $^{\circ}$ C overnight. Single colonies were inoculated into 5 mL LB cultures containing 100  $\mu$ g/mL ampicillin and grown overnight at 37  $^{\circ}$ C with shaking (225 rpm). Following overnight growth, plasmids were purified from cultures using EZ-10 Spin Column Plasmid DNA kit (BioBasic) per manufacturer's instructions and successful ligation was confirmed by DNA sequencing (Genewiz).

**3.4.16 pCAF CpgY transfection.** Following confirmation of CpgY insertion the pCAF CpgY plasmid was then transfected into HEK 293FT cells.  $1 \times 10^6$  cells/well were plated in DMEM ((Dulbecco's Modified Eagle's Medium, Corning) containing 10% FBS and 1% penicillin/streptomycin) in a 6-well clear bottom plate. Cells were allowed to incubate 16-18 hr at 37  $^{\circ}$ C 5% CO<sub>2</sub> before transfection. Transfections used DMEM in the absence of FBS, 4  $\mu$ g pCAF CpgY DNA, and a range of Lipofectamine 2000 transfection reagent (Thermo fischer) transfection reagent (9, 10, 12, 15  $\mu$ L). After overnight incubation, DMEM (containing no FBS), DNA and transfection reagent were allowed to incubate together for 5 min at room temperature then were added to the plated cells. After the transfection mixture was added, cells were allowed to incubate for 48 hours at 37  $^{\circ}$ C 5% CO<sub>2</sub>. Cells were collected, washed in PBS, and lysed using RIPA buffer (50 mM Tris-HCl, pH 7.4, 150 mM NaCl, 2 mM EDTA, 10% v/v NP40, 0.1% v/v SDS) containing a mini Roche tablet (Sigma).

### 3.5 References

1. Garg, A., The ongoing saga of obestatin: is it a hormone? *J Clin Endocrinol Metab* **2007**, *92* (9), 3396-8.
2. Chen, C. Y.; Fujimiya, M.; Asakawa, A.; Chang, F. Y.; Cheng, J. T.; Lee, S. D.; Inui, A., At the cutting edge: ghrelin gene products in food intake and gut motility. *Neuroendocrinology* **2009**, *89* (1), 9-17.
3. Romero, A.; Kirchner, H.; Heppner, K.; Pfluger, P. T.; Tschop, M. H.; Nogueiras, R., GOAT: the master switch for the ghrelin system? *Eur J Endocrinol* **2010**, *163* (1), 1-8.
4. Takahashi, T.; Ida, T.; Sato, T.; Nakashima, Y.; Nakamura, Y.; Tsuji, A.; Kojima, M., Production of n-octanoyl-modified ghrelin in cultured cells requires prohormone processing protease and ghrelin O-acyltransferase, as well as n-octanoic acid. *J Biochem* **2009**, *146* (5), 675-82.
5. Zhu, X.; Cao, Y.; Voogd, K.; Steiner, D. F., On the processing of proghrelin to ghrelin. *J Biol Chem* **2006**, *281* (50), 38867-70.
6. Cleverdon, E. R.; McGovern-Gooch, K. R.; Hougland, J. L., The octanoylated energy regulating hormone ghrelin: An expanded view of ghrelin's biological interactions and avenues for controlling ghrelin signaling. *Mol Membr Biol* **2016**, *33* (6-8), 111-124.
7. Nakazato, M.; Murakami, N.; Date, Y.; Kojima, M.; Matsuo, H.; Kangawa, K.; Matsukura, S., A role for ghrelin in the central regulation of feeding. *Nature* **2001**, *409* (6817), 194-8.
8. Hosoda, H.; Kojima, M.; Mizushima, T.; Shimizu, S.; Kangawa, K., Structural divergence of human ghrelin. Identification of multiple ghrelin-derived molecules produced by post-translational processing. *J Biol Chem* **2003**, *278* (1), 64-70.

9. Ozawa, A.; Cai, Y.; Lindberg, I., Production of bioactive peptides in an in vitro system. *Anal Biochem* **2007**, *366* (2), 182-9.
10. Zhang, J. V.; Ren, P. G.; Avsian-Kretchmer, O.; Luo, C. W.; Rauch, R.; Klein, C.; Hsueh, A. J., Obestatin, a peptide encoded by the ghrelin gene, opposes ghrelin's effects on food intake. *Science* **2005**, *310* (5750), 996-9.
11. De Waele, K.; Ishkanian, S. L.; Bogarin, R.; Miranda, C. A.; Ghatei, M. A.; Bloom, S. R.; Pacaud, D.; Chanoine, J. P., Long-acting octreotide treatment causes a sustained decrease in ghrelin concentrations but does not affect weight, behaviour and appetite in subjects with Prader-Willi syndrome. *Eur J Endocrinol* **2008**, *159* (4), 381-8.
12. Eipper, B. A.; Milgram, S. L.; Husten, E. J.; Yun, H. Y.; Mains, R. E., Peptidylglycine alpha-amidating monooxygenase: a multifunctional protein with catalytic, processing, and routing domains. *Protein Sci* **1993**, *2* (4), 489-97.
13. Green, B. D.; Irwin, N.; Flatt, P. R., Direct and indirect effects of obestatin peptides on food intake and the regulation of glucose homeostasis and insulin secretion in mice. *Peptides* **2007**, *28* (5), 981-7.
14. Steiner, D. F., The proprotein convertases. *Curr Opin Chem Biol* **1998**, *2* (1), 31-9.
15. Morihara, K.; Oka, T., A kinetic investigation of subsites S1' and S2' in alpha-chymotrypsin and subtilisin BPN'. *Arch Biochem Biophys* **1977**, *178* (1), 188-94.
16. Perona, J. J.; Hedstrom, L.; Rutter, W. J.; Fletterick, R. J., Structural origins of substrate discrimination in trypsin and chymotrypsin. *Biochemistry* **1995**, *34* (5), 1489-99.
17. Amitai, G.; Callahan, B. P.; Stanger, M. J.; Belfort, G.; Belfort, M., Modulation of intein activity by its neighboring extein substrates. *Proc Natl Acad Sci U S A* **2009**, *106* (27), 11005-10.

18. Callahan, B. P.; Belfort, M., Branching out of the intein active site in protein splicing. *Proc Natl Acad Sci U S A* **2014**, *111* (23), 8323-4.
19. Callahan, B. P.; Topilina, N. I.; Stanger, M. J.; Van Roey, P.; Belfort, M., Structure of catalytically competent intein caught in a redox trap with functional and evolutionary implications. *Nat Struct Mol Biol* **2011**, *18* (5), 630-3.
20. Owen, T. S.; Ngoje, G.; Lageman, T. J.; Bordeau, B. M.; Belfort, M.; Callahan, B. P., Förster resonance energy transfer-based cholesterolysis assay identifies a novel hedgehog inhibitor. *Anal Biochem* **2015**, *488*, 1-5.
21. Owen, T. S.; Xie, X. J.; Laraway, B.; Ngoje, G.; Wang, C.; Callahan, B. P., Active site targeting of hedgehog precursor protein with phenylarsine oxide. *Chembiochem* **2015**, *16* (1), 55-8.
22. Studier, F. W., Protein production by auto-induction in high density shaking cultures. *Protein Expr Purif* **2005**, *41* (1), 207-34.
23. Bornhorst, J. A.; Falke, J. J., Purification of proteins using polyhistidine affinity tags. *Methods Enzymol* **2000**, *326*, 245-54.
24. Barrow, K. M.; Perez-Campo, F. M.; Ward, C. M., Use of the cytomegalovirus promoter for transient and stable transgene expression in mouse embryonic stem cells. *Methods Mol Biol* **2006**, *329*, 283-94.

## **Chapter 4: Structure-activity relationship determination of ghrelin O-acyltransferase substrate binding utilizing unnatural amino acid incorporated peptides**

Portions of this chapter, including figures and experimental, have been previously published and reproduced with permission from the publisher, Reference 57, Cleverdon, E. R.; Davis, T. R.; Houglund, J. L., Functional group and stereochemical requirements for substrate binding by ghrelin O-acyltransferase revealed by unnatural amino acid incorporation. *Bioorg Chem* **2018**, 79, 98-106. Copyright © 2018 Elsevier Inc.

## 4.1 Introduction

Ghrelin octanoylation is catalyzed by the ER membrane-bound enzyme, ghrelin *O*-acyltransferase (GOAT),<sup>1-2</sup> which is a member of the membrane-bound *O*-acyltransferase (MBOAT) family.<sup>3</sup> GOAT is one of three MBOATs, along with Porcupine (PORCN) and Hedgehog acyltransferase (Hhat), which acylate protein substrates with the other family members modifying small molecules.<sup>3-5</sup> These enzymes are topologically complex integral membrane proteins, which has limited studies towards understanding of the structures and catalytic mechanisms of these proteins. Since these enzymes modify substrates that play important roles in cell function and biological signaling, there is substantial interest in inhibitor development targeting them.<sup>3, 6-16</sup> A complete understanding of the substrate recognition elements necessary for acylation of ghrelin by GOAT is crucial for exploiting the therapeutic potential provided by this enzyme and other MBOAT family members.

As discussed in Chapter 1, ghrelin receptor activation and signaling has been linked to diseases including diabetes and obesity.<sup>17-19</sup> Ghrelin is involved in many biological functions as well as disease states all of which are a result of GHS-R1a activation.<sup>20-23</sup> Since GOAT acylation is the first step in this signaling cascade, the ghrelin-GOAT system presents a unique and largely unexploited target for inhibition as a therapeutic avenue.<sup>4, 24-27</sup> Previous studies have shown short peptides containing the first five amino acids of the ghrelin N-terminal sequence (GSSFL) can serve as substrates for GOAT-catalyzed serine octanoylation.<sup>10, 28-31</sup> Since the N-terminal region of ghrelin has been determined to be important for GOAT recognition, ghrelin mimetic peptides have the potential for high selectivity for GOAT and reduced off-target effects from binding to other protein targets. The design of ghrelin mimetic inhibitors increases our understanding of ghrelin binding and recognition by GOAT.<sup>9-10, 28-29, 31-32</sup> Through the use of small N-terminal

ghrelin peptides with amino acid substitutions and/or chemical addition/deletions, it was concluded that GOAT utilizes distinct functional group contacts with multiple positions within ghrelin for acylation to occur.<sup>28-29</sup>

In studies focused solely on ghrelin binding to GOAT, unlike studies which are based upon reactivity that includes both binding and octanoylation of the peptide,<sup>28-29, 33</sup> acylated ghrelin mimetics have been demonstrated to be efficient inhibitors of GOAT. In the first reported GOAT inhibitors, Yang and coworkers showed acylated pentapeptides inhibit GOAT-catalyzed ghrelin acylation.<sup>10</sup> These octanoylated peptides utilized the serine ester motif in ghrelin but instead use a more stable amide linkage.<sup>10</sup> Using the reported inhibitor by Yang and coworkers as a template, Darling and coworkers designed acylated ghrelin-mimetic peptides to demonstrate GOAT has a preference for acyl chains with a length of seven or eight carbons.<sup>29</sup> Ghrelin mimetic inhibitors continued to incorporate acyl chains attachments into their design which has resulted in enhanced binding from the attachment of the hydrophobic moiety.<sup>9, 34</sup> The acylated ghrelin mimetics have shown potency against GOAT. However, there are issues with their ability to cross the cell membrane without the presence of a cell-penetrating peptide sequence, biostability, as well as, the possibility of GHS-R1a receptor activation. All of these negative attributes have hindered their further therapeutic development<sup>20</sup>.

More recently, a longer ghrelin-mimetic peptide incorporating 2,3-diaminopropanoic acid (Dap), a serine analog that replaces the hydroxyl with an amine (same starting residue as used in the acylated inhibitors described above), at the third position was reported by Taylor and coworkers to serve as an inefficient substrate for GOAT-catalyzed acylation.<sup>31</sup> To further investigate the importance of the amino side chain of the non-acylated Dap residue, we have designed a series of small N-terminal ghrelin mimetics to probe binding affinity and acylation

efficiency by hGOAT (Figure 4.1). This approach fully defined the necessary residues for GOAT recognition and binding which complements previous investigations of GOAT reactivity with ghrelin mimetic peptides.

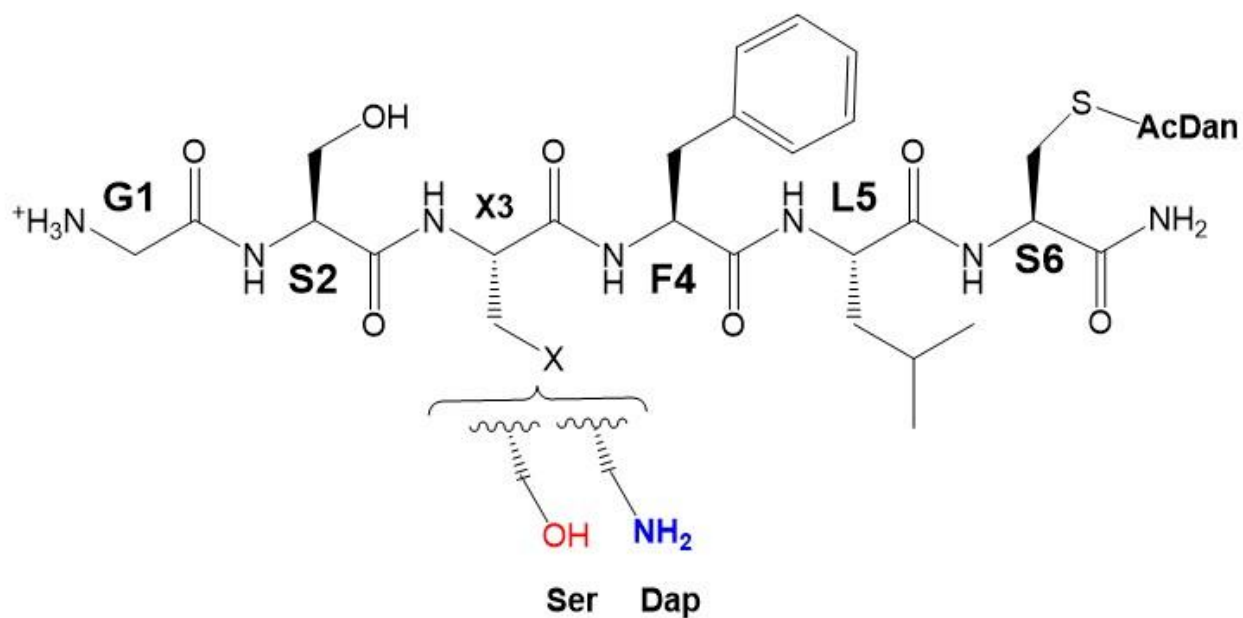


**Figure 4.1. Structure of GSSLFC<sub>AcDan</sub> and GSDapFLC<sub>AcDan</sub> peptides.** Both peptides were probed for their acylation efficiency by human GOAT (hGOAT) by fluorescent detection using RP-HPLC analysis. Serine is indicated by Ser and a hydroxyl, Dap is indicated by Dap and an amine.

## 4.2. Results

### 4.2.1 A 2, 3-diaminopropanoic acid (Dap) substituted ghrelin peptide acts as an inefficient hGOAT substrate.

Based on the reported data mentioned above that showed longer ghrelin-mimetic peptides with Dap substitution at the serine 3 (S3) position act as weak substrates for the mouse ortholog of GOAT (mGOAT),<sup>31</sup> we investigated if human GOAT (hGOAT) was able to acylate a short fluorescently labeled peptide with a Dap residue at the third position (GSDapFLC<sub>AcDan</sub>) (Figure 4.1). Since GSDapFLC<sub>AcDan</sub> acylation with octanoyl-CoA has a very similar structure to the first reported inhibitor of GOAT,<sup>10</sup> octanoylation of this peptide could lead to product inhibition. To reduce the chance of product inhibition, we explored acylation of GSDapFLC<sub>AcDan</sub> using a less active acyl donor co-substrate, decanoyl-CoA, which would yield an acylated product with lower potency as an inhibitor.<sup>29</sup> Incubation of GSDapFLC<sub>AcDan</sub> in the presence of decanoyl-CoA and hGOAT-containing microsomal fraction reproducibly produced two peaks, both of which are consistent with attachment of the longer CoA donor based on their retention time on RP-HPLC (Figure 4.2A and 4.2B). Integration of peak fluorescence showed that acylation of GSDapFLC<sub>AcDan</sub> is not as efficient as GSSFLC<sub>AcDan</sub>, which is consistent with the report from Taylor and coworkers in reactions using longer Dap-containing peptides and mGOAT (Figure 4.2C).<sup>31</sup>

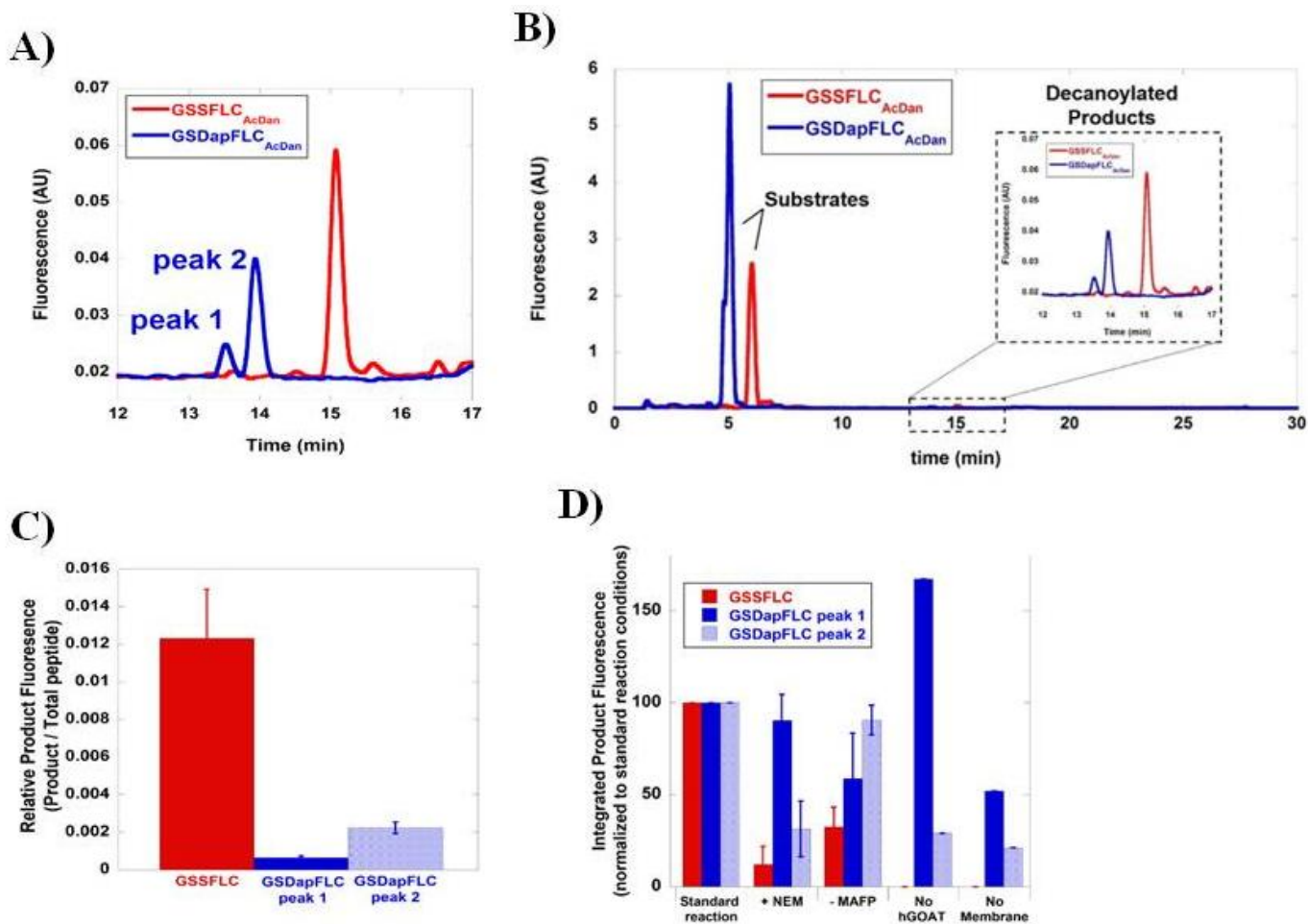


**Figure 4.2. Analysis of acylation of a ghrelin mimetic peptide substrate incorporating a Dap residue.** **A)** HPLC chromatograms showing product formation. A single acylation product is detected upon incubation of GSSFLC<sub>AcDan</sub> in the presence of hGOAT and decanoyl-CoA and two product peaks for GSDapFLC<sub>AcDan</sub> under analogous reaction conditions; red trace, GSSFLC<sub>AcDan</sub>; blue trace, GSDapFLC<sub>AcDan</sub>. **B)** Full chromatograms for analysis of acylation of ghrelin mimetic peptide substrates. Expanded view of peaks for decanoylated products observed with GSSFLC<sub>AcDan</sub> (red) and GSDapFLC<sub>AcDan</sub> (blue) from A. HPLC chromatograms from hGOAT reactions with GSSFLC<sub>AcDan</sub> (in red) and GSDapFLC<sub>AcDan</sub> (in blue) and decanoyl-CoA under analogous conditions. **C)** Normalized integrated product fluorescence (product / product+substrate) for GSSFLC<sub>AcDan</sub> and GSDapFLC<sub>AcDan</sub> acylation. **D)** Acylation of GSSFLC<sub>AcDan</sub> and GSDapFLC<sub>AcDan</sub> in the presence of multiple reaction conditions. hGOAT inhibitor (+ NEM), absence of esterase inhibitor (-MAFP), absence of hGOAT in membrane protein fraction (-hGOAT), and absence of membrane protein fraction (no membrane) compared to acylation under standard reaction conditions. All reported activities represent the average of a minimum of three independent trials, with error bars representing one standard deviation. The figure is reproduced with permission from Reference 57 (Appendix V). © 2018 Elsevier Inc.

In order to determine if the two acylation products observed with GSDapFLC<sub>AcDan</sub> require hGOAT enzymatic activity, N-ethylmaleimide (NEM) was introduced to the reaction. NEM has been shown to irreversibly inhibit hGOAT enzymatic activity.<sup>7</sup> Production of the longer eluting GSDapFLC<sub>AcDan</sub> product peak (peak 2) was susceptible to NEM treatment (Figure 4.2D), which indicated hGOAT activity was required for efficient acylation leading to that product. In contrast, the first GSDapFLC<sub>AcDan</sub> product peak (peak 1) was minimally affected by NEM treatment indicating that hGOAT was not or minimally required for product formation. Both product peaks were also observed when GSDapFLC<sub>AcDan</sub> was incubated with decanoyl-CoA without the presence of membrane fraction containing hGOAT or in buffer alone. Peak 2 is not as prevalent as in the presence of hGOAT in either of those conditions. This demonstrated that the acylation reaction with the GSDapFLC<sub>AcDan</sub> peptide occurred through both enzymatic (peak 2) and non-enzymatic routes (peak 1 and peak 2).

The presence of esterases in microsomal fractions provides an avenue for probing ester linkages as a result of hGOAT catalysis.<sup>36</sup> Treatment with the esterase inhibitor methyl arachidonyl fluorophosphonate (MAFP) inhibited esterase hydrolysis activity the microsomal fractions, while untreated microsomal fraction hydrolyzes an ester linkage such as those in S3 acylated ghrelin peptides.<sup>36</sup> When hGOAT reactions were performed without MAFP pretreatment to inactivate esterases, the first peak in the GSDapFLC<sub>AcDan</sub> reaction had a smaller integrated fluorescence value in a similar manner as the acylated product peak for the GSSFLC<sub>AcDan</sub> substrate (Figure 4.2D). The second product peak in the GSDapFLC<sub>AcDan</sub> reaction was not affected by the presence/absence of MAFP, consistent with this peak representing GSDapFLC<sub>AcDan</sub> acylation of the amino group which resulted in an esterase-resistant amide linkage. In summary, the data indicates that acylation likely occurred at both S2 (ester linkage)

and Dap3 (amide linkage) positions of the GSDapFLC<sub>AcDan</sub> substrate. The Dap3 modification was catalyzed by hGOAT, with a small minority occurring non-enzymatically, and acylation of S2 was occurring solely through a non-enzymatic pathway. This is consistent with the inability of GOAT to acylate S2 reported by other research groups.<sup>1-2, 37</sup> In either case, acylation of the Dap-containing ghrelin mimetic peptide is much less efficient than for a substrate with serine at the canonical acylation site.

Given that GSDapFLC<sub>AcDan</sub> can act as a substrate for hGOAT, enzymatic acylation of the peptide should be subject to loss of activity upon removal of residues within GOAT required for acylation of the wildtype sequence with serine at the acylation site. A number of hGOAT mutants including H338A, D234A and C235A were evaluated<sup>38</sup> and found to be catalytically inactive and were not able to catalyze the acylation of GSSFLC<sub>AcDan</sub>. If GSDapFLC<sub>AcDan</sub> is acting as an hGOAT substrate then the catalytic machinery should be necessary for this substrate as well. When GSDapFLC<sub>AcDan</sub> was under its standard reaction conditions (1 mM decanoyl-CoA, 5  $\mu$ M peptide) the catalytically inactive hGOAT mutants (H338A, D234A, and C235A) led to no observable product in comparison to wild type hGOAT. This behavior was also observed with conservative mutations of these sites H338F, D234N and C235S. It was previously proposed that H338 is not the catalytic base because the amine in the Dap's sidechain has a moderate pKa,<sup>31, 39</sup> and GOAT is able to acylate a Dap-incorporated peptide in its absence. This conclusion is not supported by examples of similar systems, as demonstrated in histone acetylation wherein lysine residues are modified using a catalytic base<sup>40</sup> or by the behavior observed during these studies. There is enhancement of product formation for the GSDapFLC<sub>AcDan</sub> substrate (peak 2) in the presence of H338 compared to when it is knocked out (as well as at C235 and D234) using an alanine or phenylalanine mutant, implying that this residue is important for enzymatic catalysis.

#### 4.2.2 A Dap-substituted peptide acts as a potent hGOAT inhibitor.

To determine if Dap incorporation at the S3 position affected peptide binding to hGOAT, ghrelin mimetic peptides with alanine (GSAFL), serine (GSSFL), or Dap (GSDapFL) were assayed as unlabeled competitive inhibitors of hGOAT acylation using GSSFLC<sub>AcDan</sub> as a substrate (Figure 4.3). No inhibition of GSSFLC<sub>AcDan</sub> octanoylation was observed with GSAFL up to 10  $\mu\text{M}$ .<sup>2, 29, 41</sup> The serine-containing GSSFL peptide exhibited an IC<sub>50</sub> value of  $53 \pm 4 \mu\text{M}$ , but S3 substitution with the amine (Dap) increases peptide potency as an hGOAT inhibitor ~380-fold (GSDapFL IC<sub>50</sub> =  $140 \pm 20 \text{ nM}$ ). The potency this unnatural amino acid incorporation indicated the free amine at the acylation site enhanced peptide binding to the hGOAT active site and provided an opportunity to explore many facets of peptide binding to GOAT.

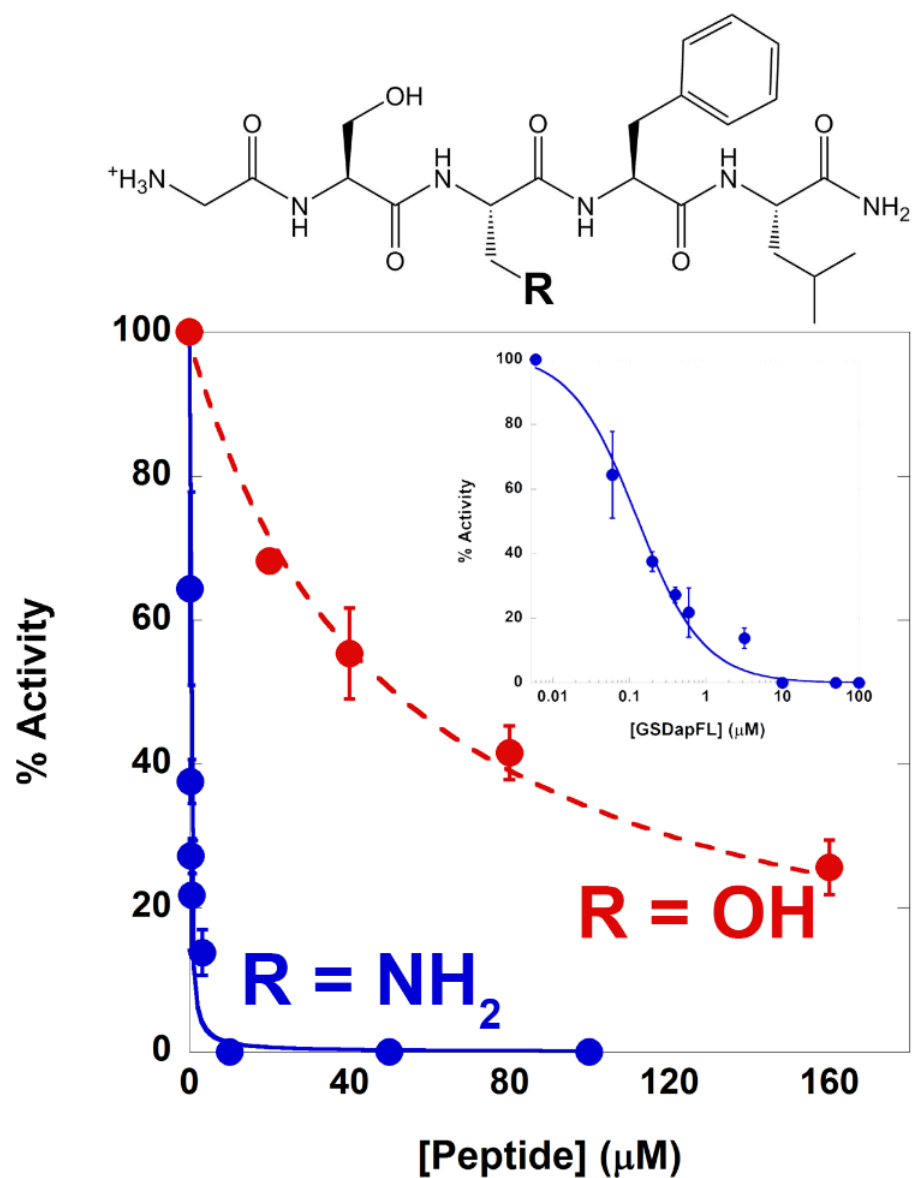


**Figure 4.3. Inhibition of hGOAT-catalyzed octanoylation of GSSFLC<sub>AcDan</sub> by GSSFL and GSDapFL.** IC<sub>50</sub> values for unlabeled GSSFL (R = OH) and GSDapFL (R = NH<sub>2</sub>) peptides were calculated from percent activity as described in the experimental section, with error bars indicating the standard deviation from a minimum of three independent measurements. The inset displays the inhibition data for GSDapFL with a logarithmic concentration scale. The figure is reproduced with permission from Reference 57 (Appendix V). © 2018 Elsevier Inc.

### 4.2.3 Length dependence of GOAT inhibition by Dap-containing peptides.

Using Dap-containing ghrelin peptides mimetics, we examined the impact of both N-terminal and C-terminal truncations on peptide binding to hGOAT (Figure 4.4). Deletion of the N-terminal glycine residue yielded the peptide SDapFL and led to a complete loss of inhibition of GOAT ( $IC_{50} > 100 \mu\text{M}$ ). Acetylation of the SDapFL peptide also led to no detectible binding to hGOAT ( $IC_{50} > 100 \mu\text{M}$ ), reflected at minimum of a 700-fold loss in peptide binding affinity compared to the GSDapFL parent upon removal of the N-terminal amino group. Length changes to the C-terminal sequence also affected peptide binding, although not as severely as the N-terminal truncations. To determine if a longer peptide with more N-terminal sequence would increase its binding affinity for the enzyme, we examined inhibition using a six amino acid ghrelin mimetic sequence (GSDapFLS). There was enhanced binding with the longer sequence but with less than a 2-fold change in  $IC_{50}$  value. Removal of L5 residue from GSDapFL (GSDapF) increased the  $IC_{50}$  ~10-fold relative to GSDapFL. An additional C-terminal truncation to GSDap resulted in complete loss of inhibition ( $IC_{50} > 100 \mu\text{M}$ ). The truncation analysis highlighted two important groups within the ghrelin sequence that are essential in peptide binding to hGOAT, the N-terminal amino group on G1 and the F4 position.

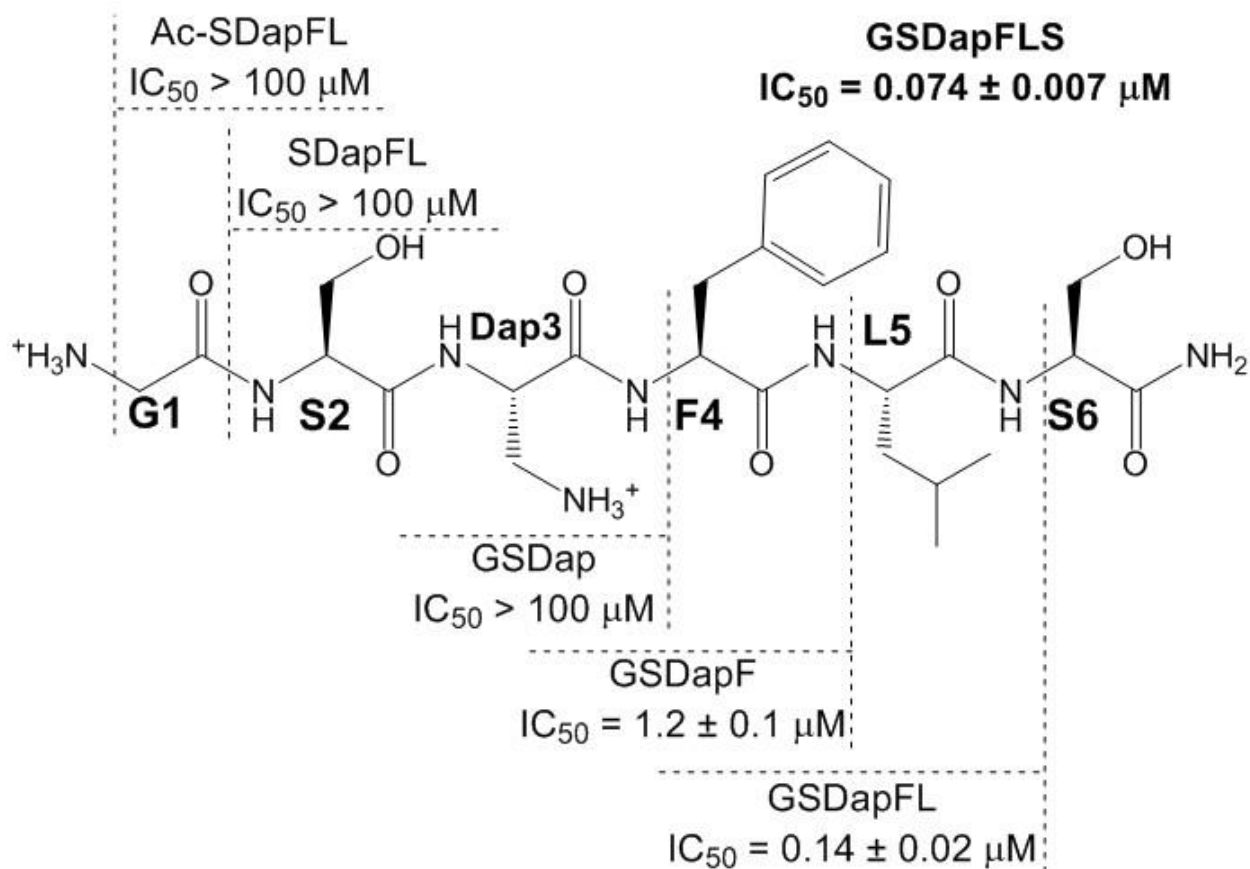


**Figure 4.4. Defining the N- and C-terminal length dependence of Dap-containing ghrelin mimetic peptide GOAT inhibitors.** The GSDapFLS peptide was truncated from the N- and C-termini as shown above, with  $\text{IC}_{50}$  values calculated for each truncated derivative as described in the experimental section. The figure is reproduced with permission from Reference 57 (Appendix V). © 2018 Elsevier Inc.

#### 4.2.4 Sequence dependence of GOAT inhibition by Dap-containing peptides

The truncation analysis of the GSDapFL peptide inhibitor highlighted the importance of the F4 residue for peptide binding to hGOAT. To probe the importance of F4's benzyl group, a series of amino acid changes were analyzed at the F4 position in the context of peptides containing either five amino acids in GSDapFL or with four amino acids in GSDapF. In the GSDapFL peptide, the phenylalanine was changed to alanine, threonine (smaller amino acids) and then tryptophan (a large amino acid, which is also hydrophobic and aromatic).<sup>29</sup> Incorporation of either alanine or threonine in the peptide led to a complete loss of binding reflected by lack of inhibition up to 100  $\mu\text{M}$  (Table 4.1). In contrast, mutation to tryptophan only reduced inhibitor potency by approximately 2-fold (GSDapWL  $\text{IC}_{50} = 0.30 \pm 0.04 \mu\text{M}$ ). In the shorter GSDapF peptide, the phenylalanine was substituted with either alanine or glycine to determine the importance of the benzyl sidechain of F4 to peptide binding in a shorter context. In both cases, no inhibition of hGOAT activity was observed up to 100  $\mu\text{M}$  which indicates the phenylalanine side chain is crucial for peptide binding which is consistent with the studies of the longer GSDapFL peptide.

| <b>Mutation</b> | <b>Peptide Sequence</b> | <b>IC<sub>50</sub> (μM)</b> |
|-----------------|-------------------------|-----------------------------|
| <i>wildtype</i> | GSDapFL                 | 0.14 ± 0.02                 |
| S2A             | GADapFL                 | 0.23 ± 0.03                 |
| F4A             | GSDapAL                 | >100                        |
| F4T             | GSDapTL                 | >100                        |
| F4W             | GSDapWL                 | 0.3 ± 0.04                  |
| L5A             | GSDapFA                 | 11 ± 2                      |
| -----           |                         |                             |
| <i>wildtype</i> | GSDapF                  | 1.2 ± 0.1                   |
| F4A             | GSDapA                  | >100                        |
| F4G             | GSDapG                  | >100                        |

**Table 4.1. Impact on mutations within GSDapFL and GSDapF peptides on inhibitor potency against hGOAT.** IC<sub>50</sub> measurements utilized the unlabeled Dap peptides as competitive inhibitors using GSSLFC<sub>AcDan</sub> as the substrate for hGOAT acylation. Based upon the decrease in integrated fluorescence value and inhibitor concentration the IC<sub>50</sub> was calculated, as described in the experimental section. The figure is reproduced with permission from Reference 57 (Appendix V). © 2018 Elsevier Inc.

Alanine amino acid incorporation at other positions in the GSDapFL peptide was used to investigate whether the importance of the functionality at F4 is unique to that position. When S2 was changed to alanine (GADapFL) the peptide was an effective inhibitor of hGOAT with an  $IC_{50}$  within 2-fold of the GSDapFL parent, while substitution of L5 to alanine decreased inhibitor potency 78.5 fold with an  $IC_{50} = 11 \pm 2 \mu\text{M}$  compared to the parent,  $IC_{50} = 0.14 \pm 0.02 \mu\text{M}$ . These studies of alanine incorporation throughout the GSDapFL peptide further demonstrate that the F4 side chain provides a necessary recognition element for ghrelin binding by hGOAT.

#### **4.2.5 D-amino acid substitution at S3 and F4 impedes ghrelin octanoylation by hGOAT.**

To investigate the stereoselectivity of substrate recognition by hGOAT, two peptides containing a D-amino acid at either the S3 or F4 position, GS(D-S)FLC<sub>AcDan</sub> and GSS(D-F)LC<sub>AcDan</sub>, were evaluated for activity as GOAT substrates since the stereoselectivity of GOAT at or near the ghrelin acylation site had not been previously reported. In enzymatic characterization studies in the 1970s, chymotrypsin was observed to proteolyze peptide substrates bearing D-amino acids slower than ones containing L-amino acids using identical peptide sequences (Figure 4.5).<sup>42-44</sup> Using this information about the relative rate of digestion between D- and L-substrates, chymotrypsin digestion was used to confirm the presence of D-F4 in the GSSFLC<sub>AcDan</sub> peptide (Figure 4.5). Using the chymotrypsin digestion as evidence of D-amino acid incorporation, we examined both the D-S3 and D-F4 peptides for their reactivity. When measured under standard reaction conditions (1.5  $\mu\text{M}$  peptide, 500  $\mu\text{M}$  octanoyl-CoA), incorporation of a D-S3 residue at the acylation site resulted in a small (<2-fold) reduction in acylation activity relative to the analogous L-GSSFLC<sub>AcDan</sub> (Figure 4.6). However, the peptide with the D-F4 substitution exhibited a more noticeable effect with peptide substrate reactivity

exhibiting ~20% of the activity of the L-wildtype substrate. This apparent loss of peptide substrate reactivity is comparable to previously reported alanine substitution at this same position in a ghrelin-mimetic substrate peptide.<sup>29</sup> These findings reinforce the data collected so far that the F4 position is playing a crucial role in ghrelin recognition by GOAT but more surprising is that the enzyme active site will acylate a substrate containing a stereochemical inversion at the acylation site.

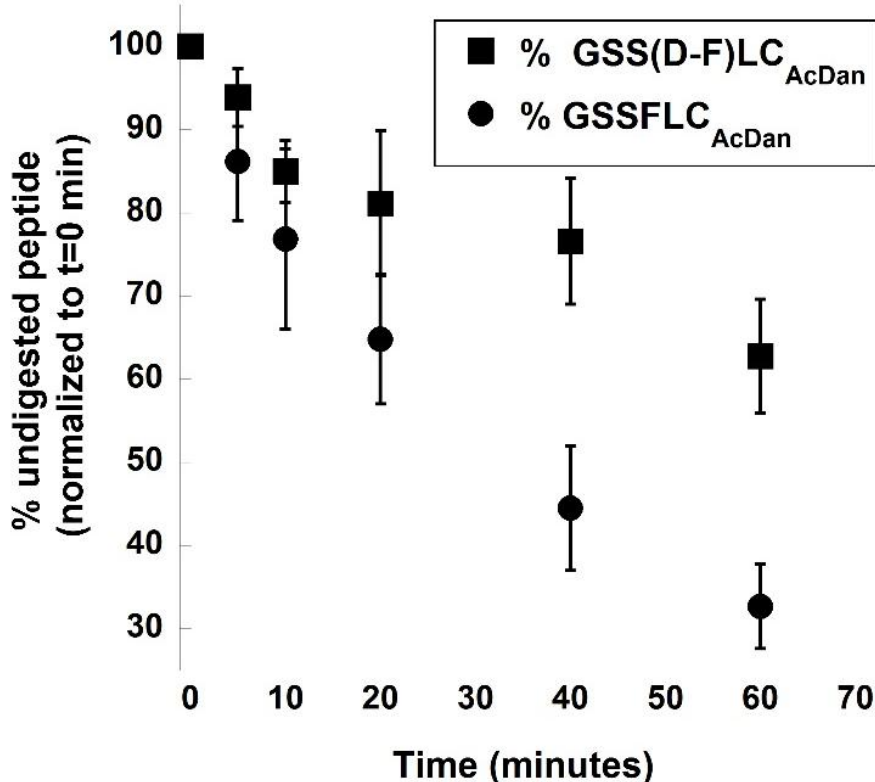


**Figure 4.5. Protection from chymotryptic digestion confirmed presence of D-phenylalanine residue in GSSFLC<sub>AcDan</sub> substrate.** GSSFLC<sub>AcDan</sub> and GSS(D-F)LC<sub>AcDan</sub> peptides were subjected to digestion by chymotrypsin. Following digestion for time points given, reactions were analyzed by HPLC to determine the amount of undigested peptide remaining. All time points are normalized to the peptide integration at the zero time point. Each data point represents the average of three independent trials, with error bars reflecting one standard deviation. The figure is reproduced with permission from Reference 57 (Appendix V). © 2018 Elsevier Inc.

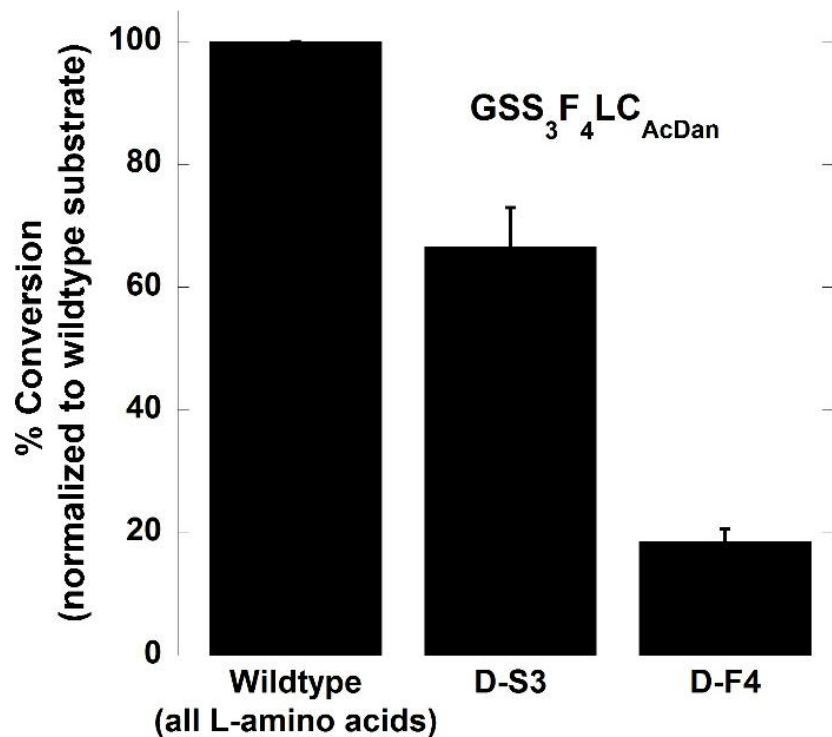


**Figure 4.6. The impact of D-amino acid substitution on peptide acylation by hGOAT.** hGOAT exhibits distinct amino acid stereoselectivity at the S3 and F4 positions. Product formation for peptide substrates with D-amino acid mutations at the S3 and F4 positions of the GSSFLC<sub>AcDan</sub> substrate peptide, shown as % peptide conversion to octanoylated product normalized to the wildtype substrate peptide containing all L-amino acids. The figure is reproduced with permission from Reference 57 (Appendix V). © 2018 Elsevier Inc.

#### 4.2.6 hGOAT tolerates backbone methylation within ghrelin peptides

In addition to amino acid side chains, the GSDapFL peptide contains the N-terminal amino group and backbone amides which could be important recognition elements for hGOAT within ghrelin. The removal of the N-terminal amine had been shown to eliminate ghrelin peptide binding and reactivity,<sup>29</sup> but the backbone amide groups had not been investigated in the same manner. To probe possible ghrelin-hGOAT interactions, the N-terminal amine of G1 and the peptide backbone amides at each position, excluding Dap3, were methylated. These methylated peptides were evaluated for their ability to inhibit hGOAT acylation of the ghrelin mimetic GSSFLC<sub>AcDan</sub> peptide substrate (Table 4.2). G1 amino group methylation with sarcosine resulted in a small improvement in binding affinity as reflected by an IC<sub>50</sub> value of  $0.088 \pm .001$   $\mu$ M, consistent with the reactivity of a peptide substrate with an N-terminal sarcosine modification in a previous study.<sup>29</sup> Backbone amide N-methylation was similarly tolerated at two of the three sites examined, methylation at F4 and L5 resulted in increased binding affinity to the enzyme compared to the non-methylated peptides by a small amount. However, N-methylation of the S2 backbone amide led to complete loss of inhibition at concentrations up to 100  $\mu$ M. The loss of enzyme binding affinity with N-methylation at the backbone amide of S2 indicated a possible binding contact between ghrelin and GOAT at this position, possibly involving a hydrogen bond involving the amide hydrogen group or binding disruption upon incorporation of the larger methyl group.

| <b>Methylation Site(s)</b> | <b>Peptide Sequence</b>                     | <b>IC<sub>50</sub> (μM)</b> |
|----------------------------|---|-----------------------------|
| <i>none</i>                | GSDapFL                                     | 0.14 ± 0.02                 |
| G1                         | SarSDapFL                                   | 0.088 ± .001                |
| S2                         | G <sub>N-Me</sub> SDapFL                    | >100                        |
| F4                         | GSDap <sub>N-Me</sub> FL                    | 0.097 ± 0.013               |
| L5                         | GSDapF <sub>N-Me</sub> L                    | 0.062 ± 0.009               |
| G1, F4                     | SarSDap <sub>N-Me</sub> F                   | 1.5 ± 0.1                   |
| G1, F4, L5                 | SarSDap <sub>N-Me</sub> F <sub>N-Me</sub> L | 6 ± 1                       |

**Table 4.2. Impact of peptide backbone methylation on Dap peptide inhibitor potency against hGOAT.** IC<sub>50</sub> measurements utilized the unlabeled Dap peptides as competitive inhibitors using GSSLFC<sub>AcDan</sub> as the substrate for hGOAT acylation. Based upon the decrease in integrated fluorescence value and inhibitor concentration the IC<sub>50</sub> was calculated, as described in the experimental section. The figure is reproduced with permission from Reference 57 (Appendix V). © 2018 Elsevier Inc.

With all of the single-site methylations except for the S2 position within the GSDapFL peptide yielding small but detectible improvements in peptide binding to hGOAT, the next approach was to investigate the impact of multiple simultaneous methylations in the sequence. Methylation at G1 (sarcosine), F4, and L5 led to the design of two methylated analogs of the GSDapF and GSDapFL peptides, SarSDap<sub>N-Me</sub>F and SarSDap<sub>N-Me</sub>F<sub>N-Me</sub>Leu (Table 4.2). Each of those methylated peptides served as hGOAT inhibitors, with the IC<sub>50</sub> value for the shorter peptide comparable to its unmethylated counterpart within 11-fold. This result indicates that the simultaneous methylations in the peptides did not prove to be additive since SarSDap<sub>N-Me</sub>F and SarSDap<sub>N-Me</sub>F<sub>N-Me</sub>Leu had IC<sub>50</sub> higher than their unmethylated parent peptides, although they are hypothetically more cell permeable than their parent peptides.<sup>45-46</sup> The cell permeability affects their potency since in order to bind to GOAT they will need to cross the cell membrane. Although, cell-based studies of GOAT inhibition suggested that these peptides do not exhibit sufficient cell permeability to target GOAT within the cell (Section 4.2.7). The SarSDap<sub>N-Me</sub>F peptide exhibited sufficient potency against hGOAT in enzyme-based studies to support further development of ghrelin-derived substrate mimetics as GOAT inhibitors.

#### **4.2.7 Cell studies into Dap-peptide permeability**

SarSDap<sub>N-Me</sub>F was chosen to pursue cell studies since it is shorter, has a smaller IC<sub>50</sub> value than the SarSDap<sub>N-Me</sub>F<sub>N-Me</sub>Leu peptide and is compliant with some of Lipinski's rules for orally available drug molecules.<sup>47-48</sup> The effect on cell viability of this peptide was determined using an Alamar blue assay<sup>49</sup> in two different human cell lines, HEK 293FT and PC3 cell lines. Both of these cell lines were modified to stably produce the cellular machinery for ghrelin acylation to occur (proghrelin and GOAT are both present). In both cases, there was no loss of cell viability observed up to 100  $\mu$ M (Figure 4.7A) using Alamar blue (described in detail,

materials and methods section 4.4.7).<sup>49</sup> Other Dap peptides described previously were also measured on PC3 cells up to 100  $\mu$ M and there was no loss of cell viability was observed (Figure 4.7B).

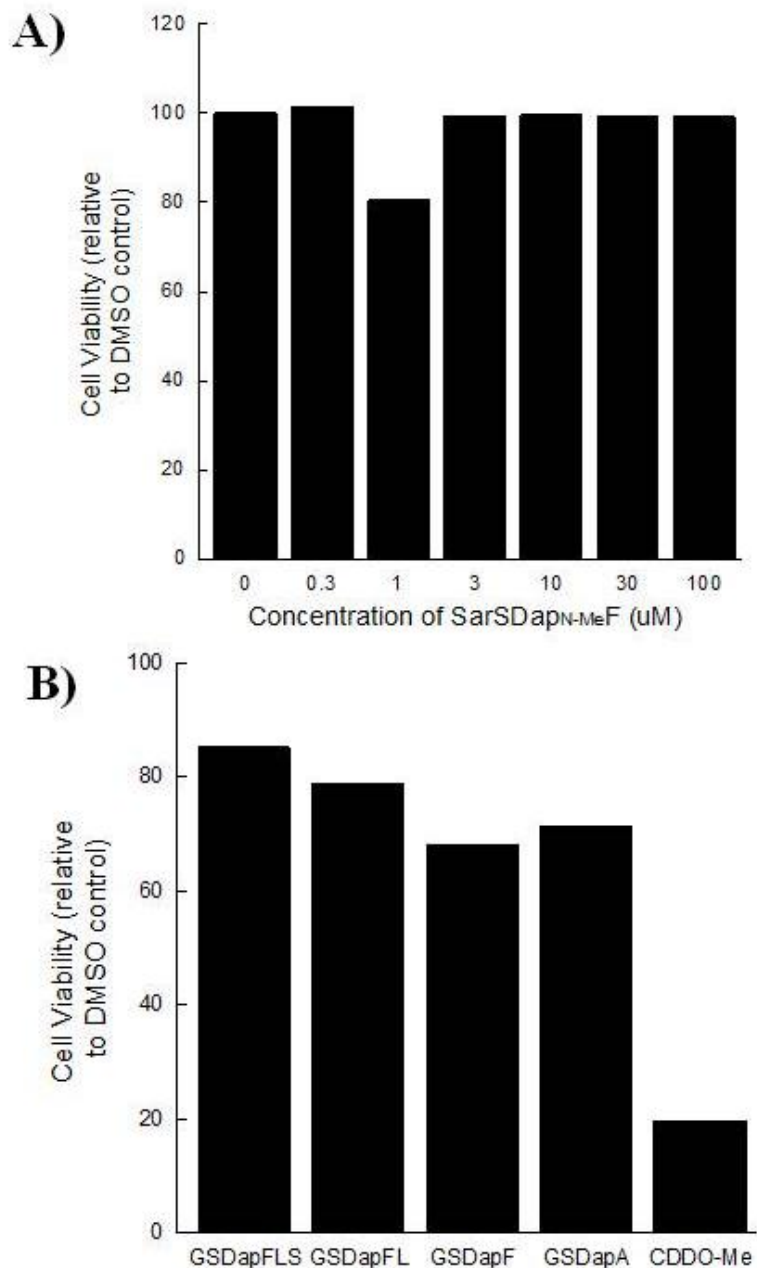


**Figure 4.7 Cell viability of Dap-incorporated peptides in PC3 or HEK 293FT cells.** Cell viability is expressed relative to the cells treated with DMSO which show no cell death at 1% v/v. A lower cell viability percentage means more cell death. **A) Cell viability of SarSDap<sub>N-MeF</sub> in HEK 293FT cells expressing mGOAT.** The inhibitor was dissolved in DMSO with 1% DMSO to total cell volume. The peptide was incubated with 10% v/v Alamar blue for 24 hours with 100 μL of 2 X 10<sup>5</sup> cells/mL to each well in a 96-well clear bottom plate. Absorbance readings at 500 and 670 nm was read for analysis. **B) Cell viability of multiple Dap-incorporated peptides in PC3 cells expressing hGOAT.** The inhibitors were dissolved in DMSO with 1% DMSO to total cell volume. The peptides were incubated with 10% v/v Alamar blue for 24 hours with 100 μL of 2 X 10<sup>5</sup> cells/mL to each well in a 96-well clear bottom plate. Absorbance at 500 and 670 nm was read for analysis. The peptides were at a concentration of 100 μM as well as the steroid CDDO-Me which is a positive control for cell death.

The lack of cytotoxicity observed for these peptides may suggest these inhibitors are incapable of permeating the cell membrane, which would block binding to and inhibiting GOAT localized in the ER membrane.<sup>50</sup> To determine whether these peptides were inhibiting GOAT within cells, an ELISA (enzyme-linked immunosorbent assay) was used to determine the production of acylated ghrelin by GOAT in HEK 293FT cells in the presence and absence of Dap-containing ghrelin mimetic peptides. Using the SarSDap<sub>N-Me</sub>F peptide inhibitor, a small decrease in acyl ghrelin was observed at 30  $\mu$ M peptide concentration. However, due to the detection limit of the ELISA antibodies and the cell line we were unable to measure total (unacylated and acylated) ghrelin levels. Consequently, we were unable to conclusively analyze the efficacy of SarSDap<sub>N-Me</sub>F inhibition of acyl ghrelin levels in the mGOAT expressing HEK 293FT cell line. Following up on unsuccessful ELISA measurements, the Dap-containing peptides were probed for their cell permeability; since the reason that there was no measurable effect on acylation was a result of low permeability. Cells were incubated with Dap-containing peptides then lysed and the lysate labeled with fluorescamine. Fluorescamine specifically labels primary amines, such as a Dap residue which is present in SarSDap<sub>N-Me</sub>F (Figure 4.8).<sup>51-52</sup> This cell lysate was then analyzed using RP-HPLC to detect the presence of Dap-containing peptides (Figure 4.9). In comparison to the control lysate (no peptide added, black trace in Figure 4.9) or the peptide alone (purple trace in Figure 4.9) there was no evidence that peptides were present in the cell lysate. The HPLC chromatograms are unclear as to the presence of the peptide in the cell due to background from cellular proteins or peptides.

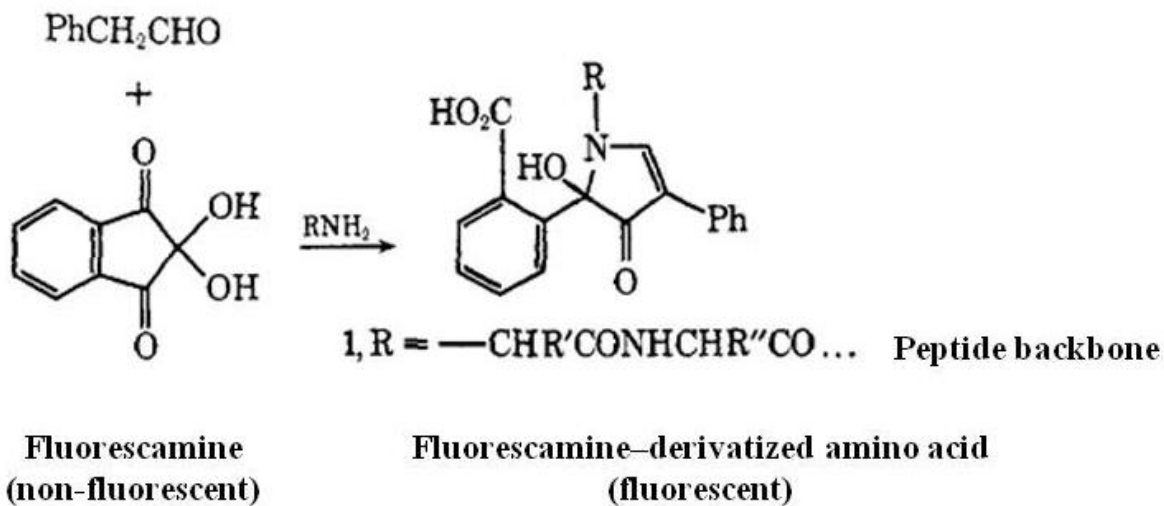


**Figure 4.8. Schematic of fluorescamine labeling.** Fluorescamine was used in cell studies to determine the cell permeability of Dap containing peptides. Initially in the absence of a primary amine, fluorescamine is non-fluorescent then is derivatized to its fluorescent counterpart. Figure is reproduced with permission from Reference 52 (Appendix VI) © 1972 American Chemical Society.

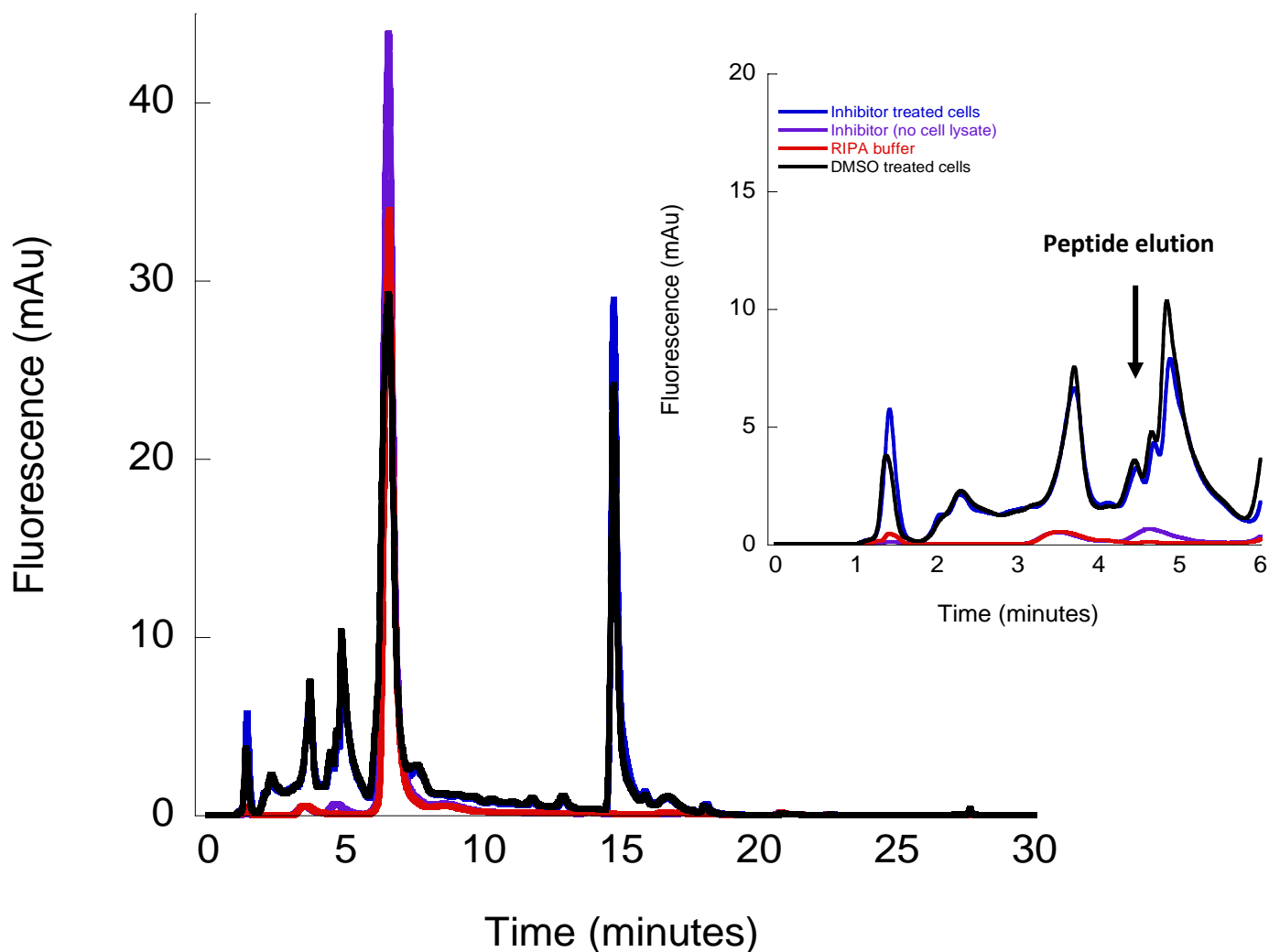


**Figure 4.9. Fluorescamine labeling of SarSDapN-MeF-treated HEK 293FT cells.** Cells treated with SarSDap<sub>N-Me</sub>Phe (dissolved in DMSO) or DMSO (vehicle) were pelleted, lysed using RIPA buffer containing a Roche protease inhibitor tablet, fluorescamine labeled, protein precipitated with ammonium sulfate, and supernatants were analyzed via RP-HPLC. Blue trace 100  $\mu$ M SarSDap<sub>N-Me</sub>Phe-treated cells, red trace RIPA buffer (buffer control), purple trace 25  $\mu$ M SarSDap<sub>N-Me</sub>Phe without cell lysate present (peptide control), black trace DMSO treated cells. The peak at 4.5 minutes is elution of fluorescamine-labeled SarSDap<sub>N-Me</sub>Phe indicated in the inset with a black arrow.

### 4.3 Conclusions

A number of N-terminal ghrelin peptides containing a Dap substitution were screened to study the binding to hGOAT and hGOAT's ability to catalyze acylation of amino groups. Incorporation of a Dap residue at S3 (the acylation site) led to a noticeable decrease in the efficiency of hGOAT-catalyzed peptide acylation and the appearance of an increased amount of non-enzymatic acylation. GSDapFLC<sub>AcDan</sub> in the presence of hGOAT and decanoyl-CoA led to two distinct products with one consistent with acylation that occurred at the serine hydroxyl group at the S2 position and the other acylation that occurred at the Dap side chain amino group. The appearance of two distinct product peaks with acylation of GSDapFLC<sub>AcDan</sub> did not occur with a substrate containing two serine residues, GSSFLC<sub>AcDan</sub>. The behavior seen with GSDapFLC<sub>AcDan</sub> suggested that the adjacent serine and Dap residues resulted in an increased non-enzymatic catalysis of side chain acylation of these amino acids. While Dap incorporated peptides with longer sequences had been used to investigate GOAT's acylation reaction as mechanistic probes,<sup>31</sup> the non-enzymatic acylation observed with the short peptides used in our experimental analysis and the overall limited reactivity reduces the ability of these Dap-based peptides as tools for investigating ghrelin acylation by GOAT.

One of the more unexpected results from these studies is that replacement of the S3 (hydroxyl) position with Dap3 (amine) significantly enhance peptide binding to hGOAT. GSDapFL and GSDapFLS peptides are the first examples of non-acylated peptide "substrate-mimetic" inhibitors of hGOAT with sub-micromolar IC<sub>50</sub> values. It is clear that the incorporation of Dap in ghrelin mimetic peptides enhanced binding to hGOAT; however, the exact chemical interactions/mechanism occurring which led to this result is unknown. There is a possibility that the amine side chain is involved in an electrostatic or hydrogen-bond within the hGOAT active

site. If these chemical interactions are occurring we can look to serine proteases or hydrolases as examples for acylation of S3 in GSSFLC<sub>AcDan</sub> by hGOAT, in which, the serine hydroxyl acts as a nucleophile in a transition-state interaction. When an amine is present such as in GSDapFL, the transition-state interaction mentioned above is converted to a ground-state interaction which could greatly contribute to the increase in binding to GOAT.<sup>53-55</sup> Regardless of the molecular basis for the binding to GOAT seen with Dap-incorporated peptides, these small ghrelin mimetics provide a scaffold which can be easily modified in order to study ghrelin binding and the necessary recognition elements by GOAT. Structure-activity relationship of Dap-incorporated peptides binding to GOAT described has led to the identification of critical aspects of a pharmacophore which defines a new class of GOAT inhibitors (Figure 4.10). There were key findings regarding ghrelin recognition elements by GOAT like the importance of the N-terminal amino group and the finding that the minimum length for the peptide is a four amino acid, “GSSF”, sequence for binding to GOAT.<sup>10, 28-30</sup> Methylation at G1’s N-terminal amine, sarcosine, shown in this study and others to be tolerated in both activity- and inhibition-based studies, these studies also provided evidence that GOAT is tolerant of backbone amide methylation at multiple distinct sites within the ghrelin peptide scaffold. This does not necessarily mean they acted in an additive manner since peptides containing methylations at multiple positions led to a decreased IC<sub>50</sub> values. Methylation of peptides has been shown to improve peptide stability and cell permeability,<sup>45-46, 56</sup> so determining GOAT’s tolerance for peptide methylation provides a possible new avenue to increase activity in biological systems. There was also another important finding in which there was a distinction between the binding-based studies described throughout this chapter and the previously published activity-based studies into ghrelin’s recognition by GOAT,<sup>28-29</sup> since substitution or deletion at the F4 position

lead to a loss of binding. This indicated that the F4 position is central for ghrelin binding to hGOAT which was not identified using activity-based screenings. One such example that shows this discrepancy is GOAT's tolerance for alanine mutations at this site in GOAT activity-based acylation assays.<sup>10,29</sup> The result observed with the importance of F4 for ghrelin binding in this study may be reflected in ghrelin species conservation since phenylalanine is highly conserved at the fourth position within ghrelin sequences across vertebrates (99.5% identity, 100% similar)<sup>57</sup> (Figure 4.11). These studies have completed the characterization of elements needed for GOAT recognition within the N-terminal ghrelin sequence, and the avenue is to study the downstream elements in ghrelin and proghrelin which might play a role in the interaction of ghrelin and GOAT leading to acylation of ghrelin at S3.<sup>29,31</sup>

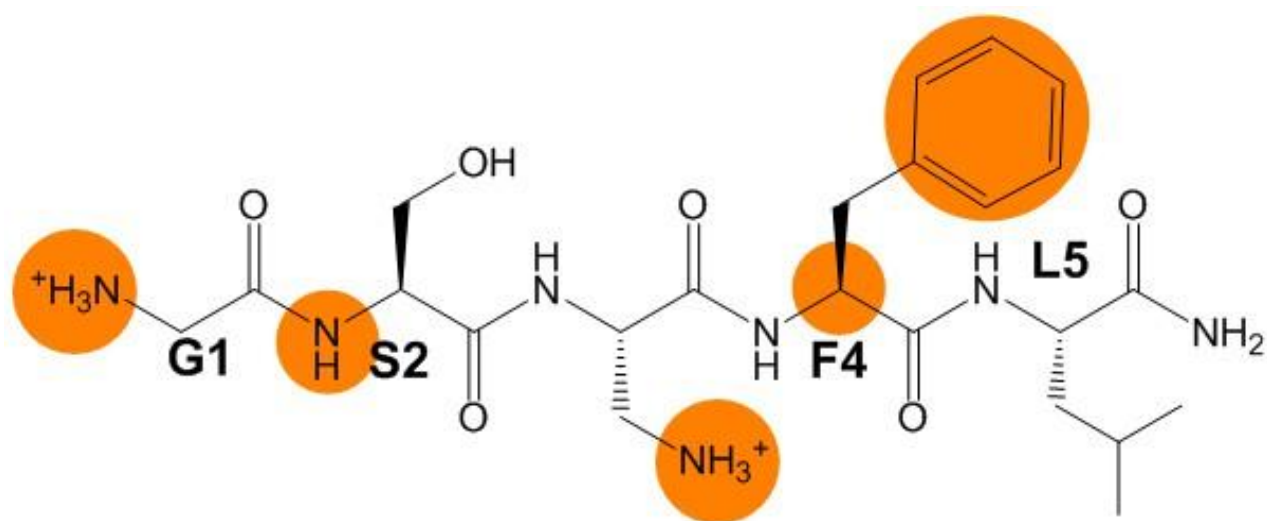


**Figure 4.10. Functional groups composing the pharmacophore for GOAT substrate-mimetic inhibitors, as defined by Dap-containing peptide inhibitor structure-activity analysis.** Chemical groups implicated in ghrelin binding to GOAT are highlighted in orange. The figure is reproduced with permission from Reference 57 (Appendix V). © 2018 Elsevier Inc.

| BAA89371.1 Homo sapiens, Human proghrelin                     | G1    | S2   | S3    | F4           | L5   |
|---|-------|------|-------|--------------|------|
| Result from alignment analysis across 185 vertebrate species: |       |      |       |              |      |
| <b>% Conserved</b>  | 100.0 | 89.7 | 98.4  | <b>99.5</b>  | 99.5 |
| <b>% Similar</b>  | n/a   | 97.8 | 100.0 | <b>100.0</b> | 99.5 |

**Figure 4.11. Conservation analysis indicates the F4 position is conserved.** The first five amino acids of all known ghrelin sequences, 185, across vertebrate classes were aligned and their % similarity and % conservation were calculated using Clustal W protein sequence alignment. The figure is adapted with permission from Reference 57 (Appendix V). © 2018 Elsevier Inc.

The potency of the Dap-incorporated peptides provides a way to target the ghrelin/GOAT/GHS-R1a endocrine signaling pathway. As previously mentioned, the small peptides evaluated during the studies in this chapter constitute a new class of inhibitors since all of the previously characterized ghrelin-mimetic GOAT inhibitors have contained either an acyl or acyl-mimetic group at the third position.<sup>9-10, 29, 34, 58</sup> Since the acyl group is a major recognition element for the GHS-R1a receptor, there is a high probability that there will be unintended interaction of acylated ghrelin mimetics with the GHS-R1a receptor.<sup>20</sup> This cross-reactivity is less likely to be an issue with a peptide like GSDapFL which does not contain a hydrophobic moiety at the Dap residue. The GSDapFL-based peptides should not have the same receptor activation issues that other product mimetic peptides have had, but the commonality between them is that there are problems with cell permeability.<sup>10, 34</sup> There have been two recent reports indicating that GOAT exists exposed in the plasma membrane of cells instead of the canonical ER; the first study used mouse tibial bone marrow adipocytes and the second used mouse and rat hippocampal neurons.<sup>59-60</sup> It is possible that Dap-containing ghrelin mimetic peptides could be potentially used as imaging agents to detect extracellular-facing GOAT without the possibility of GHS-R1a receptor labeling.<sup>59-60</sup> This hypothesis is supported by the fluorescamine-labeling data in this chapter indicating that Dap-containing peptides are not cell permeable or at least not detectable in cell lysate. Another important finding from this work is the tolerance of GOAT for D-amino acids and backbone amide methylations in distinct positions, which could increase the biostability of these molecules against proteolytic degradation in the bloodstream.<sup>45, 61</sup>

The issues seen with the low cell permeability of the ghrelin mimetic Dap-incorporated peptides is one of the most omnipresent challenges with peptide-based GOAT inhibitors. There have been attempts to increase cell permeability using cell-penetrating sequences since none

have been successful in the absence of such a motif.<sup>34, 41</sup> However, there are other approaches such as using established peptidomimetic medicinal chemistry.<sup>45, 56, 61</sup> Substrate-mimetic peptides are powerful new candidates for a scaffold to develop the next generation of GOAT inhibitors, since they increased the specificity of binding to GOAT and are targets for attachment of covalent warheads to target essential residues necessary for GOAT function.<sup>7</sup> We have designed an unnatural amino acid incorporated peptide scaffold which is useful to establish the binding and necessary recognition elements within GOAT's active site which can be used for rational inhibitor design targeting this intriguing and therapeutically unexploited system.

## 4.4 Materials and Methods

**4.4.1 General methods.** All data were plotted and analyzed using Kaleidagraph (Synergy Software, Reading, PA, USA). Octanoyl and decanoyl coenzyme A (octanoyl-CoA and decanoyl-CoA) were solubilized at a concentration of 5 mM in 10 mM Tris-HCl (pH 7.0), aliquoted into low-adhesion microcentrifuge tubes, and stored at -80 °C. Methyl arachidonyl fluorophosphonate (MAFP) was purchased from Cayman Chemical (Ann Arbor, MI) as a stock in methyl acetate and diluted into DMSO prior to use. Acrylodan (Anaspec) was solubilized in acetonitrile, with the stock concentration determined by absorbance at 393 nm on dilution into methanol ( $\epsilon = 18,483 \text{ M}^{-1} \text{ cm}^{-1}$  per manufacturer's data sheet). Dap-containing peptides were purchased from Pepmic (Suzhou, China) with >90% purity verified by reverse phase high-pressure liquid chromatography (HPLC) and peptide mass confirmed by matrix-assisted laser desorption/ionization time-of-flight (MALDI-TOF) mass spectrometry (Table 4.3).

| Peptide sequence                            | Purity (%) | Calculated mass for (M+H) <sup>+</sup> | Observed mass for (M+H) <sup>+</sup> |
|---|------------|--|--------------------------------------|
| GSDapFLS                                    | 98%        | 594.93                                 | 595.35                               |
| GSDapFL                                     | 99%        | 507.96                                 | 508.55                               |
| GSDapWL                                     | 98%        | 546.88                                 | 547.35                               |
| GSDapTL                                     | 98%        | 461.78                                 | 462.30                               |
| GSDapAL                                     | 98%        | 431.75                                 | 432.25                               |
| GSDapFA                                     | 98%        | 465.77                                 | 466.25                               |
| GADapFL                                     | 98%        | 491.85                                 | 492.30                               |
| GSDapF                                      | 98%        | 394.80                                 | 395.35                               |
| GSDapA                                      | 99%        | 317.70                                 | 319.35                               |
| GSDapG                                      | 99%        | 303.67                                 | 305.30                               |
| GSDap                                       | 96%        | 247.62                                 | 248.20                               |
| SDapFL                                      | 99%        | 449.90                                 | 451.40                               |
| [Ac]SDapFL                                  | 97%        | 492.83                                 | 493.30                               |
| SarSDapFL                                   | 98%        | 522.09                                 | 522.35                               |
| G <sub>N-Me</sub> SDapFL                    | 97%        | 521.85                                 | 522.35                               |
| GSDapF <sub>N-Me</sub> L                    | 97%        | 521.85                                 | 522.35                               |
| GSDap <sub>N-Me</sub> FL                    | 96%        | 521.85                                 | 522.35                               |
| SarSDap <sub>N-Me</sub> F <sub>N-Me</sub> L | 96%        | 550.09                                 | 550.40                               |
| SarSDap <sub>N-Me</sub> F                   | 95%        | 422.94                                 | 423.30                               |

**Table 4.3 Analytical data of Dap-containing peptides.** Peptides were analyzed by RP-HPLC and MALDI-TOF mass spectrometry, percent purity and m/z values were provided by Pepmic (Suzhou, China). The figure is reproduced with permission from Reference 57 (Appendix V). © 2018 Elsevier Inc.

The GSSFLC<sub>NH2</sub> peptide for fluorescent labeling with acrylodan was synthesized by Sigma–Genosys (The Woodlands, TX, USA) in the Pepscreen format. Peptides containing D-amino acids were synthesized by BioBasic (Amherst, NY), with the presence of D-phenylalanine in the GSS<sup>62</sup>LC<sub>AcDan</sub> peptide verified by chymotryptic digestion as described below. Peptides were solubilized in a 1:1 mixture of water and acetonitrile and stored at -80 °C. Concentrations for peptides containing cysteine residues, such as GSSLFC and GSDapFLC, were determined spectrophotometrically at 412 nm by reaction of the cysteine thiol with 5,5'-dithiobis(2-nitrobenzoic acid) using  $\epsilon_{412} = 14,150 \text{ M}^{-1} \text{ cm}^{-1}$ .<sup>63</sup> Concentrations for peptides containing Dap residues were determined using fluorescamine labeling and fluorescence relative to a GSDapFLC peptide external standard with correction for the numbers of primary amine groups.<sup>64-65</sup>

**4.4.2 Peptide fluorescent labeling.** Peptide substrates with C-terminal cysteine residue sidechains were labeled with an acrylodan fluorophore and HPLC purified per our previously reported protocol.<sup>28-29</sup> Acrylodan labeling was verified by MALDI–TOF mass spectrometry (Table 4.4) and acrylodan labeled peptide concentrations were determined by UV absorbance measurement at 360 nm.<sup>66</sup>

| Sequence                    | Calculated exact mass<br>(Daltons) | Experimental mass<br>(Daltons) |
|-----------------------------|------------------------------------|--------------------------------|
| GSSFLC <sub>Acдан</sub>     | 837.40 (M+H)                       | 875.153 (M+K)                  |
| GSDapFLC <sub>Acдан</sub>   | 836.41 (M+H)                       | 874.417 (M+K)                  |
| GS(D-S)FLC <sub>Acдан</sub> | 837.40 (M+H)                       | 877.022 (M+ K)                 |
| GSS(D-F)LC <sub>Acдан</sub> | 837.40 (M+H)                       | 877.035 (M+ K)                 |

**Table 4.4. MALDI-TOF mass spectrometry (m/z) characterization of acrylodan labeled hGOAT peptide substrates.** The figure is reproduced with permission from Reference 57 (Appendix V). © 2018 Elsevier Inc.

**4.4.3 hGOAT activity assays.** Assays were performed using previously reported protocols.<sup>7, 29</sup> For each assay, membrane fraction from Sf9 cells expressing hGOAT was thawed on ice and homogenized by passage through an 18-gauge needle 10 times. Assays were performed with ~10-50 µg of membrane protein, as determined by Bradford assay. Unless noted otherwise, membrane fraction was preincubated with 1 µM methyl arachidonyl fluorophosphate (MAFP) and inhibitor or vehicle as indicated in 50 mM HEPES pH 7.0 for 30 min at room temperature prior to reaction initiation.<sup>7, 36</sup> All reactions were initiated by the addition of fluorescently-labeled GSSFLC<sub>AcDan</sub> or GSDapFLC<sub>AcDan</sub> peptide substrate and acyl-CoA donor. Assays comparing the reactivity of the GSDapFLC<sub>AcDan</sub> to GSSFLC<sub>AcDan</sub> were initiated with 5 µM GSDapFLC<sub>AcDan</sub> or 1.5 µM GSSFLC<sub>AcDan</sub> and 1mM decanoyl-CoA in a total volume of 50 µL, followed by incubation at room temperature under foil for 3 hr. Assays investigating inhibition by unlabeled ghrelin-mimetic peptides Dap peptide were pretreated with the inhibitor for 30 min, followed by reaction initiation with the addition of 1.5 µM GSSFLC<sub>AcDan</sub> and 500µM octanoyl-CoA. Reactions were incubated for 3 hr at room temperature under foil. Reactions investigating the reactivity of ghrelin-mimetic peptides incorporating D-amino acids were performed in a similar manner with acrylodan-labeled D-amino acid containing substrate peptide in place of the GSSFLC<sub>AcDan</sub> peptide. All assays were stopped with the addition of 50 µL of 20% acetic acid in isopropanol, and solutions were clarified by protein precipitation with 16.7 µL of 20% trichloroacetic acid, followed by centrifugation (1,000 x g, 1 min). The supernatant was then analyzed using reverse-phase HPLC with fluorescence detection as previously described.<sup>7, 29</sup> Peak integrations for both substrate and product peaks were calculated using Chemstation for LC (Agilent Technologies). Data reported is the average of three independent determinations, with error bars representing one standard deviation.

**4.4.4 IC<sub>50</sub> determination.** For determination of IC<sub>50</sub> values, reactions were performed and analyzed as described in the presence of either inhibitor or vehicle as appropriate. The percent activity at each inhibitor concentration was calculated from HPLC integration data using equations 1 and 2: To determine an IC<sub>50</sub> value for a given inhibitor, the plot of % activity versus [inhibitor] was fit to equation 3, with % activity<sub>0</sub> denoting hGOAT activity in the presence of the vehicle alone. All reported IC<sub>50</sub> values represent the average of a minimum of three independent trials.

$$(1) \text{ \% activity} = \frac{\text{\% peptide acylation in presence of inhibitor}}{\text{\% peptide acylation in absence of inhibitor}}$$

$$(2) \text{ \% peptide octanoylation} = \frac{\text{Fluorescence of acylated peptide}}{\text{Total peptide fluorescence (acylated and non-acylated)}}$$

$$(3) \text{ \% activity} = \text{\% activity}_0 * \left( 1 - \frac{[\text{inhibitor}]}{[\text{inhibitor}] + \text{IC}_{50}} \right)$$

**4.4.5 Verification of D-F in GSS(D-F)LC<sub>AcDan</sub> by chymotryptic digestion.** To verify the presence of D-phenylalanine in the acrylodan labeled GSS(D-F)LC<sub>AcDan</sub> peptide, the peptide was subjected to digestion by chymotrypsin in parallel with the wildtype GSSFLC<sub>AcDan</sub> peptide substrate peptide. Chymotrypsin exhibits stereoselectivity for L-phenylalanine,<sup>42-44</sup> with incorporation of D-phenylalanine providing protection against chymotryptic cleavage. Chymotrypsin digestions (300 uL) contained: 3 μM peptide (GSSFLC<sub>AcDan</sub> or GSS(D-F)LC<sub>AcDan</sub>), 0.1 nM chymotrypsin, 10 mM CaCl<sub>2</sub>, 100 mM Tris, pH 7.8. Reactions were initiated by the addition of chymotrypsin and incubated at 37 °C under foil. Time points were taken at 0, 5, 10,

20, 40, and 60 min elapsed reaction time, with reactions stopped by the addition of 50  $\mu$ L 12 M HCl. Digestions were analyzed by reverse-phase HPLC using fluorescence detection.<sup>28</sup> Peak integrations for the undigested peptides were calculated using Chemstation for LC (Agilent Technologies) and plotted versus reaction time.

**4.4.6 Fluorescamine labeling of cell lysates.** A standard curve of SarSDap<sub>N-Me</sub>F in the presence of HEK 293FT: 50  $\mu$ L total reactions contained: 5  $\mu$ L SarSDap<sub>N-Me</sub>F at (50  $\mu$ M, 25  $\mu$ M, 12.5  $\mu$ M, 6.25  $\mu$ M, 3.125  $\mu$ M, 1.5  $\mu$ M, 0.75  $\mu$ M and 0  $\mu$ M peptide), 10  $\mu$ L HEK 293FT cell lysate ((3 wells of  $2 \times 10^5$  cells/well in a 24-well plate were combined), cells were plated in DMEM ((Dulbecco's Modified Eagle's Medium, Corning) containing 10% FBS, 1% v/v penicillin/streptomycin), and PBS containing 9 mg/mL fluorescamine. Reactions proceeded for 15 min then cellular proteins were precipitated with 0.75 M ammonium sulfate and supernatants were analyzed via RP-HPLC.

For inhibitor addition to cell lysate: 3, 6-wells per condition of HEK 293FT cells were plated at  $2 \times 10^5$  cells/well (plated in DMEM containing 10% FBS, 1% v/v penicillin/streptomycin) in a 24-well plate and incubated 18 hr at 37 °C 5% CO<sub>2</sub>. SarSDap<sub>N-Me</sub>F was dissolved in DMSO, inhibitor (100  $\mu$ M) or a null (DMSO) was added to wells to 1% total cell volume and incubated 18 hr at 37 °C 5% CO<sub>2</sub>. After incubation cell media was aspirated and cells were trypsinized washed with PBS and lysed using RIPA buffer (50 mM Tris-HCl, pH 7.4, 150 mM NaCl, 2 mM EDTA, 10% v/v NP40, 0.1% v/v SDS ) containing a mini Roche tablet (Sigma). Fluorescamine labeling reactions: 50  $\mu$ L of cell lysate (inhibitor or DMSO treated cells) containing 9mg/mL fluorescamine proceeded for 15 min, cellular proteins were precipitated with addition of 0.75 M ammonium sulfate and supernatants were analyzed via RP-HPLC with Excitation = 365 nm, Emission = 470 nm.<sup>52</sup>

**4.4.7 Alamar blue assay.** Detection of metabolic activity since the dye is an oxidation–reduction indicator. Cellular metabolism, the mitochondria, induces reduction of Alamar Blue the effect of the conditions (inhibitor) can be quantified based on the conversion of the blue, non-fluorescent resazurin to pink, fluorescent resorufin by metabolically active cells. HEK 293FT (F11) or PC3 (hPPG #1) cells were plated using 100  $\mu$ L of  $2 \times 10^5$  cells/mL in a clear bottom 96-well microplate (Thermo scientific) containing 100  $\mu$ L of DMEM ((Dulbecco's Modified Eagle's Medium, Corning, DMEM F-12 media was used for PC3 cells, Corning) containing 10% FBS, 1% v/v penicillin/streptomycin). 0.01% puromycin v/v was added to HEK 293FT cells, 0.3% G418 (Thermo fischer) v/v was added to PC3 cells. Dap-incorporated peptides were then added to each well with 1% DMSO v/v at corresponding concentration based upon desired range (3-wells per condition). Cells were incubated for 18 hr at 37  $^{\circ}$ C 5% CO<sub>2</sub> in the presence of the peptides, 10% v/v Alamar blue (Thermo fischer) was added to each well, excluding control wells and absorbance readings at 540, 5470, 600, and 630 nm were taken at 0, 18, 24, 36, and 48 hr. The average of 3-wells per condition was taken for 570 and 600 nm. The % cell viability was calculated in relationship to the DMSO-treated cells containing no peptide (Equation 4). The cells were also inspected visually for morphology and cell health.

$$(4) \quad \left( \frac{\text{X condition Average absorbance (570 nm)} - \text{X condition Average absorbance (600 nm)}}{\text{(DMSO average absorbance (570 nm)} - \text{DMSO average absorbance (600 nm)}} \right) * 100\%$$

## 4.5 References

1. Gutierrez, J. A.; Solenberg, P. J.; Perkins, D. R.; Willency, J. A.; Knierman, M. D.; Jin, Z.; Witcher, D. R.; Luo, S.; Onyia, J. E.; Hale, J. E., Ghrelin octanoylation mediated by an orphan lipid transferase. *Proc Natl Acad Sci U S A* **2008**, *105* (17), 6320-5.
2. Yang, J.; Brown, M. S.; Liang, G.; Grishin, N. V.; Goldstein, J. L., Identification of the acyltransferase that octanoylates ghrelin, an appetite-stimulating peptide hormone. *Cell* **2008**, *132* (3), 387-96.
3. Hofmann, K., A superfamily of membrane-bound O-acyltransferases with implications for wnt signaling. *Trends Biochem Sci* **2000**, *25* (3), 111-2.
4. Chang, S. C.; Magee, A. I., Acyltransferases for secreted signalling proteins (Review). *Mol Membr Biol* **2009**, *26* (1), 104-13.
5. Resh, M. D., Fatty acylation of proteins: The long and the short of it. *Prog Lipid Res* **2016**, *63*, 120-31.
6. Masumoto, N.; Lanyon-Hogg, T.; Rodgers, U. R.; Konitsiotis, A. D.; Magee, A. I.; Tate, E. W., Membrane bound O-acyltransferases and their inhibitors. *Biochem Soc Trans* **2015**, *43* (2), 246-52.
7. McGovern-Gooch, K. R.; Mahajani, N. S.; Garagozzo, A.; Schramm, A. J.; Hannah, L. G.; Sieburg, M. A.; Chisholm, J. D.; Houglund, J. L., Synthetic Triterpenoid Inhibition of Human Ghrelin O-Acyltransferase: The Involvement of a Functionally Required Cysteine Provides Mechanistic Insight into Ghrelin Acylation. *Biochemistry* **2017**, *56* (7), 919-931.
8. De Vriese, C.; Gregoire, F.; Lema-Kisoka, R.; Waelbroeck, M.; Robberecht, P.; Delporte, C., Ghrelin degradation by serum and tissue homogenates: identification of the cleavage sites. *Endocrinology* **2004**, *145* (11), 4997-5005.

9. Zhao, F.; Darling, J. E.; Gibbs, R. A.; Hougland, J. L., A new class of ghrelin O-acyltransferase inhibitors incorporating triazole-linked lipid mimetic groups. *Bioorg Med Chem Lett* **2015**, *25* (14), 2800-3.
10. Yang, J.; Zhao, T. J.; Goldstein, J. L.; Brown, M. S., Inhibition of ghrelin O-acyltransferase (GOAT) by octanoylated pentapeptides. *Proc Natl Acad Sci U S A* **2008**, *105* (31), 10750-5.
11. Yoneyama-Hirozane, M.; Deguchi, K.; Hirakawa, T.; Ishii, T.; Odani, T.; Matsui, J.; Nakano, Y.; Imahashi, K.; Takakura, N.; Chisaki, I.; Takekawa, S.; Sakamoto, J., Identification and Characterization of a New Series of Ghrelin O-Acyl Transferase Inhibitors. *SLAS Discov* **2017**, 2472555217727097.
12. Rodgers, U. R.; Lanyon-Hogg, T.; Masumoto, N.; Ritzefeld, M.; Burke, R.; Blagg, J.; Magee, A. I.; Tate, E. W., Characterization of Hedgehog Acyltransferase Inhibitors Identifies a Small Molecule Probe for Hedgehog Signaling by Cancer Cells. *ACS Chem Biol* **2016**, *11* (12), 3256-3262.
13. Petrova, E.; Rios-Esteves, J.; Ouerfelli, O.; Glickman, J. F.; Resh, M. D., Inhibitors of Hedgehog acyltransferase block Sonic Hedgehog signaling. *Nat Chem Biol* **2013**, *9* (4), 247-9.
14. Ho, S. Y.; Alam, J.; Jeyaraj, D. A.; Wang, W.; Lin, G. R.; Ang, S. H.; Tan, E. S. W.; Lee, M. A.; Ke, Z.; Madan, B.; Virshup, D. M.; Ding, L. J.; Manoharan, V.; Chew, Y. S.; Low, C. B.; Pendharkar, V.; Sangthongpitag, K.; Hill, J.; Keller, T. H.; Poulsen, A., Scaffold Hopping and Optimization of Maleimide Based Porcupine Inhibitors. *J Med Chem* **2017**, *60* (15), 6678-6692.
15. You, L.; Zhang, C.; Yarravarapu, N.; Morlock, L.; Wang, X.; Zhang, L.; Williams, N. S.; Lum, L.; Chen, C., Development of a triazole class of highly potent Porcn inhibitors. *Bioorg Med Chem Lett* **2016**, *26* (24), 5891-5895.

16. Asciola, J. J.; Miele, M. M.; Hendrickson, R. C.; Resh, M. D., An in vitro fatty acylation assay reveals a mechanism for Wnt recognition by the acyltransferase Porcupine. *J Biol Chem* **2017**, *292* (33), 13507-13513.
17. Celi, F.; Bini, V.; Papi, F.; Santilli, E.; Ferretti, A.; Mencacci, M.; Berioli, M. G.; De Giorgi, G.; Falorni, A., Circulating acylated and total ghrelin and galanin in children with insulin-treated type 1 diabetes: relationship to insulin therapy, metabolic control and pubertal development. *Clin Endocrinol (Oxf)* **2005**, *63* (2), 139-45.
18. Poykko, S. M.; Kellokoski, E.; Horkko, S.; Kauma, H.; Kesaniemi, Y. A.; Ukkola, O., Low plasma ghrelin is associated with insulin resistance, hypertension, and the prevalence of type 2 diabetes. *Diabetes* **2003**, *52* (10), 2546-53.
19. Francois, M.; Barde, S.; Legrand, R.; Lucas, N.; Azhar, S.; El Dhaybi, M.; Guerin, C.; Hokfelt, T.; Dechelotte, P.; Coeffier, M.; Fetissof, S. O., High-fat diet increases ghrelin-expressing cells in stomach, contributing to obesity. *Nutrition* **2016**, *32* (6), 709-15.
20. Bednarek, M. A.; Feighner, S. D.; Pong, S. S.; McKee, K. K.; Hreniuk, D. L.; Silva, M. V.; Warren, V. A.; Howard, A. D.; Van Der Ploeg, L. H.; Heck, J. V., Structure-function studies on the new growth hormone-releasing peptide, ghrelin: minimal sequence of ghrelin necessary for activation of growth hormone secretagogue receptor 1a. *J Med Chem* **2000**, *43* (23), 4370-6.
21. Lim, C. T.; Kola, B.; Korbonits, M., The ghrelin/GOAT/GHS-R system and energy metabolism. *Rev Endocr Metab Disord* **2011**, *12* (3), 173-86.
22. Lim, C. T.; Kola, B.; Korbonits, M.; Grossman, A. B., Ghrelin's role as a major regulator of appetite and its other functions in neuroendocrinology. *Prog Brain Res* **2010**, *182*, 189-205.
23. Mear, Y.; Enjalbert, A.; Thirion, S., GHS-R1a constitutive activity and its physiological relevance. *Front Neurosci* **2013**, *7*, 87.

24. Gonzalez-Rey, E.; Chorny, A.; Delgado, M., Therapeutic action of ghrelin in a mouse model of colitis. *Gastroenterology* **2006**, *130* (6), 1707-20.
25. Leite-Moreira, A. F.; Soares, J. B., Physiological, pathological and potential therapeutic roles of ghrelin. *Drug Discov Today* **2007**, *12* (7-8), 276-88.
26. Romero, A.; Kirchner, H.; Heppner, K.; Pfluger, P. T.; Tschop, M. H.; Nogueiras, R., GOAT: the master switch for the ghrelin system? *Eur J Endocrinol* **2010**, *163* (1), 1-8.
27. Root, A. W.; Root, M. J., Clinical pharmacology of human growth hormone and its secretagogues. *Curr Drug Targets Immune Endocr Metabol Disord* **2002**, *2* (1), 27-52.
28. Darling, J. E.; Prybolsky, E. P.; Sieburg, M.; Hougland, J. L., A fluorescent peptide substrate facilitates investigation of ghrelin recognition and acylation by ghrelin O-acyltransferase. *Anal Biochem* **2013**, *437* (1), 68-76.
29. Darling, J. E.; Zhao, F.; Loftus, R. J.; Patton, L. M.; Gibbs, R. A.; Hougland, J. L., Structure-activity analysis of human ghrelin O-acyltransferase reveals chemical determinants of ghrelin selectivity and acyl group recognition. *Biochemistry* **2015**, *54* (4), 1100-10.
30. Ohgusu, H.; Shirouzu, K.; Nakamura, Y.; Nakashima, Y.; Ida, T.; Sato, T.; Kojima, M., Ghrelin O-acyltransferase (GOAT) has a preference for n-hexanoyl-CoA over n-octanoyl-CoA as an acyl donor. *Biochem Biophys Res Commun* **2009**, *386* (1), 153-8.
31. Taylor, M. S.; Dempsey, D. R.; Hwang, Y.; Chen, Z.; Chu, N.; Boeke, J. D.; Cole, P. A., Mechanistic analysis of ghrelin-O-acyltransferase using substrate analogs. *Bioorg Chem* **2015**, *62*, 64-73.
32. Taylor, M. S.; Hwang, Y.; Hsiao, P. Y.; Boeke, J. D.; Cole, P. A., Ghrelin O-acyltransferase assays and inhibition. *Methods Enzymol* **2012**, *514*, 205-28.

33. Garner, A. L.; Janda, K. D., cat-ELCCA: a robust method to monitor the fatty acid acyltransferase activity of ghrelin O-acyltransferase (GOAT). *Angew Chem Int Ed Engl* **2010**, *49* (50), 9630-4.
34. Barnett, B. P.; Hwang, Y.; Taylor, M. S.; Kirchner, H.; Pfluger, P. T.; Bernard, V.; Lin, Y. Y.; Bowers, E. M.; Mukherjee, C.; Song, W. J.; Longo, P. A.; Leahy, D. J.; Hussain, M. A.; Tschop, M. H.; Boeke, J. D.; Cole, P. A., Glucose and weight control in mice with a designed ghrelin O-acyltransferase inhibitor. *Science* **2010**, *330* (6011), 1689-92.
35. Saha, P. K.; Reddy, V. T.; Konopleva, M.; Andreeff, M.; Chan, L., Antidiabetic Effect and Mode of Action of the Triterpenoid, CDDO-Me, in Diet-Induced Type 2 Diabetic Mice and Lepr(db/db) Mice. *Diabetes* **2010**, *59*, A372-A372.
36. McGovern-Gooch, K. R.; Rodrigues, T.; Darling, J. E.; Sieburg, M. A.; Abizaid, A.; Houglund, J. L., Ghrelin Octanoylation Is Completely Stabilized in Biological Samples by Alkyl Fluorophosphonates. *Endocrinology* **2016**, *157* (11), 4330-4338.
37. Kojima, M.; Hosoda, H.; Date, Y.; Nakazato, M.; Matsuo, H.; Kangawa, K., Ghrelin is a growth-hormone-releasing acylated peptide from stomach. *Nature* **1999**, *402* (6762), 656-60.
38. McGovern, K. R. Enzymology And Inhibition Of Ghrelin Acylation By Ghrelin O-Acyltransferase. Dissertation, Syracuse University, Syracuse University, 2017.
39. Lan, Y.; Langlet-Bertin, B.; Abbate, V.; Vermeer, L. S.; Kong, X.; Sullivan, K. E.; Leborgne, C.; Scherman, D.; Hider, R. C.; Drake, A. F.; Bansal, S. S.; Kichler, A.; Mason, A. J., Incorporation of 2,3-diaminopropionic acid into linear cationic amphipathic peptides produces pH-sensitive vectors. *ChemBiochem* **2010**, *11* (9), 1266-72.
40. Smith, B. C.; Denu, J. M., Chemical mechanisms of histone lysine and arginine modifications. *Biochim Biophys Acta* **2009**, *1789* (1), 45-57.

41. Wellman, M. K.; Patterson, Z. R.; MacKay, H.; Darling, J. E.; Mani, B. K.; Zigman, J. M.; Houglund, J. L.; Abizaid, A., Novel Regulator of Acylated Ghrelin, CF801, Reduces Weight Gain, Rebound Feeding after a Fast, and Adiposity in Mice. *Front Endocrinol* **2015**, *6*, 144.
42. Perona, J. J.; Hedstrom, L.; Rutter, W. J.; Fletterick, R. J., Structural origins of substrate discrimination in trypsin and chymotrypsin. *Biochemistry* **1995**, *34* (5), 1489-99.
43. Morihara, K.; Oka, T., alpha-Chymotrypsin as the catalyst for peptide synthesis. *Biochem J* **1977**, *163* (3), 531-42.
44. Morihara, K.; Oka, T., A kinetic investigation of subsites S1' and S2' in alpha-chymotrypsin and subtilisin BPN'. *Arch Biochem Biophys* **1977**, *178* (1), 188-94.
45. Chatterjee, J.; Gilon, C.; Hoffman, A.; Kessler, H., N-methylation of peptides: a new perspective in medicinal chemistry. *Acc Chem Res* **2008**, *41* (10), 1331-42.
46. Chatterjee, J.; Ovadia, O.; Zahn, G.; Marinelli, L.; Hoffman, A.; Gilon, C.; Kessler, H., Multiple N-methylation by a designed approach enhances receptor selectivity. *Journal of Medicinal Chemistry* **2007**, *50* (24), 5878-5881.
47. Leeson, P., Drug discovery: Chemical beauty contest. *Nature* **2012**, *481* (7382), 455-6.
48. Lipinski, C. A.; Lombardo, F.; Dominy, B. W.; Feeney, P. J., Experimental and computational approaches to estimate solubility and permeability in drug discovery and development settings. *Adv Drug Deliv Rev* **2001**, *46* (1-3), 3-26.
49. Rampersad, S. N., Multiple applications of Alamar Blue as an indicator of metabolic function and cellular health in cell viability bioassays. *Sensors (Basel)* **2012**, *12* (9), 12347-60.
50. Taylor, M. S.; Ruch, T. R.; Hsiao, P. Y.; Hwang, Y.; Zhang, P.; Dai, L.; Huang, C. R.; Berndsen, C. E.; Kim, M. S.; Pandey, A.; Wolberger, C.; Marmorstein, R.; Machamer, C.;

- Boeke, J. D.; Cole, P. A., Architectural organization of the metabolic regulatory enzyme ghrelin O-acyltransferase. *J Biol Chem* **2013**, *288* (45), 32211-28.
51. Udenfriend, S.; Stein, S.; Bohlen, P.; Dairman, W.; Leimgruber, W.; Weigele, M., Fluorescamine: a reagent for assay of amino acids, peptides, proteins, and primary amines in the picomole range. *Science* **1972**, *178* (4063), 871-2.
52. Weigele, M.; Blount, J. F.; Teng, J. P.; Czajkowski, R. C.; Leimgruber, W., Fluorogenic ninhydrin reaction. Structure of the fluorescent principle. *Journal of the American Chemical Society* **1972**, *94* (11), 4052-4054.
53. Hedstrom, L., An overview of serine proteases. *Curr Protoc Protein Sci* **2002**, *Chapter 21*, Unit 21 10.
54. Radisky, E. S.; Lee, J. M.; Lu, C. J.; Koshland, D. E., Jr., Insights into the serine protease mechanism from atomic resolution structures of trypsin reaction intermediates. *Proc Natl Acad Sci U S A* **2006**, *103* (18), 6835-40.
55. Bachovchin, D. A.; Cravatt, B. F., The pharmacological landscape and therapeutic potential of serine hydrolases. *Nat Rev Drug Discov* **2012**, *11* (1), 52-68.
56. Pauletti, G. M.; Gangwar, S.; Knipp, G. T.; Nerurkar, M. M.; Okumu, F. W.; Tamura, K.; Siahhan, T. J.; Borchardt, R. T., Structural requirements for intestinal absorption of peptide drugs. *J Control Release* **1996**, *41* (1-2), 3-17.
57. Cleverdon, E. R.; Davis, T. R.; Hougland, J. L., Functional group and stereochemical requirements for substrate binding by ghrelin O-acyltransferase revealed by unnatural amino acid incorporation. *Bioorg Chem* **2018**, *79*, 98-106.
58. Garner, A. L.; Janda, K. D., A small molecule antagonist of ghrelin O-acyltransferase (GOAT). *Chem Commun (Camb)* **2011**, *47* (26), 7512-4.

59. Hopkins, A. L.; Nelson, T. A.; Guschina, I. A.; Parsons, L. C.; Lewis, C. L.; Brown, R. C.; Christian, H. C.; Davies, J. S.; Wells, T., Unacylated ghrelin promotes adipogenesis in rodent bone marrow via ghrelin O-acyl transferase and GHS-R1a activity: evidence for target cell-induced acylation. *Sci Rep* **2017**, *7*, 45541.
60. Murtuza, M. I.; Isokawa, M., Endogenous ghrelin-O-acyltransferase (GOAT) acylates local ghrelin in the hippocampus. *J Neurochem* **2018**, *144* (1), 58-67.
61. Tugyi, R.; Uray, K.; Ivan, D.; Fellinger, E.; Perkins, A.; Hudecz, F., Partial D-amino acid substitution: Improved enzymatic stability and preserved Ab recognition of a MUC2 epitope peptide. *Proc Natl Acad Sci U S A* **2005**, *102* (2), 413-8.
62. Dantas, V. G.; Furtado-Alle, L.; Souza, R. L.; Chautard-Freire-Maia, E. A., Obesity and variants of the GHRL (ghrelin) and BCHE (butyrylcholinesterase) genes. *Genet Mol Biol* **2011**, *34* (2), 205-7.
63. Riddles, P. W.; Blakeley, R. L.; Zerner, B., Ellman's reagent: 5,5'-dithiobis(2-nitrobenzoic acid)--a reexamination. *Anal Biochem* **1979**, *94* (1), 75-81.
64. De Bernardo, S.; Weigele, M.; Toome, V.; Manhart, K.; Leimgruber, W.; Bohlen, P.; Stein, S.; Udenfriend, S., Studies on the reaction of fluorescamine with primary amines. *Arch Biochem Biophys* **1974**, *163* (1), 390-9.
65. Nakamura, H.; Tamura, Z., Fluorometric-Determination of Secondary-Amines Based on Their Reaction with Fluorescamine. *Anal Chem* **1980**, *52* (13), 2087-2092.
66. Post, P. L.; Trybus, K. M.; Taylor, D. L., A genetically engineered, protein-based optical biosensor of myosin II regulatory light chain phosphorylation. *J Biol Chem* **1994**, *269* (17), 12880-7.

67. Willert, K.; Brown, J. D.; Danenberg, E.; Duncan, A. W.; Weissman, I. L.; Reya, T.; Yates, J. R., 3rd; Nusse, R., Wnt proteins are lipid-modified and can act as stem cell growth factors.

*Nature* **2003**, *423* (6938), 448-52.

## Chapter 5: Conclusions and future directions

### 5.1 Introduction

Ghrelin was initially identified to be the endogenous ligand of the GHS-R1a GPCR, which is one of several receptors controlling the release of growth hormone.<sup>1</sup> Since its discovery in 1999, ghrelin has been implicated in a multitude of biological processes including most notably hunger signaling, metabolism, and energy balance.<sup>2-6</sup> The attachment of an eight carbon fatty acid to an N-terminal serine of ghrelin results in recognition and activation of its receptor, the GHS-R1a, and thus is necessary for its biological activity.<sup>7</sup> This post-translational attachment of an octanoyl moiety was discovered to be catalyzed by the enzyme, ghrelin *O*-acyltransferase (GOAT).<sup>8-9</sup> This step in ghrelin maturation is an ideal candidate for regulating ghrelin signaling using inhibitors since ghrelin is the only predicted substrate for GOAT.<sup>10</sup> The goals of the work in this dissertation were to better understand how GOAT acylates ghrelin by studying the biological substrate, proghrelin, and investigating the substrate binding requirements of GOAT for peptide inhibitor development. There has been no thorough investigation into the structure of proghrelin or C-terminal processing until the work presented in this document, which has advanced our understanding of this key intermediate in the ghrelin-GOAT pathway. The second goal of the work presented was to understand the binding requirements governing the formation of the ghrelin:GOAT complex. Analysis of unnatural amino acid incorporated peptides has provided both a comprehensive picture of ghrelin-GOAT functional binding requirements as well as a potent inhibitor scaffold. This dissertation has provided crucial information to unexplored areas in the ghrelin-GOAT field which enhances our understanding of how ghrelin is acylated by GOAT and ghrelin processing.

## 5.2 Development of a method for purification and structural analysis of proghrelin

In order to pursue investigation into the structural and biological properties of proghrelin a bacterial expression system was developed to produce recombinant GST-TEV-human-Proghrelin-His<sub>6</sub> as well as GST-TEV-human-C-ghrelin-His<sub>6</sub>. The first published protocol for purifying recombinantly expressed proghrelin utilized a similar fusion protein construct.<sup>11</sup> There were complications during the purification process to obtain a homogenous product. Proghrelin displayed a unique banding pattern in which there were consistent lower molecular weight protein impurities throughout the purification, from bacterial lysis to purified protein samples. In order to combat the low molecular weight proteins, the purification method was modified to decrease the total purification time and introduction of size exclusion chromatography. A homogenous product was obtained which was verified by silver staining, Western blot and mass spectrometry. Proghrelin was then subjected to structural analysis including CD and NMR which concluded that proghrelin contains a region of alpha helical secondary structure, although the majority of the protein structure is random coil. When detergents were added to the protein there was an increase in secondary structure, particularly with SDS. Comparison of proghrelin to ghrelin in an aqueous environment indicated that the C-ghrelin region is the major contributor to proghrelin secondary structure. These results are somewhat consistent with the literature since ghrelin in an aqueous environment and in modeling studies was observed to be random coil and flexible and C-ghrelin, specifically obestatin, contained some elements of secondary structure.<sup>12-</sup>  
<sup>14</sup> The result of structural analysis suggests that proghrelin contains secondary structure and this structure may be enhanced by lipids and a membrane-like environment. This information is important when modeling or analyzing interactions between proghrelin and GOAT. GOAT is located in the ER membrane, and this membrane environment would likely affect proghrelin

structure based upon the impact of detergents observed during the studies in this dissertation and previously published data.<sup>12, 15-18</sup>

The aggregation and low solubility observed with the GST-fusion protein of C-ghrelin (GThCgH) is in juxtaposition to the behavior observed with proghrelin. The fusion construct was completely insoluble until expression conditions were modified (low temperature, 0.4 mM IPTG protein induction, and LEMO-21 *E. coli*), and even then a significant fraction of the fusion protein remained insoluble. C-ghrelin was unable to be purified from the GST fusion protein since the TEV digestion was unable to be completed. This is due possibly to GThCgH protein misfolding or availability of the TEV cleavage site to the TEV protease. When a denaturant-based purification was introduced, GThCgH was able to be purified. However, it exhibited aggregation and insolubility when the protein was buffer exchanged into a non-denaturing buffer. The expression and purification of GST-TEV-human C-ghrelin-His<sub>6</sub>, although not completely successful, provided some intriguing findings supporting the possibility that ghrelin stabilizes C-ghrelin structure and solubility. Without ghrelin present, C-ghrelin is highly unstable leading to the insoluble behavior observed in this work.

### **5.3 The cleavage of proghrelin**

During lysis and purification of proghrelin, distinct lower molecular weight proteins were observed which persisted throughout and reappeared after purification to homogeneity. Initially, this behavior was attributed to cleavage due to a bacterial protease. However, after thorough addition of protease inhibitors and purification/buffer exchanges through at least three complementary purification steps, the observed cleavage behavior of proghrelin persisted. The only condition in which no proghrelin cleavage was observed was when a strong denaturant

(3XSB or 6 M GuHCl) was included during lysis or purification. This is consistent with folded protein structure being required for cleavage activity. The unique cleavage behavior of this protein was unable to be fully characterized using Western blotting or gel-based analysis so a fluorescence-based reporter system was introduced to study proghrelin cleavage. The fluorescent proghrelin construct reproduced the results observed with purified proghrelin, in which cleavages occur over time and generated a number of discrete products. After the reporter system was verified with the full length protein, a series of N- and C-terminal truncated constructs were made to study the sequence dependent behavior of cleavage. Fluorescent gel imaging provided a facile method for monitoring the cleavage behavior of proghrelin constructs, and a section of the proghrelin sequence between amino acids 30-50 was shown to be necessary for cleavage. In parallel analysis, the cleavage behavior of proghrelin was analyzed by mass spectrometry that identified the cleavage sites within purified proghrelin and showed these sites to be clustered near the C-terminal end of obestatin. Attempts to block proghrelin cleavage by mutating single amino acid residues were not successful, suggesting that this activity is robust and tolerant to a significant degree of sequence variation. The identified cut sites and the residues that are most likely responsible for cleavage are both located in C-ghrelin. There is a possibility that the cleavage behavior observed with proghrelin is related to C-ghrelin processing to obestatin, but this remains to be conclusively proven.

#### **5.4 Unnatural amino acid-containing peptides to study GOAT binding**

A ghrelin-mimetic peptide substrate incorporating an amine (2,3-diaminopropanoic acid) in place of the serine hydroxyl group at the acylation site (GSDapFLC<sub>AcDan</sub>) was explored to determine the ability of GOAT to catalyze amide bond formation. In comparison to the wildtype

substrate with a serine at the acylation site, the Dap3 residue is accepted by the enzyme but not as well as the wildtype S3 substrate. There was also the appearance of a second ester-linked peak observed in the GSDapFLC<sub>AcDan</sub> reaction, suggesting acylation at the S2 position as well as at Dap3. The acylation at the S2 position and some at Dap3 is the result of a non-enzymatic acylation reaction which means that in solution the acylation will occur without hGOAT present. This previously unidentified non-enzymatic reaction needs to be accounted for when using Dap-incorporated peptides as mechanistic probes so as not to over interpret binding and activity in relation to GOAT.

The inefficient acylation of GSDapFLC<sub>AcDan</sub> led to instead utilizing Dap-incorporation as a tool to study hGOAT binding. The incorporation of the Dap group at the third position dramatically increased binding to hGOAT in small unlabeled peptides. Within the context of the GSDapFL peptide, amino acids were truncated or mutated to evaluate the contribution of each amino acid side chain to the peptide's binding of GOAT. The studies indicate that the G1 and F4 are the most important residues for GOAT binding. The lack of peptide binding with deletion or acetylation at the G1 position in GSDapFL indicated that these peptides are binding into the active site of GOAT. Previous reactivity studies have concluded that the N-terminal G1 is a necessary recognition motif for GOAT.<sup>10-11, 19</sup> The significance of the F4 in peptide binding is in contrast to published reactivity data suggesting that F4 is replaceable with minimal impact on substrate acylation.<sup>10, 19</sup> These studies have provided a comprehensive picture of the functional requirements for GOAT binding.

Since the incorporation of Dap into small ghrelin mimetic peptides increased the binding affinity for hGOAT dramatically, there was an effort to increase the biostability for *in vitro*

purposes by introducing backbone methylations. After investigating the effect of cooperativity of methylations at multiple positions, SarSDap<sub>N-Me</sub>F which has a high nanomolar IC<sub>50</sub>, was chosen for cell studies to evaluate its ability to inhibit *in vitro* ghrelin acylation. However, there was no effect on ghrelin acylation in cell-based studies although subsequent characterization suggests this lack of activity may result from low cell permeability of the peptide. These unnatural amino acid- incorporated peptide studies provide a peptide scaffold that could be modified to increase the cell permeability, for example introduction of a HIV-Tat sequence<sup>20</sup> which was shown to improve permeability with Go-COA-Tat.<sup>21</sup> There is also another avenue to utilize the Dap- incorporated peptides to study externally located GOAT<sup>22-23</sup> as an imaging agent which would open a window into studying a new aspect of ghrelin signaling.

## 5.5 Summary and future directions

The goals of the work were to define how GOAT recognizes and modifies ghrelin by first investigating the structure and unique processing behavior of the biological substrate of hGOAT and to define the binding requirements of hGOAT to small ghrelin-mimetic peptides. The results through this dissertation have provided multiple approaches to efficiently express and purify both proghrelin and C-ghrelin. Expression of proghrelin provides the opportunity to define the structural characteristics of this intriguing prohormone. The studies done in this work indicated that the presence of a detergent or a lipid environment enhance regions of secondary structure within proghrelin. This is in agreement with studies focused which indicate that SDS enhances secondary structure in ghrelin and obestatin.<sup>12, 14, 16-18, 24</sup> The results indicated that there are possible structural interactions occurring during ghrelin-GOAT binding and acylation that have not been accounted for previously. There has also been characterization of possible self-

processing and cleavage with proghrelin, which potentially plays a role in the processing pathway leading to the other hormone produced from proghrelin, obestatin. This work has also furthered our understanding of GOAT binding by completing the full picture of what are the functional requirements for GOAT substrate recognition. A series of ghrelin peptide mimetics with Dap-incorporation focused on binding to hGOAT instead of reactivity. Evaluating substrate reactivity can lead to over interpretation of substrate binding since reactivity encapsulates binding, catalysis and release of the substrate in the enzyme. The work that has been completed has yielded both new conclusions about the ghrelin-GOAT system as well as a variety of new methods and techniques that will aide future researchers in their efforts to characterize interactions between ghrelin and GOAT.

Even though there have been large gains in our understanding of this system through the work presented in this dissertation, future research is required to fully define the molecular basis for ghrelin processing and activity. For studies of proghrelin cleavage, it is essential that the functionally essential residue(s) for this proteolytic activity are identified to both understand this biochemically intriguing chemistry and to allow inhibition of cleavage to aid in structural studies. The studies of alanine mutations within proghrelin demonstrate that multiple simultaneous mutations may be needed to block proghrelin cleavage activity. Inhibition of proghrelin will allow for complete structural characterization and aid in characterization of proghrelin bound to GOAT. Once proghrelin is completely characterized and the processing behavior is fully understood at the molecular level, this could support the conclusion that proghrelin (C-ghrelin) does in fact self-process. This form of protein cleavage would be a completely novel finding potentially revealing a new method of protein processing.

In light of the self-cleavage behavior observed in proghrelin, purification and structural characterization of the peptide hormone motilin presents another opportunity to explore the impact of self-cleavage in hormone processing. Motilin is also a hormone found in the gastrointestinal tract which shares a degree of sequence similarity to ghrelin, with ghrelin originally named the motilin-related peptide.<sup>25-26</sup> Like ghrelin, motilin is expressed as a larger precursor protein prepromotilin and then is subsequently proteolytically cleaved to yield a 22 amino acid peptide.<sup>26-28</sup> Motilin stimulates gastrointestinal motor activity and has been proposed to play a physiological role in the regulation of fasting motility patterns and gastric emptying, with maximum secretion of motilin during fasting and after eating.<sup>26, 29</sup> Motilin also activates a GPCR for its biological activity, akin to the GHS-R1a.<sup>30</sup> Homology, localization and cooperativity between ghrelin and motilin provide motivation for studying these peptide hormones. Ghrelin and motilin signaling are connected within the body, with ghrelin administration decreasing plasma levels of motilin and inhibiting intestinal propulsive contractions.<sup>31</sup> Motilin in turn decreases plasma ghrelin levels suggesting that these gut peptides cooperatively control the function of gastric motor movement and contractions.<sup>32</sup> Another similarity to the ghrelin/proghrelin/obestatin system, processing of premotilin is proposed to generate a second potential hormone (motilin-associated peptide) alongside motilin, although the biological role of motilin-associated peptide remains unclear.<sup>33-35</sup> There is a possibility that proghrelin and premotilin have similar processing and thus cleavage behavior that was observed with proghrelin. There is also interest in the ability to control ghrelin/motilin signaling in the gastrointestinal tract,<sup>36-39</sup> which includes the ability to regulate gastric emptying, feeding and metabolism.<sup>29</sup> The possibility also exists that ghrelin mimetics can act as motilin agonists in gastrointestinal hypomotility disorders.<sup>40-41</sup> The ability to express, purify and investigate the

biological activity of this molecular cousin of ghrelin could provide another opportunity to explore and explain the cleavage behavior observed with proghrelin.

The future of the structure-activity definition found with the small unnatural amino acid incorporated peptides is to use them as scaffold for further inhibitor design. Limitations of the present scaffolds include both the lack of cell permeability and potency against GOAT. To address the first limitation, a moiety would need to be attached that would increase cell permeability if intracellular GOAT was the target, such as an HIV Tat sequence, in a similar manner as Go-CoA-Tat.<sup>21</sup> In an attempt to address potency, the scaffold could be modified with a small molecule such as a CDDO-derivative<sup>42</sup> in which the peptide would increase the specificity and the small molecule would increase the potency. There have been two recently published reports of GOAT located in the plasma membrane and not in the ER membrane.<sup>22, 43</sup> The challenges with GOAT peptide inhibitor cell permeability would not impact targeting extracellular GOAT. In this case, these potent inhibitors could be used for their binding affinity as imaging or identification agents to identify the tissues or location of extracellular GOAT.<sup>22-23</sup> These inhibitors should also be characterized against the ghrelin receptor GHS-R1a to gain a better understanding of the structure-activity relationship differences between GOAT and the ghrelin receptor and to ensure there is no unintended receptor activation if these molecules were to be pursued as *in vitro/in vivo* GOAT inhibitor.

The current candidates of GOAT assays are limited and none are ideal for detecting ghrelin *in vitro*. This lack of cost-efficient and reproducible cell-based GOAT activity assays poses a key limitation for future drug development and *in vitro* testing. An *in vitro* ghrelin acylation assay would be useful not only for determining inhibitor effectiveness before going

into *in vivo* models. It would also be useful for testing GOAT mutants and acylation efficiency in a more biological relevant model, since currently GOAT is produced in Sf9 insect cells.<sup>10, 19, 44-45</sup>

The final future direction of this project is to work further on the development of a metabolic-labeling based cell assay for detection of ghrelin acylation. Preliminary studies into an *in vitro* ghrelin acylation assay through the introduction of an alkyne-labeled octanoic acid have been attempted but have not been successful. In the future, alkyne octanoic acid incorporation would lead to the labeling of acylated ghrelin with an alkyne and enable monitoring and detection of ghrelin acylation using a copper-catalyzed azide-alkyne [3+2] cycloaddition<sup>46-47</sup> and gel-based detection. These studies have determined the cytotoxicity of octanoic acid and an optimum concentration for metabolic labeling<sup>47-50</sup> based upon the cytotoxicity determination. The permeability of octanoic and octynoic acid (alkyne octanoic acid) has been tested and increased with the use of bovine serum albumin (BSA) to the mixture. This is still an ongoing goal and necessary future direction. The method of introducing an alkyne derivative or the method of detection could be modified but the foundation of an *in vitro* assay has been laid and should be further pursued by future researchers in this laboratory.

## 5.6 References

1. Kojima, M.; Hosoda, H.; Date, Y.; Nakazato, M.; Matsuo, H.; Kangawa, K., Ghrelin is a growth-hormone-releasing acylated peptide from stomach. *Nature* **1999**, *402* (6762), 656-60.
2. Cummings, D. E.; Frayo, R. S.; Marmonier, C.; Aubert, R.; Chapelot, D., Plasma ghrelin levels and hunger scores in humans initiating meals voluntarily without time- and food-related cues. *Am J Physiol Endocrinol Metab* **2004**, *287* (2), E297-304.
3. Levin, F.; Edholm, T.; Schmidt, P. T.; Gryback, P.; Jacobsson, H.; Degerblad, M.; Hoybye, C.; Holst, J. J.; Rehfeld, J. F.; Hellstrom, P. M.; Naslund, E., Ghrelin stimulates gastric emptying and hunger in normal-weight humans. *J Clin Endocrinol Metab* **2006**, *91* (9), 3296-302.
4. Cowley, M. A.; Smith, R. G.; Diano, S.; Tschop, M.; Pronchuk, N.; Grove, K. L.; Strasburger, C. J.; Bidlingmaier, M.; Esterman, M.; Heiman, M. L.; Garcia-Segura, L. M.; Nillni, E. A.; Mendez, P.; Low, M. J.; Sotonyi, P.; Friedman, J. M.; Liu, H.; Pinto, S.; Colmers, W. F.; Cone, R. D.; Horvath, T. L., The distribution and mechanism of action of ghrelin in the CNS demonstrates a novel hypothalamic circuit regulating energy homeostasis. *Neuron* **2003**, *37* (4), 649-61.
5. Heppner, K. M.; Muller, T. D.; Tong, J.; Tschop, M. H., Ghrelin in the control of energy, lipid, and glucose metabolism. *Methods Enzymol* **2012**, *514*, 249-60.
6. Lim, C. T.; Kola, B.; Korbonits, M., The ghrelin/GOAT/GHS-R system and energy metabolism. *Rev Endocr Metab Disord* **2011**, *12* (3), 173-86.
7. Bednarek, M. A.; Feighner, S. D.; Pong, S. S.; McKee, K. K.; Hreniuk, D. L.; Silva, M. V.; Warren, V. A.; Howard, A. D.; Van Der Ploeg, L. H.; Heck, J. V., Structure-function studies on the new growth hormone-releasing peptide, ghrelin: minimal sequence of ghrelin necessary for activation of growth hormone secretagogue receptor 1a. *J Med Chem* **2000**, *43* (23), 4370-6.

8. Gutierrez, J. A.; Solenberg, P. J.; Perkins, D. R.; Willency, J. A.; Knierman, M. D.; Jin, Z.; Witcher, D. R.; Luo, S.; Onyia, J. E.; Hale, J. E., Ghrelin octanoylation mediated by an orphan lipid transferase. *Proc Natl Acad Sci U S A* **2008**, *105* (17), 6320-5.
9. Yang, J.; Brown, M. S.; Liang, G.; Grishin, N. V.; Goldstein, J. L., Identification of the acyltransferase that octanoylates ghrelin, an appetite-stimulating peptide hormone. *Cell* **2008**, *132* (3), 387-96.
10. Darling, J. E.; Zhao, F.; Loftus, R. J.; Patton, L. M.; Gibbs, R. A.; Houglund, J. L., Structure-activity analysis of human ghrelin O-acyltransferase reveals chemical determinants of ghrelin selectivity and acyl group recognition. *Biochemistry* **2015**, *54* (4), 1100-10.
11. Yang, J.; Zhao, T. J.; Goldstein, J. L.; Brown, M. S., Inhibition of ghrelin O-acyltransferase (GOAT) by octanoylated pentapeptides. *Proc Natl Acad Sci U S A* **2008**, *105* (31), 10750-5.
12. Alen, B. O.; Nieto, L.; Gurriaran-Rodriguez, U.; Mosteiro, C. S.; Alvarez-Perez, J. C.; Otero-Alen, M.; Camina, J. P.; Gallego, R.; Garcia-Caballero, T.; Martin-Pastor, M.; Casanueva, F. F.; Jimenez-Barbero, J.; Pazos, Y., The NMR structure of human obestatin in membrane-like environments: insights into the structure-bioactivity relationship of obestatin. *PLoS One* **2012**, *7* (10), e45434.
13. Silva Elipe, M. V.; Bednarek, M. A.; Gao, Y. D., <sup>1</sup>H NMR structural analysis of human ghrelin and its six truncated analogs. *Biopolymers* **2001**, *59* (7), 489-501.
14. Scrima, M.; Campiglia, P.; Esposito, C.; Gomez-Monterrey, I.; Novellino, E.; D'Ursi, A. M., Obestatin conformational features: a strategy to unveil obestatin's biological role? *Biochem Biophys Res Commun* **2007**, *363* (3), 500-5.
15. Taylor, M. S.; Ruch, T. R.; Hsiao, P. Y.; Hwang, Y.; Zhang, P.; Dai, L.; Huang, C. R.; Berndsen, C. E.; Kim, M. S.; Pandey, A.; Wolberger, C.; Marmorstein, R.; Machamer, C.;

- Boeke, J. D.; Cole, P. A., Architectural organization of the metabolic regulatory enzyme ghrelin O-acyltransferase. *J Biol Chem* **2013**, *288* (45), 32211-28.
16. Beevers, A. J.; Kukol, A., Conformational flexibility of the peptide hormone ghrelin in solution and lipid membrane bound: a molecular dynamics study. *J Biomol Struct Dyn* **2006**, *23* (4), 357-64.
17. Kukol, A., The structure of ghrelin. *Vitam Horm* **2008**, *77*, 1-12.
18. Vortmeier, G.; DeLuca, S. H.; Els-Heindl, S.; Chollet, C.; Scheidt, H. A.; Beck-Sickinger, A. G.; Meiler, J.; Huster, D., Integrating solid-state NMR and computational modeling to investigate the structure and dynamics of membrane-associated ghrelin. *PLoS One* **2015**, *10* (3), e0122444.
19. Darling, J. E.; Prybolsky, E. P.; Sieburg, M.; Hougland, J. L., A fluorescent peptide substrate facilitates investigation of ghrelin recognition and acylation by ghrelin O-acyltransferase. *Anal Biochem* **2013**, *437* (1), 68-76.
20. Pauletti, G. M.; Gangwar, S.; Knipp, G. T.; Nerurkar, M. M.; Okumu, F. W.; Tamura, K.; Siahhaan, T. J.; Borchardt, R. T., Structural requirements for intestinal absorption of peptide drugs. *J Control Release* **1996**, *41* (1-2), 3-17.
21. Barnett, B. P.; Hwang, Y.; Taylor, M. S.; Kirchner, H.; Pfluger, P. T.; Bernard, V.; Lin, Y. Y.; Bowers, E. M.; Mukherjee, C.; Song, W. J.; Longo, P. A.; Leahy, D. J.; Hussain, M. A.; Tschop, M. H.; Boeke, J. D.; Cole, P. A., Glucose and weight control in mice with a designed ghrelin O-acyltransferase inhibitor. *Science* **2010**, *330* (6011), 1689-92.
22. Hopkins, A. L.; Nelson, T. A.; Guschina, I. A.; Parsons, L. C.; Lewis, C. L.; Brown, R. C.; Christian, H. C.; Davies, J. S.; Wells, T., Unacylated ghrelin promotes adipogenesis in rodent

- bone marrow via ghrelin O-acyl transferase and GHS-R1a activity: evidence for target cell-induced acylation. *Sci Rep* **2017**, *7*, 45541.
23. Murtuza, M. I.; Isokawa, M., Endogenous ghrelin-O-acyltransferase (GOAT) acylates local ghrelin in the hippocampus. *J Neurochem* **2018**, *144* (1), 58-67.
24. De Ricco, R.; Valensin, D.; Gaggelli, E.; Valensin, G., Conformation propensities of des-acyl-ghrelin as probed by CD and NMR. *Peptides* **2013**, *43*, 62-7.
25. Asakawa, A.; Inui, A.; Kaga, T.; Yuzuriha, H.; Nagata, T.; Ueno, N.; Makino, S.; Fujimiya, M.; Niijima, A.; Fujino, M. A.; Kasuga, M., Ghrelin is an appetite-stimulatory signal from stomach with structural resemblance to motilin. *Gastroenterology* **2001**, *120* (2), 337-45.
26. Brown, J. C.; Cook, M. A.; Dryburgh, J. R., Motilin, a gastric motor activity stimulating polypeptide: the complete amino acid sequence. *Can J Biochem* **1973**, *51* (5), 533-7.
27. Dea, D.; Boileau, G.; Poitras, P.; Lahaie, R. G., Molecular heterogeneity of human motilinlike immunoreactivity explained by the processing of prepromotilin. *Gastroenterology* **1989**, *96* (3), 695-703.
28. Seino, Y.; Tanaka, K.; Takeda, J.; Takahashi, H.; Mitani, T.; Kurono, M.; Kayano, T.; Koh, G.; Fukumoto, H.; Yano, H.; et al., Sequence of an intestinal cDNA encoding human motilin precursor. *FEBS Lett* **1987**, *223* (1), 74-6.
29. Itoh, Z., *Motilin*. Academic Press: San Diego, 1990; p xvii, 264 p.
30. Muccioli, G.; Tschop, M.; Papotti, M.; Deghenghi, R.; Heiman, M.; Ghigo, E., Neuroendocrine and peripheral activities of ghrelin: implications in metabolism and obesity. *Eur J Pharmacol* **2002**, *440* (2-3), 235-54.

31. Ogawa, A.; Mochiki, E.; Yanai, M.; Morita, H.; Toyomasu, Y.; Ogata, K.; Ohno, T.; Asao, T.; Kuwano, H., Interdigestive migrating contractions are coregulated by ghrelin and motilin in conscious dogs. *Am J Physiol Regul Integr Comp Physiol* **2012**, *302* (2), R233-41.
32. Avau, B.; Carbone, F.; Tack, J.; Depoortere, I., Ghrelin signaling in the gut, its physiological properties, and therapeutic potential. *Neurogastroenterol Motil* **2013**, *25* (9), 720-32.
33. Huang, Z.; De Clercq, P.; Depoortere, I.; Peeters, T. L., Isolation and sequence of cDNA encoding the motilin precursor from monkey intestine. Demonstration of the motilin precursor in the monkey brain. *FEBS Lett* **1998**, *435* (2-3), 149-52.
34. Tomasetto, C.; Karam, S. M.; Ribieras, S.; Masson, R.; Lefebvre, O.; Staub, A.; Alexander, G.; Chenard, M. P.; Rio, M. C., Identification and characterization of a novel gastric peptide hormone: the motilin-related peptide. *Gastroenterology* **2000**, *119* (2), 395-405.
35. Coulie, B. J.; Miller, L. J., Identification of motilin-related peptide. *Gastroenterology* **2001**, *120* (2), 588-9.
36. Javid, F. A.; Bulmer, D. C.; Broad, J.; Aziz, Q.; Dukes, G. E.; Sanger, G. J., Anti-emetic and emetic effects of erythromycin in *Suncus murinus*: role of vagal nerve activation, gastric motility stimulation and motilin receptors. *Eur J Pharmacol* **2013**, *699* (1-3), 48-54.
37. Simren, M.; Abrahamsson, H.; Bjornsson, E. S., An exaggerated sensory component of the gastrocolonic response in patients with irritable bowel syndrome. *Gut* **2001**, *48* (1), 20-7.
38. Simren, M.; Abrahamsson, H.; Svedlund, J.; Bjornsson, E. S., Quality of life in patients with irritable bowel syndrome seen in referral centers versus primary care: the impact of gender and predominant bowel pattern. *Scand J Gastroenterol* **2001**, *36* (5), 545-52.

39. Simren, M.; Bjornsson, E. S.; Abrahamsson, H., High interdigestive and postprandial motilin levels in patients with the irritable bowel syndrome. *Neurogastroenterol Motil* **2005**, *17* (1), 51-7.
40. De Smet, B.; Mitselos, A.; Depoortere, I., Motilin and ghrelin as prokinetic drug targets. *Pharmacol Therapeut* **2009**, *123* (2), 207-223.
41. Gonzalez-Rey, E.; Chorny, A.; Delgado, M., Therapeutic action of ghrelin in a mouse model of colitis. *Gastroenterology* **2006**, *130* (6), 1707-20.
42. McGovern-Gooch, K. R.; Mahajani, N. S.; Garagozzo, A.; Schramm, A. J.; Hannah, L. G.; Sieburg, M. A.; Chisholm, J. D.; Hougland, J. L., Synthetic Triterpenoid Inhibition of Human Ghrelin O-Acyltransferase: The Involvement of a Functionally Required Cysteine Provides Mechanistic Insight into Ghrelin Acylation. *Biochemistry* **2017**, *56* (7), 919-931.
43. Murata, M.; Okimura, Y.; Iida, K.; Matsumoto, M.; Sowa, H.; Kaji, H.; Kojima, M.; Kangawa, K.; Chihara, K., Ghrelin modulates the downstream molecules of insulin signaling in hepatoma cells. *J Biol Chem* **2002**, *277* (7), 5667-74.
44. McGovern-Gooch, K. R.; Rodrigues, T.; Darling, J. E.; Sieburg, M. A.; Abizaid, A.; Hougland, J. L., Ghrelin Octanoylation Is Completely Stabilized in Biological Samples by Alkyl Fluorophosphonates. *Endocrinology* **2016**, *157* (11), 4330-4338.
45. Zhao, F.; Darling, J. E.; Gibbs, R. A.; Hougland, J. L., A new class of ghrelin O-acyltransferase inhibitors incorporating triazole-linked lipid mimetic groups. *Bioorg Med Chem Lett* **2015**, *25* (14), 2800-3.
46. Holub, J. M.; Kirshenbaum, K., Tricks with clicks: modification of peptidomimetic oligomers via copper-catalyzed azide-alkyne [3+2] cycloaddition. *Chem Soc Rev* **2010**, *39* (4), 1325-1337.

47. Meldal, M.; Tornøe, C. W., Cu-catalyzed azide-alkyne cycloaddition. *Chem Rev* **2008**, *108* (8), 2952-3015.
48. Charron, G.; Zhang, M. M.; Yount, J. S.; Wilson, J.; Raghavan, A. S.; Shamir, E.; Hang, H. C., Robust fluorescent detection of protein fatty-acylation with chemical reporters. *J Am Chem Soc* **2009**, *131* (13), 4967-75.
49. Martin, B. R.; Cravatt, B. F., Large-scale profiling of protein palmitoylation in mammalian cells. *Nat Methods* **2009**, *6* (2), 135-8.
50. Menendez, J. A.; Colomer, R.; Lupu, R., Why does tumor-associated fatty acid synthase (oncogenic antigen-519) ignore dietary fatty acids? *Med Hypotheses* **2005**, *64* (2), 342-9.

## Rights and Permissions

[Authors](#)

[STM Publishers](#)

[Non-commercial requests](#)

[Commercial requests](#)

[Archiving policy](#)

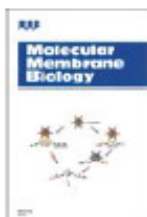
[Copyright policy](#)

[Sharing and public posting of articles](#)

## Non-commercial requests

Authors may reproduce an article, in whole or in part, in a thesis or dissertation at no cost providing the original source is attributed.

If you wish to copy and distribute an article in whole for teaching (e.g. in a course pack) please either visit [Organizations with charitable and not-for-profit statuses](#) are usually able to re-use Portland Press content without charges, but we ask that you please write to [permissions@portlandpress.com](mailto:permissions@portlandpress.com) in the first instance.



**Title:** The octanoylated energy regulating hormone ghrelin: An expanded view of ghrelin's biological interactions and avenues for controlling ghrelin signaling

**Author:** Elizabeth R. Cleverdon, Kayleigh R. McGovern-Gooch, James L. Houglund

**Publication:** Molecular Membrane Biology

**Publisher:** Taylor & Francis

**Date:** Nov 16, 2016

Rights managed by Taylor & Francis

**LOGIN**

If you're a [copyright.com](http://copyright.com) user, you can login to RightsLink using your [copyright.com](http://copyright.com) credentials.

Already a RightsLink user or want to [learn more?](#)

### Thesis/Dissertation Reuse Request

Taylor & Francis is pleased to offer reuses of its content for a thesis or dissertation free of charge contingent on resubmission of permission request if work is published.

BACK

CLOSE WINDOW

Copyright © 2018 [Copyright Clearance Center, Inc.](http://Copyright Clearance Center, Inc.) All Rights Reserved. [Privacy statement](#). [Terms and Conditions](#).  
Comments? We would like to hear from you. E-mail us at [customer care@copyright.com](mailto:customer care@copyright.com)



**Note:** Copyright.com supplies permissions but not the copyrighted content itself.

1  
PAYMENT

2  
REVIEW

3  
CONFIRMATION

### Step 3: Order Confirmation

**Thank you for your order!** A confirmation for your order will be sent to your account email address. If you have questions about your order, you can call us 24 hrs/day, M-F at +1.855.239.3415 Toll Free, or write to us at [info@copyright.com](mailto:info@copyright.com). This is not an invoice.

**Confirmation Number: 11723302**  
**Order Date: 06/11/2018**

If you paid by credit card, your order will be finalized and your card will be charged within 24 hours. If you choose to be invoiced, you can change or cancel your order until the invoice is generated.

#### Payment Information

Elizabeth Cleverdon  
ecleverd@syr.edu  
+1 (315) 751-6390  
Payment Method: n/a

#### Order Details

##### Journal of biological chemistry

**Order detail ID:** 71243065  
**Order License Id:** 4366060255110  
**ISSN:** 1083-351X  
**Publication Type:** e-Journal  
**Volume:**  
**Issue:**  
**Start page:**  
**Publisher:** AMERICAN SOCIETY FOR  
BIOCHEMISTRY AND MOLECULAR BI  
AMERICAN SOCIETY FOR  
BIOCHEMISTRY & MOLECULAR BIOL  
**Author/Editor:**

**Permission Status:** **Granted**

**Permission type:** Republish or display content  
**Type of use:** Thesis/Dissertation

**Requestor type:** Author of requested content

**Format:** Print, Electronic

**Portion:** chart/graph/table/figure

**Number of charts/graphs/tables/figures:** 1

**The requesting person/organization:** Elizabeth Cleverdon/  
Syracuse University

**Title or numeric reference of the portion(s):** Figure 7, Chapter 1 Figure 1.1.

**Title of the article or chapter the portion is from:** Architectural Organization of the Metabolic Regulatory Enzyme Ghrelin O-Acyltransferase

|  |   |
|--|---|
| <b>Editor of portion(s)</b>                  | NA  |
| <b>Author of portion(s)</b>                  | NA  |
| <b>Volume of serial or monograph</b>         | NA  |
| <b>Page range of portion</b>                 | 12  |
| <b>Publication date of portion</b>           | November 8, 2013  |
| <b>Rights for</b>                            | Main product  |
| <b>Duration of use</b>                       | Life of current edition   |
| <b>Creation of copies for the disabled</b>   | no  |
| <b>With minor editing privileges</b>         | no  |
| <b>For distribution to</b>                   | United States and Canada  |
| <b>In the following language(s)</b>          | Original language of publication  |
| <b>With incidental promotional use</b>       | no  |
| <b>Lifetime unit quantity of new product</b> | Up to 499   |
| <b>Title</b>                                 | Ghrelin Processing and Maturation: Developing a molecular-level framework for ghrelin processing and maturation |
| <b>Instructor name</b>                       | James Houglund  |
| <b>Institution name</b>                      | Syracuse University   |
| <b>Expected presentation date</b>            | Jul 2018  |

**Note:** This item will be invoiced or charged separately through CCC's [RightsLink](#) service. [More info](#)

**\$ 0.00**

**Total order items: 1**

**This is not an invoice.**

**Order Total: 0.00 USD**



**Title:** Förster resonance energy transfer-based cholesterolysis assay identifies a novel hedgehog inhibitor

**Author:** Timothy S. Owen, George Ngoje, Travis J. Lageman, Brandon M. Bordeau, Marlene Belfort, Brian P. Callahan

**Publication:** Analytical Biochemistry

**Publisher:** Elsevier

**Date:** 1 November 2015

Copyright © 2015 Elsevier Inc. All rights reserved.

Logged in as:  
Elizabeth Cleverdon  
Account #:  
3001297093

LOGOUT

### Order Completed

Thank you for your order.

This Agreement between Elizabeth Cleverdon ("You") and Elsevier ("Elsevier") consists of your license details and the terms and conditions provided by Elsevier and Copyright Clearance Center.

Your confirmation email will contain your order number for future reference.

#### [printable details](#)

|  |   |
|--|---|
| License Number                               | 4372520994103   |
| License date                                 | Jun 19, 2018  |
| Licensed Content Publisher                   | Elsevier  |
| Licensed Content Publication                 | Analytical Biochemistry   |
| Licensed Content Title                       | Förster resonance energy transfer-based cholesterolysis assay identifies a novel hedgehog inhibitor             |
| Licensed Content Author                      | Timothy S. Owen, George Ngoje, Travis J. Lageman, Brandon M. Bordeau, Marlene Belfort, Brian P. Callahan        |
| Licensed Content Date                        | Nov 1, 2015   |
| Licensed Content Volume                      | 488   |
| Licensed Content Issue                       | n/a   |
| Licensed Content Pages                       | 5   |
| Type of Use                                  | reuse in a thesis/dissertation  |
| Portion                                      | figures/tables/illustrations  |
| Number of figures/tables/illustrations       | 1   |
| Format                                       | both print and electronic   |
| Are you the author of this Elsevier article? | No  |
| Will you be translating?                     | No  |
| Original figure numbers                      | Figure 1.   |
| Title of your thesis/dissertation            | Ghrelin Processing and Maturation: Developing a molecular-level framework for ghrelin processing and maturation |
| Publisher of new work                        | Syracuse University   |
| Author of new work                           | James Hougland  |
| Expected completion date                     | Jul 2018  |
| Estimated size (number                       | 1   |

of pages)

Requestor Location Elizabeth Cleverdon  
1-109 CST

Syracuse, NY 13210  
United States  
Attn:

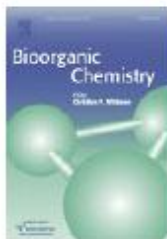
Publisher Tax ID 98-0397604

Total 0.00 USD

[ORDER MORE](#)

[CLOSE WINDOW](#)

Copyright © 2018 [Copyright Clearance Center, Inc.](#) All Rights Reserved. [Privacy statement](#). [Terms and Conditions](#).  
Comments? We would like to hear from you. E-mail us at [customercare@copyright.com](mailto:customercare@copyright.com)



**Title:** Functional group and stereochemical requirements for substrate binding by ghrelin O-acyltransferase revealed by unnatural amino acid incorporation

**Author:** Elizabeth R. Cleverdon, Tasha R. Davis, James L. Houglund

**Publication:** Bioorganic Chemistry

**Publisher:** Elsevier

**Date:** September 2018

© 2018 Elsevier Inc. All rights reserved.

**LOGIN**

If you're a [copyright.com](#) user, you can login to RightsLink using your [copyright.com](#) credentials.

Already a RightsLink user or want to [learn more?](#)

Please note that, as the author of this Elsevier article, you retain the right to include it in a thesis or dissertation, provided it is not published commercially. Permission is not required, but please ensure that you reference the journal as the original source. For more information on this and on your other retained rights, please visit: <https://www.elsevier.com/about/our-business/policies/copyright#Author-rights>

BACK

CLOSE WINDOW



**Title:** Fluorogenic ninhydrin reaction.  
Structure of the fluorescent  
principle

**Author:** M. Weigele, J. F. Blount, J. P.  
Tengi, et al

**Publication:** Journal of the American  
Chemical Society

**Publisher:** American Chemical Society

**Date:** May 1, 1972

Copyright © 1972, American Chemical Society

**LOGIN**

If you're a [copyright.com](#)  
user, you can login to  
RightsLink using your  
[copyright.com](#) credentials.

Already a [RightsLink](#) user or  
want to [learn more?](#)

**PERMISSION/LICENSE IS GRANTED FOR YOUR ORDER AT NO CHARGE**

This type of permission/license, instead of the standard Terms & Conditions, is sent to you because no fee is being charged for your order. Please note the following:

- Permission is granted for your request in both print and electronic formats, and translations.
- If figures and/or tables were requested, they may be adapted or used in part.
- Please print this page for your records and send a copy of it to your publisher/graduate school.
- Appropriate credit for the requested material should be given as follows: "Reprinted (adapted) with permission from (COMPLETE REFERENCE CITATION). Copyright (YEAR) American Chemical Society." Insert appropriate information in place of the capitalized words.
- One-time permission is granted only for the use specified in your request. No additional uses are granted (such as derivative works or other editions). For any other uses, please submit a new request.

If credit is given to another source for the material you requested, permission must be obtained from that source.

[BACK](#)[CLOSE WINDOW](#)

## Elizabeth R. Cleverdon

Syracuse University  
1-014 Center for Science and  
Technology  
Tel: (315) 443-4070  
Syracuse, NY 13244

119 Remington Avenue  
Apartment F  
[ecleverd@syr.edu](mailto:ecleverd@syr.edu)  
Tel: (315) 751-6390  
Syracuse, NY 13210

---

### Education

**Syracuse University** Syracuse, NY  
**Syracuse University** Syracuse, NY  
**University of Wyoming** Laramie, WY

Ph.D., Chemistry (2018)  
M.Phil., Chemistry (2015)  
B.S., Chemistry (2013)

### Research Experience

#### **Syracuse University**

Graduate Research Assistant (2014-Present)

Advisor: James L. Houglund

Project: Biochemical and Structural Investigation of Ghrelin Processing

- Structure and enzyme-substrate characteristics of proghrelin and ghrelin *O*-acyltransferase
- Inhibitor design and structure activity relationship determination
- Defining enzyme-substrate relationship of ghrelin-GOAT
- Structural analysis of proghrelin utilizing circular dichroism, mass spectrometry and NMR
- Development of assay for detection of *in vitro* acylation of proghrelin utilizing metabolic labeling
- Cell-based experimentation for determination of inhibitor efficacy

#### **University of Wyoming**

Undergraduate Research Assistant (2012-2013)

Advisor: Jan Kubelka

Project: Investigation into small peptide structure and chemistry

- Design, synthesis, and purification of small peptides
- Structural investigation and characterization of small peptides using Fluorescence, FTIR, ATR, circular dichroism, and DSC

### Awards and Honors

**Syracuse University Department of Chemistry Travel Award, 2017**

Syracuse University

**ACS Women's Division: Eli Lilly Travel Award, 2016**

Syracuse University

**Women in Science and Engineering (WISE) Future Professionals Program Associate (2015-2017)**

Syracuse University

**Hathaway Honors Scholarship, 2009-2013**

University of Wyoming

**President's Promise Hathaway Scholarship, 2009-2013**

University of Wyoming

**Publications**

**Cleverdon E.R.**, McGovern-Gooch K.R., Hougland J.L. "The octanoylated energy regulating hormone ghrelin: An expanded view of ghrelin's biological interactions and avenues for controlling ghrelin signaling." *Molecular Membrane Biology*. Vol. 33, Iss. 6-8, 2017.

**Cleverdon E.R.**, Davis T.R., Hougland J.L. "Functional group and stereochemical requirements for ghrelin *O*-acyltransferase substrate binding and catalysis revealed using unnatural peptides." *Bioorganic Chemistry*. Vol 79: 98-106, 2018.

Sieberg M.S., **Cleverdon E.R.**, Hougland J.L. "Ghrelin *O*-acyltransferase Assays and Inhibition" *Methods in Membrane Biology*. 2018.

*Under review*

**Presentations**

**Cleverdon E.R.**, Hougland J.L. (Oral) "Ghrelin Processing and Maturation: Developing a Molecular-Level Framework for Hormone Activation and Biological Function" 254<sup>th</sup> American Chemical Society National Meeting. Washington, D.C. August 2017.

**Cleverdon E.R.**, Hougland J.L. (Oral) "Developing a Molecular-Level Framework for Ghrelin Processing, Maturation and Biological Function" Graduate Student Elevator Talk Session. Federation of American Societies for Experimental Biology (FASEB), Protein Lipidation: Enzymology, Signaling and Therapeutics. Saxtons River, Vt. July 2017.

**Cleverdon E.R.**, Hougland J.L. (Oral) "Structural and Biochemical Investigation of Ghrelin Recognition and Processing." Northeastern Regional Meeting of the American Chemical Society. Binghamton, NY. October 2016.

**Cleverdon E.R.**, Houglund J.L. (Poster) “Developing a Molecular-Level Framework for Ghrelin Processing, Maturation and Biological Function” Federation of American Societies for Experimental Biology (FASEB), Protein Lipidation: Enzymology, Signaling and Therapeutics. Saxtons River, Vt. July 2017.

**Cleverdon E.R.**, Houglund J.L. (Poster) “Structural and Biochemical Investigation of Ghrelin Processing.” 252<sup>nd</sup> American Chemical Society National Meeting. Philadelphia, PA. August 2016.

**Cleverdon E.R.**, Houglund J.L. (Poster) “Structural and Biochemical Investigation of Ghrelin Processing.” Eli Lilly Travel Award Winner’s Poster Session. 252<sup>nd</sup> American Chemical Society National Meeting. Philadelphia, PA. August 2016.

Cabrinha, C.L., **Cleverdon E.R.**, and Houglund J.L. (Poster) “Expression and Mutation of Human Proghrelin.” Life Science Symposium at Syracuse University, Syracuse, NY. August 2015.

**Cleverdon E.R.**, Houglund J.L. (Poster) “Expression and Characterization of Expressed Human Proghrelin.” Northeastern Regional Meeting of the American Chemical Society. Ithaca, NY. June 2015.

## **Teaching Experience**

### **Undergraduate Research Mentor (2015-present)**

Houglund Laboratory  
Syracuse University

- Casey Cabrinha, Research Experience for Undergraduate (REU) summer undergraduate (Summer 2015)
- Naomi Rivera (Spring 2016-Spring 2017)

### **Teaching Assistant (2013-2017)**

CHE103: Chemistry in the Modern World (Fall 2013, 2017)  
CHE107: General Chemistry Laboratory (Spring 2014, 2015, 2017)  
CHE335: Chemical and Biochemical Analysis (Fall 2014 and 2015)  
Syracuse University